

Bentonite Based Organic-Inorganic Hybrid Materials: Application Towards Green Catalysis and as Mercury Sensor

**Thesis Submitted to AcSIR for the Award of the Degree of
DOCTOR OF PHILOSOPHY
in Chemical Sciences**



By

Maya R. J.

Registration No: 10CC11A39005

Under the Guidance of

Dr. R. Luxmi Varma



**CSIR-National Institute for Interdisciplinary Science and Technology
(CSIR-NIIST) Thiruvananthapuram-695019, Kerala, India**

August, 2017

.....*To My Father, Mother and Brother*

DECLARATION

*I hereby declare that the Ph.D. thesis entitled “**Bentonite Based Organic-Inorganic Hybrid Materials: Application Towards Green Catalysis and as Mercury Sensor**” is an independent work carried out by me at Organic Chemistry Section, Chemical Sciences and Technology Division, CSIR-National Institute for Interdisciplinary Science and Technology (CSIR-NIIST), Thiruvananthapuram under the supervision of Dr. R. Luxmi Varma, Senior Principal Scientist and Head CSTD, and it has not been submitted anywhere else for any other degree, diploma or title.*

Maya R. J.

Thiruvananthapuram

August, 2017

**NATIONAL INSTITUTE FOR INTERDISCIPLINARY SCIENCE &
TECHNOLOGY**

Council of Scientific & Industrial Research

GOVERNMENT OF INDIA
Trivandrum-695 019, India



Dr. R. Luxmi Varma
Senior Principal Scientist & Head
Chemical Sciences and Technology Division

Telephone: 91-471-2515275
Fax: 91-471-2491712

24th August 2017

CERTIFICATE

*This is to certify that the work incorporated in this Ph.D. thesis entitled “**Bentonite Based Organic-Inorganic Hybrid Materials: Application Towards Green Catalysis and as Mercury Sensor**” submitted by **Ms. Maya R. J.** to Academy of Scientific and Innovative Research (AcSIR), in fulfillment of the requirements for the award of the **Degree of Doctor of Philosophy in Chemical Sciences**, embodies original research work under my guidance. I further certify that this work has not been submitted to any other University or Institution in part or full for the award of any degree or diploma. Research material obtained from other sources has been duly acknowledged in this thesis. Any text, illustration, table, etc. used in this thesis from other sources have been duly cited and acknowledged.*

Maya R. J.

R. Luxmi Varma

Thiruvananthapuram

August, 2017

Email: luxmivarma@gmail.com, rluxmivarma@niist.res.in

ACKNOWLEDGEMENTS

*It is my great pleasure to express my deep sense of gratitude to my thesis supervisor **Dr. R. Luxmi Varma** for suggesting me the research problem and also for her excellent guidance, constant encouragement and wholehearted help that led to the successful completion of this work.*

I am grateful to Dr. A. Ajayaghosh, Director, CSIR-NIIST and former Directors Dr. Suresh Das and Dr. Gangan Prathap for providing the laboratory facilities to carry out the research work.

I would like to acknowledge Dr. R. Luxmi Varma and Dr. Mangalam S. Nair, present and former AcSIR programme coordinators at CSIR-NIIST for their timely help and advice for the academic procedures of AcSIR.

I would like to acknowledge Dr. K. R. Gopidas and Dr. D. Ramaiah, Former Heads, Chemical Sciences and Technology Division for their support.

I am very thankful to Dr. K.V. Radhakrishnan, Dr. S. Ananthakumar and Dr. Rugmini Sukumar (DAC members) for their immense support and suggestions for the completion of my research work.

I thank Dr. G. Vijay Nair, Emeritus Scientist, Organic Chemistry Section for his inspiring presence.

I would like to acknowledge Dr. A. Jayalekshmy, Dr. Kaustabh Kumar Maiti, Dr. L. Ravi Shankar, Dr. B. S. Sasidhar, Dr. Sunil Varughese and Dr. Ganesh Chandra Nandi, Scientists of Organic Chemistry Section, for their encouragement and support.

I also wish to record my heartfelt thanks to Dr. Jubi John for his valuable help and support for the successful completion of my thesis work.

I wish to express my sincere thanks to Dr. C. H. Suresh for DFT analysis.

I would like to thank Mrs. Saumini Mathew, Mr. Arun, Mr. Saran P. Raveendran, Mr. Syam and Mr. Rakesh Gokul for recording NMR spectra. Thanks are also due to Mrs. S. Viji and Ms. Aathira for mass spectral analysis and Mr. Kiran Mohan for HRTEM analysis.

I am grateful to Dr. Bhoje Gowd and Dr. J. D. Sudha for XRD analysis and TG/DTA analysis.

I am indebted to my beloved and respectful seniors Dr. Jisha Babu and Dr. Anupriya S. for their valuable suggestions and support.

I would also like to specially acknowledge Ms. Athira Krishna, Ms. Sreedevi P., Ms. Santhi S., Mr. Rajeev K. K. and Mr. Jayakrishnan A. for their unconditional love and valuable help rendered throughout my research work.

Further I would like to extend my thanks to my seniors Dr. Suchithra M.V., Dr. Nayana Joseph, Dr. Praveen Prakash, Dr. Jijy E., Dr. Ajish K. R., Dr. Sarath Chand S., Dr. Baiju T. V., Mr. Preethanuj P., Dr. Rony Rajan Paul, Dr. C. R. Sinu, Dr. Anu Jose, Dr. Sajin Francis K., Dr. Dhanya S. R., Dr. Parvathy R. and Dr. K. C. Seethalakshmi for their valuable suggestions and support during different stages of my research career.

Thanks are due to Dr. Saranya S., Mrs. Shimi M., Ms. Aparna P. S., Ms. Greeshma Gopalan, Ms. Santhini P.V., Ms. Dhanya B. P., Mr. Ajesh Vijayan, Ms. Prabha P, Mr. Sasikumar P, Ms. Sharathna S., Ms. Nitha P. R., Ms. Neethu S., Ms. Aswathy, Mrs. Meenu, Ms. Ummu Jumaila C.P., Mr. Cijil Raju, Ms. Saranya Jayaram, Ms. Irfana C. P., Mr. Jagadeesh K., Mrs. Fathimath Sulfeena C. T., Ms. Ashitha K.T., Ms. Renjitha, Ms. Maya Devi T.S., Mr. Valmiki Praveen Kumar, Mr. Mohan B., and Ms. Remya Raj P. for their friendship and help that made my journey here a memorable and delightful one.

I also wish to record my sincere thanks to Ms. Nisha N., Mr. Maniganda S., Ms. Jyothi B. Nair, Mrs. Ramya A. N., Ms. Varsha K., Mr. Sujai P. T., Ms. Saranya Giridharan, Ms. Arya, Mrs. Jamsheena, Ms. Veena, Mr. Jaggaiah G., Mr. Chandrasekhar C., Mr. Arun Kumar, Mr. Mahesha, Mrs. Jaice for their companionship and great support.

I would like to extend special thanks to Ms. Susanna Poulouse and Ms. Sirajunnisa P., for their assistance in conducting some of the experiments reported in this thesis. Thanks are also due to Mrs. Swetha J., Mrs. Akshara and Mrs. Resmi M. R the M.Sc. Project students, for their love and companionship.

I express my sincere thanks to Ms. Anjali K. Sajeev, Mrs. Raiha Mol T., Mrs. Vineetha James, Ms. Minju Thomas, Ms. D. V. M. Padmaja., Ms. Swetha S. Mrs. Remya P.R. and all other friends at Scholar's Hostel for their great companionship and support during the tenure of my research work.

I record my thanks to Dr. V. B. Manilal, Senior Principal Scientist, Mr. T.P. Poulouse, Sr.Technician and Mr. Dibin, Project Assistant PEET Division, CSIR- NIIST for their

suggestions and help to conduct my CSIR-800 project work. Mr. John, Secretary, The Balaramapuram Weavers' Industrial Co-operative Society is gratefully acknowledged for helping me to weave the banana-cotton blend fabric.

I would like to express my deep sense of gratitude to Shri Willi Paul, Senior Scientific Officer, Central Analytical Facility, SCTIMST, Poojappura for his immense help to carry out the physical characterization part of my project work and thanks are also due to Dr. Rekha M. R., Scientist D, Biosurface Technology Division, SCTIMST, BMT Wing, Poojappura for helping me to conduct the in vitro cell experiments that led to the successful completion of my CSIR-800 project.

I am grateful to UGC and CSIR New Delhi, for the financial assistance.

I would like to extend my sincere thanks to all my friends at CSIR-NIIST.

I take this opportunity to forfeit reverence to my teachers starting from my school days to those at NIIST, who motivated me and blessed me throughout my academic carrier.

I am profoundly obliged to my father, mother, brother and other family members for their support, encouragement, unconditional love and care throughout my thesis work. Without them the successful completion of this thesis would have been practically impossible.

Above all, I thank God Almighty for giving me the opportunity, strength, skills, and being with me for the successful completion of the research work.

Maya R. J.

CONTENTS

Declaration	i
Certificate	ii
Acknowledgements	iii
Contents	vi
List of figures	xii
List of tables	xiv
List of schemes	xv
Abbreviations	xvi
Preface	xviii

Chapter 1

Green Approaches Towards Catalysis and Sensing: An Overview 1-37

1.1	Introduction	1
1.2	Catalysis	2
1.3	Environmental Impact of Catalysis	4
1.4	General Considerations on Catalysis	4
1.5	Heterogeneous catalysis and Green Chemistry	5
1.6	Nano-catalysis	7
1.7	Fundamentals in Catalyst Preparation	8
	1.7.1. Preparation Techniques for Bulk Catalysts and Supports	8
	1.7.2. Basic Preparation Techniques for Supported Catalysts	10
1.8	Catalytic Applications of Supported Metal Nanoparticles	11
1.9	Supported Gold Nanoparticles as Catalysts	14
1.10	Chemosensors	17
1.11	Hybrid Sensors	20
	1.11.1. Mesoporous Silica-Based Hybrid Sensors	21
	1.11.2. Magnetic Core-Shell Particle Based Hybrid Sensors	23
	1.11.3. Magnetic Nanoparticle Based Hybrid Sensors	24

1.11.4.	Polymer Based Hybrid Sensors	24
1.11.5.	Surface-Grafted Composite Based Hybrid Sensors	25
1.11.6.	Host-Guest Interaction Based Hybrid Sensors	26
1.12	Clays	27
1.13	Objectives of the Present Investigation	30
1.14	References	31

Chapter 2

Design, Synthesis and Characterization of a Bentonite-Gold Nano hybrid as Green Heterogeneous Catalyst for the Selective Oxidation of Silanes **38-66**

2.1	Introduction	38
	2.1.1. Clay Minerals	38
	2.1.2. Bentonite as Support Material	40
	2.1.3. Silanes to Silanols Oxidation	42
2.2	Statement of the Problem	45
2.3	Results and Discussion	45
	2.3.1. Synthesis and Characterization of Bentonite-Gold Nano hybrid Heterogeneous Catalyst	45
	2.3.2. Activity of Bentonite-Gold Nano hybrid Heterogeneous Catalyst Towards Silane Oxidation	48
	2.3.3. Gram Scale Synthesis	52
	2.3.4. Recycling Experiment	54
2.4	Mechanistic Pathway	55
2.5	Conclusion	55
2.6	Experimental Section	56
	2.6.1. Materials and Methods	56
	2.6.2. Syntheses of Au nanoparticles Loaded Organofunctionalized Bentonite	56
	2.6.2.1. Synthesis of Acid Activated Bentonite (Ben-4h)	56
	2.6.2.2. Synthesis of Organofunctionalized Bentonite (Ben-MP)	56

2.6.2.3. Synthesis of Au Nanoparticles Embedded Organofunctionalized Bentonite (Au-MPBen)	57
2.6.3. General Procedure for the Catalytic Activity of Au-MPBen Towards the Oxidation of Silanes	57
2.6.4. Experimental Procedure for Mechanism Study	57
2.6.5. Calculation of Atom Economy	58
2.6.6. Calculation of TON and TOF	58
2.6.7. Recycling Experiment	59
2.6.8. Synthetic Procedure and Spectral Characterization of Silanols	59
2.7 References	63

Chapter 3

Application of Bentonite-Gold Nanohybrid Towards Green Heterogeneous Catalysis

PART A: Direct Reductive Amination of Aldehydes <i>via</i> Bentonite-Gold Nanohybrid Catalysis	67-95
3A.1 Introduction	67
3A.2 Statement of the Problem	70
3A.3 Results and Discussion	71
3A.3.1. Syntheses of Secondary Amines Using Au-MPBen catalyst	71
3A.3.2. Recycling Experiment	76
3A.3.3. Gram Scale Synthesis	77
3A.4 Mechanistic Pathway	78
3A.5 Conclusion	78
3A.6 Experimental Section	79
3A.6.1. Materials and Methods	79
3A.6.2. General Procedure for the Direct Reductive Amination of Aldehydes	79
3A.6.3. Recycling Experiment	79
3A.6.4. Gram Scale Preparation of N-benzylamine and TON and TOF Calculations	80

3A.6.5.	Synthetic Procedure and Spectral Characterization of Secondary Amines	81
3A.7	References	91
PART B: Bentonite-Gold Nanohybrid Catalyzed Oxidative Cross- Coupling of Ketones with Primary alcohols		96-120
3B.1	Introduction	96
	3B.1.1. Syntheses of α,β -Unsaturated Ketones via Claisen-Schmidt Condensation Reactions	96
	3B.1.2. Syntheses of α,β -Unsaturated Ketones via Carbon-Carbon Cross-coupling Reactions	99
3B.2	Statement of the Problem	100
3B.3	Results and Discussion	101
	3B.3.1. Syntheses of α,β -Unsaturated Ketones Using Au-MPBen Catalyst	101
	3B.3.2. Recycling Experiment	106
	3B.3.3. Gram Scale Synthesis	106
3B.4	Mechanistic Pathway	107
3B.5	Conclusion	108
3B.6	Experimental Section	108
	3B.6.1. Materials and Methods	108
	3B.6.2. General Procedure for the Oxidative C–C Coupling of Ketones and Primary Alcohols	108
	3B.6.3. Recycling Experiment	109
	3B.6.4. Gram-Scale Preparation of Chalcone (3a) and TON and TOF Calculations	109
	3B.6.5. Synthetic Procedure and Spectral Characterization of α,β - Unsaturated Ketones	110
3B.7	References	118

Chapter 4

Lower Rim Modified Calix[4]arene-Bentonite Hybrid System as a Green Reversible and Selective Colorimetric Sensor for Hg²⁺ Recognition 121-156

4.1	Introduction	121
	4.1.1. Calixarenes	122
	4.1.2. Lower Rim 1,3-Di-conjugates of Calix[4]arene as Hg ²⁺ Receptors	122
	4.1.2.1. Cyclic Conjugates	123
	4.1.2.2. Non-Cyclic Conjugates	124
	4.1.3. Organic-Inorganic Hybrid System	127
4.2	Statement of the Problem	128
4.3	Results and Discussion	129
	4.3.1. Synthesis of QHQC, 7	129
	4.3.2. Metal Ion Binding Studies	131
	4.3.3. Naked Eye Detection Studies	133
	4.3.4. ¹ H NMR Titration Studies	134
	4.3.5. Mass Spectroscopic (ESI-HRMS) Titrations Studies	137
	4.3.6. Computational Studies	138
	4.3.7. Mechanistic Pathway	139
	4.3.8. Synthesis and Characterization of QHQC _{CalBen}	140
	4.3.9. Metal Ion Binding Studies of QHQC _{CalBen}	145
4.4	Conclusion	146
4.5	Experimental Section	147
	4.5.1. Materials and Methods	147
	4.5.2. Synthesis of Di-(bromopropyl) <i>p</i> - <i>tert</i> -butylcalix[4]arene, Precursor 3	148
	4.5.3. Synthesis of 8-Hydroxyquinaldine Derivative of <i>p</i> - <i>tert</i> -butyl calix[4]arene, Precursor 5	148
	4.5.4. Synthesis of Quaternized Salt of 8-Hydroxyquinaldine Derived <i>p</i> - <i>tert</i> -butyl calix[4]arene, QHQC (7)	149
	4.5.5. Intercalation of QHQC Salt on Bentonite Clay	150

4.5.6. General Procedure for the Metal Ion Binding Studies	151
4.5.7. Calculation of LOD	151
4.6 References	151
Summary	157
List of Publications	159

LIST OF FIGURES

1.1	Principles of green chemistry	2
1.2	Schematic representation of relation between catalysis and sustainability	3
1.3	Energy profile diagram of catalyzed and uncatalyzed reaction	3
1.4	The impact of catalysis on the environmental E-factor	4
1.5	Reaction pathway for heterogeneous catalysis	6
1.6	Properties of nano-catalysis	7
1.7	Advantages of nano-catalysis	8
1.8	Proposed structures of MSIA before and after extraction with Cu^{2+}	22
1.9	Synthesis of hybrid silica hollow-sensor	22
2.1	Structure of montmorillonite clay	40
2.2	(a) XRD pattern of acid activated bentonite (Ben-4h) and organo functionalised bentonite (Ben-MP) and (2b) . IR spectra of acid activated bentonite (Ben-4h) and organofunctionalised bentonite (Ben-MP)	46
2.3	TEM images of fresh Au-MPBen (scale bar = 50 nm and 100 nm)	47
2.4	XPS spectrum of Au-MPBen	48
2.5	NMR spectra of dimethylphenylsilane and dimethylphenylsilanol	50
2.6	TEM images of Au-MPBen after 1 st and 5 th use (scale bar=50 nm)	54
3A.1	TEM image of Au-MPBen, (a) fresh and (b) after 5 th use	76
4.1	Structures of some cyclic conjugates of calix[4]arenes	123
4.2	Structures of some non-cyclic conjugates of calix[4]arene receptors	125
4.3	Structures of some non-cyclic conjugates of calix[4]arenes	126
4.4	Structures of L20 and L21	127
4.5	¹ H NMR spectrum of QHQC 7	130
4.6	¹³ C NMR spectrum of QHQC 7	131
4.7	Absorption spectra of QHQC with different metal ions in MeCN (Inset shows the magnified absorption peak at 567 nm)	132

4.8	Changes in the absorption spectra of QHQC (2.7×10^{-5} M) by the addition of Hg^{2+} ions (2.57×10^{-5} M)	133
4.9	Regression line for the determination of LOD	133
4.10	Photograph of naked eye detection of Hg^{2+} with QHQC and its reversibility with iodide solution	134
4.11	^1H NMR titration spectra of QHQC with Hg^{2+} in CD_3CN	135
4.12	Expansion of ^1H NMR titration spectrum of QHQC with Hg^{2+} in CD_3CN	135
4.13	Expansion of ^1H NMR titration spectrum of QHQC with Hg^{2+} in CD_3CN	136
4.14	Isotherm resulting from the titration of QHQC with Hg^{2+}	136
4.15	Modified Job's Plot using ^1H NMR titration data	137
4.16	Experimentally observed isotopic peak pattern of molecular ion peak of $[\text{QHQC} + \text{Hg}^{2+}]$	138
4.17	Optimized structures of (a) QHQC and (b) QHQC- Hg^{2+} complexes using DFT method	139
4.18	Photograph of (a) Na-Ben and (b) QHQC/CalBen	140
4.19	XRD patterns of Na-Ben and QHQC/CalBen	141
4.20	IR spectra of QHQC, Na-Ben and QHQC/CalBen	142
4.21	TG/DTA curves of (a) Na-Ben and (b) QHQC/CalBen	143
4.22	TGA curves of Na-Ben and QHQC/CalBen	143
4.23	Solid-state absorption spectra of QHQC and QHQC/CalBen	144
4.24	Solid-state emission spectra of QHQC and QHQC/CalBen at excitation wavelength (a) 367 nm and (b) 570nm	144
4.25	TEM images for (a) QHQC, (b) Na-Ben and (c) QHQC/CalBen	145
4.26	Photograph of naked eye detection of Hg^{2+} with QHQC/CalBen and its reversibility with iodide solution	146

LIST OF TABLES

2.1	Optimization of solvents in the oxidation of silanes	49
2.2	Comparison of various catalysts in the oxidation of silanes	51
2.3	Au-MPBen catalysed oxidation of various silanes	53
2.4	Recycling experiments of Au-MPBen catalyst	54
3A.1	Optimization of solvents for Au-MPBen catalyzed reductive amination	72
3A.2	Comparison of various catalysts in reductive amination reaction	72
3A.3	Substrate scope of reductive amination reaction	74
3A.4	Recycling experiments of Au-MPBen catalyst	77
3B.1	Optimization of solvents for the Au-MPBen-catalyzed C-C coupling of acetophenone with benzyl alcohol	102
3B.2	Comparison of various catalysts for the Au-MPBen-catalyzed C-C coupling of acetophenone with benzyl alcohol	102
3B.3	Substrate scope for the Au-MPBen-catalyzed C-C coupling of ketone with primary alcohol	104
3B.4.	Recycling experiments with the Au-MPBen catalyst	106

LIST OF SCHEMES

2.1	Synthetic methods for silanols	42
2.2	Gram scale oxidation of phenyldimethylsilane using Au-MPBen	52
2.3	Proposed mechanistic pathway for silane oxidation reaction using Au-MPBen	55
3A.1	Gram scale synthesis of N-benzylaniline using Au-MPBen	77
3A.2	Proposed mechanism for Au-MPBen catalysed reductive amination reaction	78
3B.1	Gram-scale synthesis of α,β -unsaturated ketone 3a using Au-MPBen catalyst	107
3B.2	Oxidative cross-coupling reaction of primary alcohols with ketones catalyzed by Au-MPBen	107
4.1	Synthetic pathway for the preparation of QHQC 7	130
4.2	Plausible mechanism of naked eye detection of Hg^{2+} with QHQC and its reversibility with iodide solution	140

ABBREVIATIONS

Å	: angströms	m	: multiplet
Ar	: argon	Me	: methyl
brs	: broad singlet	mg	: mg
^t Bu	: tertiary butyl	MHz	: megahertz
°C	: degree Celsius	mL	: millilitre
calcd	: calculated	mM	: millimolar
cm	: centimetre	mmole	: millimole
d	: doublet	MS	: mass spectroscopy
dd	: doublet of doublet	mV	: millivolt
DTA	: differential thermal analysis	nM	: nanomolar
equiv.	: equivalents	nm	: nanometre
eV	: electron volt	NMR	: nuclear magnetic resonance
FT	: Fourier transform	<i>O</i>	: ortho
g	: gram	<i>P</i>	: para
h	: hours	Ph	: phenyl
HRMS	: high resolution mass spectra	ppb	: parts per billion
HRTEM	: high resolution transmission electron microscopy	ppm	: parts per million
Hz	: hertz	Pt	: platinum
ICP	: inductively coupled plasma	ⁱ Pr	: isopropyl
ICT	: intramolecular charge transfer	q	: quartet
IR	: infrared	RT	: room temperature
<i>J</i>	: coupling constant	s	: singlet
K	: association constant	t	: triplet
L	: litre	THF	: tetrahydrofuran
M	: molar	TLC	: thin layer chromatography

TMS	: tetramethylsilane	XPS	: X-ray photoelectron spectroscopy
TG	: thermo gravimetry	μL	: microlitre
<i>tert</i>	: tertiary	μM	: micromolar
UV	: ultraviolet	μmol	: micromol
Vis	: visible		

PREFACE

Green chemistry is ‘the utilization of a set of principles that reduces or eliminates the use or generation of hazardous substances in the design, manufacture, and application of chemical products’. This thesis entitled “**Bentonite Based Organic-Inorganic Hybrid Materials: Application Towards Green Catalysis and as Mercury Sensor**”, describes our efforts towards development of a heterogeneous catalyst and a solid-state sensor for the selective detection of Hg^{2+} ions, using the environmentally benign bentonite as the support material.

The thesis is divided into four chapters. The first chapter of the thesis gives an overview of the various green approaches towards the two aspects dealt in this thesis- catalysis and sensing applications of hybrid materials.

The second chapter outlines the synthesis and characterization of an efficient, environmentally benign and reusable heterogeneous bentonite-gold nanohybrid catalyst (Au-MPBen) and its application towards the selective oxidation of silanes to silanols. This nanohybrid catalyst effectively oxidized various aromatic, aliphatic and sterically hindered silanes to silanols under ambient reaction conditions without the formation of disiloxanes as the by-product and is also applicable for the gram scale synthesis of silanols.

The efficacy of our bentonite-gold nanohybrid (Au-MPBen) catalyst towards green heterogeneous catalysis is discussed in Chapter 3 and this chapter is divided into two parts. Part A describes an efficient, green and reliable method for the direct reductive amination of aldehydes using Au-MPBen and the use of this heterogeneous catalyst in the presence of phenyldimethylsilane as a mild hydride donor affords a variety of secondary amines in excellent yields under ambient reaction conditions. The catalyst is recyclable, selective and is viable for the large scale synthesis of secondary amines. In Part B, we deal with the application of this catalyst for the oxidative cross-coupling reaction of ketones with primary alcohols to produce α,β -unsaturated ketones. The Au-MPBen catalyst effectively catalyzed this cascade reaction under mild conditions and water is produced as the only by-product.

The synthesis and characterization of a new lower rim functionalized 1,3-di(quateryary ammonium salt of 8-hydroxyquinaldine) derivative of *p*-tert-butylcalix[4]arene (QHQC) and its sensing properties toward Hg^{2+} ions using various physical techniques are discussed in the last chapter. The potential of this molecule to act as a reversible chemosensor for Hg^{2+} ions

selectively through naked eye detection prompted us to devise a solid state sensor with enhanced chemical and thermal stability, by intercalating it into the bentonite galleries. The characterization and Hg²⁺ sensing studies of this hybrid material are also detailed in this chapter.

It may be mentioned that each chapter of the thesis is presented as an independent unit and therefore the structural formulae, schemes and figures are numbered chapter wise.

A summary of the work is given towards the end of the thesis.

Green Approaches Towards Catalysis and Sensing: An Overview

1.1. Introduction

Green chemistry is “the utilization of a set of principles that reduces or eliminates the use or generation of hazardous substances in the design, manufacture, and application of chemical products.” The design of environmentally benign chemicals and processes are steered by the 12 principles of green chemistry as formulated by Anastas and Warner.^{1,2} The first principle depicts the fundamental idea of green chemistry that is protecting the environment from pollution. The remaining principles are focused on concepts such as atom economy, the design of energy-efficient processes, toxicity, application of raw materials from renewable sources and degradation of chemical products to simple, nontoxic substances that are safe and environmentally benign (Figure 1.1).³ Green chemistry is a versatile discipline that has been generated as a contribution of chemistry to sustainability and promotes environmental and economic affluence in order to support the environment.

Chemical developments fetch new environmental problems and dangerous unexpected side effects, which lead to the requirement for ‘greener’ chemical processes. Green chemistry supports the invention of more ecological chemical processes which lessens or even eliminates the generation of hazardous substances. Green chemistry is concerning the waste minimization at source, using non-toxic reagents, use of catalysts in place of stoichiometric reagents, improved atom efficiency, use of renewable resources and use of solvent-free or recyclable environmentally benign solvent systems.³⁻⁶ Currently, the ever-increasing concerns for a sustainable development and the realization of adverse consequences of chemical industry have created the situations for the adoption of greener technologies that protect the environment and human health in an economically advantageous approach.



Figure 1.1. Principles of green chemistry

Green chemistry is not a solution to all environmental problems but the most fundamental approach to prevent pollution and sustain the earth. This chapter comprises various green approaches towards two aspects, explicitly catalysis and sensing applications of hybrid materials. The strategic goal is the sustainable development of the chemical industry and green chemistry is one of the practical approaches towards sustainability. Catalysis plays as an important operational tool towards green chemistry which in turn to sustainability (Figure 1.2).⁷

1.2. Catalysis

Catalysis is defined as an acceleration in the rate of a chemical reaction due to the participation of an additional substance named catalyst, which will return to its original form without being consumed or destroyed at the end of the reaction and can continue to perform repeatedly. Catalyst affects only the rate of the reaction and changes neither the thermodynamics of the reaction nor the equilibrium composition. It lowers the activation energy for both forward and reverse reactions. The catalyst provides a path between reactant and product with a lower activation barrier contrast to the uncatalyzed process (Figure 1.3).

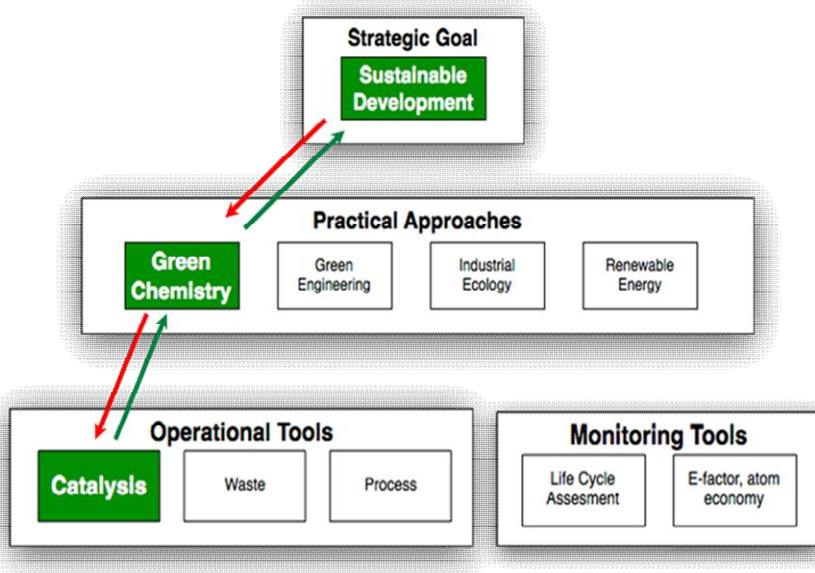


Figure 1.2. Schematic representation of relation between catalysis and sustainability

Catalysis is one of the basic pillars of green chemistry by offering atom-economical, selective, and energy-efficient solutions to several industrially important dilemmas. Catalysts have an enormous impact on the chemical industry because they facilitate reactions to occur and to formulate reaction processes more proficient. Catalysis plays a vital role in the production of a variety of chemicals and materials and more than 90 % of all chemicals are produced with the aid of catalysts.^{10,11}

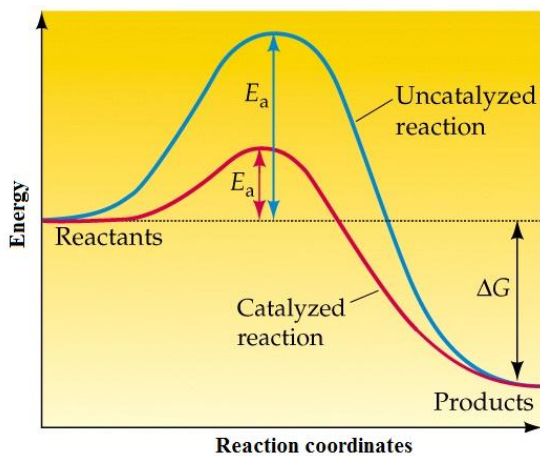


Figure 1.3. Energy profile diagram of catalyzed and uncatalyzed reaction

1.3. Environmental Impact of Catalysis

The environmental impact of catalysis is evidently demonstrated by the environmental factor (E-factor).¹² The E-factor is defined as the ratio of mass of waste produced to mass of desired product.

$$E = \frac{\text{kg of waste}}{\text{kg of desired product}}$$

The E-factor is found to be less than 0.1 in the oil refining industry where almost all chemical conversions are catalyzed. But in the pharmaceutical industry, the syntheses are clearly dominated by means of traditional, multistep and stoichiometric organic chemistry; the amount of waste generated can exceed the amount of the targeted active pharmaceutical product and the E - factor is higher than 25 (Figure 1.4).¹¹

Sector	Volumes (tons per annum)	E-Factor
Oil refining	10 ⁶ –10 ⁸	< 0.1
Bulk chemicals	10 ⁴ –10 ⁶	<1–5
Fine chemicals	10 ² –10 ⁴	5–50
Pharmaceuticals	10 ¹ –10 ³	25–100

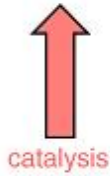


Figure 1.4. The impact of catalysis on the environmental E-factor

Another suitable measure for the ecological impact of chemical conversions is the atom economy. Calculation of the atom economy is based on molecular weights (MW) and is defined as the ratio of molecular weight of the desired product to the sum of molecular weights of all products formed in the stoichiometric equation.^{12,13}

$$\text{Atom Economy} = \frac{\text{MW of desired product}}{\text{Sum of MWs of all products formed in the stoichiometric equation}}$$

1.4. General Considerations on Catalysis

In general, catalysis is divided into two categories, homogeneous and heterogeneous. In homogeneous catalysis, the catalyst and the reactants are in the same physical phases, but in heterogeneous catalysis, both are in different phase. A large variety of homogeneous catalysts, for instance, Brønsted and Lewis acids, metals ions, metal complexes, organometallic complexes and biocatalysts (enzymes, artificial enzymes, *etc.*) are exploited

in the field of organic synthesis. In most cases, these catalysts show excellent catalytic activities and high selectivities as each single catalytic entity can act as a single active site. But, the main disadvantage of homogeneous catalysis is in difficulty to separate the products and catalyst from the reaction media. Even though, some energy intensive processes such as distillation of the reaction products or elimination of the precipitating counter-ion, *etc.* are used in order to re-utilize homogeneous catalysts, these operations may often lead to the deactivation of the catalyst. These facts emphasize the paramount significance of the preparation of heterogeneous catalysts *via* ‘heterogenize the homogeneous catalysts’ with the aim of merging the advantages of the homogenous catalyst with the capability of the heterogeneous systems to ensure reproducibility. Several methods were devised to anchor or encapsulate the homogenous catalysts; these catalysts often suffer from the drawback of leaching out of the catalyst during the catalytic run, leading to deactivation.^{14,15}

Modern society has an escalating demand for environmentally benign catalytic processes and catalysis research intended at the development of effective heterogeneous catalysts for environment-allied applications is of great interest in both academic and industrial field. Heterogeneous catalysts have a number of advantages compared to other catalytic systems including ease of separation from the reaction mixture, recyclability, minimal pollution and good thermal stability. These catalysts are easy to handle, avoid formation of inorganic salts, safe to store and has long life time.¹⁶

1.5. Heterogeneous Catalysis and Green Chemistry

Nowadays, heterogeneous catalysis constitutes the basis for numerous chemical technologies and its applications cover from the production of chemicals, energy harvesting, conversion and storage, to green technology.¹⁷ For more than one century, heterogeneous catalysts have played a key role in chemical industry and replace conventional ones to reduce the environmental pollutants. A chemical reaction with a heterogeneous catalyst occurs on the surface of a catalyst and measured catalytic performance such as activity, stability, and selectivity is the outcome of various structural and chemical factors that interrelate with each other. The mechanistic pathway for heterogeneous catalysis consists of four steps (Figure 1.5).¹⁸ First step is the adsorption of reactants on the active sites of the surface of the catalyst. It may utilize some of the bonding electrons in the molecules consequently weakening them

and creating an environment for an easier subsequent reaction steps. In the second and third steps, the molecules are arranged on the surface in the right orientation for favourable collision and the reaction occurs. In the final step, there is a rearrangement of electrons and the products are desorbed from the catalyst.

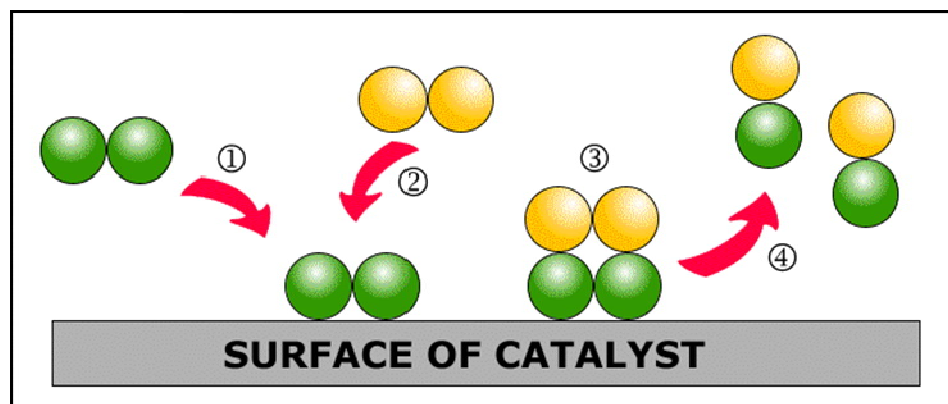


Figure 1.5. Reaction pathway for heterogeneous catalysis

The relevance of catalysis towards minimal pollution, renewable energy systems, and effectiveness formulates it as a fundamental area for green chemistry research. A green and sustainable catalyst should possess higher selectivity, higher activity, recyclability, efficient recovery from the reaction medium and cost-effectiveness.¹⁵ Green catalysis is not only targeted for the development of new catalysts with high stability and effective catalytic performances, but also considers the environmentally benign catalyst preparations. Heterogeneous catalysis is an omnipotent tool contributing to green and sustainable chemistry and acts as the key to achieve the E-factor and atom economy. The most important drawback of conventional heterogeneous catalysts is the reduced surface area compared to their homogeneous counterparts that is accessible to reactant molecules which limit their catalytic activities and lead to high consumption of expensive catalyst materials.¹⁹ One promising approach to solve this problem is to synthesize specifically engineered catalysts on nanoscale with high surface to volume ratio (S/V) by reducing the size of the catalytically active materials.^{20,21} Nanotechnology is a rapidly developing area and heterogeneous catalysts based on nano-scale materials have acquired more and more attention in synthetic organic chemistry.

1.6. Nano-catalysis

A nanomaterial is defined as a material in which one or more than one of its phase has the dimension in the nanometer (1–100 nm) size range. Some of the examples of nanomaterials include supported metal nanoparticles, nanometer sized porous materials, polycrystalline materials, *etc.* Nanomaterials are a fruitful area for green catalysis as they can be engineered suitably to possess different nano state and high surface area. The production of nanoparticles by employing green chemistry principles can lead to less hazardous chemical syntheses and an immense reduction in waste production.²² Nanostructured materials act as potential candidates for the inventive catalyst since the nano-sized particles enhance the exposed surface area of the dynamic part of the catalyst, thus dramatically increasing the contact between reactants and catalyst and mimicking the homogeneous catalysts. Conversely, their insolubility in solvents renders the easy separation of catalyst from the reaction mixture similar to heterogeneous catalysts, which in turn makes the isolation of product nonproblematic. Moreover, the activity and selectivity can be controlled by tailoring the physical and chemical properties of nano-catalyst such as size, shape, morphology and composition (Figure 1.6).²³ In view of a number of potential advantages (Figure 1.7),²⁴ nano-catalysts have been the matter of substantial attention in academic and industrial research.

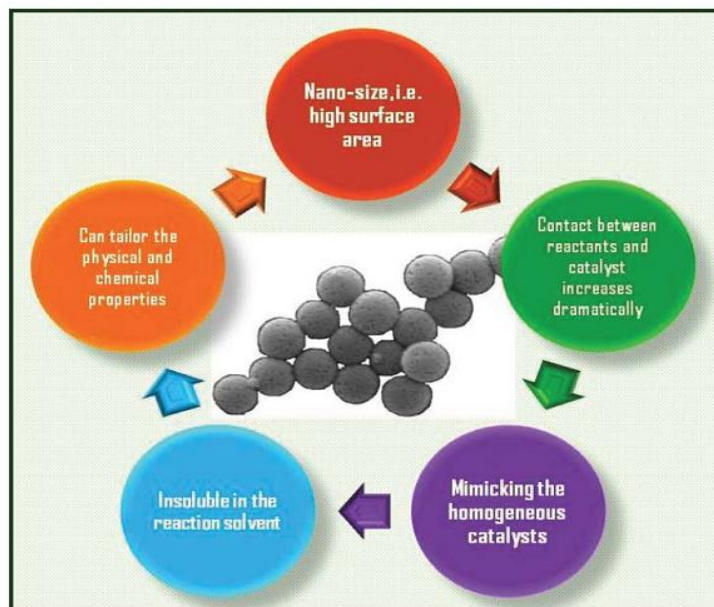


Figure 1.6. Properties of nano-catalysis

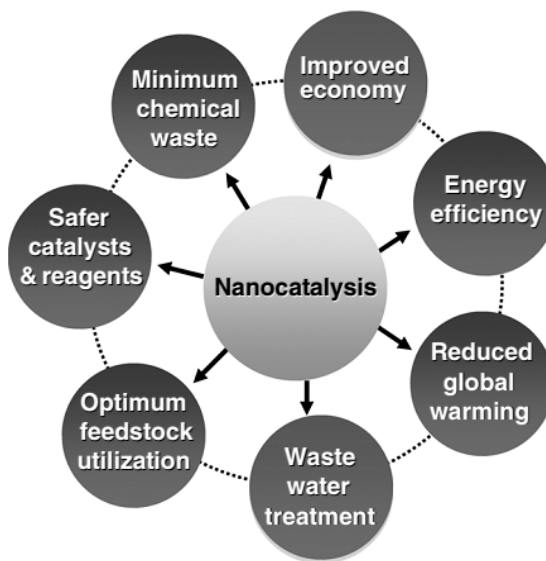


Figure 1.7. Advantages of nano-catalysis

1.7. Fundamentals in Catalyst Preparation

The design of a catalyst covers the entire aspects specifically from the selection of the active phase to the preparation method and attempt to optimize factors such as turnover number, stability, solubility, ease of separation from the reaction mixture, *etc.* Changes in the selection of metal or ligand can afford significant improvements in energy consumption, selectivity, and solvent utilization. The criteria for a good catalyst are homogeneity, uniform particle size distribution, activity, selectivity, suitable shape, mechanical stability, *etc.* Moreover, catalysts are often nano-structured and adapted pore structure. The heterogeneous catalyst may generally be a solid or an active phase is immobilized on a solid inert matrix. Generally, the catalysts are classified as bulk catalysts or supports and impregnated catalysts according to the preparation procedure. Depends upon the preparation methods, the catalytically active phase is created as a new solid phase or the active phase is fixed or introduced on a pre-existing solid through a process which inherently depends on the surface of the support.²⁵

1.7.1. Preparation Techniques for Bulk Catalysts and Supports

Precipitation and co-precipitation method, sol-gel method, solvothermal reaction, solid-state reaction and flame spray pyrolysis are the routes employed for the preparation of bulk catalysts and supports.

In the precipitation process, the desired constituent is precipitated from the solution and using this method bulk catalysts and support material are prepared. Co-precipitation is employed for the preparation of catalysts based on more than one component. In co-precipitation method, the solutions containing the salt of the metal and the salt of a compound that will be converted into the support are stirred with a base so as to precipitate as carbonate and/or hydroxides. After washing, these can be converted to oxides *via* heating.²⁶ Metal salt solutions and support precursors are mixed and then calcined. This method was widely used owing to its simplicity, reproducibility and cost-effectiveness. The co-precipitation method has some advantages such as production of nanoparticles in bulk quantities in a relatively short time, make use of inexpensive and easily available chemicals as precursors, easy control of composition and particle size, different possibilities to alter the particle surface state and homogeneity.

In sol-gel method, the porous materials are prepared by solidification from a solution phase (without precipitation). The reaction proceeds *via* two steps namely hydrolysis and condensation. The mixed oxide catalysts are synthesized by sol-gel methods. The versatility of this technique permits the control of the texture, homogeneity, composition, structural properties of solids, low calcination temperatures (reducing the undesired aggregation of the particles) and makes the feasible production of tailored materials.^{27,28} In solvothermal reaction, precursors are dissolved in hot solvents and if the solvent is water, the process is named as the hydrothermal method. Solvent other than water can afford milder reaction conditions.

The solid-state reaction method is the extensively used technique for the preparation of polycrystalline solids starting from a mixture of solid materials. Solids do not react simultaneously at room temperature at normal time gaps and it is essential to heat at higher temperatures (1000-1500 °C) to occur the reaction at an appropriate rate. The feasibility and rate of a solid-state reaction depend on reaction conditions, surface area of the solids, structural properties of the reactants, reactivity and the thermodynamic free energy.²⁹ Flame spray pyrolysis is a novel one step method for the preparation of nano-sized particles. In this process, a liquid feed metal precursor is dissolved in an organic solvent and is sprayed as micrometer sized droplets into a flame zone with an oxidizing gas. The spray is combusted

and the precursor is transferred to nanosized metal oxide or metal particles, depending on the operating conditions and the metal.³⁰

1.7.2. Basic Preparation Techniques for Supported Catalysts

Several industrial catalysts contain metals and the interaction between the support phase and the active phase can influence the catalytic activity. Impregnation method, deposition-precipitation method, inert gas condensation method and inert structured media are the techniques used for the preparation of supported catalysts.

Impregnation method is simple, economic and capable to furnish a reproducible metal loading. In this procedure, the support makes contact with certain amount of solution of the metal precursor, usually a salt and is aged for a short time, dried and calcined. There are two types of impregnation method namely incipient wetness or wet impregnation which depend on the amount of solution used for this process. In the wet impregnation method, an excess amount of solution compared to the pore volume of the support is used.²⁶ But in incipient wetness impregnation method, the volume of the solution utilized is equal or slightly less than the pore volume of the support. The loading is restricted by the solubility of the precursor in the solution.²⁵ Replacement of an ion which is in an electrostatic interaction with the surface of the support by another ion species is carried out *via* ion exchange process.

Deposition– Precipitation method includes two steps specifically precipitation from bulk solutions or from pore fluids and interaction with the support surface. The metal precursor is dissolved and the pH is adjusted to achieve a complete precipitation of the metal hydroxide. Then it is deposited on the surface of the support, calcined and reduced to the elemental metal.²⁵ The major problem is to permit the precipitation of the metal hydroxide particles inside the pores of the support, consequently, the nucleation and growth on the support surface occur which will lead to the uniform distribution of small particles on the support.²⁶

In the inert gas condensation technique, nanoparticles are produced by the evaporation of a metallic source in the presence of an inert gas, and this method is used to generate fine nanoparticles. Physical Vapour Deposition (PVD)-(no catalytic interaction) and Chemical Vapour Deposition (CVD)-(with catalytic interaction) methods are the two processes used in this technique. In chemical vapour deposition process, a solid is deposited on a heated surface from the vapour or gas phase through a chemical reaction. In thermal CVD, the

reaction is stimulated by a temperature higher than 900 °C. A typical device comprises a gas supply system, an exhaust system and a deposition chamber.^{31,32}

In inert structured media method, the particles are prepared in the structured medium by imposing constraints in the form of matrices such as zeolites, layered solids, molecular sieves, micelles or microemulsions, gels, polymers and glasses. By imposing the structure in the form of matrices, the growth kinetics can be slowed down and the size can be limited with well-defined structures.³³

The obtained heterogeneous catalysts are characterized by structural analysis, thermal analysis, spectroscopic techniques and microscopic techniques.

1.8. Catalytic Applications of Supported Metal Nanoparticles

Modern nanotechnology methods clearly propose an enormous potential for future developments of supported nanoparticles based heterogeneous catalysts.³⁴ The unsupported metal nanoparticles may undergo aggregation and poisoning under the reaction conditions which lead to the deactivation with loss of catalytic activity. In order to inhibit the aggregation and generating highly active well dispersed homogeneously sized metal nanoparticles, supports are used and the resultant materials are termed as supported metal nanoparticles. The properties of supported metal nanoparticles are associated with the specific particle morphology (shape and size), concentration, metal dispersion and the electronic properties of the metal inside the host environment.^{32,35} With the advantages of heterogeneous supports, supported metal nanoparticles are considered as ‘green’ catalysts and possess higher selectivity, yield, conversion, and catalyst recovery.

Porous and non-porous materials are used as supports for the preparation of supported metal nanoparticles. A porous material is normally a solid that consists of an organized network of pores. Various natural substances such as clays, rocks, biological tissues and synthetic materials including metal oxides, ceramics, carbonaceous materials, membranes, *etc.* can be regarded as porous materials. Nonporous materials do not have any voids or pores in their structure and these comprise metals, glass, foils, hard plastic and various polymers including polypropylene, polyethylene, *etc.* In spite of the utilization of these common supports, other biomaterials and biomass have been used for the preparation of supported metal nanoparticles. He and Zhao reported the preparation of supported metal nanoparticles

using various biopolymers as supports including chitosan, cellulose and poly(allylamine) gels.³⁶

A broad range of supported noble metal nanoparticles (Ag, Au, Pt and Pd) and supported transition-metal nanoparticles (Fe, Ni and Cu) have been reported. The supported metal nanoparticles based on transition metals have been widely used in industrial processes such as reforming, hydrogenations and Fischer-Tropsch synthesis. Metallic Au nanoparticles well dispersed on different supports with sizes ranging from 1 to 10 nm have been extensively employed in the oxidation of CO. Various supported metallic Au nanoparticles have been synthesized and exploited in a wide range of catalytic applications in oxidation, epoxidation, hydrogenation, C-C coupling reactions, *etc.*³⁶

Supported metallic Pd nanoparticles have been widely employed in C-C bond forming reactions such as Suzuki, Sonogashira, Heck and related C-C couplings. For eg. Metallic Pd nanoparticles supported on carbonaceous materials, alumina-and silica-based oxides, siliceous mesocellular foams (MCF), commercial magnetic nanoparticles, natural porous materials, mesoporous biopolymers and other polymers such as polyaniline nanofibers, polysilane, *etc.* have been accounted as highly active and reusable catalysts for the coupling of a variety of aryl chlorides and bromides with aryl boronic acids. Budarin *et al.* synthesized biopolymers based highly active, dispersed and reusable metallic Pd nanoparticles that afforded quantitative conversion of starting material to the cross-coupled product within a few minutes. Gallon *et al.* prepared polyaniline nanofibers based supported metallic Pd nanoparticles as semi-heterogeneous catalysts which is used for C-C couplings in water. Sonogashira reaction, Heck reaction, oxidations, hydrogenations, hydrodechlorinations, C-H activation, *etc.* were catalyzed by various supported Pd nanoparticles as heterogeneous catalysts.^{36,37}

Most of the supported Pt nanoparticles have been utilized in hydrogenations or in electrocatalytic oxidations for fuel cell applications, selective oxidation of CO, alkenes, alcohols, vitamin precursors such as l-sorbose to 2-keto- l-gulonic acid, and the dehydrogenation of methylcyclohexane. Metallic platinum nanoparticles supported on acidic Al-MCM-48 were reported by Campelo *et al.* for the hydroisomerization of n-alkanes. In addition, metallic Pt nanoparticles impregnated magnetic nanoparticles were used as heterogeneous catalyst for the hydrogenation of alkynes and α,β -unsaturated aldehydes.

Moreover, layered double hydroxide supported nanoplatinum catalysts were reported as good catalysts for the allylation of aldehydes.^{36,38}

Silver and silver-based compounds show antimicrobial properties. Consequently, applications of metallic Ag nanoparticles have been related to medical/biological areas and also find applications in catalytic fields. Supported metallic Ag nanoparticles found application in industry for the synthesis of epoxides and aldehydes by means of the selective oxidation of alkanes and alkenes and have employed in the hydrogenation of dyes including rose bengal, methylene blue, eosin and rhodamine 6G. Metallic Ag nanoparticles supported on alumina and calcium carbonate are selective and highly active in the epoxidation of ethylene. In recent times, Chimentao *et al.* synthesized supported Ag metal nanoparticles on alumina and MgO for the gas-phase oxidation of styrene and Mitsodume *et al.* reported supported Ag nanoparticles on hydrotalcites for the oxidant-free dehydrogenation of alcohols.^{36,39}

Supported metallic Rh nanoparticles were used as heterogeneous catalyst for the reduction of 1-alkenes, arenes, ketones, various α,β -unsaturated compounds and CO. Savastenko *et al.* reported the reduction of lean NO_x by means of supported metallic Rh nanoparticles on SiO₂. Bao and co-workers synthesized catalytically active Rh metal nanoparticles impregnated carbon nanotubes for the transformation of CO and H₂ into ethanol and alumina-supported metallic Rh nanoparticles were used for the ring opening of cyclohexane producing n-hexane with n-pentane and benzene as major products. Rh/TiO₂ materials with 0.004 % Rh loadings also found application in the partial oxidation of propylene with 13 % yield.^{36,40}

Supported metallic Ru nanoparticles are regarded as active heterogeneous catalyst in diverse catalytic processes. Silica or alumina-supported ruthenium reduces nitrogen oxide to nitrogen and the hydrogenation of aromatic compounds such as methyl benzoate, tetralin, 2-methoxycarbonylphenyl-1,3-dioxane and CO were carried out using Ru/HY and Ru/Al₂O₃ catalysts. Moreover Miyazaki *et al.* prepared supported metallic Ru nanoparticles on γ -Al₂O₃ for ammonia synthesis. Li *et al.* synthesized Ru nanoparticles on SBA-15 successfully and used for the partial oxidation of methane with oxygen to provide a mixture of CO and H₂. In addition, Pan *et al.* reported the Ru multiwalled carbon nanotubes for preparing sorbitol by the hydrogenation of glucose. Furthermore, Ru/ γ -Al₂O₃ materials and Ru nanoparticles

supported on hydroxyapatite were investigated in the Fischer-Tropsch synthesis and cis-dihydroxylation and oxidative cleavage of alkenes respectively.^{36,41}

In iron oxide nanoparticles preparation, the absolute reduction of $\text{Fe}^{2+}/\text{Fe}^{3+}$ to metallic iron is extremely challenging as compared to transition/noble metals due to its high electropositive standard reduction potential. Consequently, only a small number of reports can be found for the catalytic activity of supported metallic Fe nanoparticles. Various supported metallic Fe nanoparticles were synthesized using a range of supports including silica, MCM-41, starch and cellulose. Fe/MCM-41 materials were used in the oxidation of a wide range of alcohols using hydrogen peroxide as green oxidant under microwave irradiation.^{36,42}

Ni metal nanoparticles supported on carbon and silica have been extensively investigated for the hydrogenation of aromatic compounds in gas phase and Ni and Ni-Cu metal nanoparticles supported on inorganic materials such as sepiolite and AlPO_4 were also explored in the liquid-phase hydrogenation of propargyl alcohols and fatty acid ethyl esters. Ni/ ZrO_2 and Ni/ Al_2O_3 materials were reported for the steam reforming of methane and supported nanosized nickel on carbon nanotubes catalyzed the thermal decomposition of ammonium perchlorate, which is the common oxidizer used in composite solid propellants. Kim *et al.* synthesized Ni on multiwalled carbon nanotubes that can efficiently catalyze the gas-phase dissociation of hydrogen molecules to afford atomic hydrogen.^{36,43}

Cu metal nanoparticles on metal oxides were reported for the selective dehydrogenation of methanol and Cu- Al_2O_3 materials were investigated as an active and selective heterogeneous catalyst for the aziridination and cyclopropanation of a variety of alkenes such as styrene, cyclohexene and related aromatics. Similarly, the same metal nanoparticles were utilized in the synthesis of 1,2,3-triazoles, providing the products in moderate to high yields. Lately supported Cu metal nanoparticles were found to be active in the water gas shift reaction.^{36,44}

1.9. Supported Gold Nanoparticles as Catalysts

Bulk gold metal is regarded as inactive; conversely, gold nanoparticles or nanoporous gold possesses a high surface to volume ratio which leads to high chemical reactivity. To date, the majority of work has been focused on gold nanoparticles based heterogeneous

catalysis, due to their easy preparation methods along with remarkable synergistic effect of support on various reactions. Moreover, size or distribution of gold nanoparticles on the support can be controlled by the preparation method, and these heterogeneous catalysts often exhibit high regio and chemo-selectivity compared to other transition metals. Catalysis using supported gold nanoparticles is an area of great deal for organic chemists and researchers owing to its green and sustainable chemistry exhibited in organic transformations and the catalytic activity is directly correlated to the particle size in the nanometer scale. A variety of reactions such as oxidation of alcohols and aldehydes, hydrochlorination of ethyne, epoxidation of propylene, carbon-carbon bond formation, *etc.* are catalyzed by supported gold nanoparticles as heterogeneous catalysts. Gold nanoparticles supported on different materials such as Al_2O_3 , ZrO_2 , SiO_2 , TiO_2 , SBA-15, CeO_2 , C, *etc.* were used as heterogeneous catalysts for investigating its catalytic activity towards various reactions.⁴⁵⁻⁴⁹

Catalytic hydrogenation, one of the most important industrial reactions, was extensively studied using supported gold nanoparticles and found that supported gold nanoparticles act as a promising catalyst towards selective hydrogenation reactions. Selective hydrogenation of 1,3-butadiene, α,β -unsaturated aldehydes, *etc.* are some of the important reactions performed by supported gold nanoparticles. In industry, the catalytic hydrogenation of nitroarene is considered as an important technology and development of an effective catalyst for this hydrogenation is extremely desirable. Supported gold nanoparticles effectively carried out these conversions. In addition, the γ -butyrolactone and pyrrolidone synthesis by succinic anhydride hydrogenation or amination-hydrogenation using Au/ TiO_2 catalyst was reported. Recently, the nano-gold-catalyzed deoxygenation of epoxide, in presence of alcohols as the reducing agent with Au/hydrotalcite (HA) catalyst and Au/ TiO_2 catalyzed hydrogenative reduction of aldehydes with isopropanol as the reducing agent were reported.

Selective oxidation reactions which convert bulk chemicals to valuable products of a higher oxidation state using green oxidation systems is a fundamental goal in catalysis and nano-gold catalysts offer an excellent choice to construct green oxidation methods. Selective oxidation of benzylic and allylic C-H bonds, cyclohexane, *etc.* were carried out with the help of Au/C or Bi, Au/C, Au/ SiO_2 , Au/ CeO_2 , Au/ TiO_2 , Au/ZSM, Au/MCM-4, Au/SBA-15, Au/ Al_2O_3 , Au/TS-1 and Au-Pd/ TiO_2 as heterogeneous catalysts. Moreover, selective epoxidation of olefin especially, propylene epoxidation, with oxygen, air, or H_2/O_2 using

supported nano-gold catalysts is the major achievement in gold catalysis. Also, aldehydes and ketones are produced *via* selective oxidation of alcohols using supported gold nanoparticles. Polyols such as ethylene glycol and 1,4-diols were selectively oxidized by carbon- or alumina-supported nano-gold catalyst and Au/HT, Au/Fe₃O₄ respectively.

Nano-gold catalysts such as Au/CeO₂, Au/C, Au/ZnO and Au/TiO₂ possess very good catalytic activity towards aerobic oxidation of aldehydes. Furthermore, selective oxidation of amines explicitly imine synthesis and N-formylation of amines were successfully performed by Au/C, Au/TiO₂, Au/HAP, *etc.* Silanes oxidation and hydrosilylation reactions are other two important reactions which were efficiently achieved by supported gold nanoparticles (Au/TiO₂, Au/HAP and Au/Al₂O₃) using H₂O or molecular oxygen as oxidant. In addition, oxidation of biomass such as glucose, glycerol, cellobiose and arabinose were made by various supported gold nanoparticles as heterogeneous catalysts.

Green synthesis of vinyl chloride using a mercury-free catalytic system is an important goal in catalysis and chemical industry. This was realized by hydrochlorination of alkynes using Au-M/C (where M = Pd and Pt) bimetallic catalyst. Another important reaction is the C-C bond formation reactions, the versatile tool in synthetic organic chemistry, and nano-gold displayed specific activity in some of these types of reactions. Supported gold nanoparticles specifically Au/CeO₂ catalyzed coupling reaction such as Suzuki Miyaura and Sonogashira as well as nano-gold supported on aluminum oxyhydroxide (Au/AlO(OH)) for aerobic oxidation of alcohol and sequential C-C bond formation with ketone were also reported. Besides, benzylation of aromatics by benzyl alcohol was catalyzed by Au/SiO₂ and substituted phenols synthesized using Au/TiO₂.

Another important reaction is the C-N bond formation reaction which includes amination reactions and nucleophilic addition reactions and a variety of supported gold nanoparticles were effectively used for catalyzing these reactions. In addition, carbonylation reactions such as carbamates synthesis, carbonates synthesis and hydroformylation reaction were catalyzed by Au/polymer, Au/CeO₂, Au/SiO₂, Au/C or Co₃O₄ *etc.* Three-component coupling reactions, cyclization reactions and epoxide isomerization to allylic alcohol are some of other reactions which were accomplished by supported gold nanoparticles catalysts. Nano-gold catalysis remains as a hot research area in catalysis owing to its application toward industrially

important chemical reactions and plays a significant role in the development of green chemistry and sustainable chemical industry.

The second aspect of this chapter illustrates the green approaches towards sensing application of hybrid materials.

1.10. Chemosensors

Chemosensors are miniaturized devices that can deliver real time and online information on the presence of specific compounds or ions in even complex samples⁵⁰ and play a vital role in the analytical chemistry, environmental chemistry and bio-medicinal science.⁵¹ Chemosensors afford a precise and inexpensive identification of toxic heavy metal ions, anions and enzymes with high sensitivity and selectivity.⁵² Chemosensors utilize specific transduction techniques to report analyte information and the most extensively used techniques are optical absorption, redox potential luminescence, spectroscopic parameters, optical parameters, such as reflectivity, refractive index, *etc.*⁵³ An optical change can be evident as either an alteration to the colorimetric determination *via* UV/Vis spectroscopy, the absorbance profile of the probe, or an enhancement or quenching of the emission profile of the probe, enabling measurement of intensity and emission wavelength by fluorescence spectroscopy. In addition, an electrochemical change ensuing from a change in redox potential or current may be measured by voltammetry.

Sensors may be divided into two categories, namely electronic sensors and optical sensors⁵⁴ which depend on the type of signals produced as a result of the binding event. Electronic sensors produce changes in the electrochemical properties whereas optical sensors bring changes in the optical properties. Electronic sensors are mainly classified into five categories and they are ion-selective electrodes (ISEs), field-effect transistors (FETs), electroactive sensors, biosensors and microelectrodes. The optical sensors can be divided into two categories namely chromogenic chemosensors and fluorogenic chemosensors. In chromogenic chemosensors, the host binds the guest and signaling unit exhibits changes in colour but in fluorogenic chemosensors, the interaction between the host and the guest moiety displays the change in fluorescence properties of the signaling unit. The development of colorimetric sensors is significant as the naked eye detection can provide qualitative and quantitative information devoid of any spectroscopic instrumentation. The fluorescence

measurement is versatile, very sensitive, and gives the sub-micro molar level estimation of guest species. A wide array of optical chemosensors have been reported and based on the nature of analyte the chemosensors are broadly classified as cations sensors, anion sensors and neutral sensors.

A variety of fluorescent probes have been developed for the detection of diverse analytes *via* different types of emission mechanisms. If a fluorophore is used as the transducer component of a chemosensor, fluorescence spectroscopy is utilized for the sensing studies. Various photophysical mechanisms^{55,56} are used for the fluorescence sensing of analytes which include photoinduced electron transfer (PET), Förster resonance energy transfer (FRET), charge transfer (CT), excimer formation and aggregation induced emission (AIE) or aggregation caused quenching (ACQ).⁵⁷

PET-based chemosensors comprise of a receptor-spacer-fluorophore system or intensity-based probes which upon excitation, PET occurs from the receptor HOMO to the HOMO of the excited fluorophore. The formerly excited electron is not capable to come back to its original ground state, back-donated to the receptor and fluorescence is quenched ('off' state). When a cation binds, electrons are donated from the receptor to the cation and the redox potential of the receptor is increased. This lowers the energy of the HOMO of the receptor to less than that of the HOMO of the fluorophore. Consequently, the PET process becomes inactive and the excited electron in the LUMO of the fluorophore returns to its original ground state with fluorescence emission ('on' state).⁵⁸

Many chemosensors utilize internal (or intramolecular) charge transfer (ICT) mechanism, for which sensor molecules have both electron-rich and electron-deficient moieties within a conjugated π system that incorporates both the receptor and the fluorophore. Upon excitation, delocalization of electron density (CT) from the electron donating group to the electron accepting group occurs and a dipole moment is produced within the molecule. When an analyte binds, this dipole moment may be enhanced or reduced which depends on the nature of the analyte and the sensor molecule. The reduced dipole moment will effect in decreased molar absorptivity and absorbance and fluorescence emission will be blue-shifted. Conversely, an increased dipole moment will result in an enhancement in molar absorptivity and absorbance and fluorescence will be red-shifted. Other charge transfer methods include twisted internal charge transfer (TICT) and metal-

ligand charge transfer (MLCT). In addition, charge transfer pathways are greatly dependent on polarity of the solvent.⁵⁹

Excimers are dimers of fluorophores and are formed by the interaction of the excited state fluorophore with the same fluorophore in its ground state. Exciplexes work on a similar principle, but fluorophore in the excited state and the fluorophore in the ground state are different. The emission spectrum is red-shifted for an excimer/exciple compared to the monomer, and a dual emission from the excimer/exciple and the monomer is often observed simultaneously. Moreover, stacking or deformation of fluorophore excimers upon analyte binding may be perturbed which facilitate the exploitation of such systems as ratiometric probes by monitoring the excimer/exciple band.⁶⁰

Förster resonance energy transfer (FRET) is a non-radiative energy transfer from an excited energy donor fluorophore to an energy acceptor *via* long-range dipole-dipole interactions. When FRET operates, emission from the original excited fluorophore is not detected but from the acceptor is excited. If an appropriate fluorophore is selected, the emission wavelength is far red-shifted compared to the original excitation wavelength of the donor. The efficacy of a FRET process is established by the spectral overlap between the emission and the absorption profile of the donor and the acceptor respectively, the orientation of the dipole moments of acceptor and donor and the distance between the donor and acceptor units. Thus ratiometric probes can be achieved by the disruption of a FRET process upon analyte binding.⁶¹

Fluorophore aggregation is commonly escorted by a decrease in fluorescence intensity (aggregation-caused quenching, ACQ), owing to the formation of species with inferior fluorescence properties. The complementary phenomenon aggregation-induced emission (AIE) works with molecules that consist of 'rotors' such as phenyl groups, enabling non-radiative decay paths for electrons of excited AIE fluorophores. When such molecules aggregate, the restriction of motion (RIM) or rotation (RIR) inhibits non-radiative pathways because of steric interactions, which enables the radiative decay and fluorescence enhancement is observed.⁶²

UV/Vis absorption spectroscopy can be utilized to detect and quantify the hazardous metals ions, hydrocarbons and volatile organic compounds based on the Beer-Lambert law and the absorbing wavelengths are characteristic of each molecule and are termed as the

absorption spectrum. The UV/Vis spectrum results from the transition of electrons and the absorption spectrum consist of peaks (bands) of different wavelengths, each corresponding to a fraction of light absorbed. Certain absorption bands are considerably more pronounced and consequently more suitable for measurement. The quantity of light absorbed at a particular wavelength is proportional to the concentration and strength of the molecule at that wavelength and length of the optical path through the sample.⁶³

1.11. Hybrid Sensors

Development of sensors that consent to the sensitive, selective, and rapid recognition of metal ions and anions constitutes a significant research area in the biological, environmental, and industrial fields. In the past few decades, a variety of colorimetric and fluorescent probes for the detection of metal ions or anions were reported based on small molecule sensors.⁶⁴ However, a number of inevitable and important issues such as poor solubility in aqueous solution, low detection sensitivity, easy photobleaching, and difficulties in terms of the separation and removal of the sensors and metal ions or anions from the environmental and biological samples limit their practical applications. Consequently, developing hybrid sensing materials intended for the selective detection and efficient removal of analytes is also an active and promising research area.

A hybrid material consists of minimum two components, typically an organic and an inorganic component that are molecularly dispersed in the material. A number of hybrid materials were investigated in the field of ion recognition. The receptor-grafted inorganic supports have several significant benefits as heterogeneous hybrid sensing probes in the solid–liquid phase. The grafted receptors on the inorganic matrices can release the guest species from the contaminated aqueous solution. Subsequently, the hybrid sensing materials can be recovered and reused by suitable chemical treatments. These hybrid materials exhibit high sensitivity, selectivity, and rational absorption and fluorescence changes as a result of their superior structural properties.^{65,66} Some inorganic materials, such as mesoporous silica, Fe₃O₄ particles, polymer materials, core-shell silica materials, *etc.* can be employed as inorganic supports in hybrid sensors as these materials can possess some good structural properties.⁶⁷ According to the inorganic materials used in the hybrid material, hybrid sensors are categorized into mesoporous silica-based hybrid sensors, magnetic nanoparticle based

hybrid sensors, magnetic core-shell particle based hybrid sensors, surface-grafted composite based hybrid sensors, polymer based hybrid sensors and host-guest interaction based hybrid sensors.⁶⁸

1.11.1. Mesoporous Silica-Based Hybrid Sensors

Bhaumik and Banerjee *et al.* reported a 3-aminopropyltriethoxysilane-functionalized, 2D-hexagonal mesoporous silica MCM-41 material grafted with 4-methyl-2,6-diformyl phenol (DFP) as a hybrid sensing material^{69a} for the selective detection of Zn^{2+} with a detection limit was $6.54 \mu\text{g L}^{-1}$. Additionally, this material was successfully exploited to selectively image intracellular Zn^{2+} ions. Han *et al.* reported a Cu^{2+} sensing material RSPMOs^{69b} which showed high selectivity and sensitivity towards Cu^{2+} in ethanol-HEPES (9:1, v/v) aqueous solution with the detection limit of 6.5 ppb. A fluorescence sensor, P(OEGMA-co-RhBHA) coated MSN(CQA) was constructed by the immobilization of quinoline-based Zn^{2+} probes and RhB-based Hg^{2+} into the outer and inner surface of mesoporous silica nanoprobe (MSN) respectively and this dual optical detection channels can offer an excellent barrier for FRET between the two sensors as they showed concurrent detection for Zn^{2+} and Hg^{2+} ions.^{69c} In 2011, Li *et al.* reported a novel mesoporous silica nanoprobe decorated with a rhodamine derivative containing the thiourea group, MSN-RBH^{69d} as a chemodosimeter-functionalized nanosensor for detecting Cu^{2+} which offered a selective detection of Cu^{2+} over Hg^{2+} with an obvious solution color change (from colorless to purple), even in the presence of other metal ions in aqueous solution. The detection limit of this hybrid sensor was estimated to be $2 \mu\text{M}$ and it can be used to bio-image intracellular Cu^{2+} due to its water solubility, membrane permeability and nontoxic nature.

Tao *et al.* developed multifunctional sensing material $\text{QC}_{12}\text{Et}_3\text{Br/silica}$ material^{69e} having a strong blue-green fluorescence and its fluorescence intensity can be quenched with the binding of PPi (pyrophosphate) and PP (phosphate) anions. The detection limit of this sensor to PPi was 1.78 ppm and this synthetic strategy can provide a very important development in the large-scale fabrication of high-quality sensing materials. Moreover, an organic-inorganic silica material, SBA-P2^{69f} exhibited a high affinity for Cu^{2+} with fluorescence quenching *via* photoinduced energy transfer (PET) mechanism in water solution with a detection limit of 0.65 ppb. Kim *et al.* prepared a mesoporous silica-based

anthraquinone chemodosimeter, MSIA (Figure 1.8)⁷⁰ which exhibited high selectivity towards Cu^{2+} over other metal ions with significant color change (red to yellow) and blue-shifted absorption band in a 1: 1 stoichiometry. Furthermore, Jun and Kim *et al.* reported pellet-type nanocomposites, MSIND-Cu^{69g} and is used to selectively detect PPI in 100 % aqueous solution with a low detection limit (10 ppb) as well as excellent reusability and reproducibility.

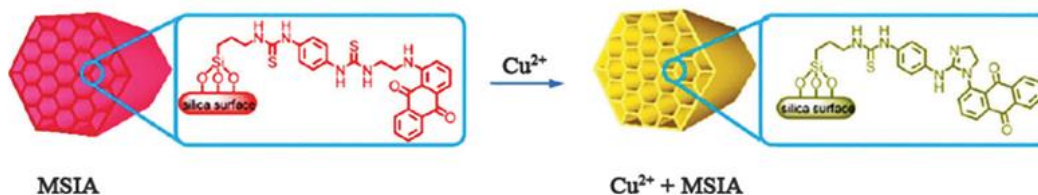


Figure 1.8. Proposed structures of MSIA before and after extraction with Cu^{2+}

In 2011, Tian *et al.* synthesized a fluorescence sensing material, MCM-2T^{69h} which exhibited a ratiometric fluorescence change towards Hg^{2+} ions with excellent sensitivity and selectivity in $\text{CH}_3\text{CN}/\text{H}_2\text{O}$ solution (1: 1, v/v) with a detection limit of 8.0×10^{-6} M. Also, this hybrid sensor showed good optical properties and removes the Hg^{2+} from aqueous solution with adsorption capacity of 234.88 mg g^{-1} . Rurack *et al.* reported a 3D hybrid material U1⁶⁹ⁱ for the colorimetric detection and removal of Hg^{2+} with a significant fluorescence response in aqueous solution with a detection limit of 0.1 ppm.

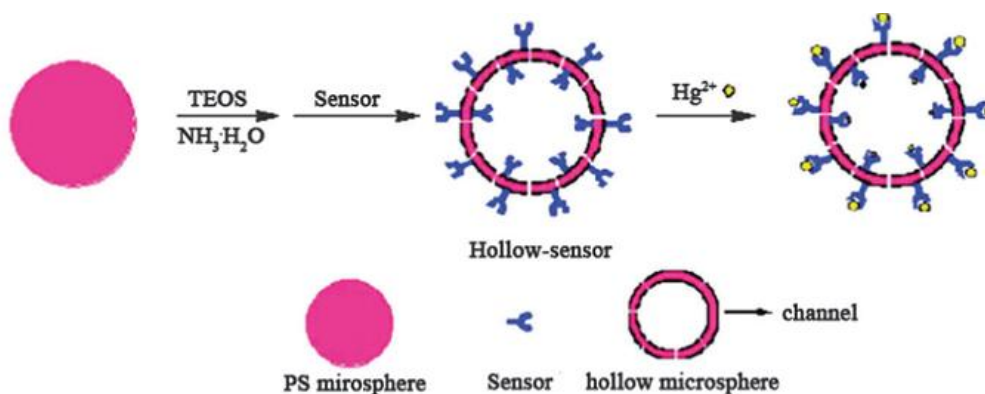


Figure 1.9. Synthesis of hybrid silica hollow-sensor

In 2015, Yan *et al.* synthesized a multifunctional organic-inorganic hybrid sensing material, RB-KCC-1^{69j} for the sensitive, selective and “naked-eye” detection of Hg^{2+} ion in

aqueous solution with the detection limit of 9.05×10^{-7} M and was effectively exploited to monitor the Hg^{2+} ions during the growth of living SMMC-7221 cells. Li and Zhang *et al.* reported a highly sensitive hollow-sensor (Figure 1.9)⁷¹ as a naked eye Hg^{2+} detector over a large pH range and removed the Hg^{2+} ions from aqueous solution with the adsorption capacity of 32.2 mg g^{-1} .

1.11.2. Magnetic Core-Shell Particle Based Hybrid Sensors

Jung's group developed a BODIPY-functionalized magnetic silica sensor, N-1^{72a} for the *in vivo* monitoring of Pb^{2+} . Upon the addition of Pb^{2+} ions, N-1 showed a chelation enhanced fluorescence (CHEF) which was characteristic of the blocking of PET and the association constant was calculated to be $1.05 \times 10^5 \text{ M}^{-1}$. Wang and He *et al.* reported hybrid sensing silica material $\text{Fe}_3\text{O}_4@\text{nSiO}_2@m\text{SiO}_2\text{-T-TRDNA}$ ^{72b} which can concurrently detect and remove the Hg^{2+} ions from the water samples and about 80 % of Hg^{2+} was removed within 1h. In 2012, Li *et al.* synthesized a novel magnetic core-shell MMS-Py^{72c} for highly selective and sensitive monitoring and removal of Hg^{2+} in aqueous solution with a detection limit of 1.72 ppb. The fluorescence properties of this hybrid sensor are stable and reversible over a pH range between 4.0 and 9.0 and it can be employed as a recyclable sensor for fast and efficient removal of Hg^{2+} .

Xiao *et al.* developed a sensitive and selective magnetic core-shell chemosensor NDPA- $\text{Fe}_3\text{O}_4@\text{SiO}_2$ ^{72d} system for detecting glutathione disulfide (GSSG). The addition of Cu^{2+} to NDPA- $\text{Fe}_3\text{O}_4@\text{SiO}_2$ solution resulted in an observable decrease in the fluorescence emission intensity at 497 nm and a new emission peak at 450 nm appeared simultaneously. In the presence of GSSG, the emission intensity of NDPA- $\text{Fe}_3\text{O}_4@\text{SiO}_2\text{-Cu}^{2+}$ was recuperated due to the strong binding of Cu^{2+} with GSSG and the detection limit was found to be 50 pM. In 2014, Liu *et al.* reported a hybrid sensor R6&MCM-41& Fe_3O_4 ^{72e} for the detection and removal of Hg^{2+} . Upon the addition of Hg^{2+} , R6&MCM-41& Fe_3O_4 exhibited “off-on” emission effect towards Hg^{2+} ions when the Hg^{2+} concentration was as high as 15×10^{-7} M. Chen's group and Yang's group reported hybrid sensing probes Rd-MCM-41@ Fe_3O_4 ^{72f} and $\text{Fe}_3\text{O}_4@\text{MCM-41}@\text{RB}$ ^{72g} for the detection of Hg^{2+} with fluorescence emission “off-on” property and these hybrid sensors can be reused for practical applications. Yan *et al.* also synthesized a multifunctional sensing material AQ- $\text{Fe}_3\text{O}_4@\text{SiO}_2@\text{KCC-1}$ ^{72h} for the detection

and removal of Zn^{2+} ions. This hybrid sensor exhibited enhanced fluorescence intensity and a high selectivity and sensitivity toward Zn^{2+} over other metal ions in the aqueous solution. A novel, 'all-in-one' hybrid sensing probe MMs⁷²ⁱ was developed by Tao *et al.* which exhibited excellent sensitivity and selectivity towards Hg^{2+} with the detection limit of 10 ppb.

1.11.3. Magnetic Nanoparticle Based Hybrid Sensors

Wu *et al.* developed a new reversible magnetic hybrid sensor $\text{Fe}_3\text{O}_4\text{-R6G}$ ^{73a} for the selective detection and removal of Hg^{2+} from aqueous solution with detection limit of 1.5×10^{-7} M. In 2013, a multifunctional hybrid material $\text{BR6G-Fe}_3\text{O}_4$ ^{73b} was reported by Wang *et al.* which showed high selectivity and sensitivity for Al^{3+} over other competing metal ions in aqueous solution at pH 7.0. This hybrid sensing probe showed a detection limit of 0.3 ppb and eliminated excess Al^{3+} in water using an external magnet which indicated that this hybrid sensor acquired practical application in toxicology and biology. Additionally, Wang's group also reported another hybrid sensor that is luminescent europium complex hybrid Fe_3O_4 nanoparticles^{73c} which can operate as a fluorescent probe for ultrasensitive detection and removal of Cu^{2+} from the aqueous solution based on the fluorescence quenching method. This multifunctional hybrid sensor exhibited high sensitivity and selectivity towards Cu^{2+} ions compared to other metal ions with the detection limit of 0.1 nM and can be used to detect Cu^{2+} in living HeLa cells.

1.11.4. Polymer Based Hybrid Sensors

Yu *et al.* reported a rhodamine and quinoline-functionalized nanofilm sensing material $\text{poly}(\text{MMA-co-RQ})$ ^{74a} as a colorimetric sensor for Fe^{3+} and PPI. In 2011, Liu *et al.* developed rhodamine functionalized sensing polymer $\text{poly}(\text{VP-co-GMA-g-RhBH})$ ^{74b} which exhibited selective and sensitive detection of Hg^{2+} in water solution with considerably enhanced fluorescence intensities, and showed color change from colorless to pink. The color change and off-on fluorescence confirmed that $\text{poly}(\text{VP-co-GMA-g-RhBH})$ could act as a naked-eye detector and selective fluorescent switcher for Hg^{2+} ions. A new FRET-based ratiometric probe using polymer particles as scaffold^{74c} was reported by Wu and Zeng *et al.* for sensing Hg^{2+} in aqueous solution and this sensor offers a method for ratiometric fluorescence sensing of metal ions in the environmental and biological field.

Yang *et al.* reported a nanofibrous film sensor PMAR^{74d} as a colorimetric and “turn-on” fluorescent sensor for Cu²⁺ in the aqueous solution with a detection limit of 1.5×10^{-6} M. In addition, Chen and Wang *et al.* synthesized the Cu²⁺ sensing probe based on the electrospun rhodamine derivative doped poly(ether sulfones) nanofibrous film^{74e} in 2013. Ozay *et al.* developed rhodamine-based colorimetric naked eye hydrogel sensors p(AAm-co-RH6GAC) and p(HEMA-co-RH6GAC)^{74f} for Fe³⁺ detection in aqueous solution and showed a minimum detection limit of 0.1 ppm for the p(HEMA-co-RH6GAC) hydrogel hybrid sensor. Moreover, the hydrogel sensors can be recycled by the treatment with EDTA. In 2011, Wu and Zeng *et al.* reported two FRET-based ratiometric hybrid sensors^{74g} for the detection of Hg²⁺ in aqueous solution utilizing polymeric nanoparticles.

Yi *et al.* developed a dual-emission ratiometric fluorescent hybrid sensor SiNP-PEIQ^{74h} which can afford naked-eye detection of Zn²⁺. This hybrid sensing probe is used for monitoring and intracellular imaging of Zn²⁺ ions and exhibited good biocompatibility, cell permeability, water dispersivity, and high selectivity and sensitivity over other metal ions with a lower detection limit of 0.5 mM. In 2010, Wu *et al.* reported a FRET-based ratiometric polymeric film probe⁷⁴ⁱ with the cross-linked polyvinyl alcohol film as the support which exhibited high selectivity for Fe³⁺ ions compared to other relative metal ions and reversibility could be achieved *via* the treatment with EDTA solution.

1.11.5. Surface-Grafted Composite Based Hybrid Sensors

Shi *et al.* reported a hybrid sensing material R6G-SiNWs^{75a} by immobilizing rhodamine 6G derivative (R6G) on the surface of silicon nanowires for the selective detection of Cu²⁺ which displayed an exceptional fluorescence enhancement over other metal ions. Moreover, the interaction between the R6G-SiNWs and Cu²⁺ is capable of releasing the fluorophore moiety from the R6G-SiNWs leading to a significant application in the living cell. In 2012, Li *et al.* synthesized a fluorescence-quenching-hybrid sensor, Rh 6G-SiO₂^{75b} by the immobilization of *p*-hydroxybenzaldehyde rhodamine 6G hydrazone on the SiO₂ nanosphere surface for the detection of NO₂⁻. The detection limit of this sensing probe was found to be 1.2 mM and the process is reversible.

A reusable dual-functional hybrid sensing material FS^{75c} for simultaneous detection and removal of Hg²⁺ in aqueous solution and serum was reported by Qian and Zhu *et al.* FS was

synthesized by grafting naphthalimide derivative of 2,6-bis(aminomethyl)pyridine to the silica particle surface and this sensing approach possessed some advantages such as simplicity, low cost and rapidity. Ren *et al.* developed a hybrid sensing probe MMZ-RH^{75d} for sensing, and removing Hg²⁺ with high selectivity over other environmentally and biologically competing metal ions. This sensor was synthesized by doping multifunctional magnetic mesoporous nanocomposites and Fe₃O₄ particles in the zeolite material and the rhodamine derivative grafted on the surface and the detection limit was calculated to be 3.2 x 10⁻⁷ M. Moreover, MMZ-RH can be employed to efficiently and rapidly remove the Hg²⁺ from the wastewater.

In 2008, Kim *et al.* reported a thiol-functionalized rhodamine-based chemodosimeter on platinum films, PFIR^{75e} which can be exploited as a molecular switch for the recognition of Cu²⁺. This hybrid sensing material exhibited a selective, sensitive, and reversible, fluorescence response to Cu²⁺ in both the organic and aqueous solution and the detection limit was about 10⁻⁵ M. Besides, at high concentration of Cu²⁺ (10⁻² M), this hybrid showed colorimetric response (colorless to pink) and can be realized by the naked eye. Shen *et al.* employed a hybrid sensor SAM-1^{75f} by the synthesis of a fluorescent self-assembled monolayer (SAM) on the glass substrate utilizing the “click” reaction to detect Hg²⁺ in aqueous solution and is unaffected over a pH range between 2.0 and 11.0.

1.11.6. Host-Guest Interaction Based Hybrid Sensors

Yang *et al.* developed a nanofibrous film based sensing material^{76a} in which the rhodamine-cyclodextrin framework was loaded on the cross-linked adamantane-functionalized poly(MMA-co-ADMA) nanofibrous film surface by host-guest interaction. The interactions can be simply controlled by the appropriate selection of geometrically complementary guest and host molecules such as β -cyclodextrin (host) and adamantane (guest). When Hg²⁺ was added to the solution of the nanofibrous film probe in DMF-H₂O, the fluorescence intensity was significantly increased, and an observable color change from white to pink-red was perceived. Furthermore, this hybrid sensing probe can sensitively and selectivity detect Hg²⁺ over other competing metal ions, and the lower limit of detection was found to be 6.0 x 10⁻⁵ M. Moreover, in 2013, Yang's group reported the fluorescent TSRh6G- β -cyclodextrin fluorophore/adamantine-functionalized magnetic nanoparticles,

TFIC MNPs^{76b} as a hybrid Hg²⁺ sensing probe and the results displayed the highly selective “turn-on” type fluorescence emission enhancement with an obvious color change from light brown to pink. The hybrid material, TFIC MNPs can be used as an efficient adsorbent for the removal of Hg²⁺ from the aqueous environments.

Organic-inorganic hybrid materials owing to its complementary or synergetic effects between organic and inorganic components, might result in enhanced performances or properties and provide promising applications in the field of optics, electronics, mechanics, ionics, energy, environment, biology and medicines as smart membrane and separation devices, catalysts, catalyst supports, functional smart coatings, sensors, smart microelectronics, cosmetics, intelligent therapeutic vectors, *etc.* Numerous hybrid material were synthesized *via* polymerization of macromonomers, functional organosilanes, and metal alkoxides, the encapsulation of organic moieties in sol-gel derived silica or metallic oxides, the organic functionalization of nanoclays, nanofillers, or other compounds possessing lamellar structures, *etc.* and template growth or self-assembly, nano-building block approaches, integrative synthesis or coupled processes, bio-inspired processes, *etc.*⁷⁷

In the organic-inorganic hybrid materials, the inorganic host matrices can offer high thermal, mechanical and chemical stability to the organic molecules. Different types of supporting materials used for the preparation of hybrid material includes metal oxides, zeolites, clay minerals, active carbon, carbon nanotubes, carbides and nitrides, magnetic nanoparticles, hydroxyapatite, hydrotalcite, *etc.*⁷⁸ Among them, clay minerals, the materials of increasing attention because of both structural features and functional relevances including environmental and biomedical uses, are widely used as support, for the preparation of hybrid materials, especially as catalysts and catalytic supports.

1.12. Clays

Clay minerals are essentially hydrous aluminosilicates having microcrystalline materials of very fine particle size usually less than 2 μ m.⁷⁹ While magnesium and iron substitute aluminium in varying degrees, alkali and alkaline earth elements are also the essential constituents in clay minerals. Clays consist of continuous two-dimensional sheets of tetrahedral silica sandwiching octahedral alumina. Water is present in both within the structure and sorbed on the surface. These substitutions cause wide diversity in clay minerals.

According to the difference of charges on clays, there are two types of clay minerals namely cationic clays and anionic clays. Cationic clays consist of negatively charged aluminosilicate layers with small cations in the interlayer space to balance the charge and anionic clays have positively charged brucite- type metal hydroxide layers with anions intercalated in the interlayer region together with water molecules. Cationic clays are widespread in nature but anionic clays are rare and are usually synthesized.⁸⁰

Based on the structure, clays can have a 1:1 and 2:1 layered structure. When one octahedral sheet is linked to one tetrahedral sheet, it is called 1:1 silicate. In 2:1 silicate, one octahedral alumina sheet is sandwiched between two tetrahedral silica sheets. Kaolin and serpentine are the examples of 1:1 silicates, smectites and vermiculites constitute 2:1 silicates. Smectites groups are widely used in various branch of industry due to their high cation exchange capacity, swelling ability and high surface area. These properties are critical for the successful development of sorbents. The most common smectite is montmorillonite whose octahedral sites are occupied mainly by Al^{3+} , but partly by Fe^{3+} and Mg^{2+} . The tetrahedral sites of montmorillonite normally contain Si^{4+} as the central atom with some Al^{3+} substitution.

The distinguishing feature of the smectite structure is that water and other polar molecules (in the form of certain organic substances) can enter into the unit layers, causing the structure to expand but kaolin does not allow expansion.⁸¹ Surface modifications of clay minerals have received attention because it allows the creation of new materials and new applications. Active sites in clay mineral surfaces are very important because they determine the chemical reactions that the clay can undergo. There are six kinds of active sites namely isomorphic substitution sites, hydrophobic sites, broken edge sites, neutral siloxane surface, metal cations occupying cation exchange sites and water molecules surrounding the exchangeable cations. Among these active sites, the first four sites are more important for modifying clays to be developed as sorbents.

Isomorphic substitution can create a kind of active site in the clay lattice of 2:1 layer silicates. For the sorption of polar and charged organic materials, isomorphic substitution sites are important. Hydrophobic sites are also one of the active sites in clays. Sorption of organic molecules on clay surfaces can create a hydrophobic nature to the clay surface. The most common example is the exchange of interlayer cations with organic cations (eg.

tetraalkylammonium cations) on montmorillonite. Smectite surfaces have a high selectivity for organic cations such as hexadecyltrimethyl ammonium cations. The edges of the particles which bear broken- end hydroxyls such as Si-OH and Al-OH are very important sites for adsorption. These active sites are dependent on pH value of the solution. In some cases, organic molecules (example phenol) do not replace the exchangeable metal cations, but coordinate directly to the metal cations which occupy the exchangeable cation sites. Neutral siloxane surface also acts as active sites in clay minerals.⁸²

General methods for the synthesis of organoclays include displacement reactions, grafting reactions, cation exchange reactions and solid-state reactions. Displacement reactions occur when water molecules in the interlayer space of smectites and vermiculites are displaced by polar molecules. The interlayer cations can be exchanged by various types of organic cations. Grafting reactions, i.e., the reaction in which covalent bonds are formed between reactive surface groups and organic species, are important steps to hydrophobise the surface of many clay mineral particles. Only the 2:1 clay minerals that provide the silanol and aluminol groups on the edge surface react with organic compounds by grafting reactions. Intercalation reaction occurs by topotactic insertion of mobile guests into an accessible crystallographic site in the layers in the layered host structures.

Cation exchange technique consists of the exchange of interlayer cations of the clay mineral by quaternary alkylammonium cations in aqueous solution. In some cases other kinds of organic compounds have been used. The quaternary alkylammonium salts are cationic surfactants and are the most used organic compounds to prepare organoclays. Modifications of clay minerals also have been performed with quaternary alkyl ammonium salts associated with other organic compounds. Organic molecules can be intercalated in dried clay minerals by solid-state reaction without the use of solvents. The absence of solvents in the preparation is environmentally good and makes the process more suitable for industrialization. The cations can remain in contact with one silicate layer, i.e., the oxygen atoms of the silicate surface occupy the coordination sites of the cations.⁸³

Natural and modified clays have attracted considerable attention owing to their enormously versatile properties.⁸⁰ The application of these clays as catalysts in organic synthesis was reported while many clay based catalysts such as claycopTM, clayzincTM, clayfenTM, envirocatTM, *etc.* are commercially available. Among them, the two most

common modified clays applied in organic synthesis are the K-10 and KSF montmorillonites. Both are synthetic clays produced from natural montmorillonites and are available from many suppliers in large quantities.⁸⁴ The most important challenges for chemists are to design clean or 'green' chemical transformations which constitute an exciting aspect of green chemistry.

Bentonite is a member of 2:1 clay minerals contains mostly montmorillonite.⁸⁵ A negative surface charge is created by the isomorphous substitution of Al^{3+} for Si^{4+} in the tetrahedral layer and Mg^{2+} for Al^{3+} in the octahedral layer. It has a very high expansion and ion exchange capacity and is very active as a catalyst in organic reactions. Clays are environmentally benign, non-corrosive, safe to handle, non-toxic, economical and recyclable.⁸⁶

1.13. Objectives of the Present Investigation

Green and sustainable chemistry based on the catalytic activity of very small and monodispersed gold particles on a suitable support has attracted tremendous attention from the synthetic community. In addition, there is a great demand to develop a simple, rapidly responsive, inexpensive, portable and environmentally benign hybrid sensor for the selective recognition of hazardous metal ions. To develop a stable, efficient and reliable organic-inorganic hybrid sensing system, selection of appropriate supporting materials is crucial and explicitly the selection of green material as support is an important criterion for sustainability. Considering the importance and several advantages of Bentonite, such as sustainability, environmentally benign nature and cost-effectiveness we chose this ubiquitous material as a support for developing organic-inorganic hybrid systems. The synthesis and characterization of two different bentonite based organic-inorganic hybrid systems and the application of one as a green catalyst towards organic reactions and the other as a solid-state colorimetric sensor for micromolar detection of mercury ions form the subject matter of this thesis.

Chapter 2 describes the synthesis and characterization of an efficient, environmentally benign and reusable heterogeneous bentonite-gold nanohybrid catalyst (Au-MPBen) and its application towards the selective oxidation of silanes to silanols under ambient reaction conditions. This nanohybrid catalyst effectively oxidized various aromatic, aliphatic and

sterically hindered silanes to silanols in excellent yields without the formation of disiloxanes as the by-product. The present silane oxidation reaction in the presence of Au-MPBen is environmentally benign, 98.7 % atom economical and proceeds with low catalyst loading.

The third chapter is divided into two parts. In Part A, an efficient, green and reliable method for the direct reductive amination of aldehydes using Au-MPBen is discussed. Use of this heterogeneous catalyst affords a variety of secondary amines in excellent yields under ambient reaction conditions in the presence of phenyldimethylsilane as a mild hydride donor. The catalyst is recyclable, selective and is well applicable for the gram-scale preparation of secondary amines. Part B describes the application of this catalyst for the efficient oxidative cross-coupling reaction of ketones with primary alcohols to produce α,β -unsaturated ketones, and water as the only by-product, under mild conditions.

In the last chapter, the synthesis and characterization of a new lower rim functionalized 1,3-di(quaternary ammonium salt of 8-hydroxyquinaldine) derivative of *p*-*tert*-butylcalix [4]arene (QHQC) and its sensing properties toward Hg^{2+} ions using various physical techniques are discussed. The capability of this molecule to act as a reversible chemosensor for Hg^{2+} ions selectively through naked eye detection prompted us to devise a solid-state sensor with enhanced chemical and thermal stability, by intercalating it into the bentonite galleries. The characterization of this hybrid material by FT-IR spectroscopy, powder XRD, TG/DTA techniques, solid-state absorption and emission studies and the studies towards its application as a colorimetric solid-state Hg^{2+} sensor are also detailed in this chapter.

1.14. References

1. V. K. Ahluwalia, M. Kidwai *New Trends In Green Chemistry*, Anamaya publisher New Delhi, 2nd edition, **2007**, 250, 5-18.
2. P.T. Anastas, J.C. Warner, *Green Chemistry: Theory and Practice*; Oxford University Press: Oxford, **1998**.
3. T. Rajale, D. D. Patil, *J. Pharm. Sci. Bioscientific Res.* **2015**, 5, 479-786.
4. P.T. Anastas, E.S. Beach, *Green Chem. Lett. Rev.* **2008**, 1, 9-24.
5. V. Dichiarante, D. Ravelli, A. Albin, *Green Chem. Lett. Rev.* **2010**, 3, 105-113.
6. I. Horva'th, P. T. Anastas, *Chem. Rev.* **2007**, 107, 2167-2168.

7. G. Rothenberg, *Catalysis: Concepts and Green Applications*, Wiley-VCH: Weinheim, **2008**, 273 pages ISBN: 978-3-527-31824-7
8. IUPAC Compendium of Chemical Terminology, Electronic version, <http://goldbook.iupac.org/C00876.html>
9. I. Chorkendorff, J.W. Niemantsverdriet, *Concepts of Modern Catalysis and Kinetics* 2nd edition, I. WILEY-VCH Verlag GmbH & Co. KGaA, Weinheim, **2007**, ISBN: 978-3-527-31672-4
10. P. T. Anastas, M. M. Kirchhoff, T. C. Williamson, *Appl. Catal. A. Gen.* **2001**, 221, 3-13.
11. J. Heveling, *J. Chem. Educ.* **2012**, 89, 1530-1536.
12. R. A. Sheldon, *Green Chem.* **2007**, 9, 1273-1283.
13. B. M. Trost, *Angew. Chem., Int. Ed. Engl.* **1995**, 34, 259-281.
14. E. Farnetti, R. Di Monte, J. Kašp, *Inorganic and Bio-Inorganic Chemistry-Vol. II - Homogeneous and Heterogeneous Catalysis*, **2009**, 50-86.
15. S. Atalay, G. Ersöz, *Novel Catalysts in Advanced Oxidation of Organic Pollutants*, Springer Briefs, **2016**, 7-22.
16. D. C. Hamilton, *Science*, **2003**, 299, 1702-1706.
17. G. Ertl, H. K. ozingen, J. Weitkamp, *Handbook of Heterogeneous Catalysis*; VCH: Weinheim, **1997**.
18. www.knockhardy.org.uk
19. M. Zach, C. H⁺ agglund, D. Chakarov, B. Kasemo, *Current Opinion in Solid State and Materials Science*, **2006**, vol. 10, 132-143.
20. J. M. Campelo, D. Luna, R. Luque, J. M. Marinas, A. A. Romero, *ChemSusChem* **2009**, 2, 18-45.
21. W. Teunissen, A. A. Bol, J. W. Geus, *Catal. Today*, **1999**, 48, 329-336.
22. S. Bhattacharya, I. Saha, A. Mukhopadhyay, D. Chattopadhyay, U. C. Ghosh, D Chatterjee, *Int. J. Chem. Sci. Technol.* **2013**, 3, 59– 64.
23. V. Polshettiwar, R. S. Varma, *Green Chem.* **2010**, 12, 743-754.
24. P. Serp, K. Philippot, *Nanomaterials in Catalysis*, 1st edition, Wiley-VCH Verlag GmbH & Co. KGaA, **2013**.
25. M. Campanati, G. Fornasari, A. Vaccari, *Catal. Today*, **2003**, 77, 299-314.

26. F. Pinna, *Catal Today* **1998**, *41*, 129-137.
27. C. J. Brinker, G. W. Scherer, *Sol-Gel science: the phys chem sol-gel process*. Academic Press, Boston, **1990**.
28. R. Prasad, P. Singh, *Bull. Chem. React. Eng. Catal.* **2011**, *6*, 63-113.
29. A. R. West, *Solid state chemistry and its applications*, Wiley, New York, **2005**.
30. M. Høj, *Nanoparticle synthesis using flame spray pyrolysis for catalysis one step synthesis of heterogeneous catalysts*. Doctoral Thesis, Technical University of Denmark, **2012**.
31. H. Malik, A. K. Singh, *Engineering physics*. Tata McGraw Hill Education Private Limited, New Delhi, **2010**.
32. R. J. White, R. Luque, V. L. Budarin, J. H. Clark, D. J. Macquarrie, *Chem. Soc. Rev.* **2009**, *38*, 481-494.
33. R. Overney, *Nanothermodynamics and nanoparticle synthesis*. Lecture Notes. **2010**.
34. B. Hvolbæk, T. V. W. Janssens, B. S. Clausen, H. Falsig, C. H. Christensen, J. K. Nørskov, *Nanotoday*, **2007**, *2*, 14-18.
35. C. A. Mirkin, *Small*, **2005**, *1*, 14-16.
36. J. M. Campelo, D. Luna, R. Luque, J. M. Marinas, A. A. Romero, *ChemSusChem* **2009**, *2*, 18-45.
37. (a) K. C. Soni, R. Krishna, S. Chandra Shekar, *Appl. Nanosci.* **2016**, *6*, 7-17; (b) M. O. Sydnes, *Catalysts* **2017**, *7*, 35, DOI:10.3390/catal7010035; (c) S. Paul, Md. M. Islamc, Sk. M. Islam, *RSC Adv.* **2015**, *5*, 42193-42221; (d) M. Opanasenko, P. Stepnicka, J. Cejka, *RSC Adv.* **2014**, *4*, 65137-65162; (e) A. Molnar, *Chem. Rev.* **2011**, *111*, 2251-2320.
38. J. Wang, H. Gu, *Molecules* **2015**, *20*, 17070-17092.
39. (a) S. Alabbad, S.F. Adil, M.E. Assal, M. Khan, A. Alwarthan, M. Rafiq H. Siddiqui, *Arabian Journal of Chemistry* **2014**, *7*, 1192-1198; (b) M. Lee, B. Y. Chen, W. Den, *Appl. Sci.* **2015**, *5*, 1272-1283; (c) X. Y. Donga, Z. W. Gaoa, K. F. Yang, W. Q. Zhanga, L. W. Xu, *Catal. Sci. & Techn.* **2013**, *00*, 1-3; (d) R. Vadakkekara, M. Chakraborty, P. A. Parikh, *Ind. Eng. Chem. Res.* **2012**, *51*, 5691-5698.
40. (a) M. Guerrero, N. T. T. Chau, S. Noël, A. D.-Nowicki, F. Hapiot, A. Roucoux, E. Monflier, K. Philippot, *Curr. Org. Chem.* **2013**, *17*, 364-399; (b) M. Michela, D. Anna,

- V. Gallo, P. Mastrorilli, G. Romanazzi, *Molecules* **2010**, *15*, 3311-3318; (c) J. Fan, Y. Gao, *J. Exp. Nanosci.* **2006**, *1*, 457-475.
41. (a) D. Wang, D. Astruc, *Molecules* **2014**, *19*, 4635-4653; (b) R. B. Nasir Baig, R. S. Varma, *ACS Sustainable Chem. Eng.* **2013**, *1*, 805-809.
42. B. I. Kharisov, H.V. Rasika Dias, O. V. Kharissova, *Arab. J. Chem.* **2014**, DOI: 10.1016/j.arabjc.2014.10.049.
43. (a) P. Frontera, A. Macario, M. Ferraro, P. Antonucci, *Catalysts* **2017**, *7*, 59, 10.3390/catal7020059; (b) H. Y. Wang, A. C. Lua, *J. Phys. Chem. C* **2012**, *116*, 26765-26775.
44. (a) A. Mandoli, *Molecules* **2016**, *21*, 1174-1217; (b) K. Lal, P. Rani *ARKIVOC* **2016**, 307-341; (c) M. B. Gawande, A. Goswami, F. X. Felpin, T. Asefa, X. Huang, R. Silva, X. Zou, R. Zboril, R. S. Varma, *Chem. Rev.* **2016**, *116*, 3722-3811.
45. M. Stratakis, H. Garcia, *Chem. Rev.* **2012**, *112*, 4469-4506.
46. Y. Zhang, X. Cui, F. Shi, Y. Deng, *Chem. Rev.* **2012**, *112*, 2467-2505.
47. T. Mitsudome, K. Kaneda, *Green Chem.* **2013**, *15*, 2636-2654.
48. F. Cardenas-Lizan, M. A. Keane, *J. Mater. Sci.* **2013**, *48*, 543-564.
49. B. S. Takale, M. Bao, Y. Yamamoto, *Org. Biomol. Chem.* **2014**, *12*, 2005-2027.
50. (a) O. S. Wolfbeis, *Fibre Optic Chemical Sensors and Biosensors*; CRC Press: Boca Raton, Vols. 1 & 2, **1991**; (b) G. Orellana, M. C. Moreno-Bondi, *Frontiers in Chemical Sensors: Novel Principles and Techniques*, Springer: New York, **2005**.
51. E. L. Que, D. W. Domaille, C. J. Chang, *Chem. Rev.* **2008**, *108*, 1517-1549.
52. J. S. Kim, D. T. Quang, *Chem. Rev.* **2007**, *107*, 3780-3799.
53. C. McDonagh, C. S. Burke, B. D. MacCraith, *Chem. Rev.* **2008**, *108*, 400-422.
54. L. Prodi, F. Bollta, M. Montalti, N. Zaccheroni, *Coord. Chem. Rev.* **2000**, *205*, 59-83.
55. M. Formica, V. Fusi, L. Giorgi, M. Micheloni, *Coord. Chem. Rev.* **2012**, *256*, 170-192.
56. J. Wu, W. Liu, J. Ge, H. Zhang, P. Wang, *Chem. Soc. Rev.* **2011**, *40*, 3483-3495.
57. J. K.-H. Wong, M. H. Todd, P. J. Rutledge, *Molecules*, **2017**, *22*, 200, DOI:10.3390/molecules22020200
58. B. Valeur, I. Leray, *Coord. Chem. Rev.* **2000**, *205*, 3-40.

59. A. P. De Silva, H. Q. N. Gunaratne, T. Gunnlaugsson, A. J. M. Huxley, C. P. McCoy, J. T. Rademacher, T. E. Rice, *Chem. Rev.* **1997**, *97*, 1515-1566.
60. J. -S. Wu, J. -H. Zhou, P. -F. Wang, X. -H. Zhang, S. -K. Wu, *Org. Lett.* **2005**, *7*, 2133-2136.
61. K. E. Sapsford, L. Berti, I. L. Medintz, *Angew. Chem. Int. Ed.* **2006**, *45*, 4562-4589.
62. Y. Hong, J. W. Y. Lam, B. Z. Tang, *Chem. Commun.* **2009**, 4332-4353.
63. (a) H. H. Qazi, A. B. Mohammad, M. Akram, *Sensors* **2012**, *12*, 16522-16556; (b) C. McDonagh, C. S. Burke, B. D. MacCraith, *Chem. Rev.* **2008**, *108*, 400-422.
64. K. P. Carter, A. M. Young, A. E. Palmer, *Chem. Rev.* **2014**, *114*, 4564-4601.
65. W. S. Han, H. Y. Lee, S. H. Jung, S. J. Lee, J. H. Jung, *Chem. Soc. Rev.* **2009**, *38*, 1904-1915.
66. Z. B. Sun, D. Guo, H. Z. Li, L. Zhang, B. Yang, S. Q. Yan, *RSC Adv.* **2015**, *5*, 11000-11008.
67. (a) X. Du, S. Z. Qiao, *Small*, **2015**, *11*, 392-413; (b) F. Ge, M. M. Li, H. Ye, B. X. Zhao, *J. Hazard. Mater.* **2012**, *211*, 366-372; (c) J. Liu, S. Z. Qiao, Q. H. Hu, G. Q. Lu, *Small*, **2011**, *7*, 425-443; (d) Y. Deng, D. Qi, C. Deng, X. Zhang, D. Zhao, *J. Am. Chem. Soc.* **2008**, *130*, 28-29; (e) W. Wang, X. L. Wang, Q. B. Yang, X. L. Fei, M. D. Sun, Y. Song, *Chem. Commun.* **2013**, *49*, 4833-4835; (f) X. Yang, M. Yang, B. Pang, M. Vara, Y. Xia, *Chem. Rev.* **2015**, *115*, 10410-10488; (g) D. Cassano, D. Rota Martir, G. Signore, V. Piazza, V. Voliani, *Chem. Commun.* **2015**, *51*, 9939-9941.
68. Z. Sun, G. Cui, H. Li, Y. Liu, Y. Tian, S. Yan, *J. Mater. Chem. B* **2016**, *4*, 5194-5216.
69. (a) K. Sarkar, K. Dhara, M. Nandi, P. Roy, A. Bhaumik, P. Banerjee, *Adv. Funct. Mater.* **2009**, *19*, 223-234; (b) X. Y. Qiu, S. H. Han, M. Gao, *J. Mater. Chem. A* **2013**, *1*, 1319-1325; (c) X. Y. Qiu, S. H. Han, Y. F. Hu, M. Gao, H. Wang, *J. Mater. Chem. A* **2014**, *2*, 1493-1501; (d) X. J. Wan, S. Yao, H. Y. Liu, Y. W. Yao, *J. Mater. Chem. A* **2013**, *1*, 10505-10512; (e) J. L. Liu, C. Y. Li, F. Y. Li, *J. Mater. Chem.* **2011**, *21*, 7175-7181; (f) S. Y. Tao, P. Fan, Y. C. Wang, C. Wang, T. Hu, C. G. Meng, *J. Mater. Chem. C* **2014**, *2*, 1962-1965; (g) Q. T. Meng, X. L. Zhang, C. He, G. J. He, P. Zhou, C. Y. Duan, *Adv. Funct. Mater.* **2010**, *20*, 1903-1909; (h) J. F. Zhang, M. Park, W. X. Ren, Y. Kim, S. J. Kim, J. H. Jung, J. S. Kim, *Chem. Commun.* **2011**, *47*, 3568-3570; (i) Q. Zou, L. Zou, H.

- Tian, *J. Mater. Chem.* **2011**, *21*, 14441-14447; (j) V. Ros-Lis, R. Casasus, M. Comes, C. Coll, M. D. Marcos, R. Martinez-Manez, F. Sancenon, J. Soto, P. Amoros, J. El Haskouri, N. Garro, K. Rurack, *Chemistry* **2008**, *14*, 8267-8278.
70. H. J. Kim, S. J. Lee, S. Y. Park, J. H. Jung, J. S. Kim, *Adv. Mater.* **2008**, *20*, 3229-3234.
71. X. J. Cheng, J. P. Li, X. H. Li, D. H. Zhang, H. J. Zhang, A. Q. Zhang, H. Huang, J. S. Lian, *J. Mater. Chem.* **2012**, *22*, 24102-24108.
72. (a) H. Y. Lee, D. R. Bae, J. C. Park, H. Song, W. S. Han, J. H. Jung, *Angew. Chem., Int. Ed. Engl.* **2009**, *48*, 1239-1243; (b) D. He, X. He, K. Wang, Y. Zhao, Z. Zou, *Langmuir* **2013**, *29*, 5896-5904; (c) Y. Wang, B. Li, L. Zhang, P. Li, L. Wang, J. Zhang, *Langmuir* **2012**, *28*, 1657-1662; (d) Y. Ma, B. Zheng, Y. Zhao, H. Yuan, Y. Cai, J. Du, D. Xiao, *Biosens. Bioelectron.* **2013**, *48*, 138-144; (e) L. Bing, *Sens. Actuators, B* **2014**, *198*, 342-349; (f) Y. T. Chen, S. Y. Mu, *Sens. Actuators, B* **2014**, *192*, 275-282; (g) Y. Jing-po, Y. Jun, L. Han, L. Fei, *Dyes Pigm.* **2014**, *106*, 168-175; (h) Z. B. Sun, H. Z. Li, D. Guo, J. Sun, G. J. Cui, Y. Liu, Y. X. Tian, S. Q. Yan, *J. Mater. Chem. C*, **2015**, *3*, 4713-4722; (i) C. Wang, S. Y. Tao, W. Wei, C. G. Meng, F. Y. Liu, M. Han, *J. Mater. Chem.* **2010**, *20*, 4635-4641.
73. (a) Z. Wang, D. Wu, G. Wu, N. Yang, A. Wu, *J. Hazard. Mater.* **2013**, *244*, 621-627; (b) L. Zhi, J. Liu, Y. Wang, W. Zhang, B. Wang, Z. Xu, Z. Yang, X. Huo, G. Li, *Nanoscale* **2013**, *5*, 1552-1556; (c) J. Liu, W. Zuo, W. Zhang, J. Liu, Z. Wang, Z. Yang, B. Wang, *Nanoscale* **2014**, *6*, 11473-11478.
74. (a) Z. X. Li, H. X. Li, C. X. Shi, W. Y. Zhang, W. Zhou, L. H. Wei, M. M. Yu, *Sens. Actuators, B* **2016**, *226*, 127-134; (b) J. Luo, S. S. Jiang, S. H. Qin, H. Q. Wu, Y. Wang, J. Q. Jiang, X. Y. Liu, *Sens. Actuators, B* **2011**, *160*, 1191-1197; (c) C. Ma, F. Zeng, G. Wu, S. Wu, *Anal. Chim. Acta* **2012**, *734*, 69-78; (d) W. Wang, X. Wang, Q. Yang, X. Fei, M. Sun, Y. Song, *Chem. Commun.* **2013**, *49*, 4833-4835; (e) M. H. Min, X. F. Wang, Y. M. Chen, L. M. Wang, H. L. Huang, J. G. Shi, *Sens. Actuators, B* **2013**, *188*, 365-371; (f) H. Ozay, O. Ozay, *Chem. Eng. J.* **2013**, *232*, 364-371; (g) C. Ma, F. Zeng, L. Huang, S. Wu, *J. Phys. Chem. B* **2011**, *115*, 874-882; (h) Y. Shi, Z. Chen, X. Cheng, Y. Pan, H. Zhang, Z. Zhang, C. W. Li, C. Yi, *Biosens.*

- Bioelectron.* **2014**, *61*, 397-403; (i) B. L. Ma, S. Z. Wu, F. Zeng, *Sens. Actuators, B* **2010**, *145*, 451-456.
75. (a) W. F. Xu, L. X. Mu, R. Miao, T. P. Zhang, W. S. Shi, *J. Lumin.* **2011**, *131*, 2616-2620; (b) L. L. Wang, B. Li, L. M. Zhang, L. G. Zhang, H. F. Zhao, *Sens. Actuators, B* **2012**, *171*, 946-953; (c) C. He, W. Zhu, Y. Xu, T. Chen, X. Qian, *Anal. Chim. Acta* **2009**, *651*, 227-233; (d) M. Yin, Z. Li, Z. Liu, X. Yang, J. Ren, *ACS Appl. Mater. Interfaces* **2012**, *4*, 431-437; (e) Y. R. Kim, H. J. Kim, J. S. Kim, H. Kim, *Adv. Mater.* **2008**, *20*, 4428-4432; (f) H. Lu, S. L. Qi, J. Mack, Z. F. Li, J. P. Lei, N. Kobayashi, Z. Shen, *J. Mater. Chem.* **2011**, *21*, 10878-10882.
76. (a) W. Wang, Y. Li, M. Sun, C. Zhou, Y. Zhang, Y. Li, Q. Yang, *Chem. Commun.* **2012**, *48*, 6040-6042; (b) W. Wang, Y. Zhang, Q. Yang, M. Sun, X. Fei, Y. Song, Y. Zhang, Y. Li, *Nanoscale* **2013**, *5*, 4958-4965.
77. C. Sanchez, B. Julian, P. Belleville, M. I. Popall *J. Mater. Chem.* **2005**, *15*, 3559-3592.
78. O. Deutschmann, H. Knozinger, K. Kochloefl, T. Turek, *Heterogeneous Catalysis and Solid Catalysts* Wiley-VCH Verlag GmbH & Co. KGaA, **2009**.
79. D. Moore, R. C. Reynolds, *X-Ray Diffraction and the Identification and Analysis of Clay Minerals* 2nd ed.; Oxford University Press, New York, **2007**.
80. A. Vaccary, *Appl. Clay Sci.* **1999**, *14*, 161-198.
81. S. W. Bailey, *American Mineralogist* **1980**, *65*, 1.
82. (a) S. Yariv; *Int. Rev. Phys. Chem.* **1992**, *11*, 345-375; (b) R. Celis, M. C. HermosIn, J. Cornejo, *Environ. Sci. Technol.* **2000**, *34*, 4593-4599; (c) T. L. Porter; M. P. Eastman; D. Y. Shang; M. E. Hagerman, *J. Phys. Chem. B* **1997**, *101*, 11106-11111; (d) W. F. Jaynes, S. A. Boyd, *Clays Clay. Miner.* **1991**, *39*, 428-436.
83. L. B. de Paiva, A. R. Morales, F. R. V. Díaz, *Appl. Clay Sci.* **2008**, *42*, 8-24.
84. G. Nagendrappa, *Appl. Clay Sci.* **2011**, *53*, 106-138.
85. G. Lagaly, *Trans. R. Soc. Lond. A*, **1984**, *311*, 315-332.
86. N. Kaur, D. Kishore, *Chem. Pharm. Res.* **2012**, *4*, 991-1015.

Design, Synthesis and Characterization of a Bentonite-Gold Nanohybrid as Green Heterogeneous Catalyst for the Selective Oxidation of Silanes

2.1. Introduction

Heterogeneous catalysis is one of the most potent tools for implementing green chemistry. The design and application of green catalyst protect environment, economy and human health; subsequently, both academic and industrial researchers have a great interest in developing greener methodologies. Hybrid nanomaterials based on natural and synthetic clay minerals which are suitably modified for achieving the properties of green catalyst are promising candidates in organic synthesis. Supported gold nanoparticles attract enormous research interest especially in green heterogeneous catalysis on account of their inimitable properties and potential that is directly correlated to their particle size. Support materials enhance the stability of the catalyst, provide increased surface area, reducing cost and allow high dispersion of active component which are essential for the high activity and selectivity of the catalyst.

2.1.1. Clay Minerals

Clays are ubiquitous and inexpensive materials which provide distinct nanometer-scaled layers and interlayers for the strategic design and preparation of a variety of active catalysts including acidic activated clay catalysts, ion exchanged catalysts, intercalated catalysts, clay-supported catalysts, pillared clay catalysts, hierarchically structured solid catalysts and inorganic and inorganic-organic hybrids. In several cases, the combinations of different protocols are executed for the catalyst preparation and the resultant materials exhibit enhanced performance or work in a synergic manner. Moreover, synthetic clay minerals such as layered double hydroxides and their derivatives showed a complementary correlation with naturally-occurring counterparts and were transformed to catalysts by proper engineering.

The invention of functional solid materials with high catalytic performance is essential to the majority of chemical processes owing to the replacement of polluting homogeneous catalysts by means of reusable heterogeneous catalysts. The clay-based heterogeneous catalysts have numerous practical and potential applications in green and sustainable catalysis including chemical, biological, photonic and electric processes.^{1,2}

In ‘clay-based catalysts’, clay minerals are used in four ways, explicitly the framework of clay minerals itself contains active species; functional nanoparticles (NPs) or clusters are built onto or within the clay nanostructure; the ions within the interlamellar space are exchanged with active components for catalytic purpose and clay minerals or their derivatives are used as catalyst supports. A variety of clay-based solids are exploited as catalyst supports and the catalytically active species are dispersed on the surface of the support by impregnation methods. Often, the support materials and catalytically active components interact to each other and function through a synergistic effect. The dispersion of expensive catalysts (e.g., Au, Pd, Ru and Rh) on such a support material significantly improves the catalytic efficiency. In addition, supported catalysts can reduce the cost of the production of catalysts in consequence of the decrease of metal dosage with easy separation and reuse.¹ Clays and clay-based catalysts can catalyze a variety of organic reactions such as oxidation, addition, epoxidation, allylation, alkylation, hydrogenation, acylation, condensation, esterification, rearrangement, isomerization, diazotization, cyclization, polymerization, *etc.*³

Grafting method is one of the important methods of functionalization of clay minerals. In grafting reactions, covalent bonds are formed between reactive surface groups and organic species which hydrophobise the surface of clay minerals. Only the 2:1 clay minerals that afford the aluminol and silanol groups on the edge surface endure grafting reactions.⁴ Moreover, the surface modifications of clay minerals using grafting reaction with silane coupling agents enhance the interfacial interaction.⁵⁻⁹ In silane-grafted clays, the organic molecule is tightly attached to the clay surface as a result of the condensation between silane and clay minerals. Besides, grafting efficacy of the silane molecules in the clay minerals depends on the silane coupling agents, nature of the clay minerals, reaction temperature, dispersing medium and so on.

Three basic models have been proposed for the interaction between clay and silane agents namely external surface, interlayer, and broken edge grafting. The interlayer grafting occurs within the clay gallery which results in the prominent enhance of the basal spacing of the clay minerals.¹⁰⁻¹² For the external surface grafting, the silylation takes place on the external surface and the basal spacing of the clay remain unchanged whereas the ‘broken’ edge grafting associated with an increase in the basal spacing of the clay mineral.

2.1.2. Bentonite as Support Material

In the area of heterogeneous catalysis, selection of support together with appropriate functionalization is the key factor for the effective performance of the catalyst. Clays are safe to handle, inexpensive, reusable, environmentally benign and promote atom economy. Use of clays as catalysts permits them to be recycled, which further enhances their economic efficacy and are extremely easy to work-up. Application of eco-friendly substances like Montmorillonite clays as catalysts for chemical reactions comprises an exciting part of green chemistry and in recent years, montmorillonite especially montmorillonite K-10 emerges as a green heterogeneous acidic catalyst in synthetic organic chemistry.^{13,14} Bentonite is a cheap, ubiquitous and environmentally benign support material among a wide range of catalyst supports. It belongs to 2:1 clay mineral and mostly containing montmorillonite. The structure of montmorillonite clay is shown in Figure 2.1.¹⁵

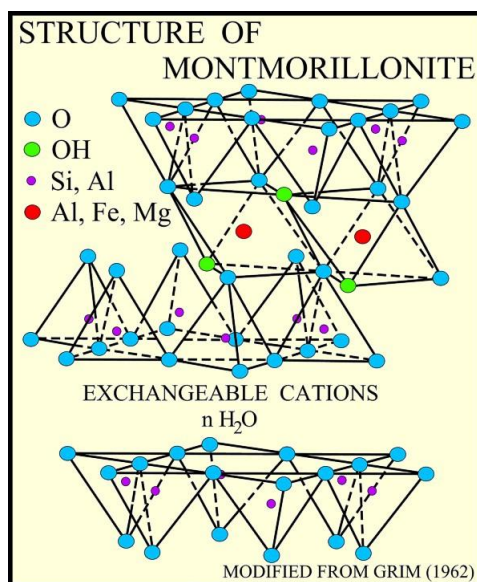


Figure 2.1. Structure of montmorillonite clay

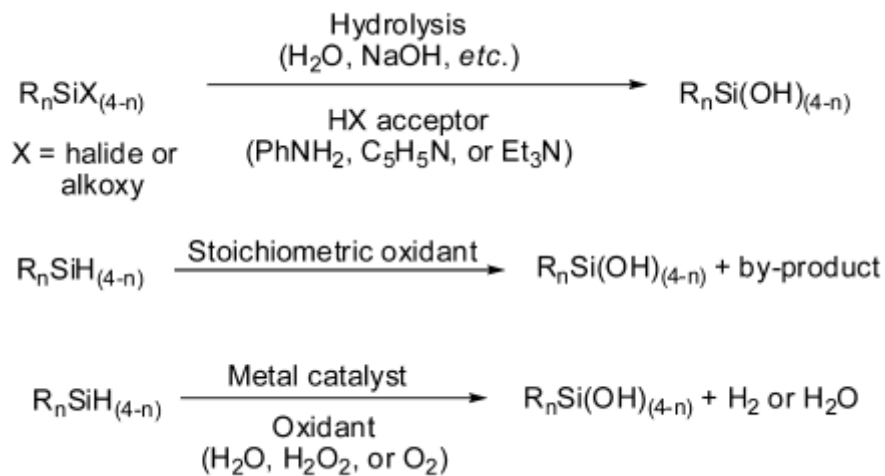
The broken bonds on the edges of bentonite lead to the formation of free hydroxyl groups, which can be utilized for chemical modification.^{16,17} When bentonite is acid activated, dealumination occurs and additional hydroxyl groups are generated in the clay skeleton, leading to the easy grafting of organic groups.¹⁸ In 1993, Mendioroz and co-workers reported Ni/Clay catalysts for vegetable oil hydrogenation in which two naturally occurring clays of Spanish origin, bentonite and palygorskite, had been used as support material.^{19a} Hu *et al.* introduced a bentonite clay-based Fe-nanocomposite for photo-Fenton discoloration and mineralization of Orange II. This heterogeneous catalyst exhibited a high catalytic activity and complete discoloration and mineralization of 0.2 mM Orange II could be attained in less than 60 and 120 min, respectively.^{19b} Yan *et al.* synthesized an acid-activated bentonite supported Au catalyst and Au-Ce catalyst for the CO oxidation and CTAB was utilized to modify the surface of the acid-activated bentonite.^{19c} Zamian *et al.* developed a propyl sulfonic acid group functionalized bentonite as the catalyst for the esterification reaction of acetic acid and 1-propanol.^{19d} This catalytic system enhanced the reaction rate and improved the yield by 12% compared to the uncatalyzed reaction.

In 2012, Ambaryarmo and co-workers prepared a variety of catalysts using noble metals (Os, Ru, Pd and Au) supported on bentonite by impregnation method for the hydrogenolysis of glycerol and found out that Os/bentonite and Ru/bentonite catalyst exhibited high activity and selectivity for hydrogenolysis at 150 °C.^{19e} In 2012, Gil and co-workers developed a heterogeneous catalyst by immobilizing a pincer-type ligand containing Pd(II) on a modified bentonite for arylation of alkenes under room temperature. This catalyst showed high selectivity and activity, could be reused three times without loss of activity.^{19f} In addition, a silicotungstic acid intercalated bentonite was employed as an efficient catalyst for the synthesis of acetal derivatives of aldehydes and ketones by M. Datta *et al.*^{19g}

Han *et al.* reported a Pd/bentonite heterogeneous catalyst for Suzuki-Miyaura coupling reaction and the catalyst is very effective towards arylboronic acid and aryl halides with different electronic substituent. All the substrates could be converted into the corresponding coupling products at room temperature with excellent yields.^{19h} Moreover, in 2017, Ghaziaskar's group reported an arenesulfonic acid-functionalized bentonite as catalyst for glycerol esterification with acetic acid. In this catalyst, bentonite acts as a support and functionalization was achieved by grafting with benzyulsulfonic acid groups.^{19d}

2.1.3. Silanes to Silanols Oxidation

Organosilicon compounds, especially silanols, are useful synthons in various fields of organic synthesis as well as in material science.²⁰⁻²⁵ Silanols are considered as nucleophilic partners in metal catalyzed carbon-carbon cross-coupling reactions,²⁶⁻²⁸ hydrogen bond donors in organocatalysis,²⁹⁻³¹ directing groups in C-H bond activation,³²⁻³⁵ and isosteres of bioactive compounds.^{36,37} Hydrolysis of chlorosilanes,^{38,39} nucleophilic substitution of siloxanes,⁴⁰ and oxidation of hydrosilanes⁴¹⁻⁴⁷ afford silanols (Scheme 2.1)⁴⁸ and we are focused on the synthesis of silanols from hydrosilanes. The classical methods for the oxidation of silanes to silanols involve the use of stoichiometric amounts of oxidants such as peracids,⁴³ dioxiranes,⁴⁴ oxaziridines,⁴⁵ permanganate,⁴⁶ osmium tetroxide,⁴⁷ silver salts,⁴⁹ ozone,^{42,50} *etc.* But these methods are not environmentally benign because of the formation of toxic by-products and generation of disiloxanes as side product consequent from the condensation of silanols. For that reason, there is a huge demand for highly efficient catalytic systems from both environmental and synthetic point of view.



Scheme 2.1. Synthetic methods for silanols

Development of efficient methods which minimizes environmental problems is a great challenge for chemists in both industrial and academic research. Even though some homogeneous transition metal catalysts such as TBA₈[Ag₄(γ -H₂SiW₁₀O₃₆)₂], [RuCl₂(*p*-cymene)]₂, [IrCl(C₈H₁₂)]₂, Re(V) complex, [Ph₃PCuH]₆, methyltrioxorhenium, diorgano telluride, *etc.* have emerged to overcome some of the above mentioned problems, their use is escorted with a difficulty of residual metal impurities, leading to serious problems in

pharmaceutical products. In the case of silane oxidation, they have often shown inadequate practical utility.^{51,52} Subsequently, heterogeneous catalytic systems have emerged as potential alternatives.

Different nanohybrid catalyst systems were developed utilizing support materials like hydroxyapatite, carbon nanotube, amorphous carbon, *etc.* with anchored metal nanoparticles (Ag, Au, Pd, *etc.*) for the selective oxidation of silanes.⁴⁸ Some of these nanometal supported heterogeneous catalysts showed a major drawback of 'leaching out' of metal nanoparticles during the reaction leading to the formation of larger nanoparticles which in turn makes them less active. Consequently, various surface modified supports were used for the stabilization of metal nanoparticles against aggregation and to produce highly active, homogeneous size dispersed metal nanoparticles. For instance, in 1966, Norman and co-workers reported metals on alumina or charcoal support such as Pd/Al₂O₃, Ru/C, Ni powder for the oxidation of hydrosilanes.^{53a} Recently, Park *et al.* developed metal nanoparticles embedded aluminum oxyhydroxide [M/AlO(OH), M = Pd, Au, Rh, Ru, and Cu] as heterogeneous catalysts for the catalytic oxidation of hydrosilanes. Among these catalysts, Pd/AlO(OH) exhibited the highest activity for a wide variety of hydrosilanes and was applicable for large-scale reactions and reusable at least for 10 times. But, the partial hydrogenation of the alkynyl group was observed in the case of some alkynylsilanes, which could be rectified using Au/AlO(OH).^{53b}

Shimizu *et al.* studied the significant effect of oxygen absorbed on the surface of palladium nanoparticles (Pd/C-500H) on the hydrolytic oxidation of hydrosilanes and found out that oxygen-absorbed Pd surfaces showed high activity.^{54a} A nanoporous gold catalyst (Au NPore) was introduced by Yamamoto and co-workers^{54b} for the hydrolytic oxidation and the gold pieces were recovered and reused at least five times devoid of the loss of activity. A variety of hydrosilanes including alkynylsilanes, dihydrosilanes and trihydrosilanes were selectively converted into the corresponding silanols. Moreover, Doris and co-workers introduced a layer-by-layer assembly of gold nanoparticles on a carbon nanotube, CNT^{54c} to construct a gold nanohybrid catalyst and described its efficacy towards oxidation of hydrosilanes and its activity was comparable to Au/AlO(OH) in the 0.20 mmol scale oxidation of dimethylphenylsilane.

Metal nanoparticles embedded in hydroxyapatite (HAP) were utilized in the hydrolytic oxidation of hydrosilanes by Kaneda *et al.* and for ruthenium catalyst (RuHAP) molecular oxygen was an essential component while that with silver catalyst (AgHAP) didn't require molecular oxygen. AgHAP catalyst exhibited higher activity than that of the RuHAP in water though this catalyst was efficient only for aromatic silanes. The limitation on substrate scope was overcome by the oxidation with AuHAP. When the concentration of nucleophiles (OH- or H₂O) on the AgHAP surface increased, silanols were formed by suppressing the condensation to disiloxane by-product.^{55a} Chang and co-workers reported a heterogeneous ruthenium catalyst [RuCl₂(*p*-cymene)]₂ on active carbon by a simple adsorption process and demonstrated its utility in the hydrolytic oxidation of silanes into silanols. The recycling experiment was carried out in tetrahydrofuran and the reaction grabbed longer times over the cycles.^{55b}

Chauhan *et al.* employed a platinum nanoparticle catalyst for the preparation of silanols, which was synthesized by the reduction of Me₂Pt(COD) with poly(methylhydro)siloxane (PMHS).^{56a} This heterogeneous catalyst was recovered by centrifugation and reused four times without considerable loss of selectivity and activity. Remarkably, synthetically valuable silanols possessing alkenyl or alkynyl functional groups were achieved in quantitative yields. Nickel catalysts such as nickel powder and Ni/AlO(OH) were investigated as the catalysts for the preparation of silanols and the activities are lower than those of other metal catalysts, and the reactions need higher temperature 60-110 °C to complete the oxidation.^{56b} Weichold and co-workers analyzed a Ti-doped zeolite as heterogeneous catalyst for the catalytic oxidation of hydrosilanes which transformed small and medium-sized hydrosilanes into the corresponding silanols with excellent selectivity and high conversion with H₂O₂ as oxidant.^{56c}

RuHAP was found to be an efficient heterogeneous catalyst for the oxidation of silanes utilizing water and molecular oxygen as oxidants.^{57a} This oxidation reaction proceeded with functional group tolerance and the catalyst was reusable with retention of selectivity and activity. Kanada and co-workers reported hydroxyapatite-supported gold nanoparticles, AuHAP for the oxidation of silanes in water and this catalytic methodology is a potential candidate for the green oxidation of silanes.^{57b} Gold NPs embedded within the poly(ionic liquid) brushes attached to a SBA-15 support was developed by Duan *et al.* which exhibited

high catalytic activity, reusability and excellent selectivity for the oxidation of diverse silanes into silanols under mild conditions.^{57c}

In 2015, Doris and group employed an organic nanotube-gold hybrid (AuONT) as a heterogeneous catalyst for the aerobic oxidation of silanes and the recyclable nanocatalyst oxidized alkyl and aryl silanes under mild conditions, in high yields without the formation of disiloxane by-product.^{58a} Moreover, Kaneda *et al.* reported Gold nanoparticles supported on hydroxyapatite (Au/HAP) for the catalytic oxidation of hydrosilanes under oxygen at 30 °C in the presence of water in acetone to afford the corresponding silanols in high yields. The catalyst was recyclable and ICP-AES analysis displayed that gold was not leached out from the catalyst during the reaction. In addition, TEM analysis revealed the absence of aggregation of gold nanoparticles on the recovered catalyst.^{58b}

Among the transition metal nanoparticles, gold plays an important role in various organic transformations by making them proceed under mild conditions with high regio- and chemo-selectivities and the details are discussed in the first chapter.

2.2. Statement of the Problem

Green and sustainable chemistry based on the catalytic activity of very small and monodispersed gold nanoparticles on a suitable support have attracted tremendous attention from the synthetic community. The selection of a support being an important aspect in designing heterogeneous catalysts, it is proposed to make use of the advantages of bentonite as a ubiquitous, environmentally benign and inexpensive support material for the design of a bentonite-gold nanohybrid heterogeneous catalyst. In order to ensure monodispersibility of Au nanoparticles inside the support material for maximum catalytic efficiency, suitably organofunctionalized bentonite is proposed to be used for the design. The details of the synthesis and characterization of the new bentonite-gold nanohybrid catalyst thus developed and its efficiency towards silane oxidation reaction are the subject matter of this chapter.

2.3. Results and Discussion

2.3.1. Synthesis and Characterization of Bentonite-Gold Nanohybrid Heterogeneous Catalyst

The assembly of the nanohybrid catalyst commenced with the acid activation of bentonite by refluxing bentonite with 4 N HCl for 4 h. The resultant product was then stirred

with (3-mercaptopropyl)trimethoxysilane (MPTMS) and phenyltriethoxysilane (PTES) at room temperature in dried toluene for 12 h under argon atmosphere to give organo functionalized bentonite (Ben-MP). The thiol group in MPTMS helps in the uniform distribution of Au nanoparticles and holds these particles strongly during the catalytic runs. The function of the PTES is to enhance the surface hydrophobicity of the catalyst which will in turn favour the adsorption of substrate molecules onto the catalyst surface. Finally, gold-bentonite nanohybrid (Au-MPBen) was synthesized by impregnating Ben-MP with HAuCl_4 followed by reduction using NaBH_4 . The Au-nanoparticles formed *in situ* then covalently link with the S atom of the thiol group of MPTMS to form the Au-S bond leading to a stable catalyst system in total. The nanohybrid system was then characterized using XRD, FT-IR, ICP-MS, XPS and TEM techniques.

The XRD spectrum of the acid activated bentonite (Ben-4h) showed a basal spacing (d value) of 12.12 Å. On examining the XRD spectrum of Ben-MP it was found that the d value had increased to 65.8 Å, arriving at a conclusion that the organic molecules (MPTMS and PTES) had successfully been intercalated into the bentonite gallery (Figure 2.2(a)).

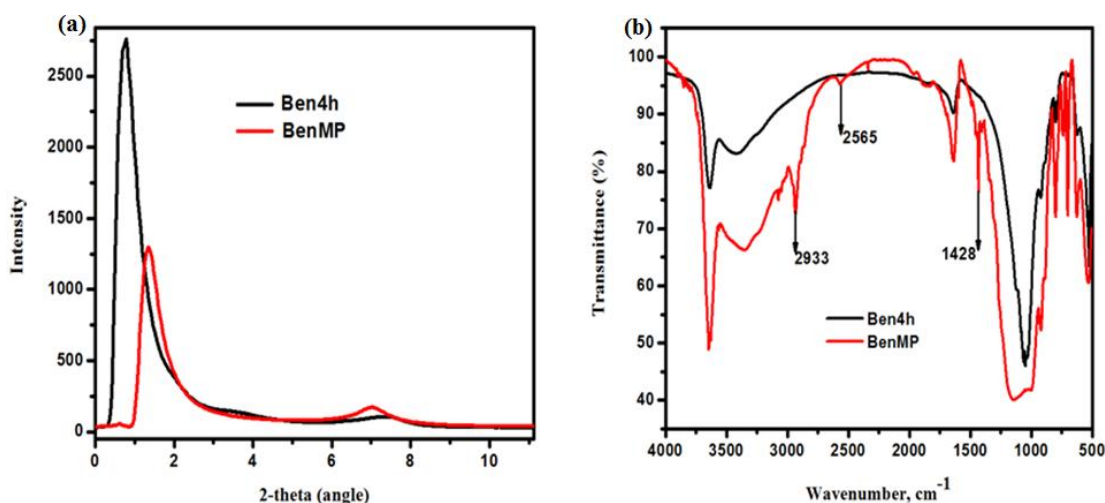


Figure 2.2(a). XRD pattern of acid activated bentonite (Ben-4h) and organofunctionalised bentonite (Ben-MP) and **(2b).** IR spectra of acid activated bentonite (Ben-4h) and organofunctionalised bentonite (Ben-MP)

To give more evidence for successful grafting, FT-IR analysis of Ben-4h and Ben-MP was performed (Figure 2.2(b)). The peak at 3646 cm^{-1} is attributed to the structural hydroxyl stretching vibrations and the peak at 3426 cm^{-1} is assigned to the OH stretching vibration of

the adsorbed water. The peak around 1051 cm^{-1} is assigned to Si-O stretching vibrations. In the organofunctionalized bentonite, peaks at 2933 cm^{-1} and 1428 cm^{-1} are attributed to the antisymmetric stretching and bending vibrations of CH_2 respectively. Peak at 2565 cm^{-1} is assigned to the presence of thiol group.

The presence of reduced gold nanoparticles on the organofunctionalized bentonite was confirmed by TEM analysis which showed the presence of mono-dispersed, spherically shaped Au nanoparticles with an average size of 4 nm on the support (Figure 2.3). This size of the Au nanoparticles is very suitable for catalysing organic reactions. Though small sized nanoparticles have the tendency to aggregate leading to the formation of inactive catalyst, the presence of thiol moiety on the clay surface was found to facilitate the mono-dispersion and stabilization of gold nanoparticles on the support. This has been unequivocally proved as detailed in subsequent pages of this chapter.

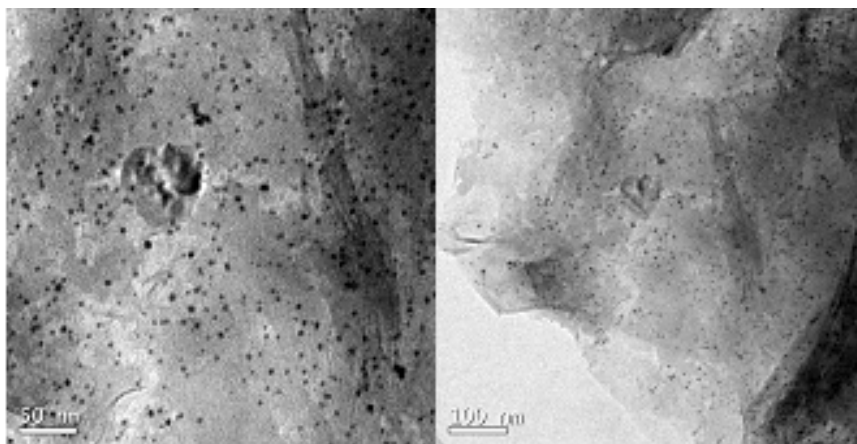


Figure 2.3. TEM images of fresh Au-MPBen (scale bar = 50 nm and 100 nm)

The gold concentration on the catalyst was measured by ICP-MS analysis and it was found to be 5.24×10^{-7} M in 1 mg of catalyst. The electronic state of the Au center was investigated using XPS analysis (Figure 2.4) which revealed that all the Au species in the catalyst were present in its metallic state, corresponding to the binding energies of 88.1 and 91.8 eV, which are characteristics of the $4f^{7/2}$ and $4f^{5/2}$ peaks of Au(0).

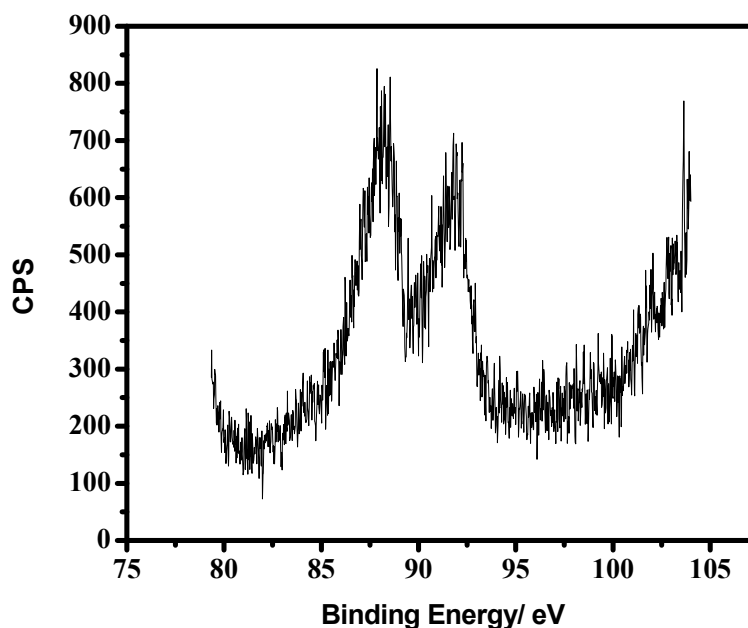


Figure 2.4. XPS spectrum of Au-MPBen

2.3.2. Activity of Bentonite-Gold Nanohybrid Heterogeneous Catalyst Towards Silane Oxidation

Upon successful synthesis and characterization of a bentonite-Au nanohybrid heterogeneous material (Au-MPBen), we decided to evaluate its performance as a catalyst for organic reactions. Considering the importance of silane-silanol conversion, as silanols are valuable nucleophilic partners in many metal catalyzed C-C coupling reactions, we chose to study the activity of the catalyst in catalyzing this reaction. Dimethylphenylsilane was chosen as the model substrate and an initial reaction was carried out in the presence of oxygen atmosphere at room temperature using THF and H₂O as solvent, dimethylphenylsilanol was afforded as product. This result prompted us to optimize the silane-silanol transformation conditions and the results are presented in table 2.1. Initially the reactions were carried out by changing the ratio of THF and H₂O and the optimized solvent condition was found to be a mixture of THF and H₂O in a ratio of 7:3. Then the reactions were performed in the presence and absence of O₂ as well as in the open air which revealed that O₂ accelerated the rate of silane oxidation (Table 2.1, entries 4, 5 & 7).

Moreover it was observed that water played an important role in the oxidation reactions of silanes and no silanol was detected in the absence of water (Table 2.1, entry 1). When the reaction was carried out using water alone as solvent, silanol was obtained in 95% yield but the reaction took 24 h for completion without the formation of disiloxane (Table 2.1, entry 6). Finally the optimized condition for the silane oxidation with Au-MPBen catalyst was found to be a combination of 0.37 mmol of silane in a 7:3 mixture of THF:H₂O (1 mL) in presence of 1 atm of O₂. This reaction afforded dimethylphenylsilanol in 99 % yield within 30 min (Table 2.1, entry 4) with 98.7 % atom economy. It's worthy to mention that disiloxane was not detected as a by-product and notably further purification was not required for this reaction. In addition, the conversion of silane to silanol was confirmed by the disappearance of the peak at δ 4.5 ppm of dimethylphenylsilane and appearance of the peak at δ 2.35 ppm of dimethylphenylsilanol in the ¹H NMR spectra (Figure 2.5).

Table 2.1. Optimization of solvents in the oxidation of silanes

$$\text{Ph}-\underset{\text{Me}}{\overset{\text{Me}}{\text{Si}}}-\text{H} + \text{H}_2\text{O} \xrightarrow[\text{solvent, RT, O}_2]{\text{Au-MPBen}} \text{Ph}-\underset{\text{Me}}{\overset{\text{Me}}{\text{Si}}}-\text{OH} + \text{H}_2$$

Entry	Solvent	Time (h)	Yield (%)
1	THF	24	0
2	THF/H ₂ O (9:1)	2.5	99
3	THF/H ₂ O (1:1)	1	99
4	THF/H ₂ O (7:3)	0.5	99
5	THF/H ₂ O (7:3)	5	99 ^a
6	H ₂ O	24	95
7	THF/H ₂ O (7:3)	3	99 ^b

Reaction conditions: phenyldimethylsilane (0.37 mmol), Au-MPBen (52 μ mol %), room temperature, solvent (1 mL), O₂ balloon (1 atm). ^a Without O₂, ^b With open air.

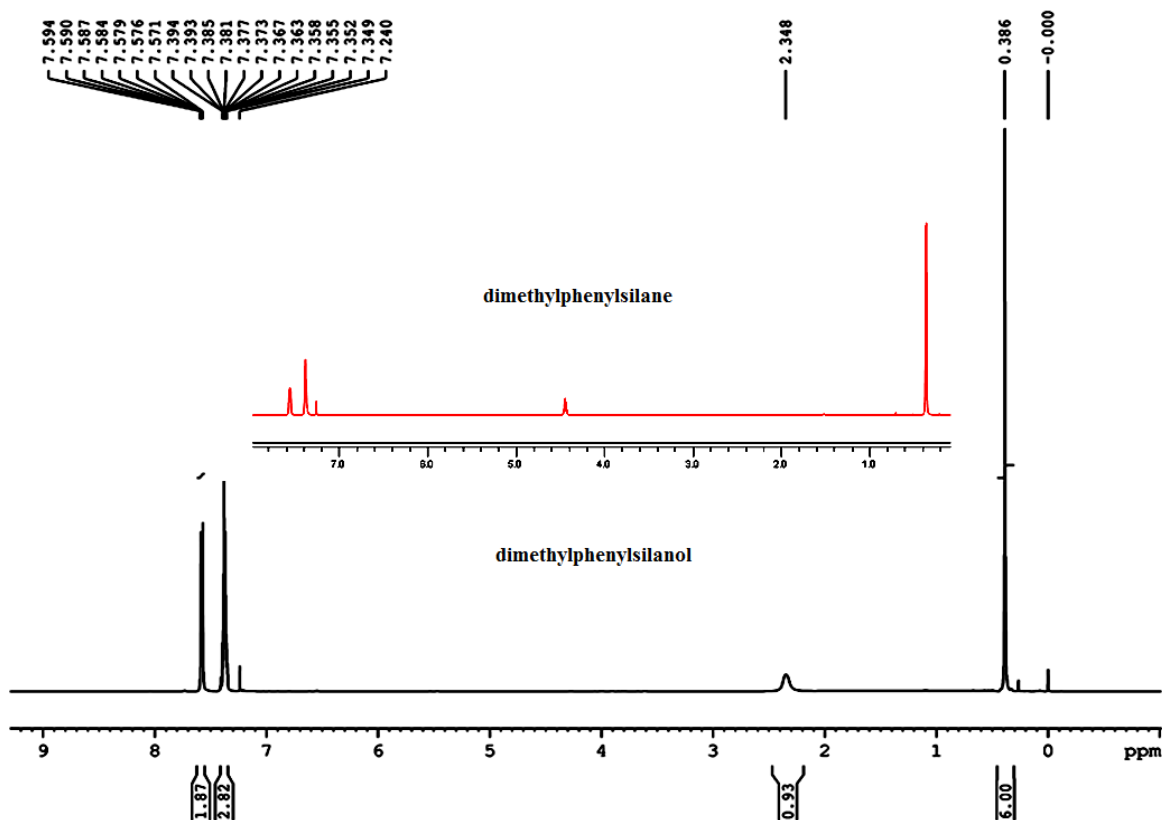
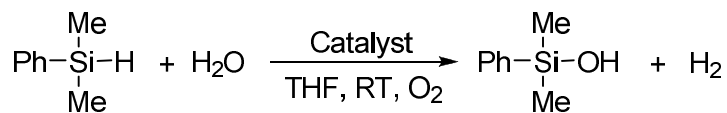


Figure 2.5. NMR spectra of dimethylphenylsilane and dimethylphenylsilanol

To highlight the supremacy of Au-MPBen catalyst, the above reaction was performed using Ben-4h, Ben-MP, Au-Ben (gold nanoparticle impregnated bentonite with no additional stabilizing agents), Au-MPBen catalytic systems and AuCl₃ (Table 2.2). When the oxidation of dimethylphenylsilane was performed with Ben-4h/ Ben-MP as catalysts, silanol was not formed even after 24 h. When Au-Ben was used as the catalyst, though the conversion of silane to silanol occurred, Au nanoparticles were found to leach out from the support, decreasing its credibility as a viable catalyst. The oxidation of silane with 0.1 mol % loading of AuCl₃ gave less than 10% of silanol. Only the Au-MPBen gave efficient conversion of silane to silanol. The covalent linkage of Au nanoparticles through the sulphur atom to the support in Au-MPBen resulted in a stable nanohybrid assembly thereby preventing leaching of Au nanoparticles.

Table 2.2. Comparison of various catalysts in the oxidation of silanes

Entry	Catalyst	Yield (%)
1	Ben-4h	0
2	Ben-MP	0
3	Ben-Au	90
4	Au-MPBen	99
5 ^a	AuCl ₃	< 10 %

Reaction conditions: phenyldimethylsilane (0.37 mmol), catalyst (52 μ mol %), room temperature, THF:H₂O / 7:3 (1 mL), 1 h, ^aAuCl₃ (0.1 mol %).

In order to prove the stability of Au nanoparticles in Au-MPBen, the oxidation of dimethylphenylsilane under the optimized condition was performed. After 15 min, half of the reaction mixture was siphoned out and the catalyst was removed by centrifugation. This reaction was kept for stirring to monitor the progress of the reaction in the absence of the catalyst. The remaining half of the reaction mixture was kept stirring without disturbance. After an additional 30 min, both the reactions were analysed. The reaction was completed in the gold-nanohybrid containing sample whereas no further progress was detected without Au-nanohybrid indicating the absence of leached out gold nanoparticles in the reaction mixture. This proves the reliability of the Au-nanohybrid as a stable catalyst.

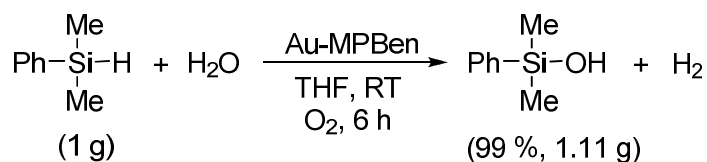
To further confirm the role of both water and oxygen in the silane oxidation reaction, two experiments were carried out. While the first reaction was performed using dried THF under oxygen atmosphere, the second reaction was run under inert atmosphere in the presence of water. It was observed that the first reaction totally failed to convert the silane to silanol. The second reaction was completed very slowly (5 h) in comparison with the optimized reaction time which was less than 30 min. But when oxygen was bubbled through the second reaction mixture and water was added to first reaction mixture, oxidation was completed within 30 min. From these observations, it is evident that water plays an important role in silane oxidation using gold-bentonite nanohybrid as catalyst and oxygen enhances the

reaction rate of silane oxidation. To elucidate the role of water as the prominent oxygen source, we carried out the oxidation reaction of phenyldimethylsilane using D₂O instead of H₂O and confirmed with the help of mass spectroscopy that D atom was transferred to the product. The same reaction was also run with CD₃OD which afforded the corresponding deuteriated methoxysilane and these observations revealed that water acts as oxidant in the silane oxidation reaction.

The generality of the silane-silanol oxidation reaction using Au-MPBen was established and the details are presented in table 2.3. The sterically hindered triisopropylsilane was quantitatively oxidized to triisopropylsilanol in 2 h. Benzyl dimethylsilanol was obtained by the reaction of benzyldimethylsilane in 99 % yield within 1 h. Diphenylmethylsilane was also converted to the corresponding silanol in 97 % yield within 3 h. Oxidation of deactivated triphenylsilane afforded triphenylsilanol in excellent yield (95 %) in 5 h. In addition, diphenylsilane was quantitatively transformed to diphenylsilanediol and 1,4-bis(dimethylsilyl)benzene was doubly oxidized into the corresponding bis-silanol within 1 h in excellent yield (99 %). Moreover no disiloxane was detected as by-product for all of the examples.

2.3.3. Gram Scale Synthesis

The applicability of Au-MPBen towards gram scale synthesis of silanol was investigated by selecting dimethylphenylsilane as model substrate (Scheme 2.2). 1 g of dimethylphenyl silane was successfully transformed to dimethylphenyl silanol in 99 % yield (1.11 g) where the turn over number (TON) and turn over frequency (TOF) were calculated as 1990 and 332 h⁻¹ respectively. But based on the fraction of gold nanoparticles that are exposed to the substrate, the TON and TOF values reached 8844 and 1475 h⁻¹ respectively. Moreover the reaction is 98.7% atom economic and environmentally benign.



Scheme 2.2. Gram scale oxidation of phenyldimethylsilane using Au-MPBen

Table 2.3. Au-MPBen catalysed oxidation of various silanes
$$\begin{array}{c}
 \text{R}_1 \\
 | \\
 \text{R}_2-\text{Si}-\text{H} \\
 | \\
 \text{R}_3
 \end{array}
 + \text{H}_2\text{O}
 \xrightarrow[\text{THF, RT, O}_2]{\text{Au-MPBen}}
 \begin{array}{c}
 \text{R}_1 \\
 | \\
 \text{R}_2-\text{Si}-\text{OH} \\
 | \\
 \text{R}_3
 \end{array}
 + \text{H}_2$$

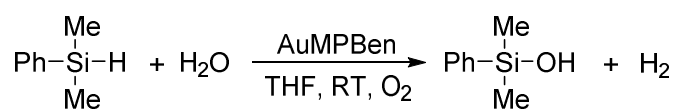
Entry	Silane	Silanol	Time (h)	Yield (%)
1			0.5	99
2			2	91
3			3	97
4			5	95
5			2	96
6			1	99
7			1	99

Reaction conditions: silane (0.37 mmol), Au-MPBen (52 μmol %), THF:H₂O / 7:3 (1 mL), O₂ (1 atm), room temperature.

2.3.4. Recycling Experiment

The recyclability of Au-MPBen for the silane oxidation was investigated by performing five consecutive reactions (Table 2.4) using the same catalyst which was recovered by simple centrifugation. After fifth run, TEM analysis showed that the morphology of the catalyst remained unchanged (Figure 2.6). These observations confirmed the higher efficacy and stability of Au-MPBen nano hybrid catalyst.

Table 2.4. Recycling experiments of Au-MPBen catalyst



Entry	Catalyst	Yield (%)
1	Fresh	99
2	Reuse 1	94
3	Reuse 2	95
4	Reuse 3	94
5	Reuse 4	96

Reaction conditions: phenyldimethylsilane (0.37 mmol), Au-MPBen (52 μmol %), THF:H₂O / 7:3 (1 mL), 30 min, O₂ (1 atm), room temperature.

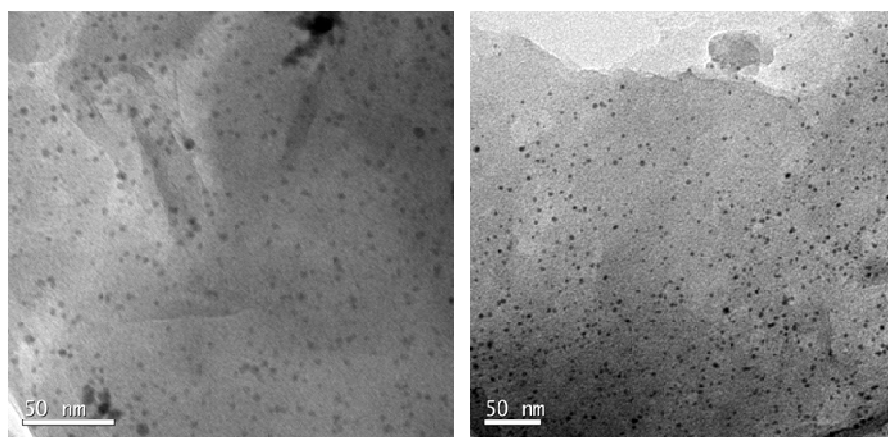
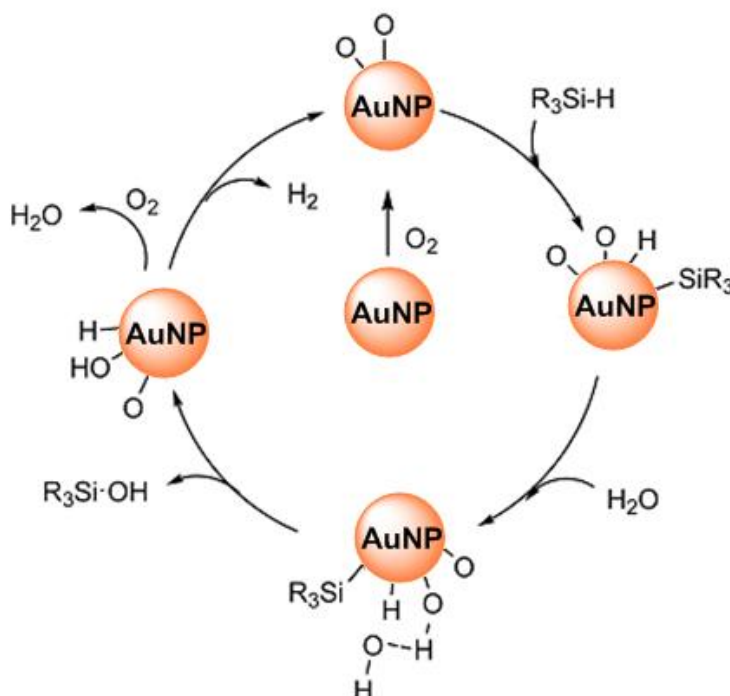


Figure 2.6. TEM images of Au-MPBen after 1st and 5th use (scale bar=50 nm)

2.4. Mechanistic Pathway

A plausible mechanism for the oxidation of silanes using Au-MPBen catalyst is illustrated in Scheme 2.3. The reaction occurs through the insertion of Si-H bond on AuNPs, followed by nucleophilic attack of water molecule producing silanol together with the generation of H₂. Oxygen adsorbed on to the surface of AuNPs enhances the silane oxidation by increasing the electron deficiency of AuNPs through charge transfer from AuNPs to O₂ for Si-H bond activation of silanes.⁵⁹



Scheme 2.3. Proposed mechanistic pathway for silane oxidation reaction using Au-MPBen

2.5. Conclusion

In conclusion, we have successfully developed a new, green and reusable, heterogeneous bentonite-gold nanohybrid catalyst, Au-MPBen which can be prepared from readily available cheap reagents, under mild reaction conditions through simple processes. This nanohybrid catalyst effectively oxidised various aromatic, aliphatic and sterically hindered silanes to silanols in excellent yields without the formation of disiloxanes. The present silane oxidation with Au-MPBen catalyst is environmentally benign, 98.7 % atom economic and proceeded with low catalyst loading. This catalyst was also applicable for the gram scale preparation of silanols.

2.6. Experimental Section

2.6.1. Materials and Methods

The bentonite clay used in the experiments was supplied by M/s Sigma Aldrich. The reagents and solvents were purchased from Alfa Aesar, Spectrochem and Merck and used without further purification. All reactions were carried out in oven dried glassware. Progress of the reactions was monitored by thin layer chromatography. Solvents were removed using Buchi E.L. rotary evaporator.

NMR spectra were recorded on Bruker Avance 500 NMR spectrometer at 500 MHz (^1H) and 125 MHz (^{13}C). Chemical shifts are reported in δ (ppm) relative to TMS as internal standard. Mass spectrum was recorded under ESI-HRMS using analyser type, orbitrap mass spectrometer (Thermo Exactive). IR spectra were recorded on Bruker Alpha-T FT-IR spectrometer and transmittances are reported in cm^{-1} . X-ray diffraction studies were carried out using a powder X-ray diffractometer (Philips X'Pert Pro) with $\text{Cu K}\alpha$ radiation. Surface morphology was analysed using a FEI, TECNAI S Transmission Electron Microscopy (TEM). The electronic structure aspects of the sample were investigated using ESCA+ Omicron Nanotechnology apparatus with Al source by XPS (X-ray photoelectron spectroscopy). Elemental analysis was performed by ICP-MS (Inductively coupled plasma mass spectroscopy) using a Thermo Scientific ICAP Qc instrument.

2.6.2. Syntheses of Au nanoparticles Loaded Organofunctionalized Bentonite

2.6.2.1. Synthesis of Acid Activated Bentonite (Ben-4h)

Bentonite (10 g) was dispersed in 200 mL 4M hydrochloric acid and refluxed for 4 h. After cooling, the supernatant liquid was discarded and the activated bentonite was repeatedly dispersed in deionised water until the supernatant liquid was free from Cl^- ions. Then it was freeze dried using lyophilizer for overnight. All measurements were done at room temperature unless otherwise stated.

2.6.2.2. Synthesis of Organofunctionalized Bentonite (Ben-MP)

0.5 g of acid activated bentonite was mixed with (3-mercaptopropyl)trimethoxysilane, MPTMS (0.525 g, 0.0027 moles) and phenyltriethoxysilane, PTES (0.502 g, 0.0021 moles) in toluene (15 mL) and stirred for 12 h at room temperature in argon atmosphere. Then the

solvent was removed by filtration and the functionalized clay was washed with the same solvent followed by drying under vacuum.

2.6.2.3. Synthesis of Au Nanoparticles Embedded Organofunctionalized Bentonite (Au-MPBen)

0.5 g of organofunctionalized bentonite was impregnated with 30 mL aqueous solution of HAuCl_4 (0.200 g, 0.005 moles) under vigorous stirring condition for 3 h. The filtrate was removed by centrifugation, resulted the formation of Au loaded organofunctionalized bentonite. Then it was dispersed in 10 mL water and reduced with NaBH_4 (0.275 g in 20 mL distilled water, 0.007 moles) which was added slowly under vigorous stirring condition at room temperature for 3 h. Finally the product was centrifuged, washed several times with distilled water and dried at 60 °C for 12 h.

2.6.3. General Procedure for the Catalytic Activity of Au-MPBen Towards the Oxidation of Silanes

To a solution of silane (0.37 mmol,) in $\text{THF:H}_2\text{O} / 7:3$ (1mL) under O_2 atmosphere, the catalyst (52 μmol %) was added. The reaction mixture was allowed to stir at room temperature till the completion of the reaction was verified by TLC. The catalyst was removed by centrifugation, washed three times with ethylacetate, dried over Na_2SO_4 and concentrated under vacuum. The product (silanol) was obtained in 99 % yield without further purification.

2.6.4. Experimental Procedure for Mechanism Study

a. Using D_2O

To a solution of dimethylphenylsilane (0.37 mmol, 50 mg) in $\text{THF:D}_2\text{O} / 7:3$ (1mL) under O_2 atmosphere, the catalyst (52 μmol %) was added. The reaction mixture was allowed to stir for overnight at room temperature. The catalyst was removed by centrifugation, washed three times with ethylacetate, dried over Na_2SO_4 and concentrated under vacuum to afford deuterium incorporated silanol in quantitative yield. This was confirmed by ESI-HRMS analysis which gave M^+ ion peak at 153.

b. Using CD₃OD

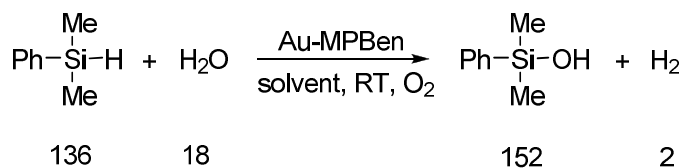
To a solution of dimethylphenylsilane (0.37 mmol, 50 mg) in THF:CD₃OD / 7:3 (1mL) under O₂ atmosphere, the catalyst (52 μmol %) was added. The reaction mixture was allowed to stir for overnight at room temperature. The catalyst was removed by centrifugation, washed three times with ethylacetate, dried over Na₂SO₄ and concentrated under vacuum to afford deuterium incorporated methoxydimethylphenylsilane in quantitative yield. This was confirmed by ESI-HRMS analysis which gave [M+H]⁺ ion peak at 170.

2.6.5. Calculation of Atom Economy

Atom economy of the reaction was calculated using the formula,

$$\text{Atom economy} = (\text{mass of product}/\text{mass of all product}) \times 100$$

For the oxidation of silane to silanol,



$$\text{Atom Economy} = (152 \times 100)/154 = 98.7\%$$

2.6.6. Calculation of TON and TOF

TON and TOF values based on the total amount of gold were calculated as

$$\begin{aligned}
 \text{TON} &= \text{total amount of product (mol)}/\text{total amount of gold (mol)} \\
 &= 0.0073/3.67 \times 10^{-6} \\
 &= 1990
 \end{aligned}$$

$$\begin{aligned}
 \text{TOF} &= \text{TON}/\text{time (h)} \\
 &= 1990/6 \\
 &= 332 \text{ h}^{-1}
 \end{aligned}$$

The fraction of gold atoms exposed to the surface of AuNP was calculated based on the work of Boudart and Djega-Mariadassou.⁶⁰ The strength or percentage of gold nanoparticles that are exposed to substrate is approximately 0.9/d, where d is the spherical metal particle diameter in nm. Thus gold nanoparticles with a diameter of 4 nm have about 22.5 % (0.9/4

nm) of their atoms lying at the surface of the AuNP. As a result, adjusted TON and TOF values based on surface atoms are 8844 and 1475 h⁻¹, respectively.

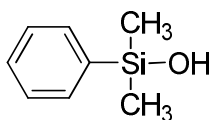
2.6.7. Recycling Experiment

To a solution of dimethylphenylsilane (0.37 mmol, 50 mg) in THF:H₂O / 7:3 (1mL) under O₂ atmosphere, the catalyst (52 μmol %) was added. The reaction mixture was allowed to stir for 30 min at room temperature. The catalyst was removed by centrifugation, washed three times with ethylacetate, dried over Na₂SO₄ and concentrated under vacuum. The product (silanol) was obtained in 99 % yield without further purification. The catalyst was reused for the second reaction after washing with THF. The oxidation reaction was repeated for four more cycles by reusing the recycled catalyst from the previous reaction. After fifth run, TEM analysis was carried out to ensure the morphology of the catalyst.

2.6.8. Synthetic Procedure and Spectral Characterization of Silanols⁵⁴

2.6.8.1. Dimethylphenylsilanol

To a solution of dimethylphenylsilane (0.37 mmol, 50 mg) in THF:H₂O / 7:3 (1mL) under O₂ atmosphere, the catalyst (52 μmol %) was added. The reaction mixture was allowed to stir for 0.5 h at room temperature. The catalyst was removed by centrifugation, washed three times with ethylacetate, dried over Na₂SO₄ and concentrated under vacuum. The product dimethylphenylsilanol was obtained in 99 % yield (55 mg) without further purification.



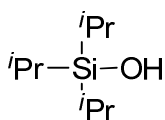
¹H NMR (500 MHz; CDCl₃) δ (ppm): 7.59-7.57 (m, 2H), 7.39-7.35 (m, 3H), 2.35 (brs, 1H), 0.39 (s, 6H).

¹³C NMR (125 MHz; CDCl₃) δ (ppm): 139.2, 133.2, 129.8, 128.0, 0.09.

MS (ESI-HRMS): Calcd for C₈H₁₂OSi, [M-H]⁻: 151.0584, Found: 151.0570.

2.6.8.2. Triisopropylsilanol

To a solution of triisopropylsilane (0.37 mmol, 59 mg) in THF:H₂O / 7:3 (1mL) under O₂ atmosphere, the catalyst (52 μmol %) was added. The reaction mixture was allowed to stir for 2 h at room temperature. The catalyst was removed by centrifugation, washed three times with ethylacetate, dried over Na₂SO₄ and concentrated under vacuum. The product triisopropylsilanol was obtained in 91 % yield (59 mg) without further purification.



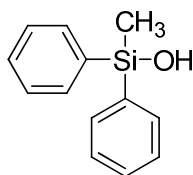
¹H NMR (500 MHz; CDCl₃) δ (ppm): 5.01 (s, 1H), 1.43 (s, 21H).

¹³C NMR (125 MHz; CDCl₃) δ (ppm): 30.3, 21.1.

MS (ESI-HRMS): Calcd for C₉H₂₂OSi, [M-H]⁻: 173.1367, Found: 173.1364

2.6.8.3. Methylphenylsilanol

To a solution of methylphenylsilane (0.37 mmol, 73 mg) in THF:H₂O / 7:3 (1mL) under O₂ atmosphere, the catalyst (52 μmol %) was added. The reaction mixture was allowed to stir for 3 h at room temperature. The catalyst was removed by centrifugation, washed three times with ethylacetate, dried over Na₂SO₄ and concentrated under vacuum. The product methylphenylsilanol was obtained in 97 % yield (77 mg) without further purification.



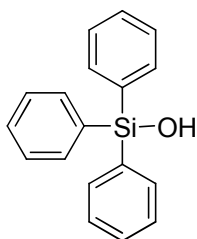
¹H NMR (500 MHz; CDCl₃) δ (ppm): 7.58-7.57 (m, 4H), 7.41-7.33 (m, 6H), 2.68 (s, 1H), 0.63 (s, 3H).

¹³C NMR (125 MHz; CDCl₃) δ (ppm): 137.2, 134.1, 130.0, 128.0, -1.16.

MS (ESI-HRMS): Calcd for C₁₃H₁₄OSi, [M-H]⁻: 213.0741, Found: 213.0739.

2.6.8.4. Triphenylsilanol

To a solution of triphenylsilane (0.37 mmol, 96 mg) in THF:H₂O / 7:3 (1mL) under O₂ atmosphere, the catalyst (52 μmol %) was added. The reaction mixture was allowed to stir for 5 h at room temperature. The catalyst was removed by centrifugation, washed three times with ethylacetate, dried over Na₂SO₄ and concentrated under vacuum. The product methyl-diphenylsilanol was obtained in 97 % yield (97 mg) without further purification.



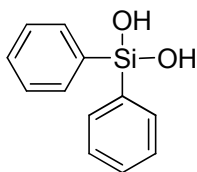
¹H NMR (500 MHz; CDCl₃) δ (ppm): 7.60 (d, 1H, 6H), 7.44-7.40 (m, 3H), 7.37-7.34 (m, 6H), 2.84 (brs, 1H).

¹³C NMR (125 MHz; CDCl₃) δ (ppm): 135.2, 135.0, 130.1, 128.0.

MS (ESI-HRMS): Calcd for C₁₈H₁₆O₂Si, [M-H]⁻: 275.0897, Found: 275.0894.

2.6.8.5. Diphenylsilanediol

To a solution of diphenylsilane (0.37 mmol, 68 mg) in THF:H₂O / 7:3 (1mL) under O₂ atmosphere, the catalyst (52 μmol %) was added. The reaction mixture was allowed to stir for 2 h at room temperature. The catalyst was removed by centrifugation, washed three times with ethylacetate, dried over Na₂SO₄ and concentrated under vacuum. The product methyl-diphenylsilanol was obtained in 96 % yield (77 mg) without further purification.



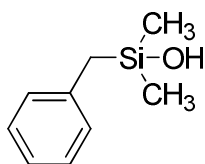
¹H NMR (500 MHz; acetone-d₆) δ (ppm): 7.57-7.56 (m, 4H), 7.26-7.18 (m, 6H), 5.86 (s, 2H).

¹³C NMR (125 MHz; acetone-d₆) δ (ppm): 138.3, 135.2, 130.3, 128.3.

MS (ESI-HRMS): Calcd for C₁₂H₁₂O₂Si, [M-H]⁻: 215.0534, Found: 215.0532.

2.6.8.6. Benzyldimethylsilanol

To a solution of benzyldimethylsilane (0.37 mmol, 56 mg) in THF:H₂O / 7:3 (1mL) under O₂ atmosphere, the catalyst (52 μmol %) was added. The reaction mixture was allowed to stir for 1 h at room temperature. The catalyst was removed by centrifugation, washed three times with ethylacetate, dried over Na₂SO₄ and concentrated under vacuum. The product benzyldimethylsilanol was obtained in 99 % yield (61 mg) without further purification.



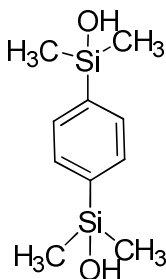
¹H NMR (500 MHz; CDCl₃) δ (ppm): 7.25-7.21 (m, 2H), 7.10-7.05 (m, 3H), 2.17 (s, 2H), 1.89 (brs, 1H), 0.13 (s, 6H).

¹³C NMR (125 MHz; CDCl₃) δ (ppm): 139.2, 128.5, 128.3, 124.4, 28.2, -0.59.

MS (ESI-HRMS): Calcd for C₉H₁₄OSi, [M-H]⁻: 165.0741, Found: 165.0739.

2.6.8.7. 1, 4-Bis(hydroxydimethylsilyl)benzene

To a solution of 1,4-bis(dimethylsilyl)benzene (0.37 mmol, 72 mg) in THF:H₂O / 7:3 (1mL) under O₂ atmosphere, the catalyst (52 μmol %) was added. The reaction mixture was allowed to stir for 1 h at room temperature. The catalyst was removed by centrifugation, washed three times with ethylacetate, dried over Na₂SO₄ and concentrated under vacuum. The product 1, 4-bis(hydroxydimethylsilyl)benzene was obtained in 99 % yield (83 mg) without further purification.



¹H NMR (500 MHz; DMSO-d₆) δ (ppm): 7.53 (s, 4H), 5.88 (brs, 2H), 0.23 (s, 12H). **¹³C NMR** (125 MHz; DMSO-d₆) δ (ppm): 141.3, 132.1, 0.57.

MS (ESI-HRMS): Calcd for C₁₀H₁₈O₂Si₂, [M-H]⁻: 225.0772, Found: 225.0771.

2.7. References

1. C. H. Zhou, *Appl. Clay Sci.* **2011**, *53*, 87-96.
2. M. Poliakoff, P. Licence, *Nature* **2007**, *450*, 810–812.
3. G. Nagendrappa, *Appl. Clay Sci.* **2011**, *53*, 106-138.
4. F. Bergaya, B. K. G. Theng, G. Lagaly, *Handbook of Clay Science*, **2006**.
5. H.P. He, J. Duchet, J. Galy, J.F. Gerard, *J. Colloid Interface Sci.* **2005**, *288*, 171.
6. N. N. Herrera, J. M. Letoffe, J. P. Reymond, E. Bourgeat-Lami, *J. Mater. Chem.* **2005**, *15*, 863-871.
7. L. Wang, K. Wang, L. Chen, C. He, Y. Zhang, *Polym. Eng. Sci.* **2006**, *46*, 215-221.
8. A. Shanmugaraj, K. Y. Rhee, S. H. Ryu, *J. Colloid Interface Sci.* **2006**, *298*, 854-859.
9. S. Yang, P. Yuan, H. He, Z. Qin, Q. Zhou, J. Zhu, D. Liu, *Appl. Clay Sci.* **2012**, *62*, 8-14.
10. K. Isoda, K. Kuroda, *Chem. Mater.* **2000**, *12*, 1702-1707.
11. A. Shimojima, D. Mochizuki, K. Kuroda, *Chem. Mater.* **2001**, *13*, 3603-3609.
12. K.W. Park, S.Y. Jeong, O.Y. Kwon, *Appl. Clay Sci.* **2004**, *27*, 21-27.
13. N. Kaur, D. Kishore, *Chem. Pharm. Res.* **2012**, *4*, 991-1015.
14. C. Peter, W. Zhen, P. Thomas, *Appl. Clay Sci.* **1999**, *15*, 11-29.
15. R.E. Grim, *Applied Clay Mineralogy*, McGraw Hill, New York, NY, **1962**.
16. A. Vaccari, *Catal. Today*, **1998**, *41*, 53-71.
17. H. Shi, T. Lan, T. J. Pinnavaia, *Chem. Mater.* **1996**, *8*, 1584-1587.
18. I. Tkac, P. Komadel, D. Muller, *Clay Miner.* **1994**, *29*, 11-19.
19. J. A. Anderson, M. T. Rodrigo, L. Daza, S. Mendioroz, *Langmuir* **1993**, *9*, 2485-2490; (b) J. Feng , X. Hu , P. L.You, *Environ. Sci. Technol.* **2004**, *38*, 269-275; (c) Z. Rongbin, Y. Liuqing, J. Yan, *Adv. Mat. Res.* **2011**, *287-290*, 1704-1707; (d) D.S. Moraes, R.S. Angélica, C.E.F. Costa, G.N. Rocha Filho, J.R. Zamian, *Appl. Clay Sci.* **2011**, *51*, 209-213; (e) N. Hamzah, W. N. R. W. Isahak, N. F. Adnan, N. M. Nordin, M. B. Kassim, M. Ambaryarmo, *Adv. Mat. Res.* **2012**, *364*, 211-216; (f) M. Ghiaci, F. Ansari, Z. Sadeghi, A. Gil, *Catal. Commun.* **2012**, *21*, 82-85; (g) R. Chaudhary, M. Datta, *JAMI*, **2013**, *3*, 193-201; (g) G. Ding, W. Wang, T. Jiang, B.

- Han, *Green Chem.* **2013**, *15*, 3396-3403. (h) M. Tangestanifard, H. S. Ghaziaskar, *Catalysts* **2017**, *7*, 211.
20. V. Chandrasekhar, R. Boomishankar, S. Nagendran, *Chem. Rev.* **2004**, *104*, 5847-5910.
21. Y. Abe, I. Kijima, *Bull. Chem. Soc. Jpn.* **1969**, *42*, 1118-1123.
22. R. Murugavel, A. Voigt, M. G. Walawalkar, H. W. Roesky, *Chem. Rev.* **1996**, *96*, 2205-2236.
23. G. Li, L. Wang, H. Ni, C. U. Pittman, Jr. *J. Inorg. Organomet. Polym.* **2001**, *11*, 123-154.
24. R. Murugavel, M. G. Walawalkar, M. Dan, H. W. Roesky, C. N. R. Rao, *Acc. Chem. Res.* **2004**, *37*, 763-774.
25. F. Guida-Pietrasanta, B. Boutevin, *Adv. Polym. Sci.* **2005**, *179*, 1-27.
26. S. E. Denmark, M. H. Ober, *Aldrichim. Acta* **2003**, *36*, 75-85.
27. S. E. Denmark, C. S. Regens, *Acc. Chem. Res.* **2008**, *41*, 1486-1499.
28. S. E. Denmark, *J. Org. Chem.* **2009**, *74*, 2915-2927.
29. N. T. Tran, T. Min, A. K. Franz, *Chem. Eur. J.* **2011**, *17*, 9897-9900.
30. A. G. Schafer, J. M. Wieting, A. E. Mattson, *Org. Lett.* **2011**, *13*, 5228-5231.
31. N. T. Tran, S. O. Wilson, A. K. Franz, *Org. Lett.* **2012**, *14*, 186-189.
32. M. Mewald, J. A. Schiffner, M. Oestreich, *Angew. Chem. Int. Ed.* **2012**, *51*, 1763-1765.
33. C. Wang, H. Ge, *Chem. Eur. J.* **2011**, *17*, 14371-14374.
34. C. Huang, B. Chattopadhyay, V. Gevorgyan, *J. Am. Chem. Soc.* **2011**, *133*, 12406-12409.
35. C. Huang, N. Ghavtadze, B. Chattopadhyay, V. Gevorgyan, *J. Am. Chem. Soc.* **2011**, *133*, 17630-17633.
36. R. Tacke, T. Schmid, M. Hofmann, T. Tolasch, W. Francke, *Organometallics* **2003**, *22*, 370-372.
37. J. K. Kim, S. M. Sieburth, *J. Org. Chem.* **2012**, *77*, 2901-2906.
38. J. A. Cella, J. C. Carpenter, *J. Organomet. Chem.* **1994**, *480*, 23-26.
39. H. M. Cho, S. H. Jeon, H. K. Lee, J. H. Kim, S. Park, M.-G. Choi, M. E. Lee, *J. Organomet. Chem.* **2004**, *689*, 471-477.

40. S. M. Sieburth, W. Mu, *J. Org. Chem.* **1993**, *58*, 7584-7586.
41. V. Chandrasekhar, R. Boomishankar, S. Nagendran, *Chem. Rev.* **2004**, *104*, 5847-5910.
42. L. Spialter, J. D. Austin, *J. Am. Chem. Soc.* **1965**, *87*, 4406.
43. (a) L. H. Sommer, L. A. Ulland, G. A. Parker, *J. Am. Chem. Soc.* **1972**, *94*, 3469-3471. (b) Y. Nagai, K. Honda, T. Migita, *J. Organomet. Chem.* **1967**, *8*, 372-373.
44. W. Adam, R. Mello, R. Curci, *Angew. Chem., Int. Ed. Engl.* **1990**, *29*, 890-891.
45. M. Cavleehioli, V. Montanari, G. Resnati, *Tetrahedron Lett.* **1994**, *35*, 6329-6330.
46. P. D. Lickiss, R. Lucas, *J. Organomet. Chem.* **1995**, *521*, 229-234.
47. K. Valliant-Saunders, E. Gunn, G. R. Shelton, D. A. Hrovat, W. T. Borden, J. M. Mayer, *Inorg. Chem.* **2007**, *46*, 5212-5219.
48. M. Jeon, J. Han, J. Park, *ACS Catal.* **2012**, *2*, 1539-1549.
49. N. Duffaut, R. Calas, J.-C. Mac, *Bull. Chem. Soc. Fr.* **1959**, 1971.
50. (a) L. Spialter, J. D. Austin, *Inorg. Chem.* **1966**, *5*, 1975; (b) L. Spialter, L. Pazdernik, S. Bernstein, W. A. Swansiger, G. R. Buell, M. E. Freeburger, *J. Am. Chem. Soc.* **1971**, *93*, 5682-5686.
51. (a) Y. Lee, D. Seomoon, S. Kim, H. Han, S. Chang, P. H. Lee, *J. Org. Chem.* **2004**, *69*, 1741-1743; (b) M. Lee, S. Ko, S. Chang, *J. Am. Chem. Soc.* **2000**, *122*, 12011-12012; (c) U. Schubert, C. Lorenz, *Inorg. Chem.* **1997**, *36*, 1258-1259; (d) E. A. Ison, R. A. Corbin, M. M. Abu-Omar, *J. Am. Chem. Soc.* **2005**, *127*, 11938-11939; (e) R. A. Corbin, E. A. Ison, M. M. Abu-Omar, *Dalton Trans.* **2009**, 2850-2855.
52. (a) W. Adam, C. M. Mitchell, C. R. Saha-Moller, O. Weichold, *J. Am. Chem. Soc.* **1999**, *121*, 2097-2103; (b) Y. Okada, M. Oba, A. Arai, K. Tanaka, K. Nishiyama, W. Ando, *Inorg. Chem.* **2010**, *49*, 383-385; (c) E. Matarasso-Tchiroukhine, *J. Chem. Soc. Chem. Commun.* **1990**, 681-682; (d) Y. Lee, D. Seomoon, S. Kim, H. Han, S. Chang, P. H. Lee, *J. Org. Chem.* **2004**, *69*, 1741-1743; (e) E. A. Ison, R. A. Corbin, M. M. Abu-Omar, *J. Am. Chem. Soc.* **2005**, *127*, 11938-11939.
53. (a) G. H., Jr. Barnes, N. E. Daughenbaugh, *J. Org. Chem.* **1966**, *31*, 885-887; (b) M. Jeon, J. Han, J. Park, *ChemCatChem.* **2012**, *4*, 521-524.

54. (a) K. Shimizu, T. Kubo, A. Satsuma, *Chem.-Eur.J.* **2012**, *18*, 2226-2229; (b) N. Asao, Y. Ishikawa, N. Hatakeyama, Menggenbateera, Y. Yamamoto, M. Chen, W. Zhang, A. Inoue, *Angew. Chem.* **2010**, *122*, 10291; *Angew. Chem. Int. Ed.* **2010**, *49*, 10093-10095; (c) J. John, E. Gravel, A. Hagege, H. Li, T. Gacoin, E. Doris, *Angew. Chem. Int. Ed.* **2011**, *50*, 7533-7536.
55. (a) T. Mitsudome, S. Arita, H. Mori, T. Mizugaki, K. Jitsukawa, K. Kaneda, *Angew. Chem.* **2008**, *120*, 8056-8058; *Angew. Chem. Int. Ed.* **2008**, *47*, 7938-7940; (b) E. Choi, C. Lee, Y. Na, S. Chang, *Org. Lett.* **2002**, *4*, 2369-2371.
56. (a) B. P. S. Chauhan, A. Sarkar, M. Chauhan, A. Roka, *Appl. Organomet. Chem.* **2009**, *23*, 385-390; (b) W. Adam, H. Garcia, C. M. Mitchell, C. R. Saha-Moller, O. Weichold, *Chem. Commun.* **1998**, 2609-2610; (c) W. Adam, A. Corma, H. García, O. Weichold, *J. Catal.* **2000**, *196*, 339-344.
57. (a) K. Mori, M. Tano, T. Mizugaki, K. Ebitani, K. Kaneda, *New J. Chem.* **2002**, *26*, 1536-1538; (b) T. Mitsudome, A. Noujima, T. Mizugaki, K. Jitsukawa, K. Kaneda, *Chem. Commun.* **2009**, 5302-5304; (c) L. Ma, W. Leng, Y. Zhao, Y. Gao, H. Duan, *RSC Adv.* **2014**, *4*, 6807-6810.
58. (a) E. Villemin, E. Gravel, D. Jawale, P. Prakash, I. N. N. Namboothiri, E. Doris, *Macromol. Chem. Phy.* **2015**, *216*, 2398-2403; (b) T. Urayama, T. Mitsudome, Z. Maeno, T. Mizugaki, K. Jitsukawa, K. Kaneda, *Chem. Lett.* **2015**, *44*, 1062-1064.
59. (a) H. M. Cho, S. H. Jeon, H. K. Lee, J. H. Kim, S. Park, M.-G. Choi, M. E. Lee, *J. Organomet. Chem.* **2004**, *689*, 471-477; (b) E. A. Ison, R. A. Corbin, M. M. Abu-Omar, *J. Am. Chem. Soc.* **2005**, *127*, 11938-11939.
60. M. Boudart, G. Djéga-Mariadassou, *Kinetics of Heterogeneous Catalytic Reactions*, Princeton University Press, Princeton, N. J., **1984**, pp 26.

Application of Bentonite-Gold Nanohybrid Towards Green Heterogeneous Catalysis

PART A

Direct Reductive Amination of Aldehydes *via* Bentonite-Gold Nanohybrid Catalysis

3A.1. Introduction

Secondary amines are the constructive intermediates with incredible potential in organic synthesis, biological systems, materials science, agrochemicals and pharmaceuticals.¹ The simplest method for the synthesis of secondary amines involves the reductive amination of carbonyl compounds *via* an intermediate imine, which is the widely utilized method in pharmaceutical industry.² Reductive amination of carbonyl compounds or reductive alkylation of amines is the reaction of aldehyde or ketones with primary or secondary amines in the presence of a reducing agent and the reaction involves the formation of the addition product aminol or carbinol amine which undergo dehydration to form the imine intermediate. The protonation of imine and subsequent reduction results in the respective alkylated amine. Direct reductive amination constitutes a more proficient and undemanding route³ contrary to indirect methods, which involves the isolation of the unstable imine intermediate.⁴ However, overalkylation of amines is a major problem of direct reductive amination of aldehydes.⁵

Traditional methods including various tin⁶ and boron⁷ complexes as catalysts for secondary amine formation often suffered from harsh reaction conditions, low selectivity, poor yields and toxic by-products. For. eg. NaBH₄ sometimes necessitated harsh reaction conditions but NaBH₃CN is highly toxic and produces toxic by-products such as HCN or NaCN. Pyridine-BH₃ is unstable to heat and must be handled with care. Catalytic hydrogenation⁸ is incompatible with the compounds that contain reducible functional groups such as cyano and nitro compounds, double and triple bonds, *etc.* In recent times, precious

metal (Rh, Ir, and Ru) based catalysts and H₂ gas have been reported to promote direct reductive amination.^{9,10} In addition, bio-relevant metals such as iron¹¹ and copper¹² based catalytic systems were also developed. In the developed methods for reductive amination, molecular hydrogen, silanes, formates, iso-propanol, and Hantzsch esters are used as hydrogen donors.^{10, 13-16} Among these, silanes act as mild hydride sources which can reduce imines in combination with Lewis or Bronsted acids. However, the homogeneous catalytic systems are plagued with the problems of catalyst-product separation and recyclability, and hence industrial applications of these catalysts, especially in the pharmaceutical industry remain as a challenge. Consequently, developing a suitable heterogeneous catalyst for the reductive amination reaction becomes significantly desirable.

The reaction of alcohols and amines through borrowing hydrogen strategy¹⁷ is one of the most powerful methods to prepare secondary amines. In this method, first step is the oxidation of alcohol followed by the formation of an imine. Finally, imine will be reduced to the *N*-alkyl amine and the hydrogen transfer process being executed by the catalyst during oxidation and reduction steps. Pd, Ru, Ir, Rh, Cu, and Fe based homogenous catalysts and Pd, Ru, Pt, Au, Ag, Ni, Mn, Cu and Fe based heterogeneous catalysts were reported for the *N*-alkylation reaction by borrowing hydrogen strategy with more or less efficiency. However, a majority of these types of reactions are conducted at high temperatures with high loadings of precious metal catalysts and a large amount of starting materials in comparatively non-polar aromatic solvents such as xylene and toluene. As a result, improved methods capable of generating secondary amines at room temperature are needed for green organic synthesis and in this context, direct reductive amination remains as a potent tool in the field of synthetic organic chemistry.

In recent times, some palladium based heterogeneous catalysts were developed for the one-pot reductive amination of aldehydes. In 2007, a recyclable Pd/C catalyzed one-pot reductive amination was established by Rhee and co-workers and this protocol utilized readily available, stable, cheap and nontoxic ammonium formate as *in situ* hydrogen donor under neutral and aqueous alcoholic conditions.¹⁸ In 2008, Hu and co-workers reported an efficient and chemoselective direct reductive amination of benzaldehyde and primary amine to directly yield *N*-monosubstituted benzylamine hydrochloride using a Pd/C catalytic hydrogenation system. This procedure was proceeded by adding a few milliliters of CHCl₃

into a conventional Pd/C catalytic system and the Pd/C catalyzed hydrodechlorination of CHCl_3 to release HCl was the essential step in this reaction. The procedure is generally applicable for diverse benzaldehydes and primary amines and N-monosubstituted benzylamine hydrochloride was obtained as a single product in quantitative yields.¹⁹ Ma *et al.* developed a simple, efficient and eco-friendly method for the reductive amination using an easily recoverable Pd/Fe₃O₄ catalyst under mild reaction conditions. This protocol afforded a variety of amines in good to excellent yields. The catalyst exhibited high activity even after eight cycles and was applicable to large-scale industrial synthesis.²⁰

In 2014, Shi *et al.* explored a simple Pd/NiO catalytic system for the reductive amination reaction under ambient reaction conditions. This catalyst showed excellent selectivity and activity in the reductive amination reaction towards a variety of amines and aldehydes and can be easily recycled for several runs without loss of activity.²¹ A convenient methodology for the reductive amination of aldehydes and hydrogenation of unsaturated ketones in the presence of an air and moisture stable and highly active gum stabilized palladium nanoparticles as recyclable heterogeneous catalysts was reported by Nasrollahzadeh.²² This catalyst can be recovered and recycled several times without considerable loss of catalytic activity.

In 2016, Mazaheri's group reported a simple, well efficient and environmentally benign method for one-pot reductive amination, using a bi-functional heterogeneous catalyst, Pd/H-hierarchical ZSM-5. This catalytic system is stable and recyclable, provides an economical and clean method for the synthesis of amines under mild reaction conditions. Moreover, this method can be used to produce a variety of amines in good to excellent yields. This catalyst exhibited high activity and stability even after six cycles and used for the large-scale industrial syntheses.²³ In addition, heterogeneous catalysts such as RANEY®-nickel, Pt/C, Pd/C, Pd/Al₂O₃, Pd/CaCO₃, Pd(OH)₂ *etc.* were used in the reductive amination reaction in the presence of dihydrogen gas as a reducing agent.²⁴ Moreover, Huang *et al.* demonstrated a supported cobalt catalyst on nitrogen doped carbon, Co@NC (800-2h), for the reductive amination of aldehydes and ketones with primary and secondary amines to generate secondary and tertiary amines respectively using H₂ gas without any additives. In addition, this catalyst is recyclable for at least 5 times and is applicable for the synthesis of biologically active N-substituted isoindolinones in one step.²⁵

Even though AuNPs exhibited high efficiency in hydride transfer processes, the exploitation of AuNPs for amine synthesis through reductive amination strategy is rare. For instance, Doris *et al.* reported a highly efficient method for the reductive amination of aldehydes *via* a CNT/gold nanohybrid catalyst using phenyldimethylsilane as hydride source.²⁶ In 2016, Xu and co-workers developed an efficient reductive amination strategy using an easily recyclable and commercially available heterogeneous Au/TiO₂ catalyst. Cost-effective and eco-friendly formic acid was utilized as transfer hydrogen reagent and this combination tolerated the formation of a range of amines from aldehydes and ketones with good reactivity.²⁷

An efficient and easily recoverable magnetic nanoparticle-supported phosphine gold(I) catalyst, Fe₃O₄@SiO₂-P-AuCl was developed by Cai *et al.* in 2016 for the direct reductive amination of aldehydes or ketones with amines with the help of commercially available and inexpensive ethyl Hantzsch ester as the hydrogen donor. The reaction was carried out at room temperature under neutral conditions and produced diverse secondary amines in excellent yields. Moreover, this heterogeneous catalyst can be recovered by applying an external magnet and reused at least ten times without deactivation.²⁸ In 2016, Shi *et al.* also reported an efficient alumina supported nano-gold as the heterogeneous catalyst, for the reductive N-methylation reaction of amine and formaldehyde under relatively mild reaction conditions. The hydrogen atoms inside the water molecules can be utilized as the hydrogen source in the direct reductive amination reaction of O-containing organic molecules with the concurrent emission of molecular oxygen.²⁹

3A.2. Statement of the Problem

As per the above discussion, it is obvious that even though a variety of heterogeneous catalysts were developed for the one-pot reductive amination of aldehydes, the exploitation of AuNPs for amine synthesis through reductive amination strategy is rare. Although the reported catalysts are dynamic for reductive amination reaction, development of more efficient, green, selective, reusable and cost-effective catalytic systems under ambient reaction condition still remain as a challenge in both industrial and academic research field and in this milieu, we introduced our newly synthesized bentonite-gold nanohybrid catalyst, Au-MPBen to examine its efficacy towards direct reductive amination reaction. This chapter

illustrates a detailed experimental investigation of the direct reductive amination of aldehydes using Au-MPBen with dimethylphenylsilane as a mild reducing agent at room temperature and explores its efficiency to afford a variety of secondary amines in excellent yield. Dimethylphenylsilane was utilized in the present reaction due to their low toxicity, mild reducing ability and in addition, due to the mild environmental impact of the byproduct silanol.

3A.3. Results and Discussion

To facilitate the applicability of our Au-MPBen catalyst towards heterogeneous catalysis, we selected the direct reductive amination reaction of aldehydes and studied its efficiency in detail which is discussed in the following sections.

3A.3.1. Syntheses of Secondary Amines Using Au-MPBen catalyst

Our studies commenced with a one-pot condensation of benzaldehyde **1** (1.0 equiv.) and aniline **2** (1.0 equiv.) in the presence of dimethylphenylsilane (1.5 equiv.) as the hydride source and a catalytic amount of Au-MPBen (420 μmol %) in acetonitrile at room temperature under an argon atmosphere. The reaction was found to be completed in an hour and after removal of the catalyst by centrifugation column chromatography was performed, the product obtained in 95 % yield was characterized to be the secondary amine **3a** by NMR and Mass spectroscopic techniques. The optimum amount of the catalyst was determined *via* performing individual experiments by changing the amount of catalyst. This promising result prompted us to investigate the effect of solvents on the reaction and the results are given in Table 3A.1 (entries 1-5). It was found that under similar reaction conditions, an optimum yield of 95 % of N- benzylaniline was produced when acetonitrile was used as the solvent.

The superiority of Au-MPBen catalyst in the direct reductive amination was established by performing the reaction using acid activated bentonite (Ben-4h), organofunctionalised bentonite (Ben-MP), gold nanoparticle impregnated bentonite (Au-Ben) with no additional stabilizing agents and bentonite-gold nanohybrid (Au-MPBen) as catalyst. When the reductive amination of benzaldehyde was performed with Ben-4h/ Ben-MP as catalysts (Table 3A.2, entry 1 & 2), N-benzyl aniline (**3a**) was not formed even after 24 h. When Au-Ben was used as the catalyst (Table 3A.2, entry 3), though the transformation of benzaldehyde to N-benzylaniline occurred, AuNPs were found to leach out from the support,

lessening its reliability as a feasible catalyst. Only the Au-MPBen (Table 3A.2, entry 4) gave the efficient conversion of benzaldehyde to N-benzylaniline.

Table 3A.1. Optimization of solvents for Au-MPBen catalyzed reductive amination

Entry	Solvent	Yield (%)
1	MeCN	95
2	THF	93
3	Toluene	70
4	Methanol	80
5	Acetone	58

Reaction conditions: benzaldehyde (0.5 mmol), aniline (0.5 mmol), dimethylphenylsilane (0.75 mmol), room temperature, Argon atmosphere, 1 h, solvent (1 mL), Au-MPBen (420 μ mol %).

Table 3A.2. Comparison of various catalysts in reductive amination reaction

Entry	Catalyst	Yield (%)
1	Ben-4h	0
2	Ben-MP	0
3	Ben-Au	80
4	Au-MPBen	95

Reaction conditions: benzaldehyde (0.5 mmol), aniline (0.5 mmol), dimethylphenylsilane (0.75 mmol), room temperature, Argon atmosphere, 1 h, MeCN (1 mL), catalyst (420 μ mol %).

In order to explore the generality of Au-MPBen catalyst in direct reductive amination reaction, under optimized reaction conditions, a variety of aldehydes and amines were reacted and the results are detailed in Table 3A.3. *Para* and *ortho* halogenated aromatic aldehydes (entries 2 & 4) provided the corresponding secondary amines (**3b** and **3d**) in quantitative yields (93-94 %) within 2 h. In the case of aldehydes containing electron releasing groups (entries 3 & 5), the reaction proceeded very efficiently within 2 h resulting in the products **3c** and **3e** in 92 and 91 % yields respectively. Besides, 2-bromoaniline and 2-iodo-4-bromoaniline (entries 9 & 10) reacted with benzaldehyde, furnishing corresponding products **3i** and **3j** in quantitative yield (93 & 91 %). Bulkier aldehydes such as 1-pyrene carboxaldehyde and 2-naphthaldehyde (entries 6 & 7) were readily converted to the desired secondary amines (**3f** and **3g**) in 85 and 89 % yield within 4 h and 2 h respectively.

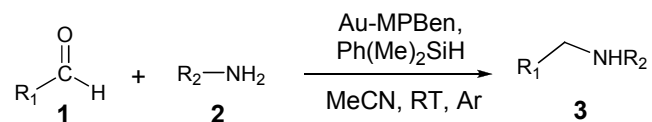
This methodology was also found to be applicable to heterocyclic aldehydes and amines. When 8-aminoquinoline (entry 8) was employed as the amino component, the corresponding secondary amine **3h** was obtained in 91% yield within 3 h. The reaction of 2-aminothiazole with benzaldehyde (entry 11) required more time (5 h) for completion and afforded the corresponding secondary amine **3k** in 71% yield. In addition, thiophen-2-aldehyde and 2-furfuraldehyde (entries 12 & 13) were converted to corresponding amines (**3l** and **3m**) in almost quantitative yields (94 and 92 %) in a short time. Furthermore, the selectivity of the Au-MPBen catalyst towards reductive amination reaction was unambiguously established by the reactions of cinnamaldehyde and perillaldehyde (entries 14 & 15) which provided the corresponding secondary amines **3n** and **3o** very effectively with 92 and 91 % yield and both the reactions were completed within 2 h.

In order to extend the substrate scope of the catalyst, aliphatic aldehydes and amines were introduced in the reaction. Propionaldehyde and butyraldehyde (entries 16 & 17) delivered the corresponding products **3p** and **3q** in good yields (80 % & 82 %) within 12 h but aliphatic amines exhibited very low reactivity towards reductive amination reaction. Even after 24 h, the reactions of isopropylamine and benzylamine with benzaldehyde did not furnish the products (**3r** & **3s**) in isolable yield.

Table 3A.3. Substrate scope of reductive amination reaction

Entry	Aldehyde 1	Amine 2	Product 3	Time (h)	Yield (%)
1				1	95
2				2	93
3				2	92
4				2	94
5				2	91
6				4	85
7				2	89
8				3	91

Table 3A.3. Continued...



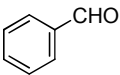
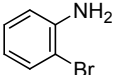
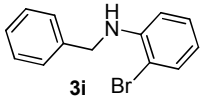
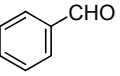
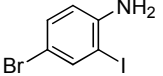
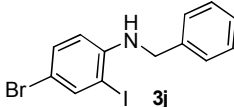
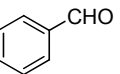
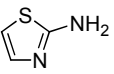
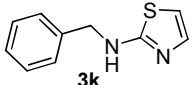
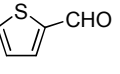
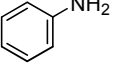
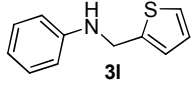
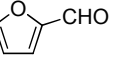
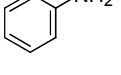
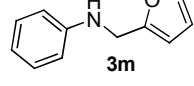
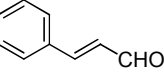
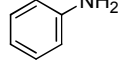
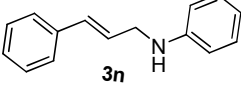
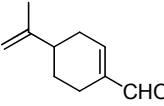
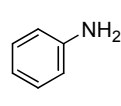
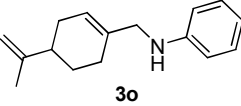
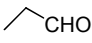
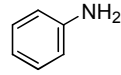
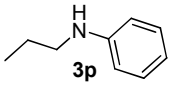
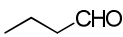
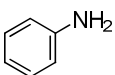
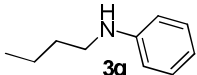
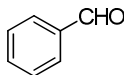
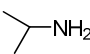
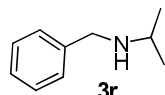
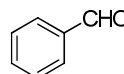
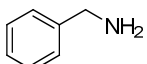
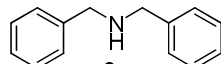
Entry	Aldehyde 1	Amine 2	Product 3	Time (h)	Yield (%)
9				2	93
10				3	91
11				5	71
12				2	94
13				2	92
14				2	92
15				2	91
16				12	80

Table 3A.3 Continued...

$$\begin{array}{c}
 \text{O} \\
 \parallel \\
 \text{R}_1-\text{C}-\text{H} \\
 \mathbf{1}
 \end{array}
 + \text{R}_2-\text{NH}_2
 \xrightarrow[\text{MeCN, RT, Ar}]{\text{Au-MPBen, Ph(Me)}_2\text{SiH}}
 \begin{array}{c}
 \text{R}_1-\text{CH}_2-\text{NHR}_2 \\
 \mathbf{3}
 \end{array}$$

Entry	Aldehyde 1	Amine 2	Product 3	Time (h)	Yield (%)
17				12	82
18				24	Trace amount
19				24	Trace amount

Reaction conditions: aldehyde (0.5 mmol), amine (0.5 mmol), dimethylphenylsilane (0.75mmol), room temperature, Argon atmosphere, MeCN (1 mL), Au-MPBen (420 μmol %).

3A.3.2. Recycling Experiment

The recyclability of Au-MPBen for direct reductive amination reaction was investigated by carrying out the reaction using benzaldehyde and aniline. Au-MPBen catalyst was recovered by centrifugation or filtration and reused in five consecutive runs without the loss of efficiency (Table 3A.4). After fifth run, TEM images (Figure 3A.1) showed no significant change in the morphology of the catalyst. These observations confirmed the high efficacy and robust nature of Au-MPBen nanohybrid catalyst.

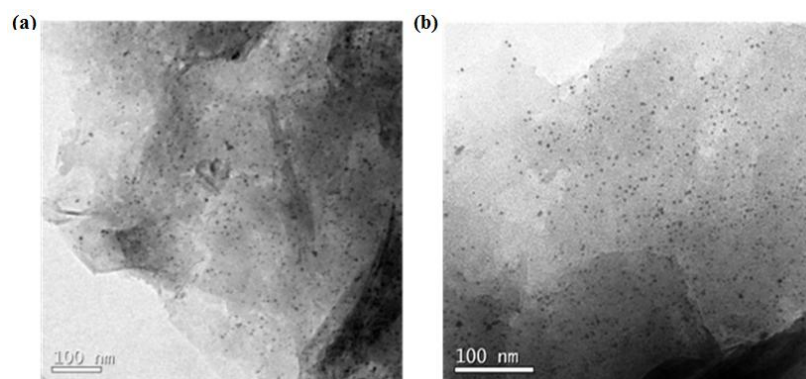
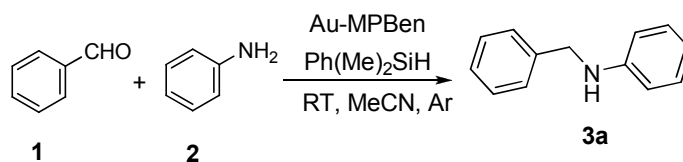


Figure 3A.1. TEM image of Au-MPBen, (a) fresh and (b) after 5th use

Table 3A.4. Recycling experiments of Au-MPBen catalyst



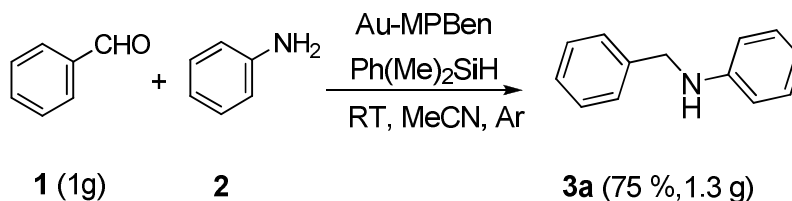
1 + 2 $\xrightarrow[\text{RT, MeCN, Ar}]{\text{Au-MPBen, Ph(Me)}_2\text{SiH}}$ 3a

Entry	Catalyst	Yield (%)
1	Fresh	95
2	Reuse 1	93
3	Reuse 2	91
4	Reuse 3	92
5	Reuse 4	94

Reaction conditions: benzaldehyde (0.5 mmol), aniline (0.5 mmol), dimethylphenylsilane (0.75 mmol), room temperature, Argon atmosphere, 1 h, MeCN (1 mL), Au-MPBen (420 μmol %).

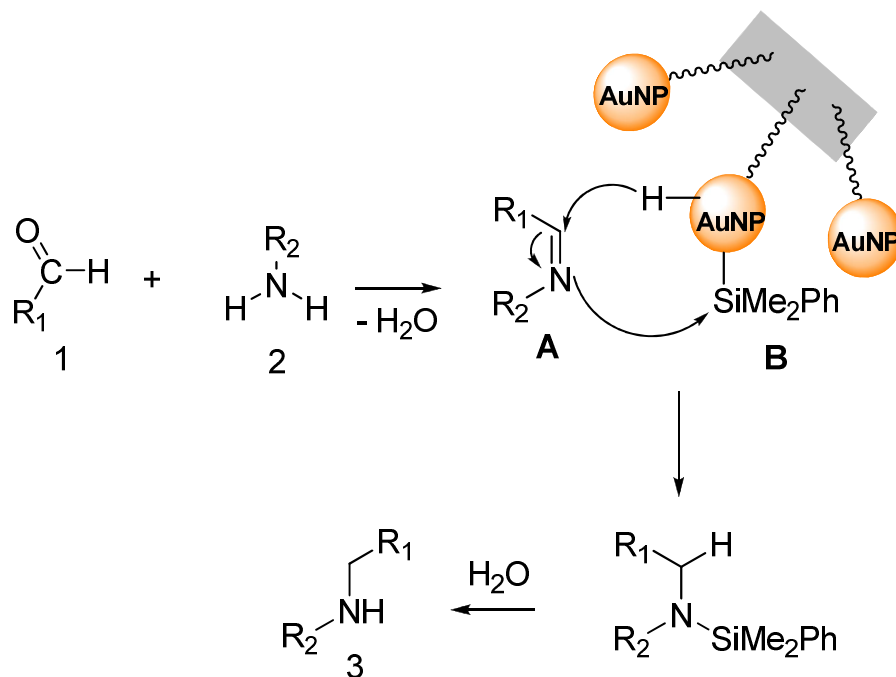
3A.3.3. Gram Scale Synthesis

The feasibility of Au-MPBen catalyst for the large scale synthesis of secondary amines was examined by performing the reaction using benzaldehyde and aniline as model reactants (Scheme 3A.1). When 1 g of benzaldehyde was treated with 0.878 g aniline in the presence of Au-MPBen (1.05 mmol %) and dimethylphenylsilane (1.92 g) as hydride source, N-benzylaniline **3a** was isolated in 75 % yield (1.3 g) within 6 h. Under these conditions, turn over number (TON) and turn over frequency (TOF) were calculated as 676 and 113 h^{-1} respectively. But based on the percentage of surface gold atoms (not the actual gold loading) that are exposed to the substrate, TON and TOF values reached to 3004 and 502 h^{-1} respectively.

**Scheme 3A.1.** Gram scale synthesis of N-benzylaniline using Au-MPBen

3A.4. Mechanistic Pathway

The presumed mechanism for the direct reductive amination of aldehydes with phenyldimethylsilane as the hydride donor is similar to the pathways suggested for similar noble metal hybrid catalysts (Scheme 3A.2).³⁰ The reaction starts with the formation of imine **A** by the condensation of aldehyde and amine. Dimethylphenylsilane undergoes oxidative insertion of Si-H bond on the surface of the gold nanoparticles, which produces an activated silane **B** that is capable of reducing the imine. This activated silane species then reacts with the imine, hydrosilylation occurs and N-silylated amine is generated. Water produced as a result of condensation reaction is used for the hydrolysis of N-silylated amine to produce corresponding secondary amine and silanol is produced as by product. Silylation of nitrogen atom and reduction are concurrent reactions that ensue during direct reductive amination reaction.



Scheme 3A.2: Proposed mechanism for Au-MPBen catalysed reductive amination reaction

3A.5. Conclusion

In conclusion, we have explored an efficient and green method for the direct reductive amination of aldehydes using a bentonite-gold nanohybrid, Au-MPBen as a heterogeneous catalyst with a mild reducing agent phenyldimethylsilane. The catalytic system has a number

of advantages such as easily separable, reusable, economical, selective, environmentally benign, and mild reaction conditions furnishing the amines in excellent yield. Au-MPBen afforded secondary amines with a wide variety of aldehydes and amines very effectively. This catalyst was also applicable for the gram scale preparation of secondary amines

3A.6. Experimental Section

3A.6.1. Materials and Methods

The reagents and solvents were purchased from Alfa Aesar, Spectrochem and Merck and used without further purification. All reactions were carried out in oven dried glassware. Progress of the reactions was monitored by thin layer chromatography, while purification was done by column chromatography using neutral alumina. Solvents were removed using Buchi E.L. rotary evaporator. All measurements were done at room temperature unless otherwise stated. NMR spectra were recorded on Bruker Avance 500 NMR spectrometer at 500 MHz (^1H) and 125 MHz (^{13}C). Chemical shifts are reported in δ (ppm) relative to TMS as internal standard and CDCl_3 was used as solvent. Mass spectrum was recorded under ESI/HRMS using analyser type, orbitrap mass spectrometer (Thermo Exactive). Surface morphology was analysed using a FEI, TECNAI S Transmission Electron Microcopy (TEM).

3A.6.2 General Procedure for the Direct Reductive Amination of Aldehydes

To a mixture of aldehyde **1** (0.50 mmol) and amine **2** (0.50 mmol) in dry MeCN (1 mL), dimethylphenylsilane (0.75 mmol) and catalyst, Au-MPBen, (420 μmol %) were added and allowed to stir at room temperature under argon atmosphere. The progress of the reaction was monitored by TLC. After the reaction, the catalyst was removed by centrifugation and washed three times with MeCN. The filtrate was concentrated under vacuum and the crude product was purified by column chromatography to afford the secondary amine (**3**).

3A.6.3. Recycling Experiment

To a mixture of benzaldehyde **1** (0.50 mmol) and aniline **2** (0.50 mmol) in dry MeCN (1 mL), phenyldimethylsilane (0.75 mmol) and catalyst, Au-MPBen, (420 μmol %) were added and allowed to stir at room temperature under argon atmosphere. The progress of the reaction was monitored by TLC. After the reaction, the catalyst was removed by centrifugation and washed three times with MeCN. The filtrate was concentrated under vacuum and the crude

product was purified by column chromatography to afford N-benzylaniline (**3a**). The catalyst was reused for the second reaction after washing with MeCN. The reductive amination reaction was repeated for four more cycles by reusing the recycled catalyst from the previous reaction. After fifth run, TEM analysis of the catalyst was carried out to check for any changes in the morphology.

3A.6.4. Gram Scale Preparation of N-benzylamine and TON and TOF Calculations

To a mixture of 1 g of benzaldehyde and 0.88 g of aniline in dry MeCN (7 mL), 1.92 g of phenyldimethylsilane and catalyst, Au-MPBen, (1.05 mmol %) were added and allowed to stir at room temperature under argon atmosphere. The progress of the reaction was monitored by TLC. After the reaction, the catalyst was removed by centrifugation and washed three times with MeCN. The filtrate was concentrated under vacuum and the crude product was purified by column chromatography. N-benzylaniline (**3a**) was obtained successfully in 75 % yield (1.3 g) within 6 h.

TON and TOF values based on the total amount of gold were calculated as

$$\text{TON} = \text{total amount of product (mol)}/\text{total amount of gold (mol)}$$

$$= 0.0071/0.0000105$$

$$= 676$$

$$\text{TOF} = \text{TON}/\text{time (h)}$$

$$= 676/6$$

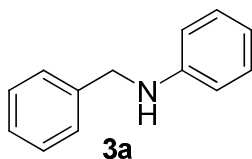
$$= 113 \text{ h}^{-1}$$

The percentage of gold atoms exposed to the surface of AuNP was calculated based on the work of Boudart and Djega-Mariadassou, which is approximately $0.9/d$, where d is the spherical metal particle diameter in nm. Thus gold nanoparticles with a diameter of 4 nm have about 22.5 % ($0.9/4 \text{ nm}$) of their atoms lying on the surface of the AuNP. As a result, adjusted TON and TOF values based on surface atoms were obtained as 3004 and 502 h^{-1} respectively.

3A.6.5. Synthetic Procedure and Spectral Characterization of Secondary Amines

3A.6.5.1. N-benzylaniline (**3a**)

To a mixture of benzaldehyde (0.50 mmol, 53 mg) and aniline (0.50 mmol, 47 mg) in dry MeCN (1 mL), dimethylphenylsilane (0.75 mmol, 102 mg) and catalyst, Au-MPBen, (420 μ mol %) were added and allowed to stir for 1 h at room temperature under argon atmosphere. After the reaction, the catalyst was removed by centrifugation and washed three times with MeCN. The filtrate was concentrated under vacuum and the crude product was purified by column chromatography (neutral alumina) to afford the N-benzylaniline (**3a**) in



¹H NMR (500 MHz, CDCl₃), δ (ppm): 7.38-7.33 (m, 4H), 7.27 (d, J = 7 Hz, 1H), 7.19-7.16 (m, 2H), 6.72 (t, J = 7.5 Hz, 1H), 6.64 (d, J = 7.5 Hz, 2H), 4.34 (s, 2H), 4.10 (brs, 1H).

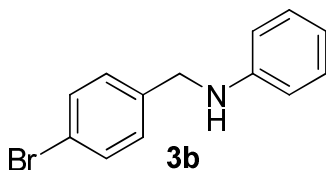
¹³C NMR (125 MHz, CDCl₃), δ (ppm): 148.2, 139.5, 129.3, 128.6, 127.5, 127.2, 117.6, 112.9, 48.4.

MS (ESI-HRMS): Calcd for C₁₃H₁₃N, [M+Na]⁺: 206.0946, Found: 206.0954.

95 % yield (87 mg).

3A.6.5.2. N-(4-bromobenzyl)aniline (**3b**)

To a mixture of 4-bromobenzaldehyde (0.50 mmol, 93 mg) and aniline (0.50 mmol, 47 mg) in dry MeCN (1 mL), dimethylphenylsilane (0.75 mmol, 102 mg) and catalyst, Au-MPBen, (420 μ mol %) were added and allowed to stir for 2 h at room temperature under argon atmosphere. After the reaction, the catalyst was removed by centrifugation and washed three times with MeCN. The filtrate was concentrated under vacuum and the crude product was purified by column chromatography (neutral alumina) to afford the N-(4-bromobenzyl)aniline (**3b**) in 93 % yield (122 mg).



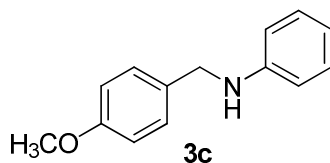
¹H NMR (500 MHz, CDCl₃), δ (ppm): 7.46-7.44 (m, 2H), 7.24 (d, *J* = 8 Hz, 2H), 7.16 (t, *J* = 8.5 Hz, 2H), 6.72 (t, *J* = 7 Hz, 1H), 6.60 (d, *J* = 7.5 Hz, 2H), 4.28 (s, 2H), 4.05 (brs, 1H).

¹³C NMR (125 MHz, CDCl₃), δ (ppm): 147.8, 138.6, 132.5, 131.7, 131.0, 129.3, 129.1, 120.9, 117.8, 112.9, 47.7.

MS (ESI-HRMS): Calcd for C₁₃H₁₂BrN, [M+H]⁺: 262.0231, Found: 262.0225.

3A.6.5.3. N-(4-methoxybenzyl)aniline (3c)

To a mixture of 4-methoxybenzaldehyde (0.50 mmol, 68 mg) and aniline (0.50 mmol, 47 mg) in dry MeCN (1 mL), dimethylphenylsilane (0.75 mmol, 102 mg) and catalyst, Au-MPBen, (420 μmol %) were added and allowed to stir for 2 h at room temperature under argon atmosphere. After the reaction, the catalyst was removed by centrifugation and washed three times with MeCN. The filtrate was concentrated under vacuum and the crude product was purified by column chromatography (neutral alumina) to afford the N-(4-methoxybenzyl)aniline (**3c**) in 92 % yield (98 mg).



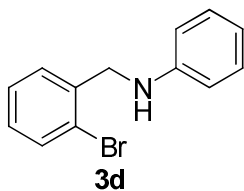
¹H NMR (500 MHz, CDCl₃), δ (ppm): 7.29 (d, *J* = 8.5 Hz, 2H), 7.19-7.16 (m, 2H), 6.89-6.87 (m, 2H), 6.73-6.70 (m, 1H), 6.64 (dd, *J*₁ = 8.5 Hz, *J*₂ = 1 Hz, 2H), 4.25 (s, 2H), 3.95 (brs, 1H), 3.79 (s, 3H).

¹³C NMR (125 MHz, CDCl₃), δ (ppm): 158.9, 148.0, 131.3, 129.2, 128.8, 117.6, 114.0, 113.0, 55.3, 47.9.

MS (ESI-HRMS): Calcd for C₁₄H₁₅NO, [M+H]⁺: 214.1232, Found: 214.1228.

3A.6.5.4. N-(2-bromobenzyl)aniline (3d)

To a mixture of 2-bromobenzaldehyde (0.50 mmol, 92 mg) and aniline (0.50 mmol, 47 mg) in dry MeCN (1 mL), dimethylphenylsilane (0.75 mmol, 102 mg) and catalyst, Au-MPBen, (420 μ mol %) were added and allowed to stir for 2 h at room temperature under argon atmosphere. After the reaction, the catalyst was removed by centrifugation and washed three times with MeCN. The filtrate was concentrated under vacuum and the crude product was purified by column chromatography (neutral alumina) to afford the N-(2-bromobenzyl)aniline (**3d**) in 94 % yield (122 mg).



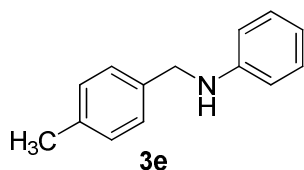
$^1\text{H NMR}$ (500 MHz, CDCl_3), δ (ppm): 7.56 (dd, $J_1 = 7.5$ Hz, $J_2 = 1$ Hz, 1H), 7.40 (dd, $J_1 = 7.5$ Hz, $J_2 = 1.5$ Hz, 1H), 7.27-7.24 (m, 1H), 7.18-7.11 (m, 3H), 6.73-6.70 (m, 1H), 6.61 (dd, $J_1 = 8.5$ Hz, $J_2 = 0.5$ Hz, 2H), 4.40 (s, 2H), 4.19 (brs, 1H).

$^{13}\text{C NMR}$ (125 MHz, CDCl_3), δ (ppm): 147.7, 138.2, 132.8, 129.3, 129.2, 128.7, 127.6, 123.3, 117.8, 113.0, 48.4.

MS (ESI-HRMS): Calcd for $\text{C}_{13}\text{H}_{12}\text{BrN}$, $[\text{M}+\text{H}]^+$: 262.0231, Found: 262.0242.

3A.6.5.5. N-(4-methylbenzyl)aniline (**3e**)

To a mixture of 4-methylbenzaldehyde (0.50 mmol, 60 mg) and aniline (0.50 mmol, 47 mg) in dry MeCN (1 mL), dimethylphenylsilane (0.75 mmol, 102 mg) and catalyst, Au-MPBen, (420 μ mol %) were added and allowed to stir for 2 h at room temperature under argon atmosphere. After the reaction, the catalyst was removed by centrifugation and washed three times with MeCN. The filtrate was concentrated under vacuum and the crude product was purified by column chromatography (neutral alumina) to afford the N-(4-methylbenzyl)aniline (**3e**) in 91 % yield (90 mg).



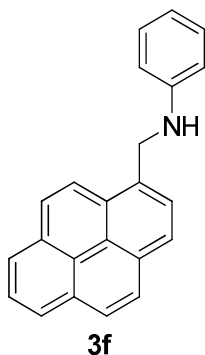
^1H NMR (500 MHz, CDCl_3), δ (ppm): 7.26 (m, 2H), 7.18-7.14 (m, 4H), 6.71 (t, $J = 5$ Hz, 1H), 6.64 (dd, $J_1 = 8.5$ Hz, $J_2 = 1$ Hz, 2H), 4.28 (s, 2H), 4.08 (brs, 1H), 2.34 (s, 3H).

^{13}C NMR (125 MHz, CDCl_3), δ (ppm): 149.1, 137.0, 129.3, 127.6, 118.0, 113.3, 48.4, 21.1.

MS (ESI-HRMS): Calcd for $\text{C}_{14}\text{H}_{15}\text{N}$, $[\text{M}]^+$: 197.1204, Found: 197.1216

3A.6.5.6. N-(pyren-1-ylmethyl)aniline (**3f**)

To a mixture of pyrene-1-carboxaldehyde (0.50 mmol, 115 mg) and aniline (0.50 mmol, 47 mg) in dry MeCN (1 mL), dimethylphenylsilane (0.75 mmol, 102 mg) and catalyst, Au-MPBen, (420 μmol %) were added and allowed to stir for 4 h at room temperature under argon atmosphere. After the reaction, the catalyst was removed by centrifugation and washed three times with MeCN. The filtrate was concentrated under vacuum and the crude product was purified by column chromatography (neutral alumina) to afford the N-(pyren-1-ylmethyl)aniline (**3f**) in 85 % yield (130 mg).



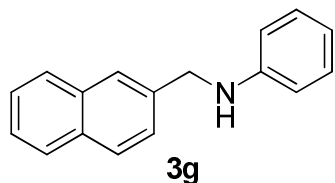
^1H NMR (500 MHz, CDCl_3), δ (ppm): 8.33 (d, $J = 9$ Hz, 1H), 8.20 (dd, $J_1 = 7.5$ Hz, $J_2 = 1.5$ Hz, 2H), 8.16-8.13 (m, 2H), 8.08-8.06 (m, 3H), 8.02 (t, $J = 7.5$ Hz, 1H), 7.24-7.22 (m, 2H), 6.79-6.75 (m, 3H), 5.00 (s, 2H), 4.15 (brs, 1H).

^{13}C NMR (125 MHz, CDCl_3), δ (ppm): 131.8, 131.3, 131.1, 130.8, 129.4, 129.1, 128.0, 127.4, 126.9, 126.0, 125.3, 125.1, 124.8, 123.0, 118.2, 113.3, 100.0, 47.0.

MS (ESI-HRMS): Calcd for $\text{C}_{23}\text{H}_{17}\text{N}$, $[\text{M}+\text{H}]^+$: 308.1439, Found: 308.1427.

3A.6.5.7. N-(naphthalen-2-ylmethyl)aniline (3g)

To a mixture of 2-naphthaldehyde (0.50 mmol, 78 mg) and aniline (0.50 mmol, 47 mg) in dry MeCN (1 mL), dimethylphenylsilane (0.75 mmol, 102 mg) and catalyst, Au-MPBen, (420 μmol %) were added and allowed to stir for 2 h at room temperature under argon atmosphere. After the reaction, the catalyst was removed by centrifugation and washed three times with MeCN. The filtrate was concentrated under vacuum and the crude product was purified by column chromatography (neutral alumina) to afford the N-(naphthalen-2-ylmethyl)aniline (**3g**) in 89 % yield (104 mg).



$^1\text{H NMR}$ (500 MHz, CDCl_3), δ (ppm): 7.84-7.79 (m, 4H), 7.54-7.45 (m, 3H), 7.19-7.16 (m, 2H), 6.72 (t, $J = 7.5$ Hz, 1H), 6.69 (d, $J = 1$ Hz, 2H), 4.50 (s, 2H), 4.17 (brs, 1H).

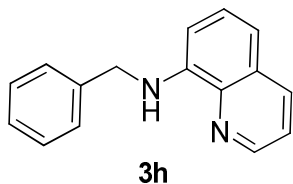
$^{13}\text{C NMR}$ (125 MHz, CDCl_3), δ (ppm): 147.2, 133.5, 132.8, 129.3, 128.4, 127.8, 127.7, 126.2, 126.0, 125.8, 125.7, 124.5, 124.0, 117.8, 113.1, 48.6.

MS (ESI-HRMS): Calcd for $\text{C}_{17}\text{H}_{15}\text{N}$, $[\text{M}+\text{H}]^+$: 234.1283, Found: 234.1275.

3A.6.5.8. N-benzylquinolin-8-amine (3h)

To a mixture of benzaldehyde (0.50 mmol, 53 mg) and 8-aminoquinoline (0.50 mmol, 72 mg) in dry MeCN (1 mL), dimethylphenylsilane (0.75 mmol, 102 mg) and catalyst, Au-MPBen, (420 μmol %) were added and allowed to stir for 3 h at room temperature under argon atmosphere. After the reaction, the catalyst was removed by centrifugation and washed three times with MeCN. The filtrate was concentrated under vacuum and the crude product was purified by column chromatography (neutral alumina) to afford the N-benzylquinolin-8-amine (**3h**) in 91 % yield (106 mg).

$^1\text{H NMR}$ (500 MHz, CDCl_3), δ (ppm): 8.72 (dd, $J_1 = 4$ Hz, $J_2 = 1.5$ Hz, 1H), 8.07 (dd, $J_1 = 8$ Hz, $J_2 = 1.5$



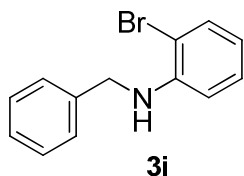
Hz, 1H), 7.44 (d, $J = 8$ Hz, 2H), 7.39-7.29 (m, 4H), 7.26 (t, $J = 7.5$ Hz, 1H), 7.06 (d, $J = 8$ Hz, 1H), 6.64 (d, $J = 7.5$ Hz, 1H), 6.60 (brs, 1H), 4.56 (s, 2H).

^{13}C NMR (125 MHz, CDCl_3), δ (ppm): 147.0, 144.7, 139.4, 136.2, 128.8, 127.9, 127.6, 127.3, 121.6, 114.3, 105.3, 47.8.

MS (ESI-HRMS): Calcd for $\text{C}_{16}\text{H}_{14}\text{N}_2$, $[\text{M}+\text{H}]^+$: 235.1235, Found: 235.1230.

3A.6.5.9. N-benzyl-2-bromoaniline (3i)

To a mixture of benzaldehyde (0.50 mmol, 53 mg) and 2-bromoaniline (0.50 mmol, 86 mg) in dry MeCN (1 mL), dimethylphenylsilane (0.75 mmol, 102 mg) and catalyst, Au-MPBen, (420 μmol %) were added and allowed to stir for 2 h at room temperature under argon atmosphere. After the reaction, the catalyst was removed by centrifugation and washed three times with MeCN. The filtrate was concentrated under vacuum and the crude product was purified by column chromatography (neutral alumina) to afford the N-benzyl-2-bromoaniline (**3i**) in 93 % yield (122 mg).



^1H NMR (500 MHz, CDCl_3), δ (ppm): 7.44 (dd, $J_1 = 8$ Hz, $J_2 = 1.5$ Hz, 1H), 7.36-7.34 (m, 4H), 7.30-7.28 (m, 1H), 7.14-7.11 (m, 1H), 6.62-6.56 (m, 2H), 4.76 (brs, 1H), 4.41 (d, $J = 4.5$ Hz, 2H).

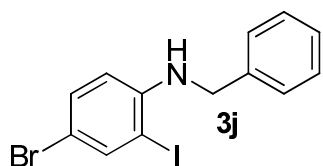
^{13}C NMR (125 MHz, CDCl_3), δ (ppm): 144.8, 138.7, 132.4, 128.7, 128.5, 127.3, 127.2, 118.0, 111.6, 109.7, 48.0.

MS (ESI-HRMS): Calcd for $\text{C}_{13}\text{H}_{12}\text{BrN}$, $[\text{M}+\text{H}]^+$: 262.0231, Found: 262.0242.

3A.6.5.10. N-benzyl-4-bromo-2-iodoaniline (3j)

To a mixture of benzaldehyde (0.50 mmol, 53 mg) and 4-bromo-2-iodoaniline (0.50 mmol, 194 mg) in dry MeCN (1 mL), dimethylphenylsilane (0.75 mmol, 102 mg) and

catalyst, Au-MPBen, (420 μmol %) were added and allowed to stir for 3 h at room temperature under argon atmosphere. After the reaction, the catalyst was removed by centrifugation and washed three times with MeCN. The filtrate was concentrated under vacuum and the crude product was purified by column chromatography (neutral alumina) to afford the N-benzyl-4-bromo-2-iodoaniline (**3j**) in 91 % yield (176 mg).



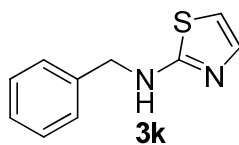
$^1\text{H NMR}$ (500 MHz, CDCl_3), δ (ppm): 7.77 (d, $J = 2$ Hz, 1H), 7.37-7.32 (m, 4H), 7.30-7.26 (m, 1H), 7.23 (dd, $J_1 = 8.5$ Hz, $J_2 = 2$ Hz, 1H), 6.38 (d, $J = 8.5$ Hz, 1H), 4.65 (brs, 1H), 4.38 (d, $J = 5.5$ Hz, 2H).

$^{13}\text{C NMR}$ (125 MHz, CDCl_3), δ (ppm): 146.3, 140.5, 138.2, 132.2, 129.0, 127.6, 127.2, 112.0, 109.0, 85.3, 48.5.

MS (ESI-HRMS): Calcd for $\text{C}_{13}\text{H}_{11}\text{BrIN}$, $[\text{M}+\text{H}]^+$: 387.9198, Found: 387.9189.

3A.6.5.11. N-benzylthiazol-2-amine (**3k**)

To a mixture of benzaldehyde (0.50 mmol, 53 mg) and 2-aminothiazole (0.50 mmol, 194 mg) in dry MeCN (1 mL), dimethylphenylsilane (0.75 mmol, 50 mg) and catalyst, Au-MPBen, (420 μmol %) were added and allowed to stir for 5 h at room temperature under argon atmosphere. After the reaction, the catalyst was removed by centrifugation and washed three times with MeCN. The filtrate was concentrated under vacuum and the crude product was purified by column chromatography (neutral alumina) to afford the N-benzylthiazol-2-amine (**3k**) in 71 % yield (67 mg).



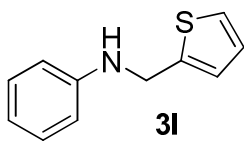
$^1\text{H NMR}$ (500 MHz, CDCl_3), δ (ppm): 7.37-7.36 (m, 4H), 7.32-7.31 (m, 2H), 7.14 (d, $J = 3.5$ Hz, 1H), 6.51 (d, $J = 4$ Hz, 1H), 4.50 (s, 2H).

$^{13}\text{C NMR}$ (125 MHz, CDCl_3), δ (ppm): 170.4, 142.5, 133.8, 128.8, 127.8, 127.6, 106.9, 49.8.

MS (ESI-HRMS): Calcd for $C_{10}H_{10}N_2S$, $[M+H]^+$: 191.0643, Found: 191.0634.

3A.6.5.12. N-(thiophen-2-ylmethyl)aniline (**3l**)

To a mixture of thiophene-2-aldehyde (0.50 mmol, 56 mg) and aniline (0.50 mmol, 47 mg) in dry MeCN (1 mL), dimethylphenylsilane (0.75 mmol, 102 mg) and catalyst, Au-MPBen, (420 μ mol %) were added and allowed to stir for 2 h at room temperature under argon atmosphere. After the reaction, the catalyst was removed by centrifugation and washed three times with MeCN. The filtrate was concentrated under vacuum and the crude product was purified by column chromatography (neutral alumina) to afford the N-(thiophen-2-yl methyl) aniline (**3l**) in 94 % yield (89 mg).



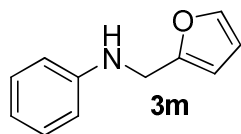
1H NMR (500 MHz, $CDCl_3$), δ (ppm): 7.22-7.18 (m, 3H), 7.02 (dd, $J_1 = 3.5$ Hz, $J_2 = 1$ Hz, 1H), 6.96 (dd, $J_1 = 5$ Hz, $J_2 = 3$ Hz, 1H), 6.75 (s, 1H), 6.69 (t, $J = 4$ Hz, 2H), 4.52 (s, 2H), 4.13 (brs, 1H).

^{13}C NMR (125 MHz, $CDCl_3$), δ (ppm): 129.3, 126.8, 125.2, 124.6, 118.3, 113.4, 43.6.

MS (ESI-HRMS): Calcd for $C_{11}H_{11}NS$, $[M+H]^+$: 190.0691, Found: 190.0687.

3A.6.5.13. N-(furan-2-ylmethyl)aniline (**3m**)

To a mixture of 2-furfuraldehyde (0.50 mmol, 48 mg) and aniline (0.50 mmol, 47 mg) in dry MeCN (1 mL), dimethylphenylsilane (0.75 mmol, 102 mg) and catalyst, Au-MPBen, (420 μ mol %) were added and allowed to stir for 2 h at room temperature under argon atmosphere. After the reaction, the catalyst was removed by centrifugation and washed three times with MeCN. The filtrate was concentrated under vacuum and the crude product was purified by column chromatography (neutral alumina) to afford N-(furan-2-yl methyl) aniline (**3m**): in 92 % yield (80 mg).



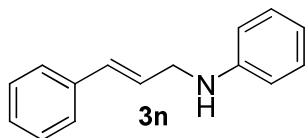
¹H NMR (500 MHz, CDCl₃), δ (ppm): 7.36 (dd, $J_1 = 2$ Hz, $J_2 = 0.5$ Hz, 1H), 7.20-7.17 (m, 2H), 6.75-6.72 (m, 1H), 6.68 (dd, $J_1 = 8.5$ Hz, $J_2 = 0.5$ Hz, 2H), 6.32-6.31 (m, 1H), 6.24 (dd, $J_1 = 3$ Hz, $J_2 = 0.5$ Hz, 1H), 4.32 (s, 2H), 4.01 (brs, 1H).

¹³C NMR (125 MHz, CDCl₃), δ (ppm): 152.7, 147.6, 141.9, 129.2, 118.0, 113.2, 110.3, 107.0, 41.5.

MS (ESI-HRMS): Calcd for C₁₁H₁₁NO, [M+H]⁺: 174.0919, Found: 174.0927.

3A.6.5.14. N-cinnamylaniline (3n)

To a mixture of cinnamaldehyde (0.50 mmol, 66 mg) and aniline (0.50 mmol, 47 mg) in dry MeCN (1 mL), dimethylphenylsilane (0.75 mmol, 102 mg) and catalyst, Au-MPBen, (420 μmol %) were added and allowed to stir for 2 h at room temperature under argon atmosphere. After the reaction, the catalyst was removed by centrifugation and washed three times with MeCN. The filtrate was concentrated under vacuum and the crude product was purified by column chromatography (neutral alumina) to afford N-cinnamylaniline (**3n**) in 92 % yield (95 mg).



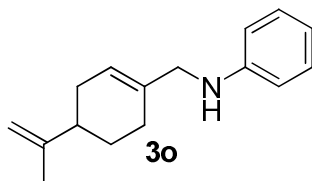
¹H NMR (500 MHz, CDCl₃), δ (ppm): 7.37 (d, $J = 7.5$ Hz, 2H), 7.31 (t, $J = 7.5$ Hz, 2H), 7.23 (s, 1H), 7.21-7.17 (m, 2H), 6.73 (s, 1H), 6.67 (d, $J = 7.5$ Hz, 2H), 6.61 (s, 1H), 6.34 (d, $J = 15.5$ Hz, 1H), 3.94 (dd, $J_1 = 5.5$ Hz, $J_2 = 1.5$ Hz, 2H), 3.88 (brs, 1H).

¹³C NMR (125 MHz, CDCl₃), δ (ppm): 148.1, 136.9, 131.6, 129.3, 128.6, 127.5, 127.1, 126.3, 117.7, 113.1, 46.2.

MS (ESI-HRMS): Calcd for C₁₅H₁₅N, [M+H]⁺: 210.1283, Found: 210.1289.

3A.6.5.15. N-((4-(prop-1-en-2-yl)cyclohex-1-enyl)methyl)aniline (3o)

To a mixture of perillaldehyde (0.50 mmol, 75 mg) and aniline (0.50 mmol, 47 mg) in dry MeCN (1 mL), dimethylphenylsilane (0.75 mmol, 102 mg) and catalyst, Au-MPBen, (420 μ mol %) were added and allowed to stir for 2 h at room temperature under argon atmosphere. After the reaction, the catalyst was removed by centrifugation and washed three times with MeCN. The filtrate was concentrated under vacuum and the crude product was purified by column chromatography (neutral alumina) to afford N-((4-(prop-1-en-2-yl)cyclohex-1-enyl)methyl)aniline (**3o**) in 91 % yield (103 mg).



^1H NMR (500 MHz, CDCl_3), δ (ppm): 7.18-7.14 (m, 2H), 6.70-6.67 (m, 1H), 6.62-6.60 (m, 2H), 5.70 (s, 1H), 4.72-4.71 (m, 2H), 3.78 (brs, 1H), 3.63 (s, 2H), 2.17-2.09 (m, 4H), 1.99-1.92 (m, 1H), 1.87-1.83 (m, 1H), 1.74 (s, 3H), 1.52-1.49 (m, 1H).

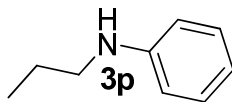
^{13}C NMR (125 MHz, CDCl_3), δ (ppm): 149.9, 134.9, 129.2, 122.4, 117.2, 112.8, 108.6, 50.0, 41.2, 30.5, 27.6, 27.2, 20.8.

MS (ESI-HRMS): Calcd for $\text{C}_{16}\text{H}_{21}\text{N}$, $[\text{M}+\text{H}]^+$: 228.1752, Found: 228.1746.

3A.6.5.16. N-propylaniline (3p)

To a mixture of propionaldehyde (0.50 mmol, 29 mg) and aniline (0.50 mmol, 47 mg) in dry MeCN (1 mL), dimethylphenylsilane (0.75 mmol, 102 mg) and catalyst, Au-MPBen, (420 μ mol %) were added and allowed to stir for 12 h at room temperature under argon atmosphere. After the reaction, the catalyst was removed by centrifugation and washed three times with MeCN. The filtrate was concentrated under vacuum and the crude product was purified by column chromatography (neutral alumina) to afford N-propylaniline (**3p**) in 80 % yield (54 mg).

^1H NMR (500 MHz, CDCl_3), δ (ppm): 7.19-7.15 (m, 2H), 7.04-7.00 (m, 1H), 6.69-6.66 (m, 2H), 3.80 (brs,



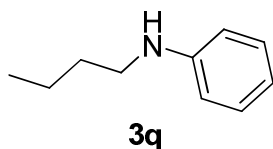
1H), 3.14-3.10 (m, 2H), 1.62-1.56 (m, 2H), 0.97 (m, 3H).

¹³C NMR (125 MHz, CDCl₃), δ (ppm): 148.9, 129.5, 129.4, 123.5, 112.6, 112.5, 51.9, 27.9, 13.9.

MS (ESI-HRMS): Calcd for C₉H₁₃N, [M+H]⁺: 136.1126, Found: 136.1142.

3A.6.5.17. N-butylaniline (3q)

To a mixture of butyraldehyde (0.50 mmol, 36 mg) and aniline (0.50 mmol, 47 mg) in dry MeCN (1 mL), dimethylphenylsilane (0.75 mmol, 102 mg) and catalyst, Au-MPBen, (420 μmol %) were added and allowed to stir for 12 h at room temperature under argon atmosphere. After the reaction, the catalyst was removed by centrifugation and washed three times with MeCN. The filtrate was concentrated under vacuum and the crude product was purified by column chromatography (neutral alumina) to afford N-propylaniline (**3p**) in 82 % yield (61 mg).



¹H NMR (500 MHz, CDCl₃), δ (ppm): 7.19 (t, 7.5Hz, 2H), 6.70 (t, 7Hz, 1H), 6.67-6.65 (m, 2H), 3.90 (brs, 1H), 3.42-3.39 (m, 2H), 1.58-1.53 (m, 4H), 0.93 (t, 7Hz, 3H).

¹³C NMR (125 MHz, CDCl₃), δ (ppm): 144.8, 127.4, 127.0, 116.4, 114.2, 49.2, 29.7, 24.6, 15.6.

MS (ESI-HRMS): Calcd for C₁₀H₁₅N, [M+H]⁺: 150.1282, Found: 150. 1273.

3A.6. References

1. M. S. Gibson, *The Chemistry of the Amino Group*, (Ed.: S. Patai) Wiley- Interscience, New York, **1968**, pp. 61; (b) A. W. Czarnik, *Acc. Chem. Res.* **1996**, *29*, 112-113; (c) J. P. Wolfe, S. Wagaw, J.-F. Marcoux, S. L. Buchwald, *Acc. Chem. Res.* **1998**, *31*, 805-818; (d) S. A. Lawrence, *Amines: Synthesis, Properties and Applications*, Cambridge University Press, Cambridge, **2004**.

2. S. Warren, P. Wyatt, *Organic Synthesis: the disconnection approach*, 2nd ed., **2008**, Oxford: Wiley-Blackwell, pp. 54
3. (a) B.-M. Park, S. Mun, J. Yun, *Adv. Synth. Catal.* **2006**, *348*, 1029-1032; (b) G. Shang, Q. Yang, X. Zhang, *Angew. Chem.* **2006**, *118*, 6508-6510; *Angew. Chem. Int. Ed.* **2006**, *45*, 6360-6362; (c) Q. Yang, G. Shang, W. Gao, J. Deng, X. Zhang, *Angew. Chem.* **2006**, *118*, 3916-3919; *Angew. Chem. Int. Ed.* **2006**, *45*, 3832-3835; (d) T. Imamoto, N. Iwadate, K. Yoshida, *Org. Lett.* **2006**, *8*, 2289-2292; (e) M. T. Reetz, O. Bondarev, *Angew. Chem.* **2007**, *119*, 4607-4610; *Angew. Chem. Int. Ed.* **2007**, *46*, 4523-4526; (f) Y.-Q. Wang, S.-M. Lu, Y.-G. Zhou, *J. Org. Chem.* **2007**, *72*, 3729-3734; (g) C. Li, C. Wang, B. Villa-Marcos, M. J. Xiao, *J. Am. Chem. Soc.* **2008**, *130*, 14450-14451; (h) Z. Han, Z. Wang, X. Zhang, K. Ding, *Angew. Chem.* **2009**, *121*, 5449-5453; *Angew. Chem. Int. Ed.* **2009**, *48*, 5345-5349; (i) W. Li, G. Hou, M. Chang, X. Zhang, *Adv. Synth. Catal.* **2009**, *351*, 3123-3127; (j) A. Baeza, A. Pfaltz, *Chem. Eur. J.* **2010**, *16*, 4003-4009.
4. (a) M. J. Palmer, M. Wills, *Tetrahedron: Asymmetry* **1999**, *10*, 2045-2061; (b) F. Spindler, H.-U. Blaser, C. Malan, B. Pugin, F. Spinder, H. Steiner, M. Studer, *Adv. Synth. Catal.* **2003**, *345*, 103-151; (c) W. Tang, X. Zhang, *Chem. Rev.* **2003**, *103*, 3029-3069; (d) T. C. Nugent, M. El-Shazly, *Adv. Synth. Catal.* **2010**, *352*, 753-819.
5. (a) M. B. Smith, J. March, *March's Advanced Organic Chemistry*; Wiley: New York, **2001**, pp. 1187; (b) A. F. Abdel-Majid, K. G. Carson, B. D. Harris, C. A. Maryanoff, R. Shath, *J. Org. Chem.* **1996**, *61*, 3849-3862; (c) R. F. Borch, H. D. Durst, *J. Am. Chem. Soc.* **1969**, *91*, 3996-3997.
6. (a) E. R. Burkhardt, B. M. Coleridge, *Tetrahedron Lett.* **2008**, *49*, 5152-5155; (b) H. Alinezhad, M. Tajbakhsh, F. Salehian, F. K. Fazli, *Tetrahedron Lett.* **2009**, *50*, 659-661; (c) W. Y. Liao, Y. F. Chen, Y. X. Liu, H. G. Duan, J. L. Petersen, X. D. Shi, *Chem. Commun.* **2009**, 6436-6438; (d) M. Tokizane, K. Sato, Sakami, Y. Imori, C. Matsuo, T. Ohta, Y. Ito, *Synthesis* **2010**, *1*, 36-42; (e) P. V. Ramachandran, P. D. Gagare, K. Sakavuyi, P. Clark, *Tetrahedron Lett.* **2010**, *51*, 3167-3169.
7. (a) H. Kato, I. Shibata, Y. Yasaka, S. Tsunoi, M. Yasuda, A. Baba, *Chem. Commun.* **2006**, *40*, 4189-4191; (b) P. D. Pham, P. Bertus, S. Legoupy, *Chem. Commun.* **2009**, *41*, 6207-6209.

8. (a) L. Xing, C. Chen, R. Zhu, B. Zhang, X. wang, Y. Hu, *Tetrahedron* **2008**, *64*, 11783-11788; (b) D. Imao, S. Fujihara, T. Yamamoto, T. Ohta, Y. Ito, *Tetrahedron* **2005**, *61*, 6988-6992.
9. (a) V. I. Tararov, A. Börner, *Synlett* **2005**, 203-211; (b) T. C. Nugenta, M. El-Shazly, *Adv. Synth. Catal.* **2010**, *352*, 753-819; (c) D. Talwar, N. P. Salguero, C. M. Robertson, J. Xiao, *Chem.-Eur. J* **2014**, *20*, 245-252.
10. (a) H. U. Blaser, H. P. Buser, H. P. Jalett, B. Pugin, F. Spindler, *Synlett* **1999**, 867-868; (b) V. I. Tararov, R. Kadyrov, T. H. Riermeier, A. Börner, *Chem. Commun.* **2000**, 1867-1868; (c) T. Gross, A. Seayad, A. Moballigh, M. Beller, *Org. Lett.* **2002**, *4*, 2055-2058; (d) Y. Chi, Y. G. Zhou, X. Zhang, *J. Org. Chem.* **2003**, *68*, 4120-4122; (e) R. Kadyrov, T. H. Riermeier, U. Dingerdissen, V. Tararov, A. Börner, *J. Org. Chem.* **2003**, *68*, 4067-4070; (f) G. D. Williams, R. A. Pike, C. E. Wade, M. Wills, *Org. Lett.* **2003**, *5*, 4227-4230; (g) D. Imao, S. Fujihara, T. Yamamoto, T. Ohta, Y. Ito, *Tetrahedron* **2005**, *61*, 6988-6992; (h) T. Bunlaksananusorn, F. Rampf, *Synlett* **2005**, *17*, 2682-2684; (i) A. Robichaud, A. N. Ajjou, *Tetrahedron Lett.* **2006**, *47*, 3633-3636; (j) L. Rubio-Pérez, F. J. Pérez-Flores, P. Sharma, L. Velasco, A. Cabrera, *Org. Lett.* **2009**, *11*, 265-268; (k) D. Steinhuebel, Y. K. Sun, K. Matsumura, N. Sayo, T. Saito, *J. Am. Chem. Soc.* **2009**, *131*, 11316-11317; (l) C. Li, B. Villa-Marcos, J. Xiao, *J. Am. Chem. Soc.* **2009**, *131*, 6967-6969; (m) B. Sreedhar, P. S. Reddy, D. K. Devi, *J. Org. Chem.* **2009**, *74*, 8806-8809.
11. S. Fleischer, S. Zhou, K. Junge, M. Beller, *Chem.-Asian J.* **2011**, *6*, 2240-2245.
12. S. Werkmeister, K. Junge, M. Beller, *Green Chem.* **2012**, *14*, 2371-2374.
13. (a) D. Dubé, A. A. Scholte, *Tetrahedron Lett.* **1999**, *40*, 2295-2298; (b) R. Apodaca, W. Xiao, *Org. Lett.* **2001**, *3*, 1745-1748; (c) B.-C. Chen, J. E. Sundeen, P. Guo, M. S. Bednarz, R. Zhao, *Tetrahedron Lett.* **2001**, *42*, 1245-1246; (d) T. Mizuta, S. Sakaguchi, Y. Ishii, *J. Org. Chem.* **2005**, *70*, 2195-2199; (e) O.-Y. Lee, K.-L. Law, C.-Y. Ho, D. Yang, *J. Org. Chem.* **2008**, *73*, 8829-8837; (f) S. Enthaler, *Catal. Lett.* **2011**, *141*, 55-61.
14. (a) M. Kitamura, D. Lee, S. Hayashi, S. Tanaka, M. Yoshimura, *J. Org. Chem.* **2002**, *67*, 8685-8687; (b) R. Kadyrov, T. H. Riermeier, *Angew. Chem.* **2003**, *115*, 5630-

- 5632; *Angew. Chem., Int. Ed.* **2003**, *42*, 5472-5474; (c) S. Ogo, K. Uehara, T. Abura, S. Fukuzumi, *J. Am. Chem. Soc.* **2004**, *126*, 3020-3021; (d) E. Byun, B. Hong, K. A. De Castro, M. Lim, H. Rhee, *J. Org. Chem.* **2007**, *72*, 9815-9817; (e) C. Wang, A. Pettman, J. Basca, J. Xiao, *Angew. Chem.* **2010**, *122*, 7710-7714; *Angew. Chem. Int. Ed.* **2010**, *49*, 7548-7552; (f) D. O'Connor, A. Lauria, S. P. Bondi, S. Sabaet, *Tetrahedron Lett.* **2011**, *52*, 129-132.
15. D. Gnanamgari, A. Moores, E. Rajaseelan, R. H. Crabtree, *Organometallics* **2007**, *26*, 1226-1230.
16. (a) S. Hoffmann, M. Nicoletti, B. List, *J. Am. Chem. Soc.* **2006**, *128*, 13074-13075; (b) R. I. Storer, D. E. Carrera, Y. Ni, D. W. C. MacMillan, *J. Am. Chem. Soc.* **2006**, *128*, 84-86; (c) A. Kumar, S. Sharma, R. A. Maurya, *Adv. Synth. Catal.* **2010**, *352*, 2227-2232.
17. (a) M. H. S. A. Hamid, P. A. Slatford, J. M. J. Williams, *Adv. Synth. Catal.* **2007**, *349*, 1555-1575; (b) T. D. Nixon, M. K. Whittlesey, J. M. J. Williams, *Dalton Trans.* **2009**, 753-762; (c) R. Yamaguchi, K. Fujita, M. Zhu, *Heterocycles* **2010**, *81*, 1093-1140; (d) G. E. Dobreiner, R. H. Crabtree, *Chem. Rev.* **2010**, *110*, 681-703; (e) G. Guillena, D. J. Ramon, M. Yus, *Chem. Rev.* **2010**, *110*, 1611-1641; (f) L. He, X.-B. Lou, J. Ni, Y.-M. Liu, Y. Cao, H.-Y. He, K.-N. Fan, *Chem.-Eur. J.* **2010**, *16*, 13965-13969; (g) C. -H. Tang, L. He. Y. -M. Liu. Y. Cao, H. -Y. He, K. -N. Fan, *Chem.-Eur.J.* **2011**, *17*, 7172-7177; (h) C. Gunanathan, D. Milstein, *Science* **2013**, *341*, 249-257; (i) L. Tang, Y. Yang, L. Wen, S. Zhang, Z. Zha, Z. Wang, *Org. Chem. Front.* **2015**, *2*, 114-118; (j) S. Bahn, S. Imm, L. Neubert, M. Zhang, H. Neumann, M. Beller, *ChemCatChem* **2011**, *3*, 1853-1864; (k) B. Cacciuttolo, O. Pascu, C. Aymonier, M. Pucheault, *Molecules* **2016**, *21*, 1042.
18. E. Byun, B. Hong, K. A. De Castro, M. Lim, H. Rhee, *J. Org. Chem.* , **2007**, *72*, 9815-9817.
19. L. Xing, C. Cheng, R. Zhu, B. Zhang, X. Wang, Y. Hu, *Tetrahedron* **2008**, *64*, 11783-11788.
20. S. Wei, Z. Dong, Z. Ma, J. Sun, J. Ma, *Catal. Commun.* **2013**, *30*, 40-44.
21. H. Yang, X. Cui, Y. Deng, F. Shi, *Synth. Commun.* **2014**, *44*, 1314-1322.
22. M. Nasrollahzadeh, *New J. Chem.*, **2014**, *38*, 5544-5550.

23. R. J. Kalbasi, O. Mazaheri, *New J. C hem.* **2016**, *40*, 9627-9637.
24. (a) P. N. Rylander, *Hydrogenation Methods*, Academic Press London, **1985**. (b) P. N. Rylander, *Catalytic Hydrogenation in Organic Synthesis*, Academic Press, New York, **1979**.
25. F. Mao, D. Sui, Z. Qi, H. Fan, R. Chen, J. Huang, *Rsc. Adv.* **2016**, *6*, 94068-94073.
26. R. Kumar, E. Gravel, A. Hagège, H. Li, D. Verma, I. N. N. Namboothiri, E. Doris, *ChemCatChem* **2013**, *5*, 3571-3575.
27. S. Liang, P. Monsen G. B. Hammond, B. Xu, *Org. Chem. Front.* **2016**, *3*, 505-509.
28. W. Yang, L. Wei, F. Yia, M. Cai, *Catal. Sci. Technol.*, **2016**, *6*, 4554-4564.
29. Z. Ke, X. Cui, F. Shi, *ACS Sustainable Chem. Eng.*, **2016**, *4*, 3921-3926.
30. M. Stratakis, H. Garcia, *Chem. Rev.*, **2012**, *112*, 4469-44.

Application of Bentonite-Gold Nanohybrid Towards Green Heterogeneous Catalysis

PART B

Bentonite-Gold Nanohybrid Catalyzed Oxidative Cross-Coupling of Ketones with Primary alcohols

3B.1. Introduction

Carbon-carbon bond forming reactions, the most essential approach to increase the molecular complexity, are utmost potent and versatile tool in synthetic organic chemistry. Carbon-carbon cross-coupling reactions, often catalyzed by the transition metals, have been extensively exploited in the areas of organic synthesis and materials science, and in the pharmaceutical, agrochemical and fine chemical industries.¹⁻⁶ Chalcones, which are α,β -unsaturated ketones, act as an important intermediate in the synthesis of a large number of pharmaceuticals and belong to one of the vital compounds as Michael acceptors in organic synthesis.^{7,8} Moreover, chalcones and their derivatives exhibit a diverse array of biological properties such as antioxidant, antimalarial, antileishmanial, anti-inflammatory, antibacterial, antimicrobial, antitumor, anticancer, radical scavenger, inhibitor of topoisomerase, *etc.*⁹⁻²² Consequently, development of efficient protocols for the synthesis of chalcone derivatives is of great interest in both academic and industrial research fields.

3B.1.1. Syntheses of α,β -Unsaturated Ketones *via* Claisen-Schmidt Condensation Reactions

Generally, α,β -unsaturated ketones are synthesized by Claisen-Schmidt condensation reactions which describe a method in which a benzaldehyde and a methyl ketone are condensed by means of acid or base catalysis. Even though chalcones are easily synthesizable, several new procedures have recently been emerged because of their

remarkable biological activities.²³ Conventionally, α,β -unsaturated ketones are synthesized by homogeneous catalysis under basic medium such as KOH, NaOH, *etc.* and acidic medium such as HCl, *p*-toluene sulfonic acid, TiCl₄, BF₃-Et₂O, *etc.*²⁴⁻²⁹ In base-mediated catalysis, the α,β -unsaturated ketone is produced from the aldol product by dehydration *via* enolate mechanism, while in acid-mediated catalysis, it is afforded *via* an enol mechanism. But these methodologies often have the disadvantages of catalyst recovery and waste-disposal problems. Chalcones were also synthesized *via* a solvent-free conditions such as grinding or microwave irradiation. The solvent-free microwave strategy avoids the influence of the solvent and decreases the by-products. It also facilitates greater flexibility for the reaction temperature and significantly reduces the reaction time.³⁰

Moreover, a variety of heterogeneous catalysts were developed for the preparation of α,β -unsaturated ketones which consent to catalyst-product separation, recyclability of the catalyst, *etc.* For instance, Pagni *et al.* developed a facile synthesis of chalcones and enones in a solvent-free aldol condensations of benzaldehyde derivatives with ketones using basic alumina as heterogeneous catalyst.³¹ In 1990, HY zeolites were employed to catalyze the Claisen-Schmidt condensation to produce *trans*- and *cis*-chalcones using acetophenone with benzaldehyde, in benzene at 80 °C together with 3,3-diphenylpropiophenone as by-product.³² Geneste and co-workers reported hydrotalcites as base catalyst for the Claisen-Schmidt condensation for the intramolecular condensation of acetonylacetone in 95 % ethanol as solvent and afforded chalcone in 20 % yield.³³ In addition, the Claisen-Schmidt condensation was performed with natural phosphate (NP) as catalyst with or without the use of a solvent.³⁴

Potassium fluoride supported on natural phosphate has a strong basic activity which could be efficiently used to promote the Claisen-Schmidt reaction of 2'-hydroxy acetophenones with benzaldehydes.³⁵ In 2005, two basic activated carbons (Na- and Cs-Norit) were used for the Claisen-Schmidt condensation between benzaldehyde and acetophenone by sonochemical irradiation and Cs-doped carbon was found to be as the optimum catalyst. A significant increase in the yield was detected when the carbon catalyst was stimulated using ultrasonic waves and offered excellent activity and selectivity towards the synthesis of several chalcones.³⁶ Yeung *et al.* reported an efficient and eco-friendly strategy to synthesize α,β -unsaturated ketones using an amino grafted zeolites by sonochemical and thermally activated methods and this simple method afforded chalcones

with nearly 100 % conversion with in 3 h.³⁷ Wu *et al.* developed a solid acidic catalyst, hydrotalcite in presence of 1,3-dibutyl-2-methylimidazoliumtetrafluoroborate ([dbmin]BF₄) as the ionic liquid to generate chalcones with a yield of 98.5 % and this method has a number of advantages such as the convenient product separation, low catalyst loading and catalyst recycling without loss of its activity.³⁸

Trabelsi *et al.* reported a solvent-free synthesis of 1,3-diaryl-2-propenones using commercial acid-clays as heterogeneous catalyst under ultrasound irradiation for the synthesis of trans-chalcones in 85-95 % yields with excellent selectivity in a short reaction time.³⁹ In 2010, Garcia and co-workers developed a simple and efficient synthetic protocol utilizing a metal-organic framework based Fe(BTC) as heterogeneous catalyst to synthesize a variety of chalcones using various aldehydes and ketones under mild reaction conditions. The catalyst could be easily recovered and reused without any loss of the product yield and could be employed for the large-scale synthesis of chalcones.⁴⁰ Moreover, Thirunarayanan and co-workers unveiled a microwave assisted sulphated titania catalyzed aldol condensation for the synthesis of some naphthalene substituted chalcones under solvent-free conditions with yields of more than 90 %.⁴¹ In 2014, Koner *et al.* employed two alkaline earth MOF compounds [Mg(HL)(H₂O)₂]_n and [Ca(H₂L)₂]_n as heterogeneous catalysts to catalyze the Claisen–Schmidt reaction and found out that [Ca(H₂L)₂]_n is more effectively catalyzed the condensation reaction compared to [Mg(HL)(H₂O)₂]_n under environmentally friendly conditions.⁴²

In 2015, a highly crystalline nanoporous metal-organic framework, IRMOF-3 was synthesized by Liu's group and used this heterogeneous catalyst for the Claisen-Schmidt reaction of benzaldehyde with acetophenone to afford chalcone as the major product. The product was obtained with a yield of 78 % under optimal reaction conditions and the catalyst was industrially viable.⁴³ Furthermore in 2017, Siddiqui *et al.* reported an efficient and recyclable silica supported copper doped phosphotungstic acid (CuPTA/SiO₂) a heterogeneous catalyst for Claisen-Schmidt condensation reaction to synthesize phenoxy pyrazolyl chalcones under solvent free conditions. The catalyst can be reused for six runs and the products were obtained in shorter time period with excellent yield.⁴⁴

3B.1.2. Syntheses of α,β -Unsaturated Ketones via Carbon-Carbon Cross-coupling Reactions

Even though a plethora of methods were reported for the synthesis of chalcones, development of highly proficient catalytic systems are significantly desirable from both synthetic and ecological point of view. One-pot synthesis is a methodology to enhance the efficacy of a reaction *via* avoiding the purification of intermediates and recently the chalcone scaffolds have been prepared by one-pot synthesis using alcohols and ketones. It is obvious that the alcohol, the greener reactant, undergoes oxidation to produce aldehyde *in situ* and the aldehyde reacts with the ketone to afford the corresponding product, α,β -unsaturated ketone. In recent times, some heterogeneous catalysts have been reported for the cross-coupling of ketones with primary alcohols to produce chalcones.

Park *et al.* reported a heterogeneous recyclable palladium catalyst, Pd/AlO(OH) which is composed of palladium nanoparticles embedded in aluminum hydroxide, for the carbon-carbon cross-coupling reaction. The C-C reaction between alcohols and ketones in the presence of oxygen to produce α,β -unsaturated ketones.⁴⁵ Uozumi and co-workers reported a water-soluble nanopalladium (nano-Pd-V) catalyst for effectively catalyzing the C-C coupling reaction of ketones and alcohols and the product was achieved in 92 % yield.⁴⁶ In 2008, Goettmann *et al.* described the synthesis and applications of sustainable catalytic systems namely mesoporous TiO₂ and TiN, to catalyze different types of aldol condensations, particularly for the alkylation of ketones with alcohols. Both mesoporous TiO₂ and TiN can be used as important alternatives to noble-metal complexes in C-C bond-forming reactions and the required reaction conditions are harsher compared to noble-metal catalysts. The synthesis of the catalyst was based on graphitic carbon nitride, which acts as the nitrogen source during nitrification of titanium oxide. It also prevents the collapse of the pores because of its favourable mechanical properties. The activity of these catalysts originated from the combination of Lewis acidic and Brønsted basic properties.⁴⁷

In 2011, Daoyong and co-workers reported an effective and simple procedure for the preparation of α,β -unsaturated ketones directly from aromatic alcohols and ketones in the presence of CrO₃ as catalyst and the product was achieved in 98 % yield. The method describes a step towards a wide range of accessible substrates and reduced cost of production.⁴⁸ Recently, Wang *et al.* employed the ceria catalyst for the cascade synthesis of

α,β -unsaturated ketones by oxidative carbon-carbon cross-coupling of ketones and primary alcohols in the absence of alkaline additives and the catalytically active sites of CeO₂ comprise surface redox and base sites. The mechanism of the reaction involves the oxidation dehydrogenation of benzyl alcohol on the redox sites and the aldol condensation of benzaldehyde and acetophenone on the base sites.⁴⁹ Although these catalysts are efficiently catalyzed the carbon-carbon bond formation, the reactions often necessitate high temperature.

In 2009, a nano-gold supported on aluminum oxyhydroxide, Au/AlO(OH) was reported as heterogeneous catalysis by Park *et al.* for the aerobic oxidation of alcohol and sequential carbon-carbon bond forming reaction with ketone to generate α,β -unsaturated ketones with the addition of 3 equiv. of Cs₂CO₃ under oxygen atmosphere at room temperature. The aromatic α,β -unsaturated ketones were afforded in 70-90 % yields, however, no desired product was obtained while using aliphatic primary alcohols as starting materials.⁵⁰ The potency of this application is to broaden the classical Claisen-Schmidt condensation using benzyl alcohols in place of aldehydes as starting materials.

3B.2. Statement of the Problem

In order to achieve greener and sustainable methodology, alcohols, which are readily accessible both from biomass and from the hydroformylation reaction of oil derivatives, can be used as the reactant in C-C coupling reactions. For that reason, catalytic systems which facilitate the production of α,β -unsaturated ketones *via* the oxidative cross-coupling of alcohols with ketones under mild reaction conditions remain as a powerful tool in synthetic organic chemistry. Although a large number of heterogeneous catalysts were reported for efficiently catalyzing the carbon-carbon bond formation reaction to produce α,β -unsaturated ketones, the reactions often necessitate high temperature. Much effort has been taken by the scientific community to develop more efficient, environmentally benign, cost-effective, selective and reusable catalytic system which affords a large substrate scope and lower catalyst loading under ambient reaction conditions. Consequent to this, in the part B section of this chapter, we present our systematic investigation on the coupling reaction of ketones with primary alcohols in the presence of Au-MPBen, the catalyst that we developed.

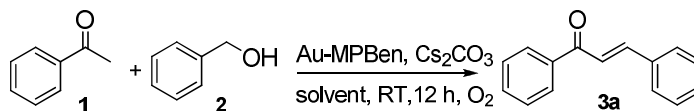
3B.3. Results and Discussion

In order to confirm the efficacy of our Au-MPBen catalyst, we selected the carbon-carbon cross-coupling reaction of ketones with primary alcohols and investigated its performance which are detailed in the following sections.

3B.3.1. Syntheses of α,β -Unsaturated Ketones Using Au-MPBen Catalyst

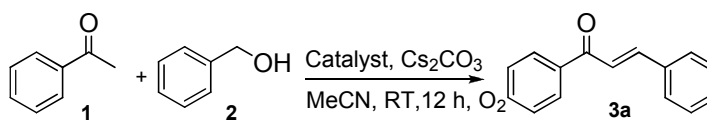
In an initial reaction, the oxidative C-C coupling reaction of ketones with primary alcohols using Au-MPBen catalyst was performed by selecting acetophenone **1** and benzyl alcohol **2** as model substrates. The reaction was carried out by reacting **1** (1.0 equiv.) and **2** (3.0 equiv.) in the presence of Cs₂CO₃ (3.0 equiv.) under oxygen atmosphere at room temperature using catalytic amount of Au-MPBen (524 μ mol %) in acetonitrile. The reaction was completed in 12 h as evidence by TLC. The catalyst was removed by centrifugation and the crude product after removal of the solvent was purified by column chromatography. The product was obtained in 90 % yield which was characterized to be the α,β -unsaturated ketone **3a**. Subsequently, we investigated the effect of different solvents in this reaction and the results are shown in Table 3B.1(entries 1-6). The reaction using acetonitrile as the solvent provided the chalcone **3a** selectively with the optimum yield of 90 % in the presence of Cs₂CO₃ as the base. Experiments using K₂CO₃, Na₂CO₃ and Cs₂CO₃ under the optimized reaction conditions revealed that Cs₂CO₃ is most efficient base for this reaction. The only by-product in this cascade reaction is water.

The supremacy of Au-MPBen catalyst in the oxidative C-C coupling was established by conducting the reaction using different catalysts such as Ben-4h (acid activated bentonite), Ben-MP (organofunctionalized bentonite), Au-Ben (gold nanoparticle-impregnated bentonite with no additional stabilizing agents) and Au-MPBen (bentonite-gold nanohybrid). The results confirmed that Ben-4h/Ben-MP catalysts (Table 3B.2, entries 1 and 2) were unable to generate the product **3a** even after 24 h. Even though Au-Ben (Table 3B.2, entry 3) catalyzed the reaction and produced the product in 80 % yield, Au NPs were found to leach out from the support which decreased its reliability as a feasible catalyst. Only Au-MPBen (Table 3B.2, entry 4) provided the α,β -unsaturated ketone **3a** effectively by oxidative C-C bond forming reaction.

Table 3B.1. Optimization of solvents for the Au-MPBen-catalyzed C-C coupling of acetophenone with benzyl alcohol

Entry	Solvent	Yield[%]
1	MeCN	90
2	Toluene	80
3	Chloroform	82
4	THF	70
5	DCM	81
6	Ethanol	65

Reaction conditions: acetophenone (0.4 mmol), benzyl alcohol (1.2 mmol), Cs₂CO₃ (1.2 mmol), room temperature, oxygen atmosphere, 12 h, solvent (2 mL), Au-MPBen (524 μmol %).

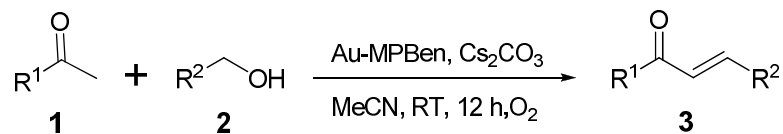
Table 3B.2. Comparison of various catalysts for the Au-MPBen-catalyzed C-C coupling of acetophenone with benzyl alcohol

Entry	Catalyst	Yield [%]
1	Ben-4h	0
2	Ben-MP	0
3	Ben-Au	75
4	Au-MPBen	90

Reaction conditions: acetophenone (0.4 mmol), benzyl alcohol (1.2 mmol), Cs₂CO₃ (1.2 mmol), room temperature, oxygen atmosphere, 12 h, MeCN (2 mL), catalyst (524 μmol %).

In order to explore the generality of our Au-MPBen catalyst in oxidative C-C coupling reaction, we extended the reaction to a wide range of ketones and primary alcohols under the optimized reaction conditions and the details are depicted in Table 3B.3. We introduced two different approaches to investigate the efficacy of Au-MPBen catalyst for the synthesis of a wide variety of α,β -unsaturated ketones. In the first approach, different ketones were allowed to react with benzyl alcohol. For instance, substituted acetophenones such as *para*-nitroacetophenone and *para*-fluoroacetophenone (entries 2 & 3) reacted with benzyl alcohol, furnishing the corresponding α,β -unsaturated ketones **3b** and **3c** in 92 and 85 % yield respectively. Besides, this methodology was found to be applicable for various heterocyclic ketones. When 2-acetylpyridine (entry 4) reacted with benzyl alcohol, the corresponding chalcone **3d** was obtained in 89 % yield. In addition, 2-acetylfuran and 2-acetylthiophene (entries 5 & 6) were converted to the corresponding products **3e** and **3f** in almost quantitative yields (91 and 93 %). The reaction is also well applicable for the cross-coupling reaction between α,β -unsaturated ketone such as benzilideneacetone and benzyl alcohol (entry 7) and afforded the desired product, dibenzilideneacetone **3g** in 82 % yield. Furthermore, in order to extend the substrate scope of the catalyst for diverse ketones, aliphatic ketones were introduced in the reaction. Cyclopropyl ethanone and 2-butanone (entries 8 & 9) provided the corresponding chalcones **3h** and **3i** in good yields (83 & 84 %).

In the second approach, various primary alcohols were allowed to react with acetophenone or its derivatives to ensure the tolerance of catalyst. 9-fluorenamethanol, the N-protecting reagent used in peptide synthesis underwent the oxidative C-C bond formation with *p*-nitroacetophenone (entry 10) and the desired product, **3j** was achieved in 91 % yield. This sequential oxidation-addition protocol is well suitable for different polycyclic primary alcohols. When 1-pyrenemethanol was employed as the alcohol component (entry 11), the reaction occurred effectively and resulted in the product **3k** in 80 % yield. Moreover, 1-naphthalenemethanol and 9-anthracenemethanol (entries 12 & 13) were converted to the corresponding α,β -unsaturated ketones **3l** and **3m** in almost quantitative yields (82 & 85). Meanwhile, the aliphatic primary alcohols (entries 14 & 15) didn't afford the desired products even after 24 h.

Table 3B.3. Substrate scope for the Au-MPBen-catalyzed C-C coupling of ketone with primary alcohol

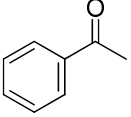
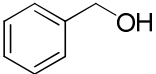
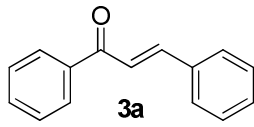
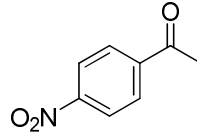
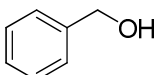
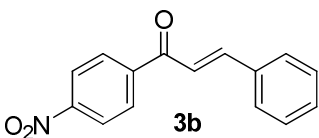
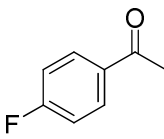
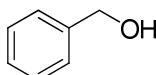
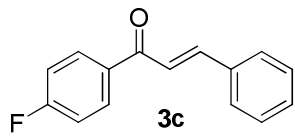
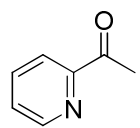
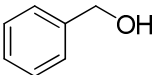
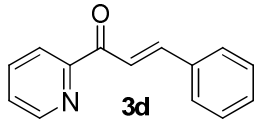
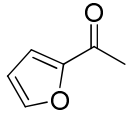
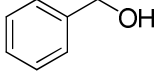
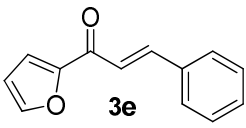
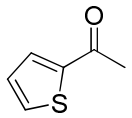
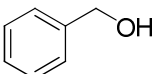
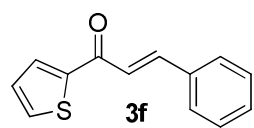
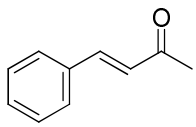
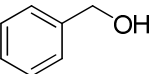
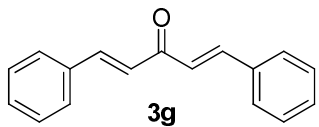
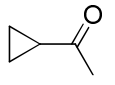
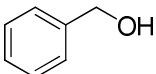
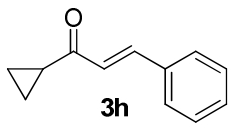
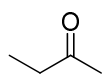
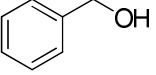
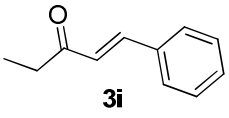
Entry	Ketone 1	Alcohol 2	Product 3	Yield[%]
1				90
2				92
3				85
4				89
5				91
6				93
7				82
8				83
9				84

Table 3B.3. Continued...

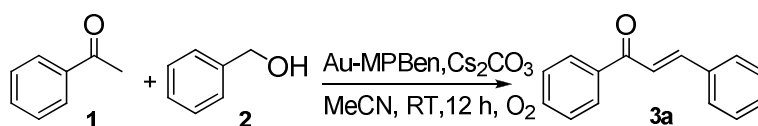
Entry	Ketone 1	Alcohol 2	Product 3	Yield[%]
10				91
11				80
12				82
13				85
14			No reaction	0
15			No reaction	0

Reaction conditions: ketones (0.4 mmol), primary alcohols (1.2 mmol), Cs₂CO₃ (1.2 mmol), room temperature, oxygen atmosphere, 12 h, MeCN (2 mL), Au-MPBen (524 μmol %).

3B.3.2. Recycling Experiment

The recyclability of Au-MPBen catalyst for the oxidative C-C coupling of ketones with primary alcohols was examined by performing the reaction using acetophenone and benzyl alcohol. The catalyst was recovered by centrifugation, reused in five successive runs (Table 3B.4). Even after the fifth run, the efficiency of the catalyst remained almost unchanged. This observation confirmed the efficacy and stability of Au-MPBen nanohybrid catalyst.

Table 3B.4. Recycling experiments with the Au-MPBen catalyst

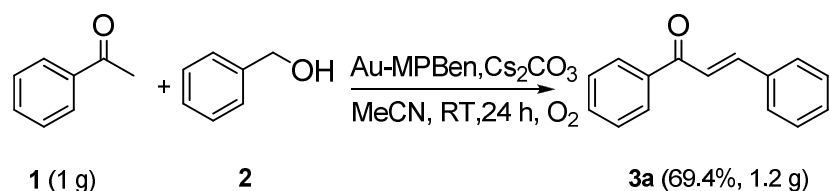


Entry	Catalyst	Yield [%]
1	Fresh	90
2	Reuse 1	88
3	Reuse 2	89
4	Reuse 3	87
5	Reuse 4	89

Reaction conditions: acetophenone (0.4 mmol), benzyl alcohol (1.2 mmol), Cs₂CO₃ (1.2 mmol), room temperature, oxygen atmosphere, 12 h, MeCN (2 mL), Au-MPBen (524 μmol %).

3B.3.3. Gram Scale Synthesis

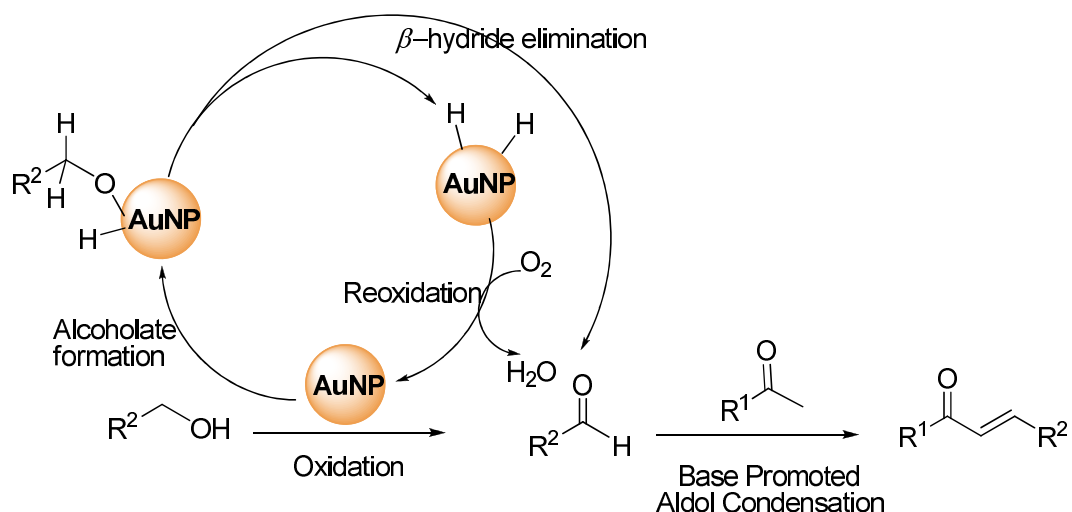
The applicability of Au-MPBen catalyst towards the gram scale synthesis of α,β -unsaturated ketones was studied by selecting acetophenone and benzyl alcohol as model substrates (Scheme 3B.1). When 1 g of acetophenone **1** was treated with benzyl alcohol **2** in the presence of Au-MPBen (1.572 mmol %) and Cs₂CO₃ as base, the product **3a** (1.2 g) was isolated in 69.4 % yield within 24 h where the turnover number (TON) and turnover frequency (TOF) were calculated as 367 and 15 h⁻¹, respectively. But the adjusted TON and TOF values according to the percentage of gold atoms (not the actual gold loading) that are exposed to the substrate reached to 1629 and 67 h⁻¹, respectively.



Scheme 3B.1. Gram-scale synthesis of α,β -unsaturated ketone **3a** using Au-MPBen catalyst

3B.4. Mechanistic Pathway

The proposed reaction mechanism for Au-MPBen catalyzed oxidative C-C coupling reaction of primary alcohols with ketones is exemplified in scheme 3B.2. The important steps that lead to the formation of α,β -unsaturated ketones involve the oxidative dehydrogenation of alcohol followed by aldol condensation of aldehyde with ketone. The oxidation reaction of alcohols starts with the adsorption of alcohol molecules on the surface of gold nanoparticles to generate metal alcoholates. Subsequently, metal alcoholate species undergo β -hydride elimination and produce the active carbonyl product, aldehyde and a metal-hydride intermediate. Then metal-hydride is oxidized by oxygen to restore the gold surface and water is produced as the by-product. Eventually, the base, Cs_2CO_3 catalyzed aldol condensation occurs between aldehyde and ketone to generate the desired α,β -unsaturated ketone.



Scheme 3B.2. Oxidative cross-coupling reaction of primary alcohols with ketones catalyzed by Au-MPBen

3B.5. Conclusion

In conclusion, we have explored an efficient, green and sustainable method for the oxidative C–C coupling of ketones and primary alcohols to produce α,β -unsaturated ketones using a bentonite-gold nano hybrid (Au-MPBen) as a heterogeneous catalyst in the presence of Cs_2CO_3 as base. The cascade C-C bond formation strategy using our Au-MPBen catalyst is environmentally benign, economical, selective, easily separable and reusable, and works under mild reaction conditions. This nanohybrid system afforded a wide variety of α,β -unsaturated ketones in excellent yield with water as the only byproduct. In addition, this heterogeneous catalyst was well applicable for the gram scale synthesis of α,β -unsaturated ketones.

3B.6. Experimental Section

3B.6.1. Materials and Methods

The reagents and solvents were purchased from Sigma Aldrich, Alfa Aesar, Spectrochem and Merck, and used without further purification. All reactions were carried out in oven dried glassware. Progress of the reactions was monitored by thin layer chromatography, while purification was done by column chromatography using silica 100-200 mesh. Solvents were removed using Buchi E.L. rotary evaporator. All measurements were done at room temperature unless otherwise stated. NMR spectra were recorded on Bruker Avance 500 NMR spectrometer at 500 MHz (^1H) and 125 MHz (^{13}C). Chemical shifts are reported in δ (ppm) relative to TMS as internal standard and CDCl_3 was used as solvent. Mass spectrum was recorded under ESI/HRMS using analyser type, orbitrap mass spectrometer (Thermo Exactive). Surface morphology was analyzed using a FEI, TECNAI S Transmission Electron Microscope (TEM).

3B.6.2. General Procedure for the Oxidative C–C Coupling of Ketones and Primary Alcohols

To a mixture of ketone **1** (0.40 mmol) and primary alcohol **2** (1.2 mmol) in MeCN (2 mL), Cs_2CO_3 (1.2 mmol) and the catalyst, Au-MPBen, (524 μmol %) were added and the mixture was allowed to stir at room temperature under oxygen atmosphere. The progress of the reaction was monitored by TLC. After completion of the reaction, the catalyst was removed by centrifugation and washed three times with MeCN. The filtrate was concentrated

under vacuum and the crude product was purified by column chromatography (silica 100-200 mesh) to afford α, β -unsaturated ketone **3a**.

3B.6.3. Recycling Experiment

To a mixture of acetophenone **1** (0.40 mmol, 49 mg) and benzyl alcohol **2** (1.2 mmol, 130 mg) in MeCN (2 mL), Cs₂CO₃ (1.2 mmol, 391 mg) and the catalyst, Au-MPBen, (524 μ mol %) were added and the mixture was allowed to stir at room temperature under oxygen atmosphere. The progress of the reaction was monitored by TLC. After completion of the reaction, the catalyst was removed by centrifugation and washed three times with MeCN. The filtrate was concentrated under vacuum and the crude product was purified by column chromatography to afford α, β -unsaturated ketone **3a**. The catalyst was reused for the second reaction after washing with MeCN. The C-C coupling reaction was repeated for four more cycles by reusing the recycled catalyst from the previous reaction.

3B.6.4. Gram-Scale Preparation of Chalcone (3a) and TON and TOF Calculations

To a mixture of 1 g of acetophenone and 2.7 g of benzyl alcohol in MeCN (10 mL), 8.1 g of Cs₂CO₃ and the catalyst, Au-MPBen, (1.572 mmol %) were added and the mixture was allowed to stir at room temperature under oxygen atmosphere. The progress of the reaction was monitored by TLC. After completion of the reaction, the catalyst was removed by centrifugation and washed three times with MeCN. The filtrate was concentrated under vacuum and the crude product was purified by column chromatography. α, β -unsaturated ketone **3a** was obtained successfully within 24 h; yield: 1.2 g (69.4 %).

Based on the total amount of gold TON and TOF values were calculated as follows:

$$\begin{aligned} \text{TON} &= \text{total amount of product (mol)}/\text{total amount of gold (mol)} \\ &= 0.0058/0.00001572 = 367 \end{aligned}$$

$$\text{TOF} = \text{TON}/\text{time (h)} = 367/24 = 15 \text{ h}^{-1}$$

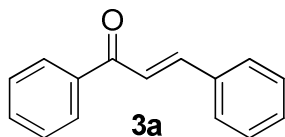
Based on the work of Boudart and Djega-Mariadassou, the fraction of gold atoms exposed to the surface of AuNPs was calculated which is approximately $0.9/d$, where d is the diameter of spherical metal nanoparticle in nm. Accordingly, AuNPs with a diameter of 4 nm

have about 22.5 % (0.9/4 nm) of their atoms lying on the surface of the AuNP. Consequently, based on the surface atoms adjusted TON and TOF values were achieved as 1629 and 67 h⁻¹, respectively.

3B.6.5. Synthetic Procedure and Spectral Characterization of α,β -Unsaturated Ketones⁵¹⁻⁵⁴

3B.6.5.1. 1,3-diphenylprop-2-en-1-one (3a)

To a mixture of acetophenone (0.40 mmol, 48 mg) and benzyl alcohol (1.2 mmol, 130 mg) in MeCN (2 mL), Cs₂CO₃ (1.2 mmol, 390 mg) and the catalyst, Au-MPBen, (524 μ mol %) were added and the mixture was allowed to stir for 12 h at room temperature under oxygen atmosphere. After the reaction, the catalyst was removed by centrifugation and washed three times with MeCN. The filtrate was concentrated under vacuum and the crude product was purified by column chromatography to afford the product **3a** in 90 % yield (75 mg).



¹H NMR (500 MHz, CDCl₃), δ (ppm): 8.04-8.01 (m, 2H), 7.82 (d, J = 15.7 Hz, 1H), 7.67-7.64 (m, 2H), 7.59 (m, J = 6.7, 4.0, 1.3 Hz, 1H), 7.52 (ddd, J = 9.1, 8.0, 7.0 Hz, 3H), 7.44-7.41 (m, 3H).

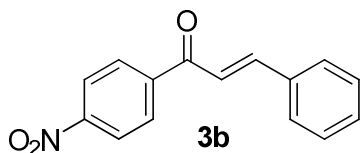
¹³C NMR (125 MHz, CDCl₃), δ (ppm): 189.6, 143.9, 138.4, 137.2, 133.9, 131.8, 129.5, 128.4, 128.0, 127.9, 127.6, 127.5, 127.4, 127.3, 127.2, 121.1.

MS (ESI-HRMS): Calcd for C₁₅H₁₂O, [M+H]⁺: 209.0966, Found: 209.0962.

3B.6.5.2. 1-(4-nitrophenyl)-3-phenylprop-2-en-1-one (3b)

To a mixture of 4-nitroacetophenone (0.40 mmol, 66 mg) and benzyl alcohol (1.2 mmol, 130 mg) in MeCN (2 mL), Cs₂CO₃ (1.2 mmol, 390 mg) and the catalyst, Au-MPBen, (524 μ mol %) were added and the mixture was allowed to stir for 12 h at room temperature under oxygen atmosphere. After the reaction, the catalyst was removed by centrifugation and washed three times with MeCN. The filtrate was concentrated under vacuum and the crude

product was purified by column chromatography to afford the product **3b** in 92 % yield (93 mg).



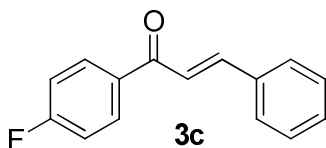
¹H NMR (500 MHz, CDCl₃), δ (ppm): 8.39-8.34 (m, 2H), 8.16-8.13 (m, 2H), 7.85 (d, *J* = 15.7 Hz, 1H), 7.67 (dd, *J* = 7.2, 2.2 Hz, 2H), 7.51-7.43 (m, 4H).

¹³C NMR (125 MHz, CDCl₃), δ (ppm): 189.1, 146.9, 141.9, 134.3, 131.3, 129.9, 129.5, 129.1, 128.7, 128.4, 125.6, 123.9, 121.4.

MS (ESI-HRMS): Calcd for C₁₅H₁₁NO₃, [M+H]⁺: 254.0817, Found: 254.0815.

3B.6.5.3. 1-(4-fluorophenyl)-3-phenylprop-2-en-1-one (**3c**)

To a mixture of 4-fluoroacetophenone (0.40 mmol, 55 mg) and benzyl alcohol (1.2 mmol, 130 mg) in MeCN (2 mL), Cs₂CO₃ (1.2 mmol, 390 mg) and the catalyst, Au-MPBen, (524 μmol %) were added and the mixture was allowed to stir for 12 h at room temperature under oxygen atmosphere. After the reaction, the catalyst was removed by centrifugation and washed three times with MeCN. The filtrate was concentrated under vacuum and the crude product was purified by column chromatography to afford the product **3c** in 85 % yield (77 mg).



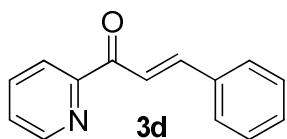
¹H NMR (500 MHz, CDCl₃), δ (ppm): 8.07 (dd, *J* = 8.9, 5.4 Hz, 2H), 7.82 (d, *J* = 15.7 Hz, 1H), 7.67-7.63 (m, 2H), 7.51 (d, *J* = 15.7 Hz, 1H), 7.45-7.41 (m, 3H), 7.19 (t, *J* = 8.7 Hz, 2H).

¹³C NMR (125 MHz, CDCl₃), δ (ppm): 193.4, 165.6 (d, *J* = 290.2 Hz, CF), 145.1, 139.4, 131.7 (*J* = 9.5 Hz, CH), 131.1 (*J* = 9.2 Hz, CH), 130.7, 129.4, 128.3, 126.5, 121.6, 115.8, 115.7 (*J* = 21.9 Hz, CH).

MS (ESI-HRMS): Calcd for C₁₅H₁₁FO, [M+H]⁺: 227.0872, Found: 227.0867.

3B.6.5.4. 3-phenyl-1-(pyridin-2-yl)prop-2-en-1-one (3d)

To a mixture of 2-acetylpyridine (0.40 mmol, 48 mg) and benzyl alcohol (1.2 mmol, 130 mg) in MeCN (2 mL), Cs₂CO₃ (1.2 mmol, 390 mg) and the catalyst, Au-MPBen, (524 μmol %) were added and the mixture was allowed to stir for 12 h at room temperature under oxygen atmosphere. After the reaction, the catalyst was removed by centrifugation and washed three times with MeCN. The filtrate was concentrated under vacuum and the crude product was purified by column chromatography to afford the product **3d** in 89 % yield (74 mg).



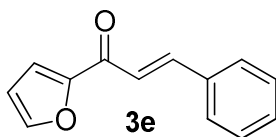
¹H NMR (500 MHz, CDCl₃), δ (ppm): 8.76-8.74 (m, 1H), 8.31 (d, *J* = 16.0 Hz, 1H), 8.20 (dt, *J* = 7.9, 1.0 Hz, 1H), 7.95 (d, *J* = 16.1 Hz, 1H), 7.88 (td, *J* = 7.7, 1.7 Hz, 1H), 7.74 (dd, *J* = 6.5, 3.1 Hz, 2H), 7.51-7.49 (m, 1H), 7.42 (dd, *J* = 5.0, 1.9 Hz, 3H).

¹³C NMR (125 MHz, CDCl₃), δ (ppm): 189.5, 154.3, 148.9, 144.8, 137.0, 130.6, 130.1, 128.9, 128.1, 126.9, 123.0, 120.9.

MS (ESI-HRMS): Calcd for C₁₄H₁₁NO, [M+H]⁺: 210.0919, Found: 210.0914.

3B.6.5.5. 1-(furan-2-yl)-3-phenylprop-2-en-1-one (3e)

To a mixture of 2-acetylfuran (0.40 mmol, 44 mg) and benzyl alcohol (1.2 mmol, 130 mg) in MeCN (2 mL), Cs₂CO₃ (1.2 mmol, 390 mg) and the catalyst, Au-MPBen, (524 μmol %) were added and the mixture was allowed to stir for 12 h at room temperature under oxygen atmosphere. After the reaction, the catalyst was removed by centrifugation and washed three times with MeCN. The filtrate was concentrated under vacuum and the crude product was purified by column chromatography to afford the product **3e** in 91 % yield (72 mg).



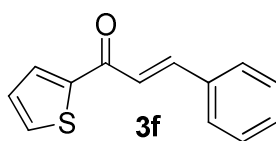
^1H NMR (500 MHz, CDCl_3), δ (ppm): 7.89 (d, J = 15.8 Hz, 1H), 7.67-7.64 (m, 3H), 7.48-7.40 (m, 4H), 7.34-7.30 (m, 2H).

^{13}C NMR (125 MHz, CDCl_3), δ (ppm): 173.6, 158.5, 152.9, 146.7, 139.0, 135.1, 130.5, 128.9, 128.3, 124.5, 117.0, 114.0.

MS (ESI-HRMS): Calcd for $\text{C}_{13}\text{H}_{10}\text{O}_2$, $[\text{M}+2\text{H}]^{2+}$: 200.0837, Found: 200.0857.

3B.6.5.6. 3-phenyl-1-(thiophen-2-yl)prop-2-en-1-one (3f)

To a mixture of 2-acetylthiophene (0.40 mmol, 50 mg) and benzyl alcohol (1.2 mmol, 130 mg) in MeCN (2 mL), Cs_2CO_3 (1.2 mmol, 390 mg) and the catalyst, Au-MPBen, (524 μmol %) were added and the mixture was allowed to stir for 12 h at room temperature under oxygen atmosphere. After the reaction, the catalyst was removed by centrifugation and washed three times with MeCN. The filtrate was concentrated under vacuum and the crude product was purified by column chromatography to afford the product **3f** in 93 % yield (79 mg).



^1H NMR (500 MHz, CDCl_3), δ (ppm): 7.86 (d, J = 15.3 Hz, 1H), 7.70 (d, J = 3.8 Hz, 3H), 7.65-7.63 (m, 3H), 7.13 (dd, J = 4.7, 4.0 Hz, 3H).

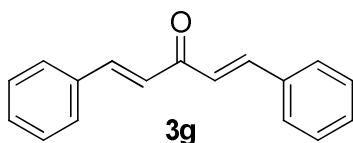
^{13}C NMR (125 MHz, CDCl_3), δ (ppm): 190.8, 144.6, 140.5, 133.8, 133.1, 132.5, 129.8, 129.0, 128.5, 128.2, 125.4, 121.6.

MS (ESI-HRMS): Calcd for $\text{C}_{13}\text{H}_{10}\text{OS}$, $[\text{M}+\text{H}]^+$: 215.0530, Found: 215.0528.

3B.6.5.7. 1,5-diphenylpenta-1,4-dien-3-one (3g)

To a mixture of benzilideneacetone (0.40 mmol, 58 mg) and benzyl alcohol (1.2 mmol, 130 mg) in MeCN (2 mL), Cs_2CO_3 (1.2 mmol, 390 mg) and the catalyst, Au-MPBen, (524 μmol %) were added and the mixture was allowed to stir for 12 h at room temperature under oxygen atmosphere. After the reaction, the catalyst was removed by centrifugation and

washed three times with MeCN. The filtrate was concentrated under vacuum and the crude product was purified by column chromatography to afford the product **3g** in 82 % yield (76 mg).



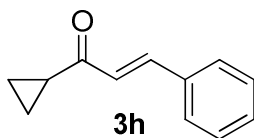
¹H NMR (500 MHz, CDCl₃), δ (ppm): 7.57-7.53 (m, 2H), 7.48 (dd, *J* = 7.1, 1.9 Hz, 4H), 7.42-7.40 (m, 2H), 7.35 (d, *J* = 1.6 Hz, 2H), 6.91 (d, *J* = 12.7 Hz, 2H), 6.18 (d, *J* = 12.7 Hz, 2H).

¹³C NMR (125 MHz, CDCl₃), δ (ppm): 188.9, 143.4, 139.9, 130.5, 129.6, 129.4, 129.0, 128.9, 128.4, 128.3, 127.2, 126.7, 125.4.

MS (ESI-HRMS): Calcd for C₁₇H₁₄O, [M+H]⁺: 235.1123, Found: 235.1118.

3B.6.5.8. 1-cyclopropyl-3-phenylprop-2-en-1-one (**3h**)

To a mixture of cyclopropylethanone (0.40 mmol, 34 mg) and benzyl alcohol (1.2 mmol, 130 mg) in MeCN (2 mL), Cs₂CO₃ (1.2 mmol, 390 mg) and the catalyst, Au-MPBen, (524 μmol %) were added and the mixture was allowed to stir for 12 h at room temperature under oxygen atmosphere. After the reaction, the catalyst was removed by centrifugation and washed three times with MeCN. The filtrate was concentrated under vacuum and the crude product was purified by column chromatography to afford the product **3h** in 83 % yield (58 mg).



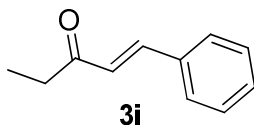
¹H NMR (500 MHz, CDCl₃), δ (ppm): 7.62 (d, *J* = 16.1 Hz, 1H), 7.57 (dd, *J* = 6.7, 2.9 Hz, 2H), 7.40 (dd, *J* = 4.9, 1.8 Hz, 3H), 6.88 (d, *J* = 16.1 Hz, 1H), 2.29-2.22 (m, 1H), 1.17 (dt, *J* = 7.0, 3.4 Hz, 2H), 1.00-0.97 (m, 2H).

¹³C NMR (125 MHz, CDCl₃), δ (ppm): 200.1, 142.0, 134.7, 130.3, 128.9, 128.3, 126.5, 19.7, 11.4.

MS (ESI-HRMS): Calcd for C₁₂H₁₂O, [M+H]⁺: 173.0966, Found: 173.0961.

3B.6.5.9. 1-phenylpent-1-en-3-one (3i)

To a mixture of 2-butanone (0.40 mmol, 29 mg) and benzyl alcohol (1.2 mmol, 130 mg) in MeCN (2 mL), Cs₂CO₃ (1.2 mmol, 390 mg) and the catalyst, Au-MPBen, (524 μmol %) were added and the mixture was allowed to stir for 12 h at room temperature under oxygen atmosphere. After the reaction, the catalyst was removed by centrifugation and washed three times with MeCN. The filtrate was concentrated under vacuum and the crude product was purified by column chromatography to afford the product **3i** in 84 % yield (54 mg).



¹H NMR (500 MHz, CDCl₃), δ (ppm): 7.97 (dd, *J* = 8.3, 1.3 Hz, 1H), 7.55 (t, *J* = 2.9 Hz, 2H), 7.41-7.38 (m, 3H), 6.75 (d, *J* = 16.2 Hz, 1H), 2.71 (q, *J* = 7.3 Hz, 2H), 1.18 (t, *J* = 7.3 Hz, 3H).

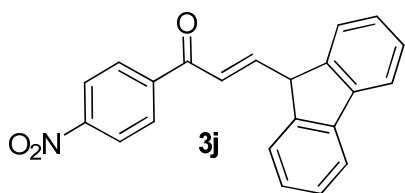
¹³C NMR (125 MHz, CDCl₃), δ (ppm): 201.0, 142.2, 133.1, 130.4, 128.9, 128.2, 126.0, 31.6, 14.1.

MS (ESI-HRMS): Calcd for C₁₁H₁₂O, [M+H]⁺: 161.0966, Found: 161.0963.

3B.6.5.10. 3-(9H-fluoren-9-yl)-1-(4-nitrophenyl)prop-2-en-1-one (3j)

To a mixture of 4-nitroacetophenone (0.40 mmol, 66 mg) and 9-fluorenamethanol (1.2 mmol, 235 mg) in MeCN (2 mL), Cs₂CO₃ (1.2 mmol, 390 mg) and the catalyst, Au-MPBen, (524 μmol %) were added and the mixture was allowed to stir for 12 h at room temperature under oxygen atmosphere. After the reaction, the catalyst was removed by centrifugation and washed three times with MeCN. The filtrate was concentrated under vacuum and the crude product was purified by column chromatography to afford the product **3j** in 91 % yield (124 mg).

¹H NMR (500 MHz, CDCl₃), δ (ppm): 7.74 (d, *J* = 7.5 Hz, 1H), 7.69 (d, *J* = 7.5 Hz, 1H), 7.55-7.44 (m, 1H), 7.37 (td, *J* = 7.4, 1.0 Hz, 1H), 7.30 (td, *J* = 7.5, 1.1 Hz, 1H), 7.24-6.34 (m, 8H), 6.08 (s, 1H), 4.19-3.84 (m, 1H).

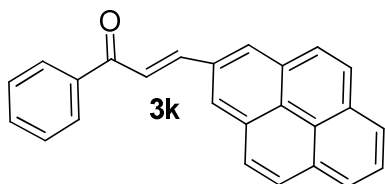


^{13}C NMR (125 MHz, CDCl_3), δ (ppm): 194.0, 144.4, 142.1, 140.5, 140.3, 139.9, 134.7, 134.2, 129.4, 129.3, 129.1, 127.0, 126.9, 126.5, 125.9, 125.7, 124.9, 124.4, 120.3, 119.6, 29.7.

MS (ESI-HRMS): Calcd for $\text{C}_{22}\text{H}_{15}\text{NO}_3$, $[\text{M}+\text{H}]^+$: 342.1130, Found: 342.1357.

3B.6.5.11. 3-(9H-fluoren-9-yl)-1-(4-nitrophenyl)prop-2-en-1-one (3k)

To a mixture of acetophenone (0.40 mmol, 48 mg) and 1-pyrenemethanol (1.2 mmol, 279 mg) in MeCN (2 mL), Cs_2CO_3 (1.2 mmol, 390 mg) and the catalyst, Au-MPBen, (524 μmol %) were added and the mixture was allowed to stir for 12 h at room temperature under oxygen atmosphere. After the reaction, the catalyst was removed by centrifugation and washed three times with MeCN. The filtrate was concentrated under vacuum and the crude product was purified by column chromatography to afford the product **3k** in 80 % yield (106 mg).



^1H NMR (500 MHz, CDCl_3), δ (ppm): 8.37 (d, $J = 9.2$ Hz, 2H), 8.20 (t, $J = 6.8$ Hz, 4H), 8.10 (d, $J = 9.2$ Hz, 2H), 8.06 – 8.04 (m, 4H), 8.02 (t, $J = 6.8$ Hz, 2H), 7.66 (d, $J = 7.8$ Hz, 2H).

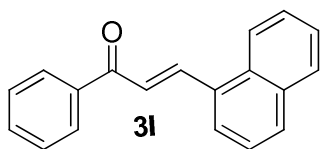
^{13}C NMR (125 MHz, CDCl_3), δ (ppm): 193.1, 134.4, 131.5, 130.9, 130.2, 129.2, 127.8, 127.7, 127.6, 126.0, 125.1, 125.0, 123.4, 123.1.

MS (ESI-HRMS): Calcd for $\text{C}_{25}\text{H}_{16}\text{O}$, $[\text{M}+\text{H}]^+$: 333.1279, Found: 333.1272.

3B.6.5.12. 3-(naphthalen-1-yl)-1-phenylprop-2-en-1-one (3l)

To a mixture of acetophenone (0.40 mmol, 48 mg) and 1-naphthalenemethanol (1.2 mmol, 190 mg) in MeCN (2 mL), Cs_2CO_3 (1.2 mmol, 390 mg) and the catalyst, Au-MPBen, (524 μmol %) were added and the mixture was allowed to stir for 12 h at room temperature under oxygen atmosphere. After the reaction, the catalyst was removed by centrifugation and washed three times with MeCN. The filtrate was concentrated under vacuum and the crude

product was purified by column chromatography to afford the product **3l** in 82 % yield (85 mg).



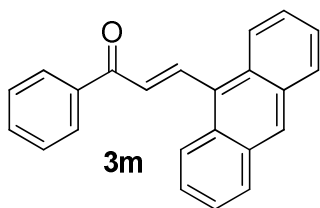
$^1\text{H NMR}$ (500 MHz, CDCl_3), δ (ppm): 9.26 (d, $J = 9.2$ Hz, 2H), 8.12 (d, $J = 8.2$ Hz, 2H), 8.01 (dd, $J = 7.0, 1.3$ Hz, 2H), 7.94 (d, $J = 8.2$ Hz, 2H), 7.72-7.66 (m, 2H), 7.65 (dd, $J = 8.2, 7.1$ Hz, 2H), 7.62-7.59 (m, 2H).

$^{13}\text{C NMR}$ (125 MHz, CDCl_3), δ (ppm): 193.6, 136.7, 135.3, 133.8, 133.0, 131.4, 130.5, 129.7, 129.1, 128.6, 128.5, 128.4, 128.2, 127.0, 124.9.

MS (ESI-HRMS): Calcd for $\text{C}_{19}\text{H}_{14}\text{O}$, $[\text{M}+\text{H}]^+$: 259.1123, Found: 259.1118.

3B.6.5.13. 3-(anthracen-9-yl)-1-phenylprop-2-en-1-one (**3m**)

To a mixture of acetophenone (0.40 mmol, 48 mg) and 1-anthracenemethanol (1.2 mmol, 250 mg) in MeCN (2 mL), Cs_2CO_3 (1.2 mmol, 390 mg) and the catalyst, Au-MPBen, (524 μmol %) were added and the mixture was allowed to stir for 12 h at room temperature under oxygen atmosphere. After the reaction, the catalyst was removed by centrifugation and washed three times with MeCN. The filtrate was concentrated under vacuum and the crude product was purified by column chromatography to afford the product **3m** in 85 % yield (105 mg).



$^1\text{H NMR}$ (500 MHz, CDCl_3), δ (ppm): 9.00 (d, $J = 9.0$ Hz, 2H), 8.72 (s, 1H), 8.47 (s, 1H), 8.28 (d, $J = 8.7$ Hz, 2H), 8.08 (d, $J = 8.6$ Hz, 2H), 8.00 (d, $J = 8.3$ Hz, 2H), 7.71-7.67 (m, 2H), 7.42 (m, 4H).

$^{13}\text{C NMR}$ (125 MHz, CDCl_3), δ (ppm): 193.1, 143.9, 142.9, 138.6, 138.2, 135.3, 134.2, 132.2, 131.1, 129.3, 129.2, 128.5, 127.7, 127.6, 127.3, 125.9, 125.7, 125.5, 124.1, 123.6, 123.5, 122.3.

MS (ESI-HRMS): Calcd for $\text{C}_{23}\text{H}_{16}\text{O}$, $[\text{M}+\text{H}]^+$: 309.1279, Found: 309.1271.

3B.7. References

1. de Meijere, F. Diederich, Eds. ; *Metal-Catalyzed Cross-Coupling Reactions* , Vol.1 and 2, 2nd ed.: Wiley-VCH: Weinheim, New York, **2004**.
2. J. Magano, J. R. Dunetz, *Chem. Rev.* **2011**, *111*, 2177-2250.
3. C. Torborg, M. Beller, *Adv. Synth. Catal.* **2009**, *351*, 3027-3043.
4. K. C. Nicolaou, P. G. Bulger, D. Sarlah, *Angew. Chem. Int. Ed.* **2005**, *44*, 4442-4489.
5. J.-P. Corbet, G. Mignani, *Chem. Rev.* **2006**, *106*, 2651-2710.
6. S. D. Roughley, A. M. Jordan, *J. Med. Chem.* **2011**, *54*, 3451-3479.
7. M. Loudon, *Organic Chemistry* 5th Ed. Roberts & Company Publishers, **2009**, 1047.
8. Y. Budak, M. B. M. Gürdere, Keçeci, M. Ceylan, *Bull. Chem. Soc. Ethiop.* **2010**, *24*, 85-91.
9. M. J. Rashmi, O.P. Chourasia, J. T. Rao, *E-J. Chem.* **2004**, *1*, 178-183.
10. S. J. Won, C. T. Liu, L. T. Tsao, J. R. Weng, H. H. Ko, J. P. Wang, C. N. Lin, *Eur. J. Med. Chem.* **2005**, *40*, 103-112.
11. J. Tatsuzaki, K. F. Bastow, K. N. Goto, S. Nakamura, H. Itokawa, K.H Lee, *J. Nat. Prod.* **2006**, *69*, 1445-1449.
12. J. M Yun, M. H. Kweon, H. Kwon, J. K. Hwang, H. Mukhtar, *Carcinogenesis.* **2006**, *27*, 1454-1464.
13. P. S. Kumar, S. G. Babu, D. Mukesh, *Chem. Pharm. Bull.* **2007**, *55*, 44-49.
14. E. G. W. M. Schijlen, C. H. Ricde Vos, S. Martens, H. H. Jonker, F. M. Rosin, J. W. Molthoff, Y. M. Tikunov, G. C. Angenent, A. J. van Tunen, A. G. Bovy, *Plant Physiol.* **2007**, *144*, 1520-1530.
15. M. Cabrera, M. Simoens, G. Falchi, M. L. Lavaggi, O. E. Piro, E. E. Castellano, A. Vidal, A. Azqueta, A. Monge, A. L. de Ceraín, G. Sagrera, G. Seoane, H. Cerecetto, M. González, *Bioorg. Med. Chem.* **2007**, *15*, 3356-3367.
16. G. Yoon, B. Y. Kang, S. H. Cheon, *Arch. Pharm. Res.* **2007**, *30*, 313-316.
17. M. Ceylan, H. Gezegen, *Turk .J. Chem.* **2008**, *32*, 55-61.
18. Y. R. Prasad, P. P. Kumar, P. R. Kumar, A. R. Rao, *E-J. Chem.* **2008**, *5*, 144-148.
19. M. R. Jayapal, N. Y. Sreedhar, *J. pharm. Sci. Res.* **2010**, *2*, 644-647.

20. R. Kumar, D. Mohanakrishnan, A. Sharma, N. K. Kaushik, K. Kalia, A. K. Sinha, *Eur. J. Med. Chem.* **2010**, *45*, 5292-5301.
21. L. C. Tavares, S. Johann, T. M. A. Alves, J. C. Guerra, E. M. S. Fagundes, P. S. Cisalpino, A. J. Bortoluzzi, G. F. Caramori, R. M. Piccoli, H. T. S. Braibante, M. E. F. Braibante, M. G. Pizzolatti, *Eur. J. Med. Chem.* **2011**, *46*, 4448-4456.
22. R. Abonia, D. Insuasty, J. Castillo, B. Insuasty, J. Quiroga, M. Noguerras, J. Cobo, *Eur. J. Med. Chem.* **2012**, *57*, 29-40.
23. C. Zhuang, W. Zhang, C. Sheng, W. Zhang, C. Xing, Z. Miao, *Chem. Rev.* **2017**, *117*, 7762-7810.
24. A. Mitsutani, *Catal. Today* **2002**, *73*, 57-63.
25. G. Cave, C. Raston, *Chem. Commun.* **2000**, 2199-2200.
26. N. Calloway, L. Green, *J. Am. Chem. Soc.* **1937**, *59*, 809-811.
27. G. Sipos, F. Sirokman, *Nature* **1964**, *202*, 489-490.
28. E. Le Gall, F. Texier-Boullet, J. Hamelien, *Synth. Commun.* **1999**, *29*, 3651-3657.
29. T. Narendar, K. P. Reddy, *Tetrahedron Lett.* **2007**, *48*, 3177-3180.
30. (a) N. M. Rateb, H. F. Zohdi, *Synth. Commun.* **2009**, *39*, 2789-2794; (b) P. Kulkarni, *Curr. Microwave Chem.* **2015**, *2*, 144-149; (c) X. F. Liu, D. H. Shi, *Appl. Chem. Ind.* **2009**, *38*, 1210-1213; (d) Q. Xu, Z. G. Yang, D. L. Yin, F. Zhang, *Catal. Commun.* **2008**, *9*, 1579-1582.
31. R. Varma, G. Kabalka, L. Evans, R. Pagni, *Synth. Commun.* **1985**, *15*, 279-284.
32. A. Corma, M. Climent, H. Garcia, J. Primo, *Catal. Lett.* **1990**, *4*, 85-91.
33. A. Guida, M. H. Lhouty, D. Ticht, F. Figueras, P. Geneste, *Appl. Catal. A* **1997**, *64*, 251-264.
34. S. Sebti, A. Saber, A. Rhihil, R. Nazih, R. Tahir, *Appl. Catal. A* **2001**, *206*, 217-220.
35. D. Macquarrie, R. Nazih, S. Sebti, *Green Chem.* **2002**, *4*, 56-59.
36. C. Duran-Valle, I. Fonseca, V. Calvino-Casilda, M. Picallo, A. Lopez-Peinado, R. Martin-Aranda, *Catal. Today* **2005**, *107*, 500-506.
37. E. P. Rondón, R. M. M. Aranda, B. Casal, C. J. D. Valle, W. N. Lau, X. F. Zhang, K. L. Yeung, *Catal. Today* **2006**, *114*, 183-187.
38. H. Wu, H. Q. Ye, D. C. Chen, *Ind. Catal.* **2006**, *14*, 34-37.

39. M. Chtouron, R. Abdelhedi, M. Frikha, M. Trabelsi, *Ultrason. Sonochem.* **2010**, *17*, 246-249.
40. A. Dhakshinamoorthy, M. Alvaro, H. Garcia, *Adv. Synth. Catal.* **2010**, *352*, 711-717.
41. P. Janaki, K. G. Sekar, G. Thirunarayanan, *ILCPA*, **2014**, *28*, 16-22.
42. D. Saha, T. Maity, S. Koner, *Dalton Trans.* **2014**, *43*, 13006–13017.
43. S. Wu, X. Ma, J. Ran, Y. Zhang, F. Qina, Y. Liu, *RSC Adv.* **2015**, *5*, 14221-14227.
44. S. Siddiqui, M. U. Khan, Z. N. Siddiqui, *ACS Sustainable Chem. Eng.* **2017**, DOI: 10.1021/acssuschemeng.7b01467.
45. M. S. Kwon, N. Kim, S. H. Seo, I. S. Park, R. K. Cheedra, J. Park, *Angew. Chem.* **2005**, *117*, 7073-7075; *Angew. Chem. Int. Ed.* **2005**, *44*, 6913-6915.
46. Y. M. A. Yamada, Y. Uozumi, *Tetrahedron* **2007**, *63*, 8492-8498.
47. A. Fischer, P. Makowski, J. O. Muller, M. Antonietti, A. Thomas, F. Goettmann, *ChemSusChem* **2008**, *1*, 444-449.
48. Li, Y. Chen, Daoyong, *Chin. J. Chem.* **2011**, *29*, 2086-2090.
49. Z. Zhang, Y. Wang, M. Wang, J. Lu, C. Zhang, L. Li, J. Jiang, F. Wang, *Catal. Sci. Technol.* **2016**, *6*, 1693-1700.
50. S. Kim, S. W. Bae, J. S. Lee, J. Park, *Tetrahedron* **2009**, *65*, 1461-1466.
51. I. Muthuvel, S. Dineshkumar, K. Thirumurthy, S. Rajasri, G. Thirunarayanan, *Indian J. Chem.* *55B*, **2016**, 252-260.
52. D. Wang, Y. Zhang, A. Harris, L. N. S. Gautam, Y. Chen, X. Shi, *Adv. Synth. Catal.* **2011**, *353*, 2584 – 2588.
53. X. F. Zhou, Y. Y. Sun, Y. D. Wu, J. J. Dai, J. Xu, Y. Huang, H. J. Xu, *Tetrahedron* **2016**, *72*, 5691-5698.
54. M. Rueping, T. Bootwicha, H. Baars, E. Sugiono, *Beilstein J. Org. Chem.* **2011**, *7*, 1680-1687.

Lower Rim Modified Calix[4]arene-Bentonite Hybrid System as a Green Reversible and Selective Colorimetric Sensor for Hg²⁺ Recognition

4.1. Introduction

Design and development of reliable and economic organic-inorganic hybrid systems as sensors that can recognize hazardous metal ions by direct visual observation is an intriguing endeavor among the scientific community and have received much attention in diverse fields.^{1,2,3} Mercury is a well-known and extremely poisonous heavy metal that exists in different forms as elemental mercury, ionic mercury and organic mercury complexes and can cause severe problems to human health and the environment.^{4,5} Mercury exposure even at very low concentration can lead to serious neurological, kidney and digestive diseases due to the easy passage of Hg²⁺ through biological membranes.⁶⁻⁸ These adverse effects urge the necessity for the development of new and improved methods in a pursuit of identifying Hg²⁺ ions⁹ which are cost effective and environmentally benign.

Conventional approaches toward Hg²⁺ determination such as atomic absorption, emission spectroscopy, ICP-MS, electrochemical measurements, gas chromatography, *etc.* are time-consuming processes involving multistep sample preparation and sophisticated instrumentation. Much effort is being focused towards discovering reliable, inexpensive and environmentally benign ways of detecting hazardous ions. Subsequently, developing new ion receptors have become an important goal in both academic and industrial fields. Although a large number of highly sensitive and selective Hg²⁺ sensors based on a variety of macrocyclic molecular platforms are established, calixarene-based chemosensors¹⁰⁻¹⁸ received great attention owing to their advantages such as flexible core, hydrophobic cavity, easy functionalization at the upper or lower rims for substrate binding, *etc.*¹⁹ Moreover, calixarene incorporated receptors would utilize further advantages emerging from its supramolecular behavior.

4.1.1. Calixarenes

Calixarenes, the macrocyclic receptors, are synthesized by base-catalyzed condensation reaction of *p-tert*-butyl phenol with formaldehyde.²⁰ Depending upon the substituent groups present at the lower rim as well as at the *para*-position, calix[n]arenes (where n= 4, 6, etc.) can exist in different conformations. As the number of phenyl ring units change, the shape and size of the cavity also get altered. The complexation properties depend on the conformation and donor groups present in the calixarene conjugates. Moreover, the conformation of a calix[n]arene conjugates can be changed by the presence of particular ions.²¹⁻²⁴ Among various calix[n]arenes, calix[4]arene plays as an important building block because of its capability to exist in cone conformation and the ease of functionalization at lower and upper rims.^{25,26} Calix[4]arene derivatives are well-known for their high binding efficiency and selectivity toward ions and molecules.^{24,27,28}

The binding behaviour of the parent calix[4]arene can be improved by functionalizing at its lower rim, as the resultant conjugates can afford preorganized binding cores appropriate for various ions and molecules.^{29,30} Though mono-, di-, tri-, and tetra-functionalizations are feasible, particularly the 1,3-disubstitution at the lower rim of the calix[4]arene has become more attractive owing to the presence of two phenolic OH and its ability to retain the cone-conformation. Conversely, such structures are flexible and upon complexation, the conformation may alter. In fact, the binding efficiency of the calix[4]arene conjugates towards various guest species depends on the nature of the guest species, ring size, number of binding groups attached and conformation of the arms. Usually, the recognition events are observed either by visual methods or by spectroscopy or both.^{29,11,31-33} Such conjugates with chromogenic units sense the guest species *via* fluorescence, absorption, and/or color changes. For this rationale, it is essential to assimilate a chromophore into the binding core either directly or through a spacer.

4.1.2. Lower Rim 1,3-Di-conjugates of Calix[4]arene as Hg²⁺ Receptors

There are two types of 1,3-di-conjugates of calix[4]arene namely cyclic conjugates and non-cyclic conjugates.

4.1.2.1. Cyclic Conjugates

An azophenol-type ionophore (L1) was reported for the selective chromogenic detection of Hg^{2+} ions in the presence of other ions, such as alkali, alkaline earth and heavy metal ions.³⁴ Amido-crown conjugate of calix[4]arene (L2) exhibited selectivity toward Hg^{2+} ions with a blue shift of 38 nm in UV-Visible spectroscopy, while no changes were detected with other ions.³⁵ Chen *et al.* developed a cyclic amido-dansyl conjugate (L3) which forms a 1:1 complex and exhibited high fluorescence sensitivity with Hg^{2+} ions *via* the formation of N_4 binding core.³⁶ In the case of L1 and L2, no proposed structures were known for Hg^{2+} binding.

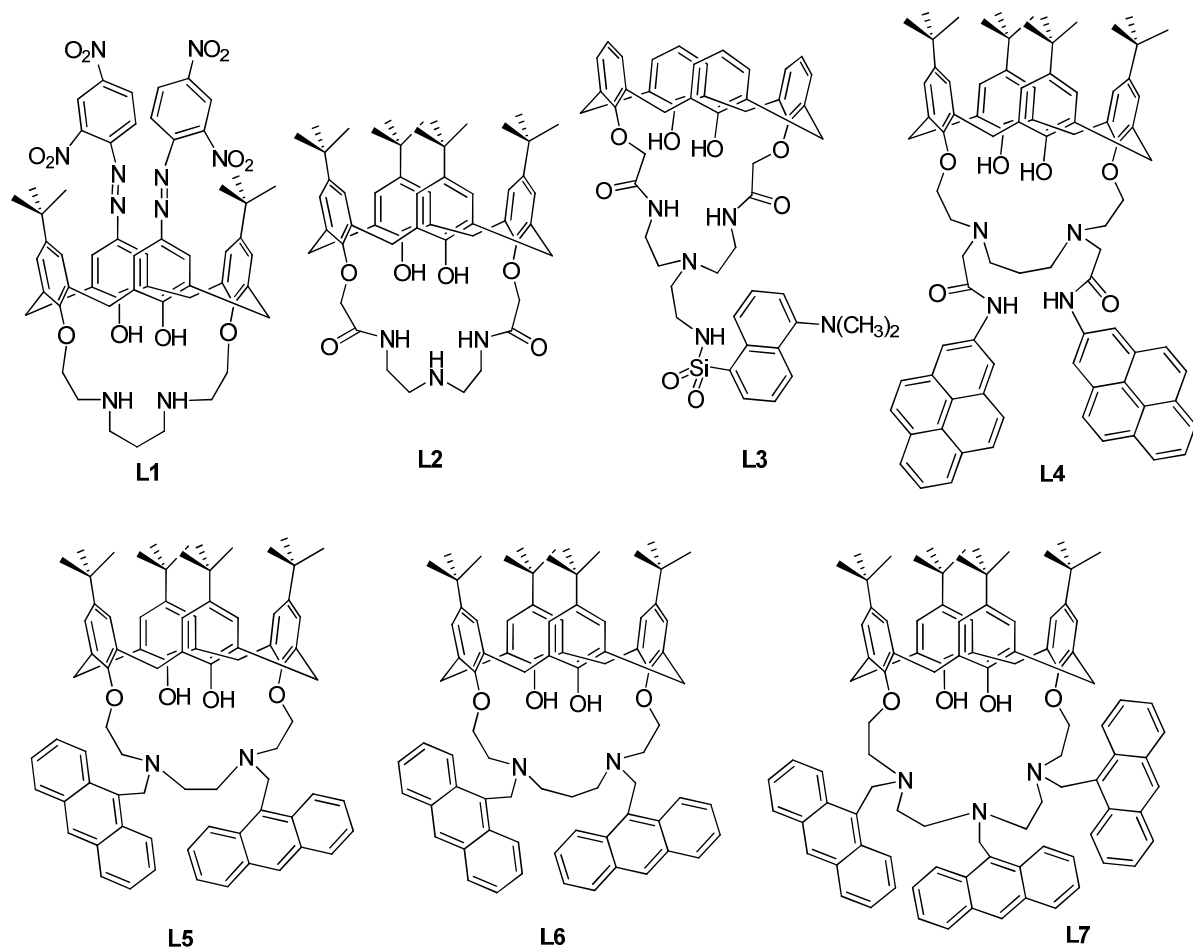


Figure 4.1. Structures of some cyclic conjugates of calix[4]arenes

A calix[4]arene receptor appended with pyrenylacetamide (L4)³⁷ was reported by Chang and co-workers which recognized Hg^{2+} ions *via* fluorescence quenching even in the presence of other alkali, alkaline earth and heavy metal ions, in methanol with an association constant of $4.5 \times 10^4 \text{ M}^{-1}$. The fluorescence emission of L4 originates from the monomer and weak excimer in methanol and it is reverse in 50 % aqueous methanol. Upon binding with Hg^{2+} emissions of L4 is quenched, demonstrating an ON-OFF type receptor. In addition, a series of aza crown derivatives of calix[4]arene with an anthracene fluorophore (L5, L6 and L7)³⁸ were synthesized by Chang *et al.* in 2002 to check their ability to recognize Hg^{2+} ions and found out that L6 showed highest fluorescence enhancement towards Hg^{2+} . The non-selectivity of L7 is mainly due to the occurrence of more number of nitrogen donor centers in the system which indicates that for optimal binding, only the required number of ligating nitrogen centers is essential. The higher selectivity of L6 is attributed to the flexibility of the spacer unit present that brings better coordination between Hg^{2+} ions and the nitrogen donor centers. The structures of some cyclic conjugates of calix[4]arenes are shown in Figure 4.1.

4.1.2.2. Non-Cyclic Conjugates

In 2008, Rao *et al.* introduced an amido-benzimidazole conjugate (L8) which exhibited high selectivity towards Hg^{2+} by forming a 1:1 complex in 1:1 aqueous acetonitrile.³⁹ The bent arm of L8 undergoes conformational changes in the presence of Hg^{2+} ion to create a suitable binding core. The isolated complex exhibited different TEM, AFM, and SEM features compared to the receptor (L8). Amido-pyridylcalix[4]arene derivative, L9, was studied for its complexation with Hg^{2+} , Zn^{2+} and Ag^+ by ^1H NMR spectroscopy and electrochemistry.⁴⁰ ^1H NMR spectral titration proved the formation of the complex with Hg^{2+} through the pyridyl and amide units. The electrochemical studies also confirmed the metal-ligand binding. A calix[4]arene incorporated with two dansyl fluorophores and two long chain triethoxysilane groups (L10) embedded in mesoporous silica exhibited the ability to detect Hg^{2+} ions in water by forming a 1:1 complex.⁴¹ In addition, a series of calix[4]arenes possessing dansyl fluorophore (L11, L12 & L13) were developed as mercury sensor and they were studied by absorption and fluorescence spectroscopy.⁴² Also, the solvent-dependent recognition property of thioether conjugate of calix[4]arene, L14 were studied by ^1H NMR spectroscopy, thermodynamics and electrochemistry.^{43,44} CdSe/ZnS quantum dots (QDs)

capped with thioether derivative of calix[4]arene showed selective recognition to Hg^{2+} ions with a detection limit of 15 nM.⁴⁵ The structures of these non-cyclic receptors are displayed in Figure 4.2.

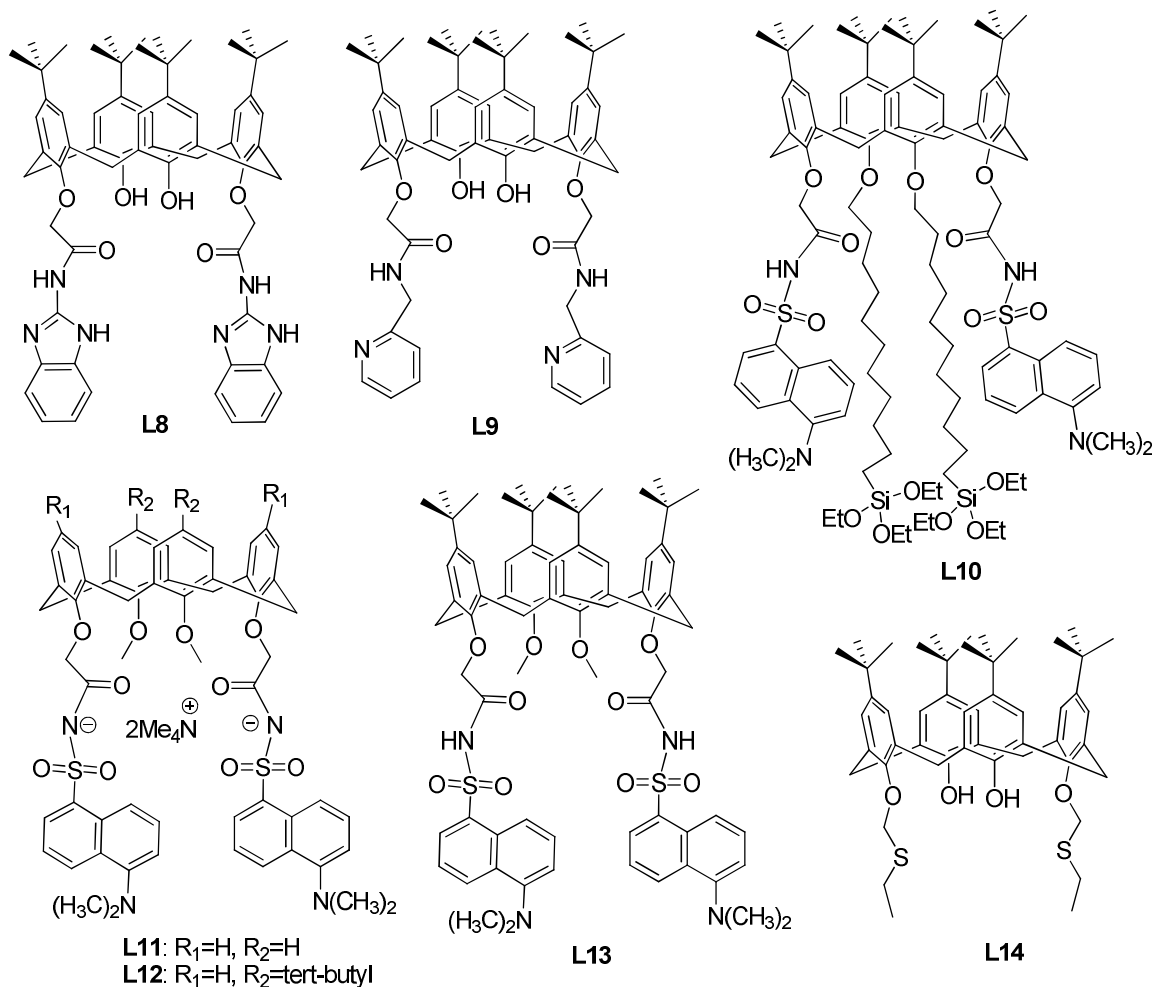


Figure 4.2. Structures of some non-cyclic conjugates of calix[4]arene receptors

A benzothiazole appended conjugate of calix[4]arene, L15 that was coated on glassy carbon electrode was employed by Zhang and co-workers which detected Hg^{2+} ions selectively in aqueous medium by cyclic and square wave voltammetric techniques⁴⁶ and the detection limit was found to be 25 nM. He *et al.* reported a nicotinic moieties appended calix[4]arene, L16 as Hg^{2+} and Ag^+ sensor and its liquid membrane transport and silver selective electrode properties were investigated.⁴⁷ Moreover, Li and co-workers developed a triazole linked 8-oxyquinoline conjugate (L17) which displayed selectivity for Hg^{2+} by fluorescence

quenching.⁴⁸ In addition, a double branched calixarene conjugate appended with one amidopyrenylmethyl moiety and a rhodamine B unit, L18⁴⁹ performed as a 1:1 stoichiometric chemosensor for Hg^{2+} and Al^{3+} . On the basis of the emission properties, it has been feasible to distinguish Hg^{2+} from other heavy ions, Pb^{2+} and Cd^{2+} using a terminal- NH_2 bound calix[4]arene conjugate, L19.⁵⁰ The structures of these non-cyclic receptors are displayed in Figure 4.3.

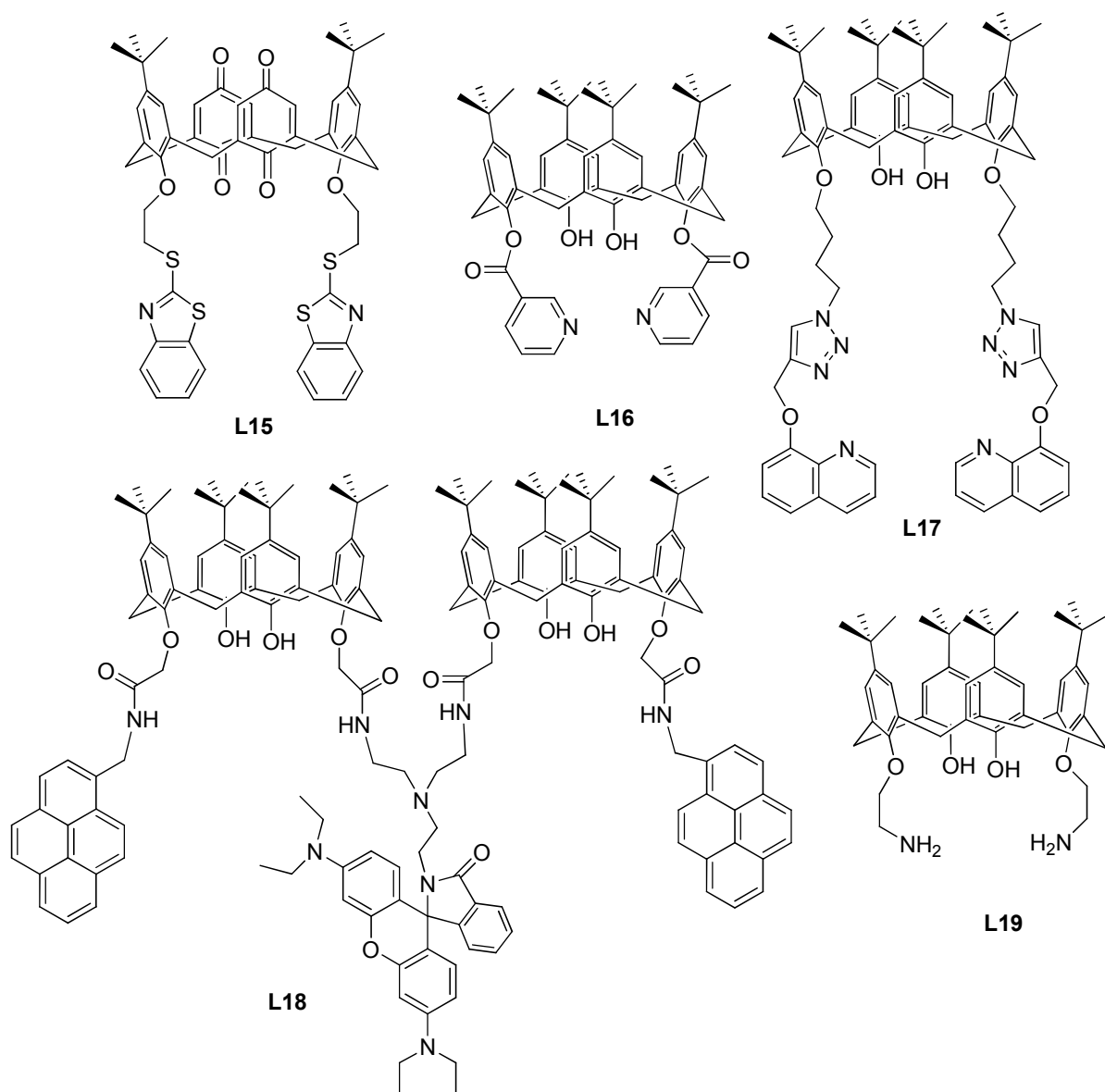


Figure 4.3. Structures of some non-cyclic conjugates of calix[4]arenes

Moreover, a 1,3-alternate thiacalix[4]arene and an anthracene-oxyquinoline dyad based Hg^{2+} sensors (Figure 4.4.) were reported from our group. Varma *et al.* developed a 1,3-

alternate thiacalix[4]arene derivative bearing four 8-quinolinoloxo groups through flexible propyl chains (L20)⁵¹ as a reversible ON-OFF fluorescent Hg^{2+} sensor in partially aqueous systems which exhibited only marginal affinity toward Cr^{3+} and Ag^+ , and no affinity toward other transition metal ions. The system performed as four independent entities of mixed N/S/O donor sites in a thiacalixarene scaffold. The unusual formation of a tetramercury complex with L20 was substantiated by fluorescence, UV-Vis, NMR, and MALDI-TOF mass spectral analysis. An oxyquinoline-anthracene dyad (L21)⁵² was synthesized and characterized which showed excellent selectivity and adequate sensitivity for the recognition of Hg^{2+} ions in MeCN/ H_2O system. When L21 binds Hg^{2+} , unfolding of the dyad from its initial folded conformation take place. The sensing event was characterized by spectrofluorometric studies and showed a marked color change from greenish-blue to blue fluorescence.

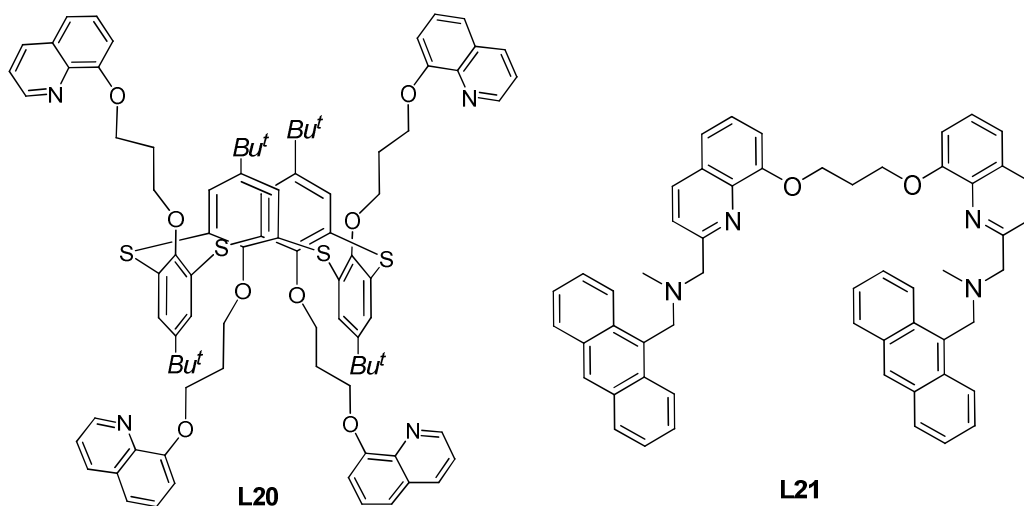


Figure 4.4. Structures of L20 and L21

4.1.3 Organic-Inorganic Hybrid System

Development of solid-state colorimetric sensors *via* naked eye detection have received much current interest and investigations are currently being pursued by researchers in the area of nano-thin films, molecular imprinted polymers, modified sol-gel membranes, *etc.*⁵³⁻⁶³ In recent times, a variety of supporting materials are used for the immobilization of organic molecules to fabricate organic-inorganic hybrid system for the determination of mercury ions and the details are elaborately discussed in the first chapter. Incorporation of organic

molecules into the inorganic host matrices are of great interest as the resulting hybrid material can have high mechanical, thermal and chemical stability compared to organic molecules. Clays, one of the promising candidates in materials sciences, afford an incredible potential for the development of hybrid systems due to their low-cost, environmentally benign nature, good adsorptive capacity, high stability, large specific surface area, *etc.*⁶⁴⁻⁶⁹ Moreover, Bentonite is a 2:1 clay which has the capacity to expand its interlayer when treated with water that is utilized for the intercalation of a variety of organic moieties.⁷⁰

4.2. Statement of the Problem

Development of colorimetric sensors for the detection of hazardous metal ions has immense significance in various fields such as medicinal and biological, environmental and security. Even though a large number of chemosensors are developed which have several advantages such as selectivity, sensitivity and low-cost, syntheses of novel materials containing organic functional molecules with recyclability and environmentally benign nature are of great interest. Calixarenes, the third best receptor molecules, easily synthesizable and readily functionalizable with suitable binding cores, are considered as excellent molecular scaffolds for the recognition of ions. Consequently, developing suitably functionalized calixarene-based molecular receptors capable of selectively detecting Hg^{2+} is an interesting area of research. As our group was successful in developing Hg^{2+} ion selective chemosensors containing quinoline moieties, it was proposed to incorporate similar chelating moieties into calix[4]arene scaffold through a suitable spacer which may exhibit affinity to Hg^{2+} . Moreover, exploration of solid-state colorimetric sensors for hazardous metal ions by naked eye detection is highly desirable and there is a great demand to develop a simple, rapidly responsive, inexpensive, portable and environmentally benign metal ion sensor material for the selective recognition of Hg^{2+} ions. To facilitate a stable, efficient and reliable mercury sensing system, selection of appropriate supporting materials is crucial. In this context, bentonite, owing to its remarkable potential for the development of organic-inorganic hybrid systems, is selected as a support. In addition, calixarene-bentonite hybrid systems are not reported as Hg^{2+} sensors in the literature. This chapter discloses the synthesis, characterization and application of an economically affordable, green and reversible lower rim modified calixarene-bentonite hybrid system (QHQCalBen) as a

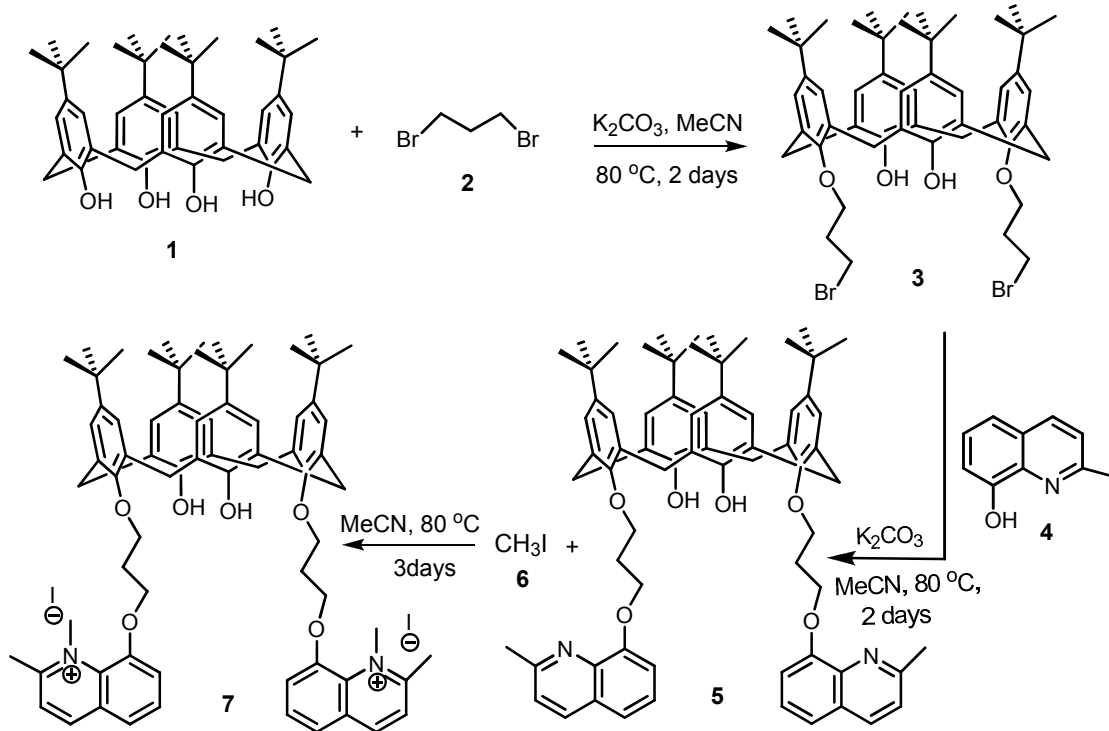
colorimetric sensor for the selective and rapid monitoring of Hg^{2+} ions using naked eye detection. In addition, bentonite facilitates the realization of the sensor as a recyclable one.

4.3. Results and Discussion

The key steps which led to the development of the organic-inorganic hybrid system (QHCalBen) included the synthesis of lower rim functionalized 1,3-di(quaternary ammonium salt of 8-hydroxyquinaldine) derivative of *p-tert*-butylcalix[4]arene (QHQC) as the cone conformer and its intercalation into the sodium-bentonite gallery *via* ion-exchange method. The synthesized QHQC itself imparts selectivity and reversibility towards Hg^{2+} ions in the solution state, the QHCalBen hybrid system shows properties analogous to QHQC in acetonitrile as well as in MeCN/H₂O (1:9, v/v) system and is reusable.

4.3.1. Synthesis of QHQC, **7**

The receptor, QHQC **7** was synthesized *via* three steps starting from *p-tert*-butylcalix[4]arene as shown in Scheme 4.1. In brief, the precursor **3**⁷¹ was prepared from *p-tert*-butylcalix[4]arene and 1,3-dibromopropane with K₂CO₃ as base in refluxing acetonitrile. In the next stage, **3** was treated with 8-hydroxyquinaldine and K₂CO₃ in dry acetonitrile at 80 °C fetched the HQ-calix[4]arene **5**.⁷² Subsequently, the precursor **5** on treatment with excess methyl iodide in refluxing acetonitrile afforded QHQC **7** in 73.3 % yield. The precursors and the main receptor molecule **7** were characterized by various spectral techniques such as ¹H NMR, ¹³C NMR, ESI/HRMS and FT-IR. In the ¹H NMR spectrum (Figure 4.5), two doublets discernible at δ 4.24 and 3.37 ppm for the bridged methylene hydrogens revealed the existence of the molecule **7** in cone conformation and it was further confirmed by ¹³C NMR spectrum (Figure 4.6) which showed the peaks at δ 31.7 and 31.0 ppm for the corresponding carbons. The peak at δ 4.69 ppm in the ¹H NMR spectrum and the peak at δ 46.6 ppm in the ¹³C NMR spectrum were attributed to the methyl group attached to nitrogen atom of quinaldine ring in consequence of the quaternization of precursor **5**. The structure of the QHQC **7** was finally confirmed by mass spectral analysis, which showed a molecular ion peak at m/z 1077.6653.



Scheme 4.1. Synthetic pathway for the preparation of QHQC 7

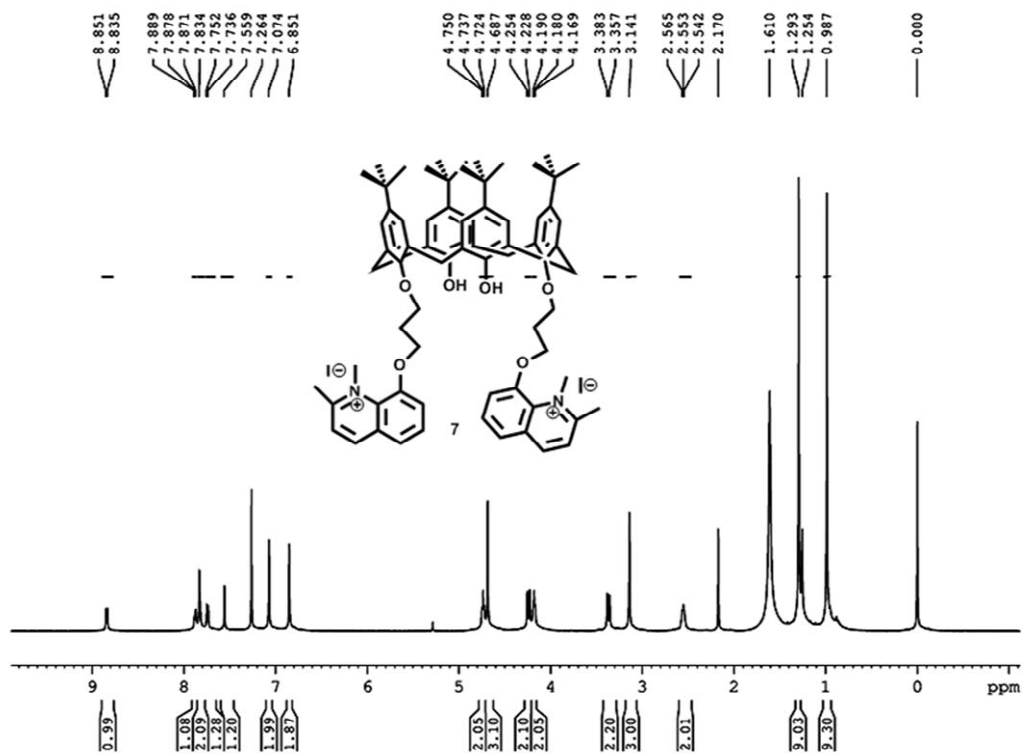


Figure 4.5. ^1H NMR spectrum of QHQC 7

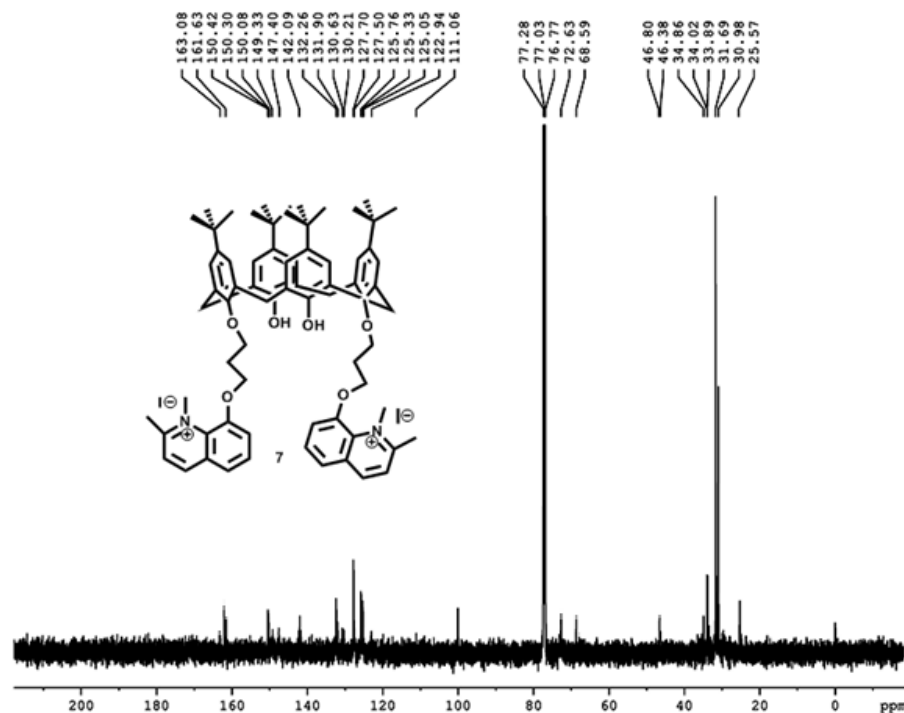


Figure 4.6. ^{13}C NMR spectrum of QHQC 7

The rationale behind the synthesis of positively charged arms on the calixarene derivative (compound 7) by quaternization process is the intercalation of organic moieties in the interlayers of bentonite by ion exchange method which is possible only if the molecule is positively charged. Moreover, the compound 7 is violet colored and furnishes naked eye detection with Hg^{2+} ions. But the compound 5 which has neutral arms did not give the same result.

4.3.2. Metal Ion Binding Studies

In order to find out the efficacy of our organic-inorganic hybrid system as a solid-state colorimetric sensor, it is necessary to scrutinize the binding properties of the QHQC alone. Hence, its ion recognition properties were explored using various techniques such as absorption, ESI/HRMS and 1H NMR experiments and most importantly by visual detection. The binding affinity of QHQC 7 towards different metal ions was investigated by UV-Visible spectroscopy. The absorption spectrum of QHQC exhibited a strong absorption band at 256 nm, and a weak broad band at 567 nm in acetonitrile medium. In order to obtain an insight into the receptor ability of 7 toward metal ions, such as Mn^{2+} , Fe^{2+} , Al^{3+} , Co^{2+} , Ni^{2+} , Cu^{2+} , Zn^{2+} , Hg^{2+} , Ag^+ , Ba^{2+} , Cd^{2+} , Na^+ , Mg^{2+} , Cr^{3+} and Ca^{2+} , the perchlorates of metals were

added to the acetonitrile solution of **7** and UV-Vis spectral changes were investigated (Figure 4.7). QHQC showed a pronounced selectivity towards Hg^{2+} ions which could be recognized by the disappearance of the absorption peak at 567 nm along with the enhancement in intensity of the peak at 256 nm upon addition of Hg^{2+} ions. In the case of Al^{3+} ions and Fe^{2+} ions, even if the peak at 567 nm vanished, visual colour change was not observed. Other metal ions have no effect on the absorption spectrum of QHQC. Moreover, QHQC showed good selectivity towards Hg^{2+} in the presence of interfering ions like Ba^{2+} , Mn^{2+} , Ni^{2+} , Zn^{2+} , Mg^{2+} , Ca^{2+} , Ag^+ , Co^{2+} , Na^+ *etc.* The UV-Visible absorption spectra of QHQC with Hg^{2+} titration (Figure 4.8) showed that no isosbestic points were formed but the peak at 567 nm disappeared and the intensity of peak at 256 nm increased. The detection limit (LOD) of Hg^{2+} was calculated as three times the standard deviation of the background noise and was found to be 2.95×10^{-6} M (Figure 4.9). The response time of quinaldine functionalized calix[4]arene receptor (QHQC) is very fast and within seconds, recognition of Hg^{2+} takes place.

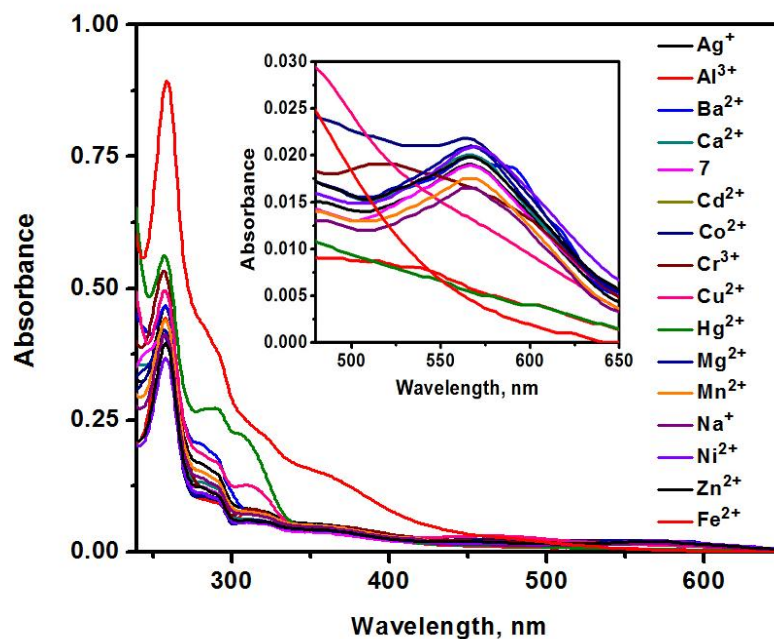


Figure 4.7. Absorption spectra of QHQC with different metal ions in MeCN (Inset shows the magnified absorption peak at 567 nm)

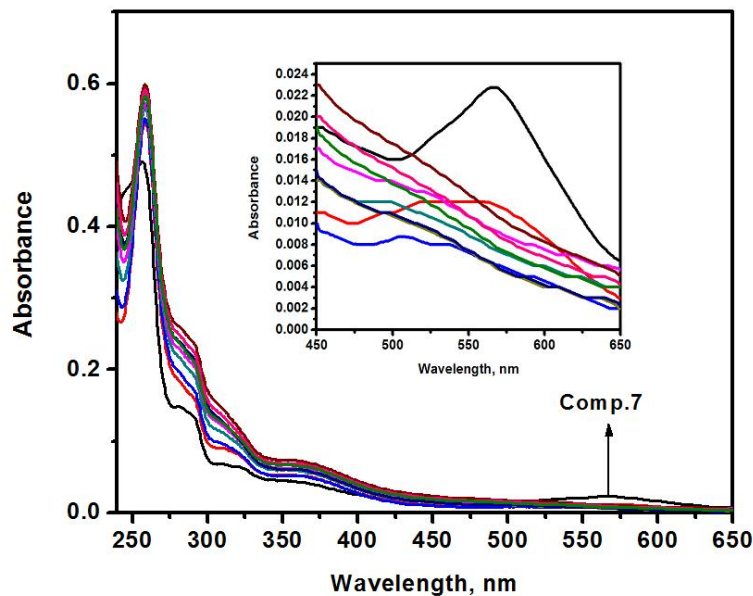


Figure 4.8. Changes in the absorption spectra of QHQC (2.7×10^{-5} M) by the addition of Hg^{2+} ions (2.57×10^{-5} M)

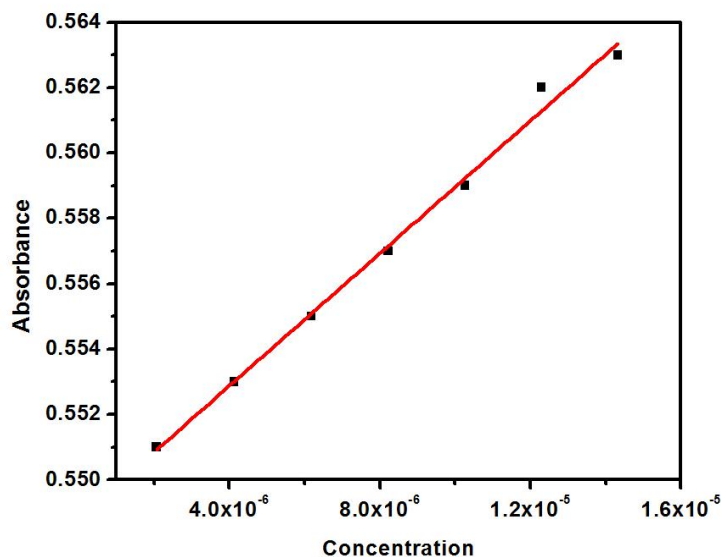


Figure 4.9. Regression line for the determination of LOD

4.3.3. Naked Eye Detection Studies

One important aspect of the system is that it could be used for the naked eye detection of Hg^{2+} ions and its reversibility can be achieved by the addition of iodide ions. The violet coloured QHQC 7 (9×10^{-6} M in MeCN), changed its colour to light brown by the addition of

Hg^{2+} (1×10^{-6} M in MeCN) and the absorption peak at 567 nm disappeared. But when iodide (6.8×10^{-6} M in MeCN) solution was added to the above system, the violet colour reappeared immediately and the absorption peak at 567 nm re-emerged. Further addition of Hg^{2+} ions to the above solution revealed the repeatability of the system (Figure 4.10). For a chemical sensor to be widely employed for the detection of specific analytes, reversibility of the system is the most essential aspect and consequently QHQC 7 is a good candidate for the naked eye detection of Hg^{2+} ions.



Figure 4.10. Photograph of naked eye detection of Hg^{2+} with QHQC and its reversibility with iodide solution

4.3.4. ^1H NMR Titration Studies

To disclose the nature of the interaction of QHQC with Hg^{2+} , ^1H NMR titrations (Figure 4.11) were carried out. When it was treated with one equivalent of Hg^{2+} , there were only minimal up-field shifts in the δ values of quinaldine ring protons (0.018-0.010 ppm). The $-\text{OCH}_2$ protons attached to quinaldine ring and $-\text{N}-\text{CH}_3$ protons were also recorded minute up-field shifts (0.008 ppm) indicating the formation of Hg^{2+} complex through the oxygen connected to quinaldine moiety. When more equivalents of Hg^{2+} ions were added, the pattern of spectrum remained the same suggesting that only one equivalent of mercury was getting coordinated to the QHQC. These shifts were unable to differentiate from the NMR spectra at a glance, expansion of titration spectra (Figure 4.12 & 4.13) facilitated to understand these chemical shifts. The absence of alterations observed in the chemical shift of other protons in the macrocyclic molecule excluded the interaction of other oxygens attached to arene cavity of calixarene derivative 7. When iodide solution (3 equiv.) was added to the above system,

Hg^{2+} detached from the host molecule and it instantly regained the original spectrum. From these evidences, it is obvious that the Hg^{2+} binds only weakly to the organic molecule thereby contributing to the reversibility of the system. Reversibility is applicable for more than five cycles with the actual sample.

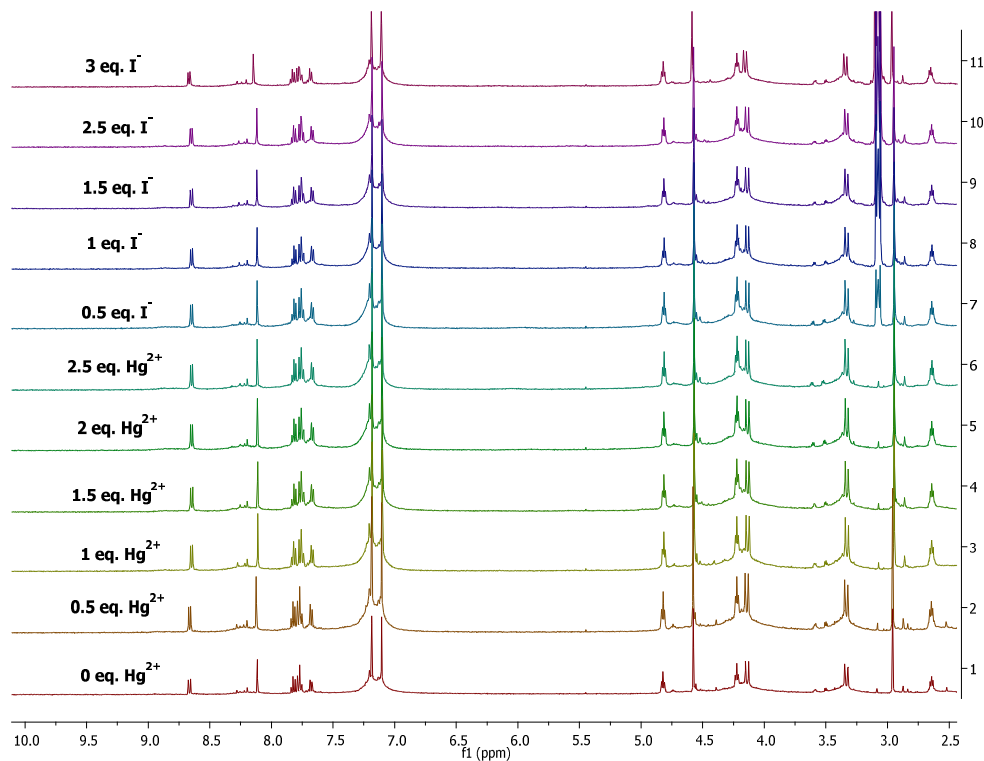


Figure 4.11. ^1H NMR titration spectra of QHQC with Hg^{2+} in CD_3CN

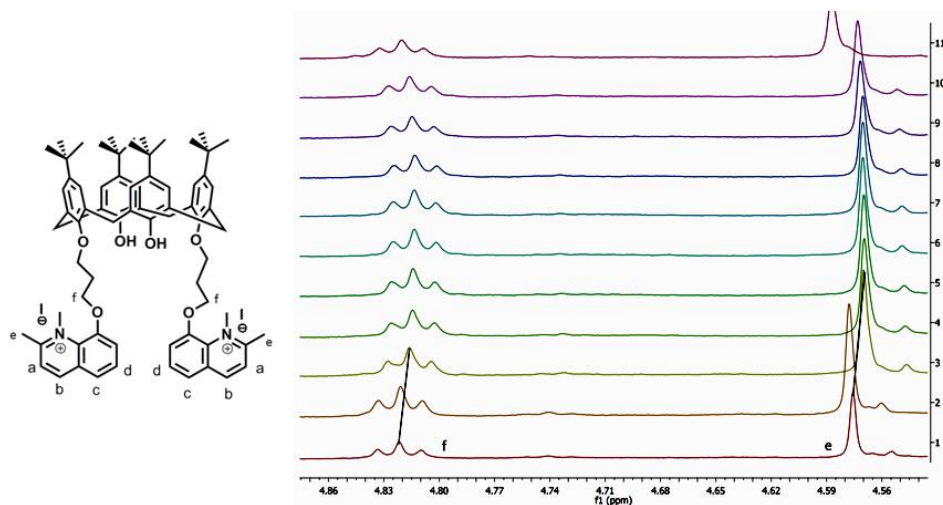


Figure 4.12. Expansion of ^1H NMR titration spectrum of QHQC with Hg^{2+} in CD_3CN

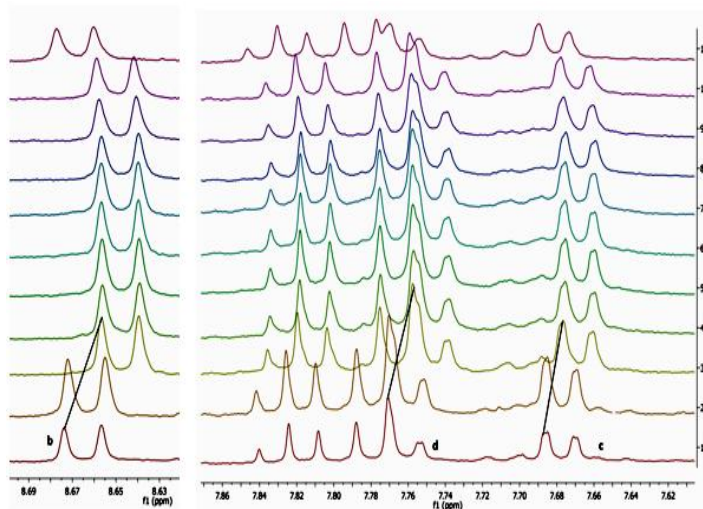


Figure 4.13. Expansion of ^1H NMR titration spectrum of QHQC with Hg^{2+} in CD_3CN

The binding constant of Hg^{2+} with QHQC was calculated based on the ^1H NMR titration data by a nonlinear curve fitting procedure for the guest induced chemical shift for selected peak using commercially available GraphPad Prism software⁷³ and the association constant found to be 1852 M^{-1} (Figure 4.14). To substantiate the stoichiometry of the guest-host complex formed, we carried out modified Job's plot experiment using ^1H NMR titration data and from the binding isotherm (Figure 4.15), the maxima were obtained at 0.5 mole fraction and the stoichiometry was confirmed as 1:1.

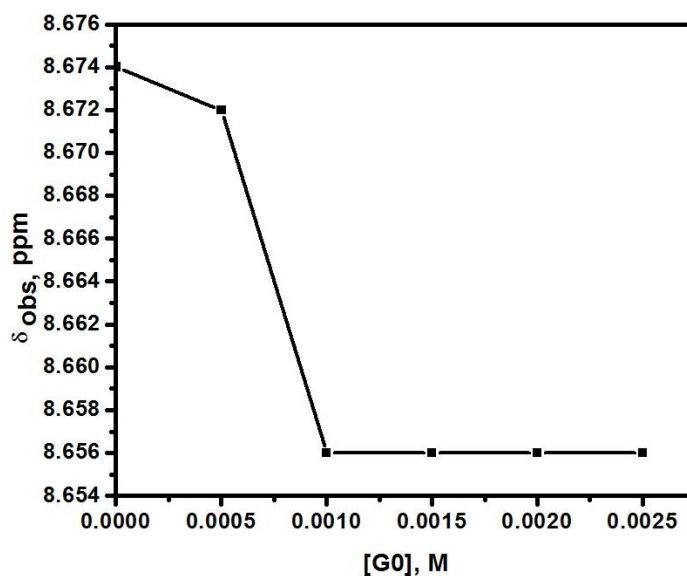


Figure 4.14. Isotherm resulting from the titration of QHQC with Hg^{2+}

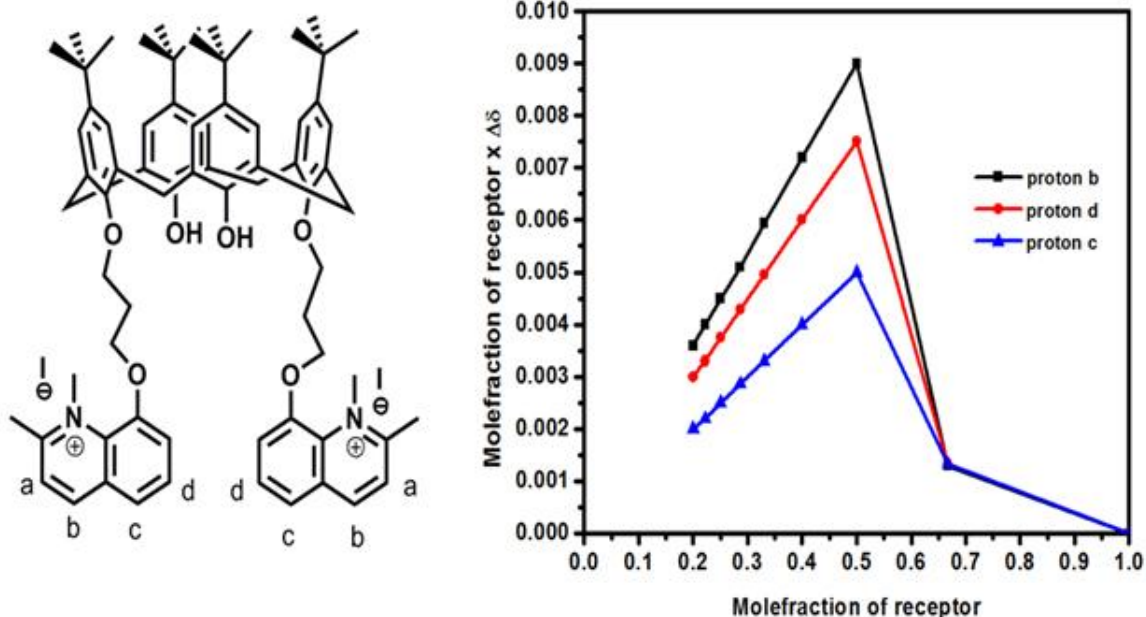


Figure 4.15. Modified Job's Plot using $^1\text{HNMR}$ titration data

4.3.5. Mass Spectroscopic (ESI-HRMS) Titrations Studies

In order to confirm the stoichiometry of the complex, Electron Spray Ionization Mass Spectroscopic (ESI-MS) titrations of QHQC with Hg^{2+} were carried out. Upon addition of one equivalent of Hg^{2+} , a molecular ion peak at m/z of 1274.8008 was obtained which could be assigned to the formation of 1:1 complex. However, when the titration was performed using more equivalents of Hg^{2+} additional molecular ion peaks were not observed. Furthermore the isotopic peak pattern observed for the molecular ion peak (Figure 4.16) authenticates the presence of mercury (II) ions and thus established the 1:1 binding of QHQC with Hg^{2+} . The reversibility of the system was further proved by the addition of iodide solution and conducting ESI/MS analysis. Consequently, a peak at m/z of 1077.6353 was obtained that corresponded to the $[M+H]^+$ peak of the receptor molecule 7, confirming the release of Hg^{2+} from the complex. When Hg^{2+} ions were again added to the above solution and carried out mass analysis, peak at m/z of 1274.8263 $[QHQC+Hg^{2+}]$ reappeared which revealed the repeatability of the system to recognize Hg^{2+} ions.

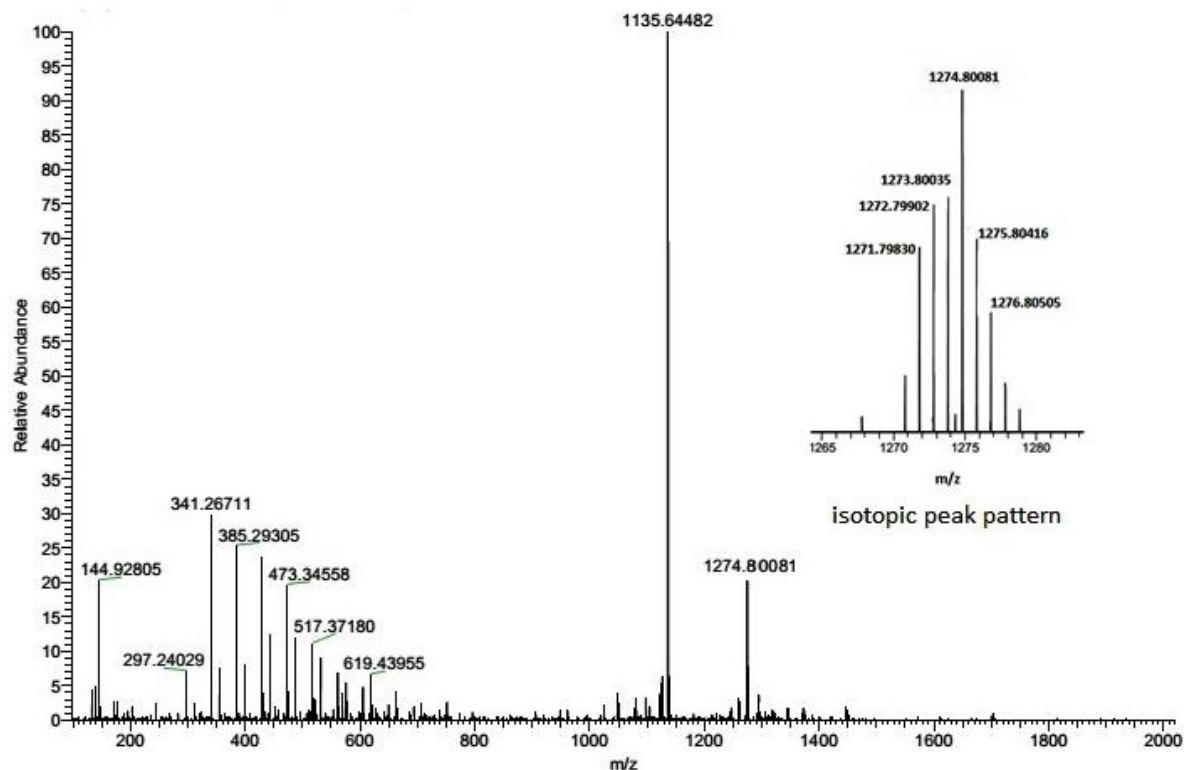


Figure 4.16. Experimentally observed isotopic peak pattern of molecular ion peak of $[\text{QHQC} + \text{Hg}^{2+}]$

4.3.6. Computational Studies

The binding energy of Hg^{2+} with QHQC was calculated using density functional theory method and was found to be 32.3 kcal/mol. Also the reaction is exergonic by 14.0 kcal/mol. Optimized structure of (a) QHQC and (b) QHQC-Hg^{2+} complex using B3LYP/Gen^{74,75} level density functional theory method as implemented in Gaussian09⁷⁶ are shown in Figure 4.17. Gen indicates basis set comprising of LanL2DZ for (Hg, I) and 6-31G* for (N, C, O, H). The O...Hg...O angle is 158.4°. The geometry adopted by Hg^{2+} in the complex is distorted octahedra; four oxygens from two perchlorate moieties occupy the equatorial plane and two oxygens linked with the quinoline moieties occupy the axial positions.

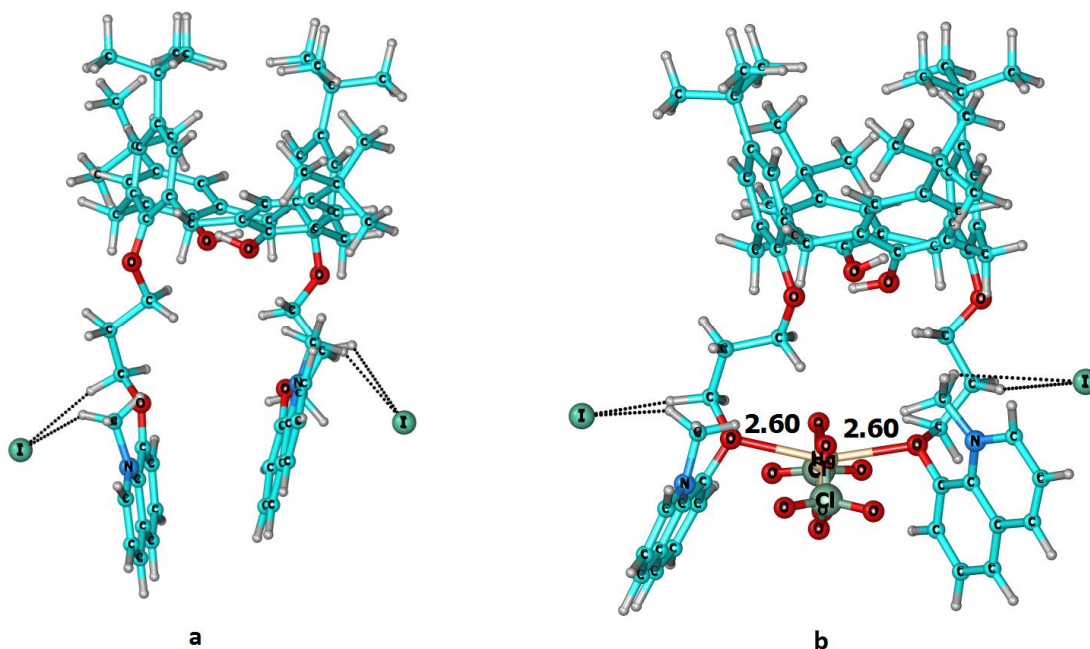
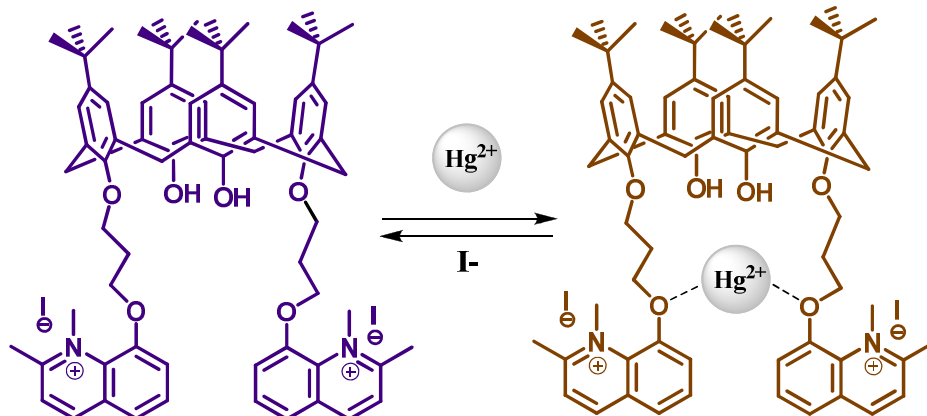


Figure 4.17. Optimized structures of (a) QHQC and (b) QHQC- Hg^{2+} complexes using DFT method

4.3.7. Mechanistic Pathway

The reason for the violet colour of the compound **7**(QHQC) is presumably due to the electron transfer process (charge transfer)⁷⁷⁻⁷⁸ from oxygen atom (oxygen attached to quinaldine moiety) to quinaldine ring of QHQC. When Hg^{2+} binds with QHQC through its etherial oxygen (oxygen attached to quinaldine moiety), the quenching of electron transfer process from oxygen atom to quinaldine ring occurs as a consequence of the formation of 1:1 Hg^{2+} -QHQC complex. This leads to the colour change from violet to light brown. When iodide solution was added to the above solution, Hg^{2+} was easily released from the complex. This may be due to the formation of more stable HgI_2 compared to weak Hg^{2+} -QHQC complex. The process is reversible and reusability of the technique was examined by carrying out the experiment several times using Hg^{2+} and iodide solution. The schematic representation of the plausible mechanism is shown in Scheme 4.2.



Scheme 4.2. Plausible mechanism of naked eye detection of Hg^{2+} with QHQC and its reversibility with iodide solution

On the basis of the stimulating properties of the macrocyclic receptor (QHQC) and its rapid detection of Hg^{2+} ions, we decided to construct the organic-inorganic hybrid system, QHQC/bentonite and assess its credibility as a naked eye sensitive colorimetric solid-state sensor for Hg^{2+} ions.

4.3.8. Synthesis and Characterization of QHQC/bentonite

The support material, bentonite used for the development of hybrid system QHQC/bentonite is economical and environmentally benign. QHQC intercalated bentonite clay (QHQC/bentonite) was synthesized *via* cation-exchange method by stirring QHQC with sodium bentonite (Na-Ben) in acetonitrile at room temperature for 24 h and the organic-inorganic hybrid was obtained as a violet colored solid (Figure 4.18). The hybrid material was characterized using FT-IR spectroscopy, Powder XRD, TG/DTA techniques and solid-state absorption and emission studies.

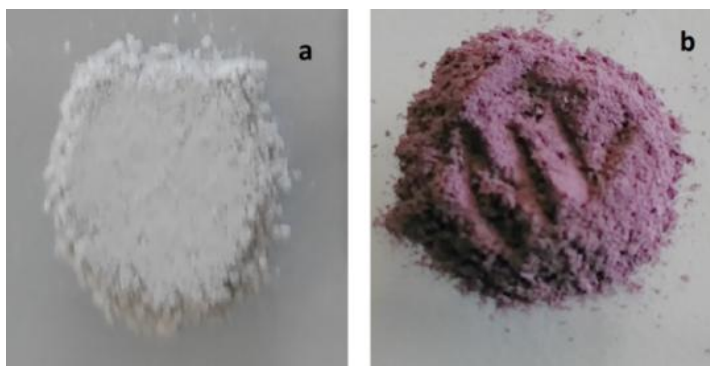


Figure 4.18. Photograph of (a) Na-Ben and (b) QHQC/bentonite

The X-ray diffraction (XRD) patterns of Na-Ben and QHQCAlBen are shown in Figure 4.19. Na-Ben showed a diffraction peak which corresponds to the basal spacing (d-spacing) value ($d_{(001)}$) of 13.4 Å. The QHQCAlBen sample exhibited a peak at 'd' value of 30.7 Å which is greater than the d-spacing of Na- Ben by 17.3 Å indicating the successful intercalation of QHQC 7 into the bentonite gallery. The peaks present in the hybrid which are the same (or small shift in the position) as that of Na-Ben suggests that Na-Ben is not completely converted to QHQCAlBen.

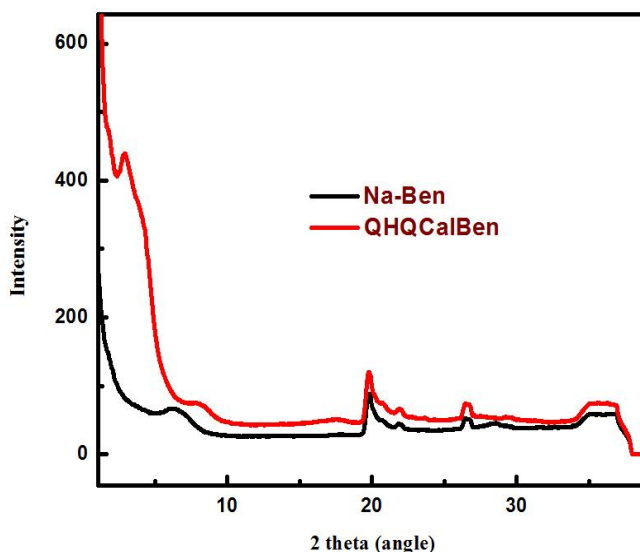


Figure 4.19. XRD patterns of Na-Ben and QHQCAlBen

The energy minimization studies of the molecule 7 using ChemBio3D Ultra 11.0 software showed that this molecule has an approximate length of 17 Å. From the XRD patterns of organoclay it is evident that the interlamellar space has been increased by 17.3 Å from the original value of Na-Ben and successful intercalation of QHQC moieties into bentonite gallery has taken place.

To give more evidence for successful intercalation, FT-IR analysis was performed. FT-IR spectra of QHQC, Na-Ben and QHQCAlBen are shown in Figure 4.20. QHQC and QHQCAlBen showed major peaks at 2955, 2358, and 1480 cm^{-1} . The peak at 3621 cm^{-1} is attributed to the structural hydroxyl stretching vibrations and peak at 3440 cm^{-1} is assigned to the OH stretching vibration of the adsorbed water. Bands observed around 1633 cm^{-1} are due to the bending vibration of OH group in water molecules. The peak around 1035 cm^{-1} is

assigned to Si-O-Si stretching vibrations. Band at 794 cm^{-1} is attributed to the presence of silica. In the case of organomodified bentonite sample, the profile in the OH stretching region showed clear perturbation, which is due to the displacement of the sodium ions (along with its hydration shell) by the organic moiety. The band at 3621 cm^{-1} is owing to the inner OH groups inaccessible to QHQC. Additional well-defined absorption bands observed at approximately 2955 cm^{-1} , 1480 cm^{-1} , 2358 cm^{-1} and are attributable to sp^3 -CH stretching, $-\text{CH}_2$ bending and $-\text{C}-\text{N}$ stretching respectively. From these information, it is unambiguously established that organic moiety is intercalated into the bentonite gallery. Moreover, we noticed that there were no significant changes in the peak of QHQC/ben compared to those of pure QHQC, which indicates that the conformation of QHQC is unaffected in the hybrid state.

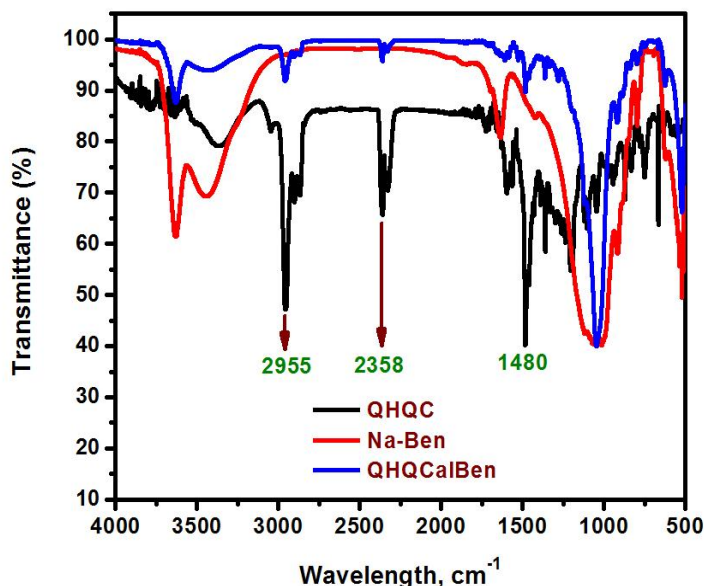


Figure 4.20. IR spectra of QHQC, Na-Ben and QHQC/ben

TG/DTA analysis provided a simple method to measure the content of organic molecules and physisorbed water in the intercalated bentonite. Na-Ben showed two major peaks [Figure 4.21.(a)] around $87\text{ }^{\circ}\text{C}$ and $704\text{ }^{\circ}\text{C}$, corresponding to the loss of physically adsorbed water and dehydroxylation of bentonite respectively. The decomposition of QHQC/ben exhibited peaks at $64\text{ }^{\circ}\text{C}$, $313\text{ }^{\circ}\text{C}$, $625\text{ }^{\circ}\text{C}$ and $731\text{ }^{\circ}\text{C}$. For Na-Ben, there is no obvious mass loss in the range $200\text{ }^{\circ}\text{C}$ - $600\text{ }^{\circ}\text{C}$. Thus the mass losses between $200\text{ }^{\circ}\text{C}$ - $600\text{ }^{\circ}\text{C}$ are attributed to the organic molecules intercalated in the interlayers of bentonite. Peaks at

313 °C and 625 °C are assigned as decomposition of intercalated QHQC from QHQC/Ben. Furthermore, the melting point of QHQC was found to be 180 °C. The decomposition of QHQC when intercalated in bentonite galleries takes place at elevated temperature compared to the organic molecule itself. Consequently, confinement of organic molecules into bentonite contributed to its enhanced thermal stability [Figure 4.21.(b)].

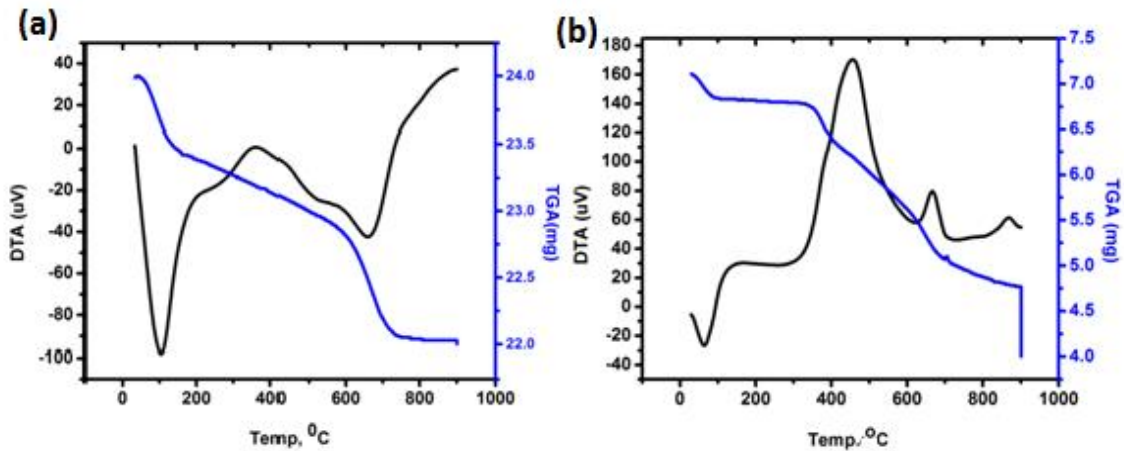


Figure 4.21. TG/DTA curves of (a) Na-Ben and (b) QHQC/Ben

The loading of QHQC into the bentonite gallery for the formation of the organic-inorganic hybrid system was determined by TGA (Figure 4.22) and it was found to be 19 wt%.

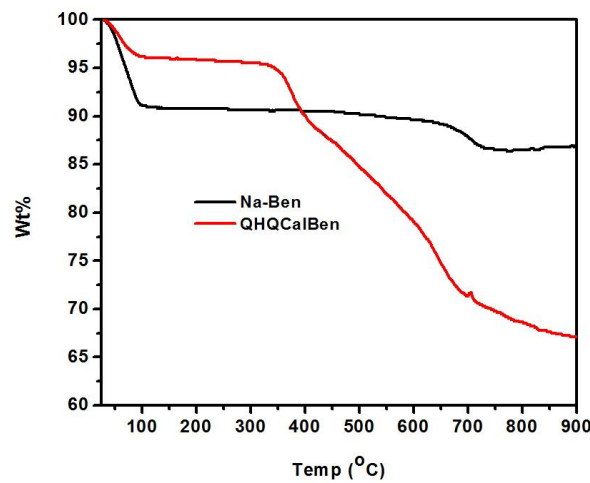


Figure 4.22. TGA curves of Na-Ben and QHQC/Ben

The solid-state absorption and emission studies proved that the hybrid system, QHQC/ben exhibited significant absorption and emission which originated from the organic moiety intercalated in the bentonite gallery. The absorption spectra of QHQC and QHQC/ben in the solid-state (Figure 4.23) show that peak at 577 nm for the receptor **7** is blue-shifted to 563 nm in the hybrid system. But in the case of solid-state emission (Figure 4.24), upon excitation at 367 nm, peak around 426 nm of **7** is red shifted to 482 nm for the hybrid. When the excitation wave length was changed to 570 nm, emission band at 702 nm for **7** is blue-shifted to 680 nm in the hybrid system. The construction of heterogeneous system might have caused changes in chemical environment owing to the interaction of organic moiety with inorganic moiety and hence the reported shifting of absorption and emission peaks. These data further confirmed the intercalation of the macrocyclic molecule into the bentonite.

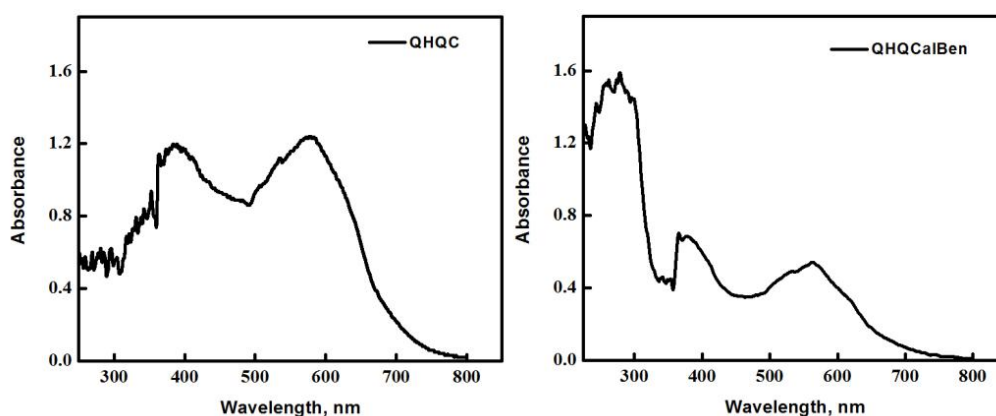


Figure 23. Solid-state absorption spectra of QHQC and QHQC/ben

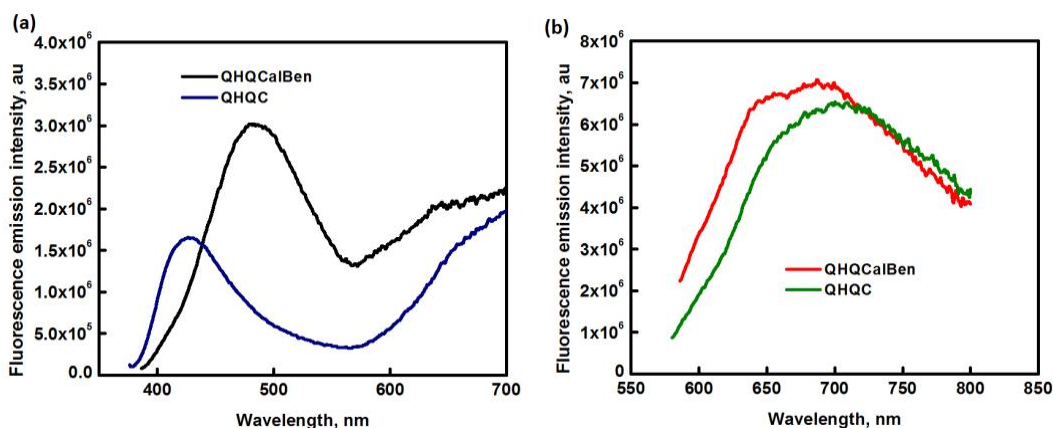


Figure 4.24. Solid-state emission spectra of QHQC and QHQC/ben at excitation wavelength (a) 367 nm and (b) 570nm

To dwell into the aggregation behavior of QHQC when intercalated into galleries of bentonite, we carried out transmission electron microscopic analysis. The images of TEM revealed that QHQC molecules have spherical morphology (a) and are not in the aggregated state. But the morphology of QHQC/ben (c) showed that QHQC molecules are aggregated as a result of intercalation of QHQC into the bentonite galleries (Figure 4.25).

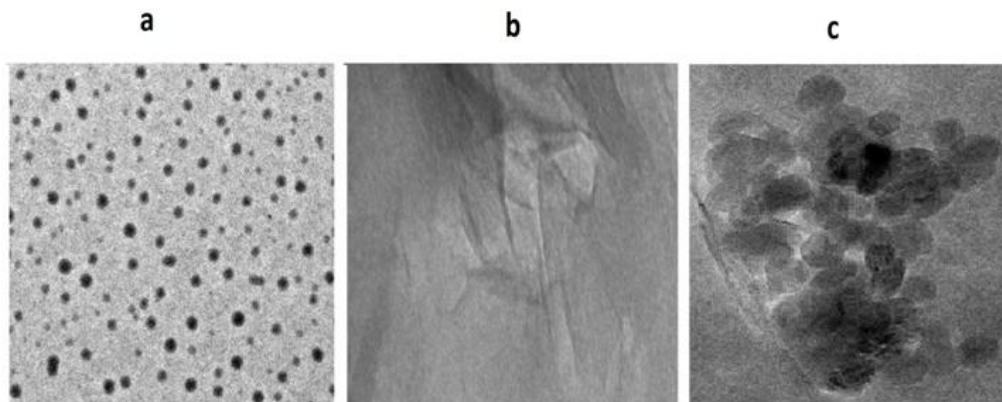


Figure 4.25. TEM images for (a) QHQC, (b) Na-Ben and (c) QHQC/ben

4.3.9. Metal Ion Binding Studies of QHQC/ben

The organic-inorganic hybrid system QHQC/ben was evaluated for its reliability as a naked eye sensitive colorimetric sensor for Hg^{2+} ions. Accordingly, the response of the hybrid system towards the selective sensing of hazardous Hg^{2+} ions was studied by adding Hg^{2+} ions (1×10^{-6} M) to 2 mg of QHQC/ben. Immediately the colour of the solid sample changed from violet to light brown. When iodide solution was added to the above system, the violet colour of the hybrid reappeared (Figure 4.26) and was found to be proficient to bind Hg^{2+} ions recurrently. This showed that the hybrid system also displayed properties analogous to QHQC in acetonitrile. Additionally, the sensor exhibited naked eye detection in MeCN/ H_2O (1:9, v/v) system comparable to acetonitrile. Complexation with Hg^{2+} ions, is the property of QHQC which is intercalated into the bentonite galleries. Here bentonite acts only as a support material for the receptor QHQC and hold it in its interlayers and imparts characteristic functionality to the hybrid. Furthermore, QHQC was not extracted out from QHQC/ben during the complexation process. Consequently, the mechanism of naked eye detection of Hg^{2+} and its reversibility with iodide solution is identical for both QHQC and QHQC/ben.

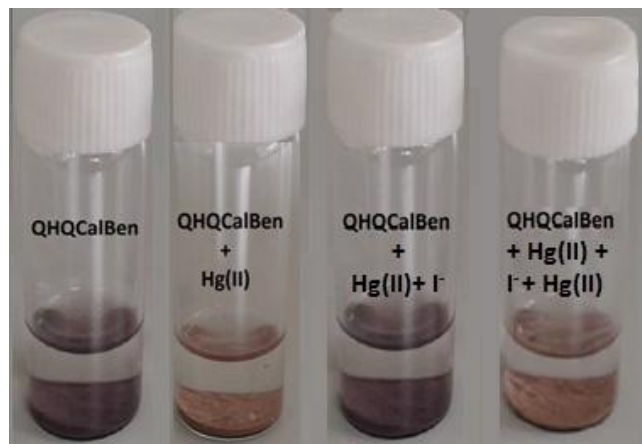


Figure 4.26. Photograph of naked eye detection of Hg^{2+} with QHQCalBen and its reversibility with iodide solution

QHQCalBen showed similar complexation properties as that of QHQC. When the detection limit of QHQCalBen using different concentration of Hg^{2+} ions was checked, it was found that it could recognize the Hg^{2+} ions upto micromolar concentration. It was also observed that the solid-state sensor did not show any considerable response when similar experiments were conducted with other metal ions. Accordingly, QHQCalBen can be used as a selective and reversible solid-state sensor for Hg^{2+} recognition. Owing to the inexpensive and environmentally benign bentonite as the supporting material production of QHQCalBen can be cost-effective and the hybrid sensor can be inferred as economically affordable. In addition, this solid-state sensor is a violet coloured powder and not sensitive to different environment. As a result, this bentonite-hybrid sensor is deduced as portable. Due to the reversibility of the system with iodide solution and constancy even after consecutive experiments, QHQCalBen is established as a reusable hybrid sensor selective to Hg^{2+} .

4.4. Conclusion

In conclusion, we have successfully synthesized and characterized a new lower rim functionalized 1,3-di(quaternary ammonium salt of 8-hydroxyquinaldine) derivative of *p*-tert-butylcalix[4]arene (QHQC) as cone conformer and analyzed its sensing properties toward Hg^{2+} ions using various techniques such as absorption, visual color change, ESI/HRMS and ^1H NMR experiments. Our results revealed that the synthesized molecule is highly capable of recognizing Hg^{2+} ions selectively through naked eye detection following a marked colour change from violet to light brown. The molecule acts as a reversible

chemosensor as it regains the violet colour in the presence of iodide ions, and the detection limit of Hg^{2+} was found to be 2.95×10^{-6} M. In view of these findings an organic-inorganic hybrid system was synthesized by intercalating QHQC into the bentonite galleries and characterized using FT-IR spectroscopy, Powder XRD, TG/DTA techniques and solid-state absorption and emission studies. This hybrid system successfully performed as a colorimetric solid-state Hg^{2+} sensor which showed properties analogous to QHQC. In addition, the sensor is thermally stable, environmentally benign, economically affordable, reversible, portable and reusable.

4.5. Experimental Section

4.5.1. Materials and Methods

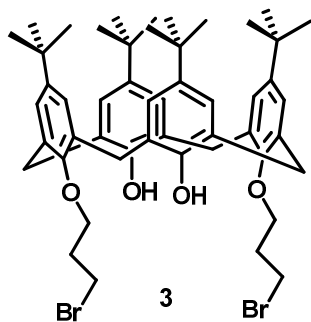
The bentonite clay used in the experiments, *p*-tert-butylcalix[4]arene, 1,3-dibromopropane, 8-hydroxyquinoline and metal perchlorates were purchased from M/s Sigma Aldrich. Acetonitrile was provided by Merck. Other materials used were potassium carbonate (SDFCL), and iodomethane (Spectrochem). Deionized water was used throughout the experiments.

All reactions were carried out in oven dried glassware. Progress of the reactions was monitored by thin layer chromatography, while purification was done by column chromatography. NMR spectra were recorded on Bruker Avance 500 NMR spectrometer (AV 500) at 500 MHz (1H) and 125 MHz (^{13}C). Chemical shifts were reported in δ (ppm) relative to TMS as internal standard, $CDCl_3$ and CD_3CN were used as solvents. IR spectra were recorded on a Perkin-Elmer Spectrum One FT-IR spectrometer (neat KBr). Mass spectra were recorded under ESI/HRMS using analyzer type, Orbitrap mass spectrometer (Thermo Exactive). Absorption spectra were recorded using a Shimadzu UV-2450 spectrophotometer. X-ray diffraction studies were carried out using a powder X-ray diffractometer (Philips X'Pert Pro) with $Cu K\alpha$ radiation. Thermal stability measurements were performed at a heating rate of $10\ ^\circ C\ min^{-1}$ in nitrogen atmosphere using Shimadzu DTG-60 equipment. Absorption spectra of the solid samples were measured with a UV-Vis Spectrophotometer (Shimadzu UV-3600) with an integrating sphere attachment, (ISR-3100) using barium sulfate as a reference. Emission spectra of solid samples were recorded using FluoroLog-322 (Horiba) spectrometer. Surface morphology was analyzed using a FEI,

TECNAI S Transmission Electron Microcopy (TEM). Energy minimization studies were done by ChemBio3D Ultra 11.0 software. All measurements were done at room temperature unless otherwise stated.

4.5.2. Synthesis of Di-(bromopropyl)*p*-*tert*-butylcalix[4]arene, Precursor 3

A mixture of *p*-*tert*-butylcalix[4]arene (0.0015 moles, 1 g) and K₂CO₃ (0.0038 moles, 0.532 g) in dry acetonitrile (20 mL) was stirred at 80 °C for 10 minutes. To this reaction mixture, 1,3-dibromopropane (0.0015 moles, 0.311 g) was added drop wise or slowly during 0.5 h and refluxed for 48 h. Completion of the reaction was checked by TLC. Acetonitrile and excess dibromopropane was removed by vacuum. The residue was quenched by 10-30 mL 5 % HCl and chloroform. Then organic layer was extracted with chloroform, washed with water and dried over sodium sulphate. White solid residue obtained was subjected to column chromatography (60-120 mesh silica gel) using dichloromethane-hexane (20 %). Product **3** was obtained as white powder (1.1 g) in 81 % yield.



IR ν_{\max} : 3379, 2963, 2909, 2865, 1753, 1602, 1488, 1382, 1352, 1299, 1200, 1125, 1042, 943, 867, 815, 777, 633, 543 cm⁻¹.

¹H NMR (500 MHz, CDCl₃), δ (ppm): 7.65 (s, 2H), 7.05 (s, 4H), 6.87 (s, 4H), 4.26 (d, $J = 13$ Hz, 4H), 4.11 (t, $J = 5.5$ Hz, 4H), 4.00 (t, $J = 6.5$ Hz, 4H), 3.35 (d, 13Hz, 4H), 2.54-2.50 (m, 4H), 1.27 (s, 18H), 1.01 (s, 18H).

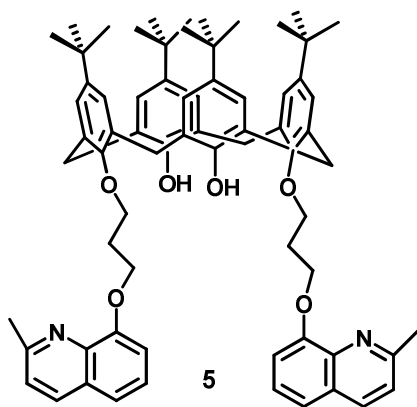
¹³C NMR (125 MHz, CDCl₃), δ (ppm): 149.5, 148.8, 146.4, 140.7, 132.9, 131.7, 126.8, 124.9, 124.6, 124.2, 71.6, 33.2, 32.8, 31.7, 30.7, 30.2.

MS (ESI-HRMS): Calcd for C₅₀H₆₆Br₂O₄, [M+Na+2H]⁺: 913.3382, Found: 913.3212.

4.5.3. Synthesis of 8-Hydroxyquinaldine Derivative of *p*-*tert*-butylcalix[4]arene, Precursor 5

A mixture of 8-hydroxy quinaldine (0.0022 moles, 0.357 g) and K₂CO₃ (0.0034 moles, 0.473 g) in dry acetonitrile (10 mL) was stirred at 80 °C for 10 minutes. To this reaction

mixture, compound **3** (0.0006 moles, 0.500g) was added and refluxed for 48 h. Completion of the reaction was checked by TLC. The reaction mixture was cooled to room temperature and dilute HCl was added for neutralization. Slowly, solid was formed in the reaction mixture which was extracted with chloroform; organic layer was washed with water and dried over sodium sulphate. The crude product was purified by column chromatography (60-120 mesh silica gel) using ethylacetate-hexane (15%). Product **5** was obtained as slight yellow solid (0.380g) in 64.6 % yield.



IR ν_{\max} : 3364, 3053, 2955, 2872, 1594, 1563, 1480, 1427, 1359, 1314, 1254, 1239, 1095, 1042, 861, 830, 739 cm^{-1} .

1H NMR (500 MHz, $CDCl_3$), δ (ppm): 7.92 (d, $J = 8$ Hz, 2H), 7.61 (s, 2H), 7.34 (d, $J = 8$ Hz, 2H), 7.24-7.21 (m, 4H), 7.12 (d, $J = 7.5$ Hz, 2H), 6.99 (s, 4H), 6.80 (s, 4H), 4.50 (t, 6.5 Hz, 4H), 4.26 (d, $J = 13$ Hz, 4H), 4.22 (t, $J = 6$ Hz, 4H), 3.27 (d, $J = 13$ Hz, 4H), 2.72 (s, 6H), 2.57-2.52 (m, 4H), 1.27 (s, 18H), 0.97 (s, 18H).

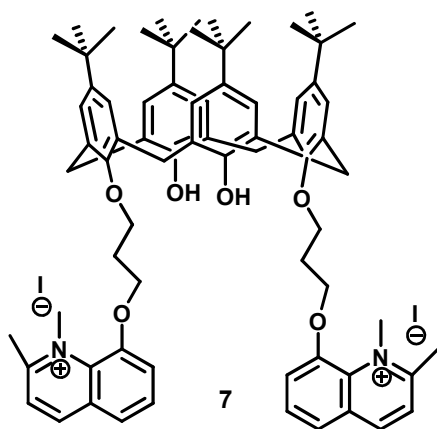
^{13}C NMR (125 MHz, $CDCl_3$), δ (ppm): 157.8, 154.1, 150.7, 149.6, 146.9, 141.3, 140.2, 135.9, 132.7, 127.6, 125.9, 125.5, 124.9, 122.3, 119.3, 109.6, 65.9, 33.9, 31.7, 31.0, 29.7, 25.6.

MS (HRMS): Calcd for $C_{70}H_{82}N_2O_6$, $[M+H]^+$: 1047.6251, Found: 1047.6265.

4.5.4. Synthesis of Quaternized Salt of 8-Hydroxyquinoline Derived *p-tert-butyl* calix[4]arene, QHQC (**7**)

Compound **5** (0.0003 moles, 0.288 g) in dry acetonitrile (10 mL) was refluxed for 5 minutes. Methyl iodide (excess) was added slowly to the above solution and allowed to stir for 72 h at 80 °C. Then acetonitrile was removed under vacuum and the crude product

obtained was purified by column chromatography [alumina, chloroform: methanol (9:1)]. The product 7 was obtained as dark violet coloured solid (0.260 g) in 73.3 % yield.



IR ν_{\max} : 3371, 3053, 2955, 2895, 2865, 2358, 2327, 1594, 1480, 1359, 1193, 1110, 1049, 860, 830, 747, 657 cm^{-1} .

¹H NMR (500 MHz, CDCl_3), δ (ppm): 8.84 (d, $J = 8$ Hz, 2H), 7.89-7.83 (m, 6H), 7.74 (d, $J = 8$ Hz, 2H), 7.56 (s, 2H), 7.07 (s, 4H), 6.85 (s, 4H), 4.74 (t, $J = 6.5$ Hz, 4H), 4.69 (s, 6H), 4.24 (d, $J = 13$ Hz, 4H), 4.18 (t, $J = 5$ Hz, 4H), 3.37 (d, $J = 13$ Hz, 4H), 3.14 (s, 6H), 2.55 (m, 4H), 1.29 (s, 18H), 0.99 (s, 18H).

¹³C NMR (125 MHz, CDCl_3), δ (ppm): 163.1, 161.6, 150.4, 150.3, 150.1, 149.3, 147.4, 142.1, 132.3, 131.9, 130.6, 130.2, 127.7, 127.5, 125.8, 125.3, 125.0, 122.9, 111.1, 72.6, 68.6, 46.8, 46.4, 34.9, 34.0, 31.7, 31.0, 25.6.

MS (HRMS): Calcd for $\text{C}_{72}\text{H}_{88}\text{I}_2\text{N}_2\text{O}_6$, $[\text{M}-\text{I}_2+\text{H}]^+$: 1077.6709, Found: 1077.6653

4.5.5. Intercalation of QHQC Salt on Bentonite Clay

Intercalation of QHQC into clay surface consists of two processes namely preparation of Na-Bentonite (Na-Ben) and intercalation of QHQC on Na-Bentonite. Na-Ben was prepared by mixing bentonite with 1 N NaCl using a mechanical stirrer (600 rpm) for 24 h at room temperature. After that, the residue was separated by centrifugation, washed with distilled water until chloride ions were not detected in the supernatant solution upon addition of 0.1 M AgNO_3 solution. Subsequently, it was kept at -4°C and dried in a lyophilizer.

About 0.100 g of Na-Ben was dispersed in 50 mL acetonitrile and 0.112 g of QHQC in 50 mL acetonitrile was added to it, allowed to stir for 24 h at room temperature. Then it was allowed to stand for overnight, filtered off, washed with acetonitrile (until there was no unreacted QHQC in supernatant solution) and dried under vacuum. The resultant product was

designated as QHQC/CalBen and characterized using FT-IR spectroscopy, PXRD (Powder X-ray Diffraction) and TG/DTA.

4.5.6. General Procedure for the Metal Ion Binding Studies

Metal perchlorate solutions were made in HPLC grade acetonitrile. Metal ion titration was carried out by adding small volume of metal solutions in quartz cuvette. After addition of the metal perchlorate to the cuvette using micro pipette, the absorption spectra were recorded. The stock solutions of metal ions and chromophore were prepared in acetonitrile. The UV absorption studies were performed using a micromolar solution of chromophore with appropriate amounts of metal ions. In the selectivity experiment, to a solution of QHQC 7 (9×10^{-6} M) in acetonitrile, 10 equiv. of different cations each (Mn²⁺, Al³⁺, Co²⁺, Ni²⁺, Cu²⁺, Zn²⁺, Hg²⁺, Ag⁺, Ba²⁺, Cd²⁺, Na⁺, Mg²⁺, Cr³⁺, Zn²⁺, Fe²⁺ and Ca²⁺) were added and absorbance were recorded. For reversibility experiment, tetrabutylammonium iodide in acetonitrile was used as iodide source. ¹H NMR titrations were carried out using Hg(ClO₄)₂ and tetrabutylammonium iodide in CD₃CN at room temperature.

4.5.7. Calculation of LOD

LOD is calculated using the formula,

$$\text{LOD} = 3\sigma / S$$

Where, σ is the standard deviation of blank and S is the slope of the regression line.

4.6. References

1. M. Suresh, C. Anand, J. E. Frith, D. S. Dhawale, V. P. Subramaniam, E. Strounina, C. I. Sathish, K. Yamaura, J. J. Cooper-White, A. Vinu, *Sci. Rep.* **2016**, *6*, 21820, DOI: 10.1038/srep21820
2. S. A. El-Safty, *J. Mater. Sci.* **2009**, *44*, 6764-6774.
3. Š. Korent Urek, N. Frančič, M. Turel, A. Lobnik, *J. Nanomater.* **2013**, *2013*, 13.
4. T. C. Hutchinson, K. M. Meema, *Lead, Mercury, Cadmium and Arsenic in the Environment*, Wiley: New York, **1987**.

5. G. M. Gadd, *Heavy Metal Pollutants: Environmental and Biotechnological Aspects*. In: Lederberg J (ed) *Encyclopedia of microbiology*, 2nd edn; Academic: San Diego, **2000**.
6. P. Grandjean, P. Weihe, R. F. White, F. Debes, *Environ. Res.* **1998**, *77*, 165-172.
7. T. Takeuchi, N. Morikawa, H. Matsumoto, Y. Shiraishi, *Acta Neuropathol.* **1962**, *2*, 40-57.
8. J. J. Gutknecht, *J. Membr. Biol.* **1981**, *61*, 61-66.
9. P. D. Selid, H. M. Xu, E. M. Collins, *Sensors* **2009**, *9*, 5446-5459.
10. R. Joseph, B. Ramanujam, A. Acharya, A. Khutia, C. P. Rao, *J. Org. Chem.* **2008**, *73*, 5745-5758.
11. I. Leray, B. Valeur, *Eur. J. Inorg. Chem.* **2009**, *24*, 3525-3535.
12. Y. Yanfei, C. Xiaodan, S. Malgorzata, A. Richard, A. Bartsch, *Tetrahedron* **2010**, *66*, 447-454.
13. C. P. Rao, R. Joseph, *Chem. Rev.* **2011**, *111*, 4658-4702.
14. A. Bandela, J. P. Chinta, C. P. Rao, *Dalton Trans.* **2011**, *40*, 11367-11370.
15. J. Dessingou, K. Tabbasum, A. Mitra, V. K. Hinge, C. P. Rao, *J. Org. Chem.* **2012**, *77*, 1406-1413.
16. J. Ma, M. Song, I. Boussouar, D. Tian, H. Li, *Supramol. Chem.* **2015**, *27*, 444-452.
17. H. Li, Y. Zhang, X. Wang, D. Xiong, Y. Bai, *Mater. Lett.* **2007**, *61*, 1474-1477.
18. D. Tian, H. Yan, H. Li, *Supramol. Chem.* **2010**, *22*, 249-255.
19. S. Shinkai, *Tetrahedron* **1993**, *49*, 8933-8968.
20. (a) C. D. Gutsche, R. Muthukrishnan, *J. Org. Chem.* **1978**, *43*, 4905-4906. (b) C. D. Gutsche, M. Iqbal, D. Stewart, *J. Org. Chem.* **1986**, *51*, 742-745.
21. L. Mandolini, R. Ungaro, *Calixarenes in Action*; Imperial College Press: London, **2000**.
22. (a) C. D. Gutsche, *Acc. Chem. Res.* **1983**, *16*, 161-170. (b) C. D. Gutsche, B. Dhawan, J. A. Levine, K. H. No, L. J. Bauer, *Tetrahedron* **1983**, *39*, 409-426.
23. (a) I. Oueslati, R. Abidi, H. Amri, P. Thuery, M. Nierlich, Z. Asfari, J. Harrowfield, J. Vicens, *Tetrahedron Lett.* **2000**, *41*, 8439-8443. (b) S. Shinkai, K. Fujimoto, T. Otsuka, H. L. Ammon, *J. Org. Chem.* **1992**, *57*, 1516-1523. (c) D. Beer, M. G. B. Drew, P. A. Gale, P. B. Leeson, M. I. Ogden, *J. Chem. Soc., Dalton Trans.* **1994**,

- 3479-3485. (d) P. J. Dijkstra, J. A. J. Brunink, K.-E. Bugge, D. N. Reinhoudt, S. Harkema, R. Ungaro, F. Ugozzoli, E. Ghidini, *J. Am. Chem. Soc.* **1989**, *111*, 7567-7575.
24. J. Vicens, V. Bohmer, *Calixarenes, a Versatile Class of Macrocyclic Compounds*; Kluwer Academic Publishers: Dordrecht, The Netherlands, **1991**.
25. (a) K. Iwamoto, S. Shinkai, *J. Org. Chem.* **1992**, *57*, 7066-7073. (b) S. K. Sharma, C. D. Gutsche, *Tetrahedron* **1994**, *50*, 4087-4104.
26. E. M. Collins, M. A. McKervey, E. Madigan, M. B. Moran, M. Owens, G. Ferguson, S. J. Harris, *J. Chem. Soc. Perkin Trans. 1* **1991**, 3137-3142.
27. C. D. Gutsche, *Calixarenes Revisited, Monographs in Supramolecular Chemistry*; J. F. Stoddart, Ed.; Royal Society of Chemistry: Cambridge, UK, Vol. 1, **1998**.
28. A. Dondoni, A. Marra, *Chem. Rev.* **2010**, *110*, 4949-4977.
29. J. S. Kim, D. T. Quang, *Chem. Rev.* **2007**, *107*, 3780-3799.
30. B. S. Creaven, D. F. Donlon, J. McGinley, *Coord. Chem. Rev.* **2009**, *253*, 893-962.
31. B. Valeur, I. Leray, *Coord. Chem. Rev.* **2000**, *205*, 3-40.
32. B. Valeur, I. Leray, *Inorg. Chim. Acta* **2007**, *360*, 765-774.
33. A. P. de Silva, H. Q. N. Gunaratne, T. Gunnlaugsson, A. J. M. Huxley, C. P. McCoy, J. T. Rademacher, T. E. Rice, *Chem. Rev.* **1997**, *97*, 1515-1566.
34. M. J. Choi, M. Y. Kim, S.-K. Chang, *Chem. Commun.* **2001**, 1664-1665.
35. H. M. Chawla, S. P. Singh, S. Upreti, *Tetrahedron* **2006**, *62*, 9758-9768.
36. Q.-Y. Chen, C.-F. Chen, *Tetrahedron Lett.* **2005**, *46*, 165-168.
37. J. H. Kim, A.-R. Hwang, S.-K. Chang, *Tetrahedron Lett.* **2004**, *45*, 7557-7561.
38. N. R. Cha, M. Y. Kim, Y. H. Kim, J.-I. Choe, S.-K. Chang, *J. Chem. Soc., Perkin Trans. 2* **2002**, 1193-1196.
39. R. Joseph, B. Ramanujam, A. Acharya, A. Khutia, C. P. Rao, *J. Org. Chem.* **2008**, *73*, 5745-5758.
40. J. J. Colleran, B. S. Creaven, D. F. Donlon, J. McGinley, *Dalton Trans.* **2010**, *39*, 10928-10936.
41. R. Metivier, I. Leray, B. Lebeau, B. Valeur, *J. Mater. Chem.* **2005**, *15*, 2965-7973.
42. U. Ocak, M. Ocak, K. Surowiec, R. A. Bartsch, M. G. Gorbunova, C. Tu, Surowiec, M. A. *J. Inclusion Phenom. Macrocyclic Chem.* **2009**, *63*, 131-139.

43. A. F. Danil de Namor, S. Chahine, E. E. Castellano, O. E. Piro, *J. Phys. Chem. A* **2005**, *109*, 6743-6751.
44. A. F. Danil de Namor, S. Chahine, E. E. Castellano, O. E. Piroc, H. D. J. Brooke, *Chem. Commun.* **2005**, 3844-3846.
45. H. Li, Y. Zhang, X. Wang, D. Xiong, Y. Bai, *Mater. Lett.* **2007**, *61*, 1474-1477.
46. J. Lu, X. He, X. Zeng, Q. Wan, Z. Zhang, *Talanta* **2003**, *59*, 553-560.
47. Y. Liu, B.-T. Zhao, L.-X. Chen, X.-W. He, *Microchem. J.* **2000**, *65*, 75-79.
48. D. Tian, H. Yan, H. Li, *Supramol. Chem.* **2010**, *22*, 249-255.
49. A. B. Othman, J. W. Lee, J.-S. Wu, J. S. Kim, R. Abidi, P. Thuery, J. M. Strub, A. Van Dorsselaer, J. Vicens, *J. Org. Chem.* **2007**, *72*, 7634-7640.
50. R. Joseph, A. Gupta, C. P. Rao, *J. Photochem. Photobiol., A* **2007**, *188*, 325-329.
51. L. Praveen, V. B. Ganga, R. Thirumalai, T. Sreeja, M. L. P. Reddy, R. Luxmi Varma, *Inorg. Chem.* **2007**, *46*, 6277-6282.
52. L. Praveen, J. Babu, M. L. P. Reddy, R. Luxmi Varma, *Tetrahedron Lett.* **2012**, *53*, 3951-3954.
53. G. Wirnsberger, B. J. Scott, G. D. Stucky, *Chem. Commun.* **2001**, 119-120.
54. L. Nicole, C. Boissiere, D. Grosso, P. Hesemann, J. Moreau, C. Sanchez, *Chem. Commun.* **2004**, *20*, 2312-2313.
55. S. J. Lee, S. S. Lee, J. Y. Lee, J. H. Jung, *Chem. Mater.* **2006**, *18*, 4713-4715.
56. E. Palomares, R. Vilar, A. Green, J. R. Durrant, *Adv. Funct. Mater.* **2004**, *14*, 111-115.
57. J. Liu, Y. Lu, *Chem. Mater.* **2004**, *16*, 3231-3238.
58. M. Comes, M. D. Marcos, F. Sancenon, J. Soto, L. A. Villaescusa, P. Amoros, D. Beltran, *Adv. Mater.* **2004**, *16*, 1783-1786.
59. L. F. Capitan-Vallvey, C. Raya, E. L. Lopez, M. D. F. Ramos, *Anal. Chim. Acta.* **2004**, *524*, 365-372.
60. M. A. Kalinina, N. V. Golubev, O. A. Raitman, S. L. Selector, V. V. Arslanov, *Sens. Actuators, B* **2006**, *114*, 19-27.
61. D. L. Rodman, H. Pan, C. W. Clarier, W. Feng, Z. L. Xue, *Anal. Chem.* **2005**, *77*, 3231-3237.
62. A. R. Potyrailo, *Angew. Chem. Int. Ed.* **2006**, *45*, 702-723.

63. A. B. Desacalzo, K. Rurack, H. Weisshoff, R. M. Martinez-Manez, M. D. Marcos, P. Amoros, K. Hoffmann, J. Soto, *J. Am. Chem. Soc.* **2005**, *127*, 184-200.
64. A. C. D. Newman, *Chemistry of Clays and Clay Minerals*. Monograph No. 6; Mineralogical Society: New York, **1987**.
65. H. van Olphen, *An Introduction to Clay Colloid Chemistry*, 2nd ed; John Wiley and Sons: New York, **1977**.
66. R.E. Grim, *Clay Mineralogy, International Series in Earth and Planetary Sciences*, 2nd ed; Pergamon Press: New York, **1968**.
67. T. Shichi, K. Takagi, *J. Photochem. Photobiol. C: Photochem. Rev.* **2000**, *1*, 113-130.
68. S. Takagi, M. Eguchi, D. A. Tryk, H. Inoue, *J. Photochem. Photobiol. C: Photochem. Rev.* **2006**, *7*, 104-126.
69. M. Ogawa, K. Kuroda, *Chem. Rev.* **1995**, *95*, 399-438.
70. L. Petra, P. Billik, P. Komadel, *Appl. Clay Sci.* **2015**, *115*, 174-178.
71. Z. T. Li, G.-Z. Ji, C.-X. Zhao, S.-D. Yuan, H. Ding, C. Huang, A.-L. Du, M. Wei, *J. Org. Chem.* **1999**, *64*, 3572-3584.
72. I. A. Bagatin, H. E. Toma, *New J. Chem.* **2000**, *24*, 841 -844.
73. H. J. Motulsky, A. Christopoulos, GraphPad Software Inc., San Diego, CA, **2003**.
74. A. D. Becke, *Phys. Rev. A* **1988**, *38*, 3098-3100.
75. C. Lee, W. Yang, R. G. Parr, *Phys. Rev. B*, **1988**, *37*, 785-789.
76. M. J. Frisch, G. W. Trucks, H. B. Schlegel, G. E. Scuseria, M. A. Robb, J. R. Cheeseman, G. Scalmani, V. Barone, B. Mennucci, G. A. Petersson, H. Nakatsuji, M. Caricato, X. Li, H. P. Hratchian, A. F. Izmaylov, J. Bloino, G. Zheng, J. L. Sonnenberg, M. Hada, M. Ehara, K. Toyota, R. Fukuda, J. Hasegawa, M. Ishida, T. Nakajima, Y. Honda, O. Kitao, H. Nakai, T. Vreven, J. A. Montgomery, Jr., J. E. Peralta, F. Ogliaro, M. Bearpark, J. J. Heyd, E. Brothers, K. N. Kudin, V. N. Staroverov, R. Kobayashi, J. Normand, K. Raghavachari, A. Rendell, J. C. Burant, S. S. Iyengar, J. Tomasi, M. Cossi, N. Rega, J. M. Millam, M. Klene, J. E. Knox, J. B. Cross, V. Bakken, C. Adamo, J. Jaramillo, R. Gomperts, R. E. Stratmann, O. Yazyev, A. J. Austin, R. Cammi, C. Pomelli, J. W. Ochterski, R. L. Martin, K. Morokuma, V. G. Zakrzewski, G. A. Voth, P. Salvador, J. J. Dannenberg, S. Dapprich, A. D.

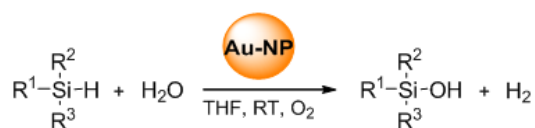
- Daniels, Ö. Farkas, J. B. Foresman, J. V. Ortiz, J. Cioslowski, D. J. Fox, Gaussian 09, Revision **D.01**, Gaussian, Inc., Wallingford CT, **2009**.
77. I. Leray, Z. Asfari, J. Vicens, B. Valeur, *J. Chem. Soc. Perkin Trans. 2* **2002**, 1429-1434.
78. I. Leray, Z. Asfari, J. Vicens, B. Valeur, *J. Fluoresc.* **2004**, *14*, 451-458.
79. Y. M. Zhang, W. J. Qu, G. Y. Gao, B. B. Shi, G. Y. Wu, T. B. Wei, Q. Lin, H. Yao, *New J. Chem.* **2014**, *38*, 5075-5080.
80. Y. Shiraishi, C. Ichimura, S. Sumiya, T. Hirai, *Chem. -Eur. J.* **2011**, *17*, 8324-8332.
81. J. Yang, Z. Wang, Y. Li, Q. Zhuang, W. Zhao, J. Gu, *RSC Adv.* **2016**, *6*, 69807-69814.

SUMMARY

The thesis entitled “**Bentonite Based Organic-Inorganic Hybrid Materials: Application Towards Green Catalysis and as Mercury Sensor**” embodies the results of our investigations carried out in the area of bentonite based organic-inorganic hybrid systems for application towards green catalysis and as a solid state sensor for detection of micromolar levels of mercury ions.

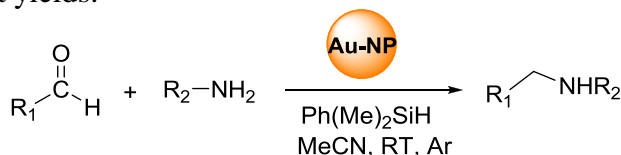
The introductory chapter of the thesis gives an overview of the various green approaches towards two aspects, explicitly catalysis and sensing applications of hybrid materials. A definition of the present work is also incorporated in this chapter.

Chapter 2 describes the synthesis and characterization of an efficient, environmentally benign and reusable heterogeneous bentonite-gold nanohybrid catalyst (Au-MPBen). The applicability of this catalyst towards the selective oxidation of silanes to silanols was investigated under ambient reaction conditions and it was found that this nanohybrid catalyst afforded aromatic, aliphatic and sterically hindered silanols in excellent yields without the formation of disiloxanes as by-product and was recyclable. The present methodology for silane oxidation reaction is environmentally benign, 98.7 % atom economical and proceeded with low catalyst loading (Scheme 1).



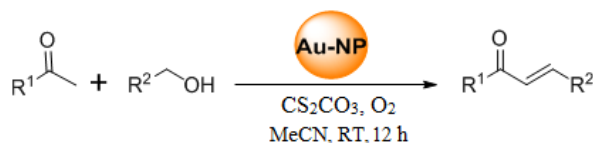
Scheme 1

Chapter 3 deals with the efficacy of Au-MPBen catalyst towards two different organic reactions and this chapter is divided into two parts. In Part A, an efficient and green method for the direct reductive amination of aldehydes using Au-MPBen catalyst is discussed (Scheme 2). The reaction was performed in the presence of phenyldimethylsilane as a mild hydride donor under ambient reaction conditions and afforded a wide array of secondary amines in excellent yields.



Scheme 2

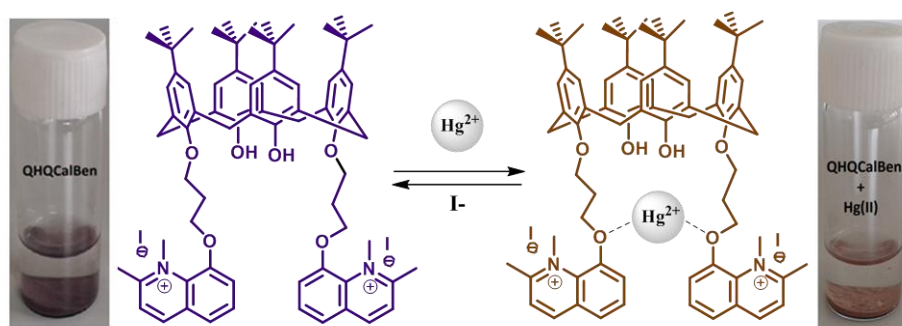
We extended the scope of our catalyst towards the oxidative cross-coupling reaction of ketones with primary alcohols in presence of Cs_2CO_3 as base and the details are presented in Part B of the third chapter (Scheme 3). This cascade C-C bond formation strategy is environmentally benign, economical, selective, easily separable, reusable and works under mild reaction conditions and generated a variety of α,β -unsaturated ketones with water as the only by-product.



Scheme 3

The remarkable property of this heterogeneous catalyst is its applicability towards the gram scale synthesis of silanols, secondary amines and α,β -unsaturated ketones.

In the final chapter, the synthesis and characterization of a new lower rim functionalized calix[4]arene derivative (QHQC) and its sensing properties toward Hg^{2+} ions using various physical techniques are discussed. The behavior of QHQC as a reversible and selective Hg^{2+} sensor through naked eye detection prompted us to devise a solid state Hg^{2+} sensor (QHQC/ben) with enhanced chemical and thermal stability, by intercalating it into the bentonite galleries. This hybrid material (QHQC/ben) was characterized and assessed its feasibility as colorimetric solid state Hg^{2+} sensor and the results are also detailed in this chapter (Scheme 4)



Scheme 4

In conclusion, we have been successful in synthesizing two organic-inorganic hybrid systems based on bentonite. One has been explored as a green heterogeneous catalyst for different organic reactions and other as a solid state sensor for the selective detection of Hg^{2+} ions.

List of Publications

1. A bentonite-gold nanohybrid as a heterogeneous green catalyst for selective oxidation of silanes. **R. J. Maya**, Jubi John, R. Luxmi Varma. *Chem. Commun.* **2016**, 52, 10625-10628.
2. Direct reductive amination of aldehydes via environmentally benign bentonite-gold nanohybrid catalysis. **R. J. Maya**, Susanna Poullose, Jubi John, R. Luxmi Varma, *Adv. Synth. Catal.* **2017**, 359, 1177-1184.
3. Lower rim modified calix[4]arene-bentonite hybrid system as a green, reversible and selective colorimetric sensor for Hg²⁺ recognition. **R. J. Maya**, Athira Krishna, P. Sirajunnisa, C. H. Suresh, R. Luxmi Varma, *ACS Sustainable Chem. Eng.* **2017**, 5, 6969-6977.
4. An efficient and environmentally benign bentonite-gold nanohybrid catalyzed oxidative cross coupling of ketones with benzylic primary alcohols. **R. J. Maya**, R. Luxmi Varma, *Asian J. Org. Chem.* **2017**, 6, 1486-1491.
5. Colorimetric detection of Al(III) ions based on triethylene glycol appended 8-propyloxyquinoline ester. B. Jisha, M. R. Resmi, **R. J. Maya**, R. Luxmi Varma, *Tetrahedron Lett.* **2013**, 54, 4232-4236.

Contributions to Academic Conferences

1. Triethylene glycol appended 8-propoxyquinoline ester as selective colorimetric sensor towards Al(III) ions, **Maya R. J.**, Sreedevi P., Jisha Babu, R. LuxmiVarma, TFOC-2014, October 9-11, Trivandrum.
2. Synthesis & characterisation of propyloxycoumarin appended silane grafted bentonite: Application towards removal of phenol as organic pollutant, **Maya. R. J.**, R. Luxmi Varma, NDCS- 2015, Oct. 16-18, 2015, BITS- Pilani (PP-165).